DEVELOPMENT OF MICROPARTICLE - NANOPARTICLE POWDER MIXTURES FOR THE USE IN DRY POWDER INHALERS

Inaugural - Dissertation

zur
Erlangung des Doktorgrades der
Mathematisch - Naturwissenschaftlichen Fakultät der
Heinrich - Heine - Universität Düsseldorf

vorgelegt von
Viktoriya Mykhaylova
aus Lemberg

Düsseldorf, Januar 2009

Aus dem Institut für Pharmazeutische Technologie und Biopharmazie der Heinrich - Heine - Universität Düsseldorf

Gedruckt mit der Genehmigung der
Mathematisch - Naturwissenschaftlichen Fakultät der
Heinrich - Heine - Universität Düsseldorf

Referent: Prof. Dr. N.A. Urbanetz

Koreferent: Prof. Dr. P. Kleinebudde

Tag der mündlichen Prüfung: 25.05.2009

MEINEN ELTERN

MEINEM VERSTORBENEN BRUDER

RUSLAN

Content

A. Preface

The use of inhaled drugs for the treatment of respiratory diseases, such as bronchial asthma, chronic bronchitis or chronic obstructive pulmonary diseases (COPD) has increased tremendously during the last decades. Compared with systemic therapy, aerosols have many clinical advantages. For example, the therapeutic effect can be achieved with a fraction of the dose needed when the drug is administered systemically. Thereby, the risk of extrapulmonary and systemic side - effects is reduced. The onset of action is faster after pulmonary application. This is very important for drugs, like bronchodilators, which are used for the treatment of acute bronchospasm (Moren, 1993).

For many years, aerosol therapy was used mostly for the treatment of airways diseases. Lately, aerosols have been used for the treatment of extrapulmonary diseases like diabetes mellitus or cancer. Also the interest in the systemic therapy with peptide drugs, hormones and antibiotics increases (Lohrmann, 2005). It is of great advantage that the surface of the lung of the grown - up person is ca. 100 m^2 and works as a highly permeable membrane. The pulmonary application is free of pain. The problems with poor resorption and first - pass - effect can be avoided and the bioavailability of drugs may be increased.

Drug delivery to the lung is not problem - free. Some aerosol ingredients may cause irritation and bronchospasm. Not all patients are able to use available devices for inhalation properly.

There are three main possibilities for the pulmonary application: metered dose inhalers, nebulisers and dry powder inhalers. The most frequently used delivery systems are pressurized metered dose inhalers. Also, the usage of dry powder inhalers is on the rise. The advantages of the latter are, that the formulation does not need environmentally harmful propellants, and active ingredients, which are usually instable in fluid media, can be used. Nebulisers may be used for aerosol generation also, but they are usually too large for the usage as portable devices (Moren, 1993).

The main concern with most inhaled aerosols is the deposition at the desired location in the respiratory tract. The deposition is dependent on the particle size of the aerosol and breathing pattern of the patient. Particles may be too large to pass the oropharynx and larynx and to deposit in the deep parts of the lung. The optimal aerodynamic diameter of the particles must be between 1 µm and 5 µm. Larger particles stay in the upper airways, whereas smaller ones are be exhaled again.

To ensure the arriving of the active ingredient powder at the site of action usually the powder has to be micronised. Micronised powders are usually very cohesive leading to poor flowability, mass uniformity upon dosing and redispersion, which cause the amount of the active ingredient in the low part of the lung to vary.

In order to get an easy - flowing powder, which is ready for use in dry powder inhalers, drug particles are often mixed with coarse carrier particles. The diameter of the carrier particles varies mostly between 50 µm and 200 µm. As carrier materials lactose, glucose or mannitol are reported to be in use (Steckel et al., 2004; Saint - Lorant et al., 2007). Upon inhalation the drug particles must separate from the carrier in order to reach the alveolar part of the lung. The drug particle fraction, which is separated from the carrier particles during inhalation, is largely dependent on the interparticle interactions between drug and carrier. If the interactions between

the two interacting partners are stronger than between the particles of the same fraction, the drug particles tend to stick on the carrier particles, ensuring thereby highly homogeneous free - flowing interactive mixtures with good mass uniformity. It might be difficult to detach the drug particles from the surface of the carrier during inhalation due to high interparticle interactions. At the beginning of the inhalation process, Van der Waals and electrostatic forces play the dominating role. After the entrance of the powder in the mouth - throat area and mixing with warm and humid air, the powder may start to gain water and capillary forces may increase immensely (Moren, 1993). If the interactions between the drug and the carrier are too weak, the particles tend to agglomerate with the particles of the same fraction resulting in the decomposition of the powder mixture. In order to control the amount of drug, which reaches the targeted parts of the lung several ideas, such as addition of fines or formation of "soft pellets", which represent agglomerates of micronised drug particles were proposed and tested (Moren, 1993).

Goal of this study is the evaluation of an innovative formulation approach for the use in dry powder inhalers, designed to work without coarse carriers using drugs coated with nanoparticles. Nanoparticles are used as spacers between drug particles, thus reducing interparticle interactions (Huber et al., 2003; Mykhaylova et al., 2006).

To prove the viability of this concept, a model was chosen consisting of spray - dried and micronised powders as the model substance for the active ingredient, and colloidal silicon dioxide (Aerosil® R972), as the model substance for the nanoparticles covering the drug particles. Mixtures of microparticles and nanoparticles were prepared by conventional mixing using the TURBULA® shaker mixer or by electrostatically supported mixing (Huber, 2001; Mykhaylova et al., 2006) using the high speed homogenator ULTRA - TURRAX®.

Amount of active ingredient presumably reaching the respiratory tract was determined by aerodynamic assessment of fine particles in vitro using the Next Generation Pharmaceutical Impactor (European Pharmacopoeia 6.0). Different methods to characterise the flowability of the mixtures were evaluated in order to obtain a measure for the uniformity of mass, as well as the uniformity of mass itself, using a multidose dry powder inhaler was, determined.

B. Introduction

1. Inhalation therapy

1.1 Anatomy of the respiratory tract

It is very important to be acknowledged with the anatomy of the lung in order to understand the deposition of the drug powder in this organ. The respiratory tract can be divided into the upper (nose, nasal and paranasal passages, mouth, pharynx, larynx, trachea and bronchi) and lower parts (bronchioles and alveoli) and viewed as a series of branching passageways. According to Figure 1 the anatomy of the lung is similar to the structure of a tree, the branching starts at the bottom of the trachea. The lower airways are further divided into conducting and respiratory zone. In the conducting zone humidification, gas buffering, transference as well as air warming take place. In the respiratory zone the gas exchange takes place. With increasing airway generation the diameter of the single airway decreases, however, the total cross section of all airways of one generation increases with increasing airway generation.

Moving through the upper respiratory tract, at each branch, the air has to change the direction sharply, causing instability of the air stream. In the lower airways the air stream becomes more stable and exhibits laminar flow. This region includes the main sites of action for anti - asthmatic drugs (Zeng et al., 2001).

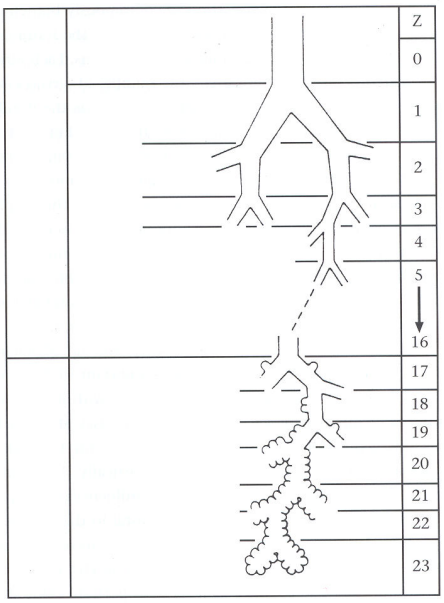

Figure 1: Lung model according to Weibel, modified by Zeng (taken from Zeng et al., 2001)

1.2 Lung deposition

The transport of particles in the airways is mainly determined by aerodynamic characteristics: particle size, shape, density and gas velocity. Particle shape is one of the most important, but one of the most uncontrollable factors in powder technology. It is not very unusual, that particles, which had undergone similar treating procedures, possess different shapes.

Instead of the geometric diameter, it seems quite reasonable to use the aerodynamic equivalent diameter for the characterisation of the behaviour of particles travelling through the airways. The aerodynamic diameter is defined as the diameter of the unit - density (1 g/cm^3) sphere, that has the same gravitational settling velocity in the air as the particle under examination. The aerodynamic diameter of a sphere is expressed as:

$$d_{ae} = d_g \cdot \rho_p^{\frac{1}{2}} \qquad \textbf{Equation 1}$$

where d_{ae} and d_g are the aerodynamic and geometric diameter of the particle, respectively, and ρ_p is the particle density. A spherical particle with the diameter of 5 µm and the density of 4.0 g/cm^3 aerodynamically behaves the same as a spherical particle with the diameter of 10 µm and the density 1.0 g/cm^3 (Moren, 1993).
During inhalation, the particles are separated from the flow streamlines, may contact the respiratory surface and may be deposited or captured in the respiratory tract by different mechanisms. The most important deposition mechanisms are impaction, sedimentation and diffusion (Figure 2).

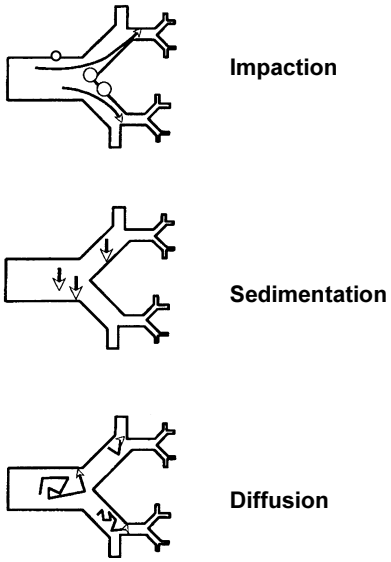

Figure 2: The most important deposition mechanisms of the particles in the lung (taken from Lohrmann, 2005)

- Impaction - inhaled air follows the path through the airways. When the air stream changes direction, the inhaled particles tend to keep their trajectories. If the particles possess a sufficient momentum, they will not follow the air stream, but impact on any barrier in their way. The deposition by impaction is governed by a function known as Stokes´ number:

$$STK = \frac{\rho_p \cdot d_p^2 \cdot V_a}{18 \cdot \eta_a \cdot R_a}$$ **Equation 2**

where ρ_p is the particle density, d_p the particle diameter, V_a the air velocity, η_a the air viscosity and R_a the airway radius. The higher the Stokes´ number is, the more the particle is likely to be deposited by impaction. Impaction may be increased by raising the air flow rate, particle size or particle density. Impaction is usually undesirable, because it is the most likely deposition mechanism in the upper airways;

- Sedimentation - inhaled particles settle in the airways under the influence of gravity. This process is time - dependent. The sedimentation velocity V_t of particles can be calculated according to Stokes´ Law:

$$V_t = \frac{(\rho_p - \rho_a) \cdot d_p^2 \cdot g}{18 \cdot \eta_a}$$ **Equation 3**

where ρ_p is the particle density, ρ_a the density of the air, d_p the particle diameter, η_a the air viscosity and the g gravitational acceleration. It is assumed, that the flow within the lung is laminar, which is true for the lower airways. While the most important deposition mechanism in the upper airways is impaction, due to the high air velocity, sedimentation is the most significant deposition mechanism of particles in the low parts of the lung, where the air velocity is low;

- Diffusion - particles with diameters smaller than 1 µm underlay the Brownian motion in the air stream due to collisions with gas molecules. Brownian motion increases with decreasing particle size. Therefore diffusion plays a certain role for particle deposition in the deep lung (Zeng et al., 2001). Particle movement may be described as follows:

$$\Delta = \sqrt{6 \cdot D \cdot t}$$ **Equation 4**

where Δ is the root mean square displacement with the time t and D is the diffusion coefficient of the particles:

$$D = K \cdot T / 3 \cdot \pi \cdot \eta_a \cdot d_p$$ **Equation 5**

with K the Boltzmann constant, T the absolute temperature, η_a the gas viscosity and d_p the particle diameter.

Two further deposition mechanisms interception and electrostatic deposition are underpart. In summary, aerodynamic particle size is the most important factor of the powder formulation in relation to particle deposition (Zeng et al., 2001; Podczeck, 1997 (c); Buckton, 1988).

1.3 Application devices

1.3.1 Preliminary remarks

To ensure the penetration of active ingredients in the deep parts of the lung, the application devices have to generate an aerosol of drug solution droplets or drug particles in the range between 1 µm and 5 µm. The device must ensure reproducible drug dosing and physico - chemical stability during storage. The metered dose inhalers, nebulisers and dry - powder inhalers match the requirements and therefore have found their way into commercial markets.

1.3.2 Metered dose inhalers

Pressurized metered dose inhalers (MDIs) are widely used for the treating of airway diseases, because of their compactness, convenience and readiness to use. MDIs are powered by propellants, which give the necessary vapour pressure and desired spray characteristics. The dose leaves the canister via a metering chamber.

For a long time, chlorofluorocarbons (CFC) were used as propellants. Now, these CFC propellants are no longer allowed for the use, because they are considered environmentally harmful and also contribute to global warming. Therefore, alternative non - CFC propellants, hydrofluoroalkanes, have been developed. The hydrofluoroalkanes are less harmful, but still likely to raise environmental concerns. Replacement of the one kind of the propellant by the other is not an easy task, they have different physico - chemical properties such as polarity altering drug solubility. Vapour pressure and density are likely to influence the deposition of the drug in the lung.

Aside from cough reflexes, some patients stop the inspiration, minimizing the deposition of the aerosol into the airways, because of the unpleasant feeling of the cool cloud in the throat. Several mistakes, due to the inability of many patients to synchronise aerosol actuation with inspiration, reduce the deposition level. To solve these problems, inhalation aids, spacers, fitted to the mouthpiece of the conventional MDI, can be used. The spacers take up the aerosol cloud in their body, reducing thereby the need for coordination between actuation and inhalation (Zeng et al., 2001; Podczeck, 1997 (b)). Due to the use of spacers, the speed of the droplets coming out of the canister is reduced and larger particles are separated in the spacer. The aerosol deposition in the mouth/throat area may be reduced and the lung deposition may be increased (Steckel, 2003 (a)).

1.3.3 Nebulisers

Nebulisers are usually used by patients who have difficulties using other devices successfully, especially children under 4 years. They are usually used for the treatment of hospitalised or non - ambulatory patients. They are helpful when large doses of the active ingredient have to be administered, which cannot be delivered with the help of MDIs or dry powder inhalers. Nebulisers are easy to use and require no coordination during the use, due to the continuous generation and delivery of the aerosol. Inhalation may be done through a mouth - piece or face mask. Nebulisers are able to generate small droplets, which penetrate deeply into the lung.

Nebulisers are used to convert the drug solution or suspension into a spray. In case of the jet nebuliser the device is powered by compressed gas from a compressor, in case of ultrasonic

nebulisers, by a high - frequency sound wave. By jet nebulisers the gas, air or oxygen is forced through a narrow bore inlet and across the top of a capillary tube. Lower end of the tube is immersed in a liquid to be nebulised. By leaving the inlet, the gas expands and generates the negative pressure which draws the liquid up the capillary tube and into the gas stream. The expansion of the gas breaks the liquid into droplets, the smaller droplets are delivered to the patient and the larger ones are returned to the liquid after the contact with the baffles. Ultrasonic nebulisers do not need a carrier gas. The solution or suspension is atomised with the help of the piezoelectric crystal transducer, using an alternating current, which causes the shape of the crystal to shrink and expand in turn. The originated vibration is amplified by a stainless steel shim and transferred to the solution or suspension in the nebuliser reservoir, leading to the fragmentation of the liquid. Solutions of β_2 - agonists, corticosteroids and mucolytic substances are commercially available in form of solutions and suspensions for the nebulisation. In comparison to other inhalation devices nebulisers are bulky, more expensive and the treatment is time - consuming.

In early 2004, the company Boehringer Ingelheim Pharma GmbH & Co. KG (Ingelheim, Germany) introduced Respimat® SMI (Soft Mist™ Inhaler), a portable nebuliser, in Germany. With a new SMI technology, the inhaler releases a soft, long lasting, slow moving mist (Soft Mist™) from a liquid solution without the need for propellants. A liquid solution is pressed through a capillary tube and passes through a nozzle system that produces the Soft Mist™, with cloud properties that result in better lung deposition and high fine particle fraction. This inhalation device has a delivery mechanism that relies on the energy released from a tensioned spring rather than from propellants. A simple 180° twist of the inhaler's base compresses the spring, which draws a pre - defined, metered volume of solution through the capillary tube and into a micro - pump. The key component of the Respimat® SMI is the uniblock, which is based on the use of principles established for microchip technology. This allows fine fluid channels to be etched into the surface of silicon wafers, which are then covered by a glass plate and bonded chemically. This filter structure leads to two extremely fine outlet channels, through which the drug solution is forced by the mechanical power of the tensioned spring, producing two fine jets of liquid that converge at a carefully controlled angle. The impact of these two jets generates the slow - moving mist. Due to the innovative technology, the inhaler is easy to use and is suitable for all patients with asthma or COPD who require inhaled respiratory therapy.

1.3.4 Dry powder inhalers

Dry powder inhalers (DPIs) are the main alternative to MDIs and nebulisers, because of their environmental friendliness and compactness. The drug powders are presented in the powder form, thus it is expected that they exhibit high physico - chemical stability during storage. The vast majority of DPIs are passive breath activated devices. They rely on the patient’s inspiration to operate and there is also no risk of hand - mouth miscoordination. The patient simply inhales deeply to access the drug. It follows, that both the delivered and the fine particle dose of DPIs are dependent on the strength and duration of the patient’s inspiration. Different inhalers provide varying degrees of resistance to inhalation. The devices are portable and relatively inexpensive in comparison to nebulisers. Many different types of DPIs are commercially available, but

unfortunately none of them meets all the requirements that are important for the ideal device. DPI has not only to be simple in use, compact and inexpensive, but also to be able to produce and emit the dose reproducibly.
In some devices, the dose, filled into gelatine capsules, must be loaded before each application. Before the inhalation the capsule is pierced with metal needles. During inhalation the powder is released through the holes of the capsule walls. The powder can be also packed in a blister. Before the beginning of inhalation process the blister is pierced within the inhaler. The advantage of those devices is, that the powder stays dry until the beginning of the inhalation, hence cannot be influenced by relative humidity. Single unit devices must be reloaded every time before use. More recently multiple - dose inhalers were developed (Steckel et al., 1997). In those devices powders are presented in a reservoir. Before the inhalation the required dose is provided by a built - in metering dose unit.
In most devices, the drug particles are micronised, thus flowability and fluidisation are usually poor and tendency to agglomeration is high. The mentioned factors lead to poor uniformity of mass and low respirable fraction of the drug reaching the deep parts of the lung. Therefore, the drug particles are usually adhered to inert carrier particles with the diameter of 50 µm to 200 µm. A number of different carriers have been used, the most frequently α - lactose - monohydrate (Podzeck, 1998 (b); Zeng et al., 2001; Steckel et al., 2006). Upon inhalation, the drug is detached from the carrier. Most of the excipient particles remain in the inhaler or deposit in the mouth or upper airways. The main point is that the drug particles are detached from the carriers during the inhalation in order to be able to follow the air stream and to be deposited in the lower airways.
Turbohaler (AstraZeneca GmbH, Wedel, Germany) is a multidose inhaler, which delivers the active ingredient without the help of additives. The micronised drug particles are agglomerated in a well defined agglomeration procedure. The size of the agglomerates is usually in the range between 300 µm and 500 µm. They are called “soft pellets”. The size of the agglomerates ensures good flowability and high reproducibility of dosing. Before the inhalation the powder is metered by being pushed into a group of conical holes, which are part of the disc of the dosing unit. The agglomerates are destroyed during the inhalation process and discrete particles reach the lower airways.
During the development of the Jethaler (e.g. Budesonid - Ratiopharm® Jethaler (Ratiopharm GmbH, Ulm, Germany)) a new working principle was used. With the help of the milling cutter, which is activated by a spring tension, a defined powder dose is cut from the surface of a so - called ring tablet containing active ingredient and excipients. This process takes place during the inhalation, so the liberated particles can be immediately inhaled. An isostatic pressed ring tablet possesses a uniform porosity distribution, therefore exactly the same amount of the powder is cut from the tablet whenever the device is used. The preparation of a tablet containing active ingredient and excipients into the form of a tablet prevents the demixing of the powder fractions during storage (Gruetzmann et al., 2004).
As in the case of MDIs, only a small fraction of the dose is able to reach the deep part of the lung. Development of a dry powder inhaler is not only concentrated on the device development, but also on the process development and powder formulation development, as all of them significantly impact the drug deposition in the lung (Steckel, 2003 (b)). In relation to the powder

formulation the performance is highly affected by drug particle - drug particle and drug particle - carrier particle interactions that define drug dispersion and detachment and the eventual loss of the active ingredient. Interparticle interactions, which are too strong, lead to poor dispersion and detachment of the powder, causing impaction in the mouth area. Weak interparticle interactions cause the demixing of the powder formulation during handling and storage (Lohrmann, 2005).

So, in relation to formulation development, high reproducibility of dosing and high amount of the active ingredient deposited in the deep parts of the lung are the most important factors that have to be kept in mind.

2. Interparticle interactions in dry powder inhaler formulations

2.1 Preliminary remarks

Interactions between particles can be arranged into two classes, cohesive and adhesive interactions. Cohesion is found between particles of the same chemical and physico - chemical identity. Adhesion, in contrast, emerges between particles of different species. When the particle size of at least one of the interacting partners is under 10 μm and the particle mass is low, both, cohesion and adhesion forces between the interacting partners are stronger than the gravity force. The gravity force F_g for a spherical particle is calculated as follows:

$$F_g = \left(\frac{4}{3} \cdot \pi \cdot r_p^{\,3}\right) \rho_p \cdot g \qquad \textbf{Equation 6}$$

where r_p is the radius of the particle, ρ_p its density, g gravitational acceleration.

According to Israelachvili (Israelachvili, 2000), the interparticle interactions, which play an important role in powder mixtures, can be classified into three categories:

- Purely electrostatic, in origin arising from the Coulomb force between charges. The interactions between permanent dipoles or charges fall into this group;
- Polarisation forces arising from the dipole moments induced in atoms and molecules by the electric fields of nearby charges and permanent dipoles. All interactions in a solvent medium involve polarisation effects;
- The forces of quantum mechanical nature, such as covalent or chemical bonding and repulsive steric or exchange interactions that balance the attractive forces at very short distances.

These three groups are not considered as rigid or exhaustive. According to another classification (Linsenbuehler, 2005) the interacting forces are divided into primary and secondary ones.

The primary forces are:

- Covalent bonding forces;
- Van der Waals forces;
- Electrostatic interactions.

The secondary forces are classified as follows:

- Hydrogen bonds between moisture adsorption layers and capillary bridges;
- Solid bridges;
- Forces caused by mechanical interlocking, sintering.

Interactions between the particles in dry powder inhalers may result from a number of simultaneously acting forces, such as Van der Waals and electrostatic forces, forces caused by solid bridging or mechanical interlocking. It is very important to understand, as far as possible, the nature and the role of these forces.

2.2 Born repulsion

Very small distances between atoms, molecules or particles lead to overlapping of the electron clouds of the involved atoms and increasing of a strong repulsive force, determining how close two atoms may come together. These repulsive forces are called steric or Born repulsion. They

are very short - ranged and arise quite sharply as two molecules or particles approach each other. Due to the Born repulsion the electron clouds of the two bodies are prevented from interpenetration (Visser, 1989). According to Krupp (Krupp, 1967), the minimal contact distance for colloidal particles in vacuum is 0.4 nm. At contact of two particles, equilibrium between repulsive and attractive forces has to be established.

2.3 Van der Waals forces

2.3.1 Preliminary remarks

Particle interactions occur as a consequence of so - called long range attractive forces. Van der Waals forces play the most important role among the attractive forces. They are omnipresent and dominate in dry bulk solids. Van der Waals forces may consist of three different components: Debye forces (interactions between permanent and induced dipoles), Keesom forces (interactions between two permanent dipoles) and London forces (interactions between two induced dipoles) (Israelachvili, 2000).

In whole, Van der Waals interactions describe the interplay between two neutral materials. The calculation of these forces may be done with the help of two different models: the microscopic and the macroscopic. Hamaker (Hamaker, 1937) established the microscopic model, where he described the additivy of single intermolecular interactions between all atoms of the body under examination. Lifschitz (Lifschitz, 1956) described the macroscopic theory, where interactive forces are calculated according to optical features of the involved materials. Both theories provide material constants for the interactions. The constants can be converted into each other, what eases the calculations.

2.3.2 Microscopic model after Hamaker

According to the theory after Hamaker, the Van der Waals forces consist of three components:

- Debye or induction interactions: the interactions between permanent dipole and polarised molecule;
- Keesom or orientation interactions: the interactions between permanent dipoles;
- London or dispersion interactions: the interactions between polarised atoms and molecules. They base on the fact of time and space fluctuation of the electron density around the cores of the atoms. Therefore the positive and negative charge distribution may swing and fluctuation dipoles are resulting.

These interactions possess the following characteristics:

- Long ranging, from 0.2 nm to 10 nm (Krupp, 1967);
- Being both, attractive and repulsive;
- Exhibiting in addition to the attractive and repulsive forces also the very weak orientation component.

The total Van der Waals forces can be calculated by summarising of Debye, Keesom and London forces.

With the help of the Hamaker - Van - der - Waals constant A_H, the microscopic calculations of the Van der Waals interactions may be converted into macroscopic calculations. For the Van der

Waals interactions between two different materials 1 and 2 A_H may be calculated (Israelachvili, 2000; Linsenbuehler, 2005):

$$A_H = \pi^2 \cdot \rho_{n(1)} \cdot \rho_{n(2)} \cdot c_{VdW} \qquad \textbf{Equation 7}$$

where ρ_n is the number density of the molecules, c_{VdW} the Van - der - Waals coefficient.
According to the above mentioned considerations, the Hamaker approach has a few disadvantages:
- Influence of neighbour atoms and molecules is neglected by the calculation;
- It is assumed that the molecules are freely moving, but in real solids and liquids the molecules are more or less condensed, which may cause deviations from theory;
- The movements of the charge carriers in the solids are not respected.

2.3.3 Macroscopic model after Lifschitz

In contrast to the Hamaker model, Lifschitz proposed the macroscopic model for the calculation of the Van der Waals forces, which is based on the optical properties of the involved materials. Here, the idea of the additive behaviour of the interactions between single atoms or molecules is not taken into consideration. This model incorporates the influence of neighbour atoms on the interacting molecules. The whole model is very complicated and only approximations for special cases are available.
The Lifschitz - Van - der - Waals constant $\hbar\varpi$ can be converted into the Hamaker - Van - der - Waals constant A_H with the help of the following equation:

$$\hbar\varpi = \frac{4}{3} \cdot \pi \cdot A_H \qquad \textbf{Equation 8}$$

2.3.4 Concluding remarks

As explained in the chapter above, it is difficult to describe real systems using the macroscopic model after Lifschitz (Israelachvili, 2000), therefore, the microscopic model after Hamaker is usually preferred. According to the latter, Van der Waals forces consist of a geometric and a constant part, the Hamaker constant. The Hamaker constant depends on the material, values for solids lay in the range between 10^{-19} J and 10^{-18} J (Schubert, 1987).
Van der Waals forces F_{VdW} between two ideally smooth spheres of radii $r_{p(1)}$ and $r_{p(2)}$, separated by a distance a in vacuum can be expressed as follows:

$$F_{VdW} = \frac{A_H}{6 \cdot a^2} \cdot \frac{r_{p(1)} \cdot r_{p(2)}}{\left(r_{p(1)} + r_{p(2)}\right)} \qquad \textbf{Equation 9}$$

where, A_H is the Hamaker - Van - der - Waals constant, a the contact distance between two particles, $r_{p(1)}$ and $r_{p(2)}$ the radii of the particle 1 and particle 2.

2.4 Electrostatic forces

Electrostatic forces may also contribute to particle interactions. There are different possibilities for the particles to acquire an electrical charge, for example during grinding of a powder, dispersion from the bulk state, friction or contact with surfaces or walls as well as liquid spraying. According to Cohen´s Rule, during this contact, the material with higher permittivity will be charged positively (Gerthsen, 1997).

When two charged materials contact, they will experience attraction or repulsion, depending on whether the particles are charged equally or oppositely. The attraction forces F_A between two interacting particles are calculated according to the following equation:

$$F_A = r_p \cdot \pi \cdot \varepsilon \frac{(\Delta U)^2}{a} \qquad \textbf{Equation 10}$$

where ΔU is the potential difference as a consequence of the difference in work functions and r_p is the radius of the interacting particles, ε is the permittivity and a is the distance between the two particles.

The magnitude of the electrostatic forces F_{el} between two point charges may be calculated according to Coulomb's Law:

$$F_{el} = \frac{q_{(1)} \cdot q_{(2)}}{4 \cdot \pi \cdot \varepsilon \cdot a^2} \qquad \textbf{Equation 11}$$

where $q_{(1)}$ and $q_{(2)}$ are the electrical charges on the surface of two particles, ε is the permittivity and a is the distance between the two charges $q_{(1)}$ and $q_{(2)}$.

Electrostatic charges may arise from the contact of an uncharged particle with either a negatively or positively charged particle, due to the transfer of electrons and ions between the particles. It has been investigated, that electrically neutral particles are quite rare (Vercoulen, 1995). If a particle with the charge q approaches an uncharged particle with radius r, the inducing of the image charge of the first particle on the second particle takes place. In this case the electrostatic force F_{el} can be calculated as follows:

$$F_{el} = \frac{q^2\left(1 - \frac{a}{\sqrt{r^2 + a^2}}\right)}{16 \cdot \pi \cdot \varepsilon \cdot a^2} \qquad \textbf{Equation 12}$$

where a is the distance between the charged and the uncharged particles.

Charge might also result from the contact between two uncharged particles if they have different work functions. The work function Φ^M is the minimum energy, which an electron needs to leave

the particle. It is equal to the sum of the potential energy and the kinetic Fermi energy taken with the reverse sign:

$$\Phi^M = -\left(V_e + \varepsilon_e^F\right) \qquad \textbf{Equation 13}$$

where V_e is the potential energy for electrons in metals and ε_e^F is the kinetic energy of electrons at the Fermi level. If two solids with different work functions are separated by a small distance *a*, electrons from the material with the lower work function are transferred to the material with the higher one.

It has to be pointed out, that the electrostatic forces are mainly dependent on the chemical structures and physical states of the powders. There are some donor - acceptor series found in the literature (Zeng et al., 2001), where the relation between the donor and acceptor is reflected:

Donor $-NH_4$ > -OH > -OR > -COOR > $-CH_3$ > $-C_6H_5$ > halogen > =CO > -CN Acceptor.

Here each next member is an acceptor with respect to the previous member, which acts as a donor.

2.5 Hydrogen bonds between moisture adsorption layers

The physico - chemical properties of powders are often altered by the adsorption and/or absorption of water vapour. The sorption of water vapour by a powdered material may increase the interparticle forces between the interacting particles through hydrogen bonds between the moisture adsorption layers. Water readily forms hydrogen bonds with other polar materials and therefore can be adsorbed by a variety of materials at different temperatures and humidities. In general, the higher the relative humidity, the more a polar solid will sorb water vapour at a higher uptake rate. The thickness of the adsorption layers depends on the properties of the materials also. Additionally, the adsorption layers decrease the distance between the interacting partners leading to an increase of the interacting forces between the particles. It is of high importance for powders intended for the use in dry powder inhalers to be stored under low relative humidities. Otherwise, due to the building of hydrogen bonds, the dispersibility and fluidization of the powder may be deteriorated, leading to the deterioration of the flow behaviour, uniformity of mass and respirable fraction.

2.6 Capillary bridges

The moisture capture by particles may influence the interparticle forces by altering the surface conductivity and electrostatic charging of the particles, it may influence the surface energy of the particles and increase the interaction by hydrogen bonds of the water adsorption layers and finally by capillary forces. The interparticle interactions due to liquid bridges might be several times stronger than the gravity forces. Capillary forces are determined by the surface tension of the liquid (usually water), the size of the interacting partners and the contact angle of the liquid on the surface. The interaction forces due to liquid bridges between two spherical particles of the same size can be calculated as follows:

$$F_{CB} = 2 \cdot \pi \cdot \gamma \cdot r_p \cdot \cos \vartheta$$ **Equation 14**

where r_p is the radius of the particle, that is wetted by a liquid with the surface tension γ and contact angle ϑ.

The environmental humidity is the most secure indicator for the extent of water vapour uptake. As the humidity is increased, the thickness of the adsorbed layers also increases leading to the eventual condensation at the contact points of the particles, liquid bridges may be formed. Below a critical relative humidity the water vapour is adsorbed onto the surface of the particles and capillary forces are expected to be negligible (Buckton, 1995 (b)). Above the critical relative humidity a liquid bridge may be formed at the contact points of the particles. So, if the relative humidity is above the critical value and the water vapour condensation is allowed to reach equilibrium, a further increase of the relative humidity will enhance the capillary forces and therefore the overall interparticle forces (Zeng et al., 2001).

2.7 Solid bridges

Solid bridges may immensely increase interparticle interactions. They may be built due to chemical reactions or sintering effects. Because of the frictional movements and plastic deformation between points of interparticle contact in bulk solids, the melting temperature might be achieved (Israelachvili, 2000). With increasing temperature the mobility of the atoms enhances. Increasing temperature may also lead to formation of solid bridges, because the diffusion of atoms gets stronger (Rumpf, 1977). If the powder is loosely poured in a powder container, the particles contact each other only at relatively few points. The load at these points is directly proportional to the applied force. As the forces are concentrated over a small surface area, the pressure which acts on these parts of the particles might be extremely high. The local pressure may exceed the yield value of the material and the powder begins to flow. As a result, the area of contact between the particles gets larger and the interparticle interactions, due to Van der Waals forces and mechanical interlocking increase.

2.8 Mechanical interactions

The surface of powders for the use in dry powder inhalers is seldom smooth. If the surface of the particles is irregular, the asperities may interlock with each other thereby increasing interparticle interactions. The effects of surface smoothness on interacting forces follow many complicated mechanisms and depend on the relative scale of the surface roughness to the diameter of the interacting particles. If the surface roughness does not bring about substantial interaction due to mechanical interlocking, then increasing the surface roughness may reduce the interactive forces by means of reducing the contact area between the interacting particles (Zeng et al., 2001). However, a high degree of surface asperities and therefore roughness is often associated with increased frictional forces between the particles and usually results in poor flow properties of the powder.

2.9 Factors affecting interparticle interactions

2.9.1 Particle size

The larger the particles are, the stronger the interparticle interactions caused by Van der Waals forces. Zeng (Zeng et al., 2001) calculated the Van der Waals forces and the gravitational force as a subject of the particle size and demonstrated that with increasing of the particle size Van der Waals forces also increase. The Van der Waals forces are directly proportional to the particle size, the gravitational force, in contrast, is proportional to the cube of the particle size. The gravitational force decreases more rapidly with size reducing than the Van der Waals forces. Therefore the Van der Waals forces between small particles dominate the gravitational force. Interparticle interactions due to Van der Waals forces become important when at least one of the interacting particles exhibits a diameter under 10 μm and the separation distance between the particles is of the order of a few nanometers. Generally, the smaller the particle sizes and separation distances are, the more dominating the attractive forces are, particles are highly cohesive or adhesive and exhibit poor flowability.

2.9.2 Particle shape

Particle shape is one of the most incontrollable factors in powder technology. Different production methods produce particles with different shapes, though even particles which have undergone similar treatments may possess different shapes. Therefore, most methods for the calculation of interparticle interactions are based upon an idealised situation. Real particles are never ideal and it is extremely difficult to calculate the interactions between them (Zeng et al., 2001). The intimate contact between elongated particles may increase the contact area leading to increased attractive forces. However, the packing patterns of highly elongated or flattened particles are dependent upon the previous processing history. During the powder handling such particles may arrange themselves to the most stable conformation exhibiting a low porosity of the bulk and a dense packing of the powder on the one hand. On the other hand, there is also the possibility that elongated irregular shaped particles build up open packing of high porosity, where the separation distance between the particles is higher than between spherical particles. Thus, the irregularity of particle shape might be reported to increase the interparticle interactions, although the reverse trend is also found.

2.9.3 Texture of the surface

Interacting forces decrease with increasing distance between the interacting partners. So, any means of increasing of this distance would reduce the interparticle interactions. For example, surface asperities of the appropriate size reduce the Van der Waals force almost to zero. Real solids may have a variety of surface morphologies. Asperities of the surface may lead to changes of the contact area with respect to a smooth surface, which may cause increasing or decreasing of the interacting forces. The adhesion to a surface can be classified into three groups:

- Perfectly smooth particles adhere to each other or to a perfectly smooth plate. In this case, the common methods may be used for the prediction and calculation of the interactive forces between the partners;

- The surface asperities of the particles are much smaller than the size of the interacting partners or the surface asperities of the plate are much smaller than the size of the adhered particles. In this case the true contact area between the interacting partners is smaller in comparison to the contact area between smooth surfaces and the separation distance is large, leading to a decrease of the interactive forces in comparison to smooth surfaces;
- Surface asperities are of a larger scale than described above. The contact area and therefore the interparticle interactions are enlarged.

The particles attached to the smooth regions can be removed easier (case 1) than the entrapped ones (case 3), whereas the ones attached to surfaces with small asperities (case 2) may be removed easier than the ones attached to the smooth surface.

2.9.4 Relative humidity

Relative humidity may influence the interactive forces by two opposing mechanisms. On the one hand relative humidity may increase the interactions due to hydrogen bonds and capillary forces, in case if considerable amounts of water are condensed on the surface of the particles. On the other hand it increases the conductivity of both, the interactive particles and the surrounding atmosphere. Very low relative humidities during handling may hinder charge decay and may cause accumulation of the electrostatic charges on the surface of the powder, finally leading to an increase of interparticle interactions. The emergence of capillary bridges depends on not only relative humidity but also on the material (Zeng et al., 2001).

2.9.5 Electrical properties of the powder

Electrical charge arises from collision and friction amongst the particles during powder handling and processing. Due to the intensive movement of the material, charge transfer may be caused. This charge transfer is also called triboelectrical charging. With each normal collision, an interfacial charge transfer of electrons occurs. The charge sign of each individual group of particles largely depends upon their relative electron - donor or - acceptor properties and work functions. Water vapour condensation on the surface of the particles may improve the distribution of the charge. Crystallinity also has an effect on the charge distribution. Molecules of an amorphous material exhibit higher mobility than the ones fixed in a crystal lattice. Therefore, electrical charges may distribute relatively homogeneously on the surface of amorphous spherical particles (Zeng et al., 2001). In case of crystalline particles with edges or tips, most charges may concentrate on tips. Electrostatic forces become more significant when the particle size is reduced and the environmental humidity is low.

2.9.6 Concluding remarks

In conclusion, the most predominant interparticle forces are Van der Waals forces. Electrostatic forces become dominating at low relative humidities, in contrast, capillary forces become manifest at high relative humidities. All these forces dominate over the gravitational forces if the size of the particles is under 10 µm (Zeng et al., 2001; Podczeck, 1998 (a)).

3. Increasing drug deposition in the respiratory tract

3.1 Overview over strategies decreasing interparticle interaction

Handling and processing of fine particles is a generic industrial problem. These powders have poor flowability due to the cohesion force arising mainly from Van der Waals attraction (Yang et al., 2005). In order to get a flowable powder for use in powder inhalers, drug particles are often mixed with coarse carrier particles. The aerodynamic diameter of the drug particles in these interactive mixtures is usually between 1 µm and 5 µm. The diameter of the carriers is in the range between 50 µm and 200 µm (Lohrmann, 2005). Most commonly, the carrier consists of α - lactose - monohydrate. Mannitol and sorbitol are also considered for the use in DPI formulations (Steckel, 2003 (b)). High interactions between the drug and the coarse carrier particles or between agglomerated drug particles may result in the loss of the drug by deposition in the upper airways. In order to resign from the coarse carriers, the micronised drug particles may be agglomerated in so - called "soft pellets". The size of the pellets varies from 300 µm to 500 µm. The agglomerates are destroyed during the inhalation due to the dispersion mechanisms in DPIs and the single drug particles are able to reach the lower parts of the lungs.

Another possibility to decrease interparticle interactions in interactive mixtures, which are intended for the use in DPIs, is the use of an additional third fraction, such as carrier fines or other additives, like magnesium stearate. The desired effect of adding the carrier fines or additives is the enhancement of surface roughness and occupation of high energy sites on the carrier surface and consequently the reducing of the interactive forces between the coarse carrier and the active ingredient (Zeng et al., 1998; Zeng et al.; 1999; Tee et al., 2000; Guchardia et al., 2008; Najafabadi et al., 2006).

Kawashima (Kawashima et al., 1998) made the approach to modify the surface of hydrophobic cohesive pranlukast drug particles with hydrophilic colloidal silica in order to decrease adhesive forces. Colloidal silicon dioxide (Aerosil®) was chosen because of its highly hydrophilic and adsorbing properties. The idea was that the modification of the drug surface by hydrophilic Aerosil® reduces the adhesive forces, because hydrophilised surfaces sorb water thereby reducing hydrogen bonding.

An alternative way of improving the flow behaviour and ensuring high drug deposition in the lung by means of reducing the interparticle attractive forces is the coating of the drug particles with particles in the nanometer range, which will be discussed in the following chapter.

3.2 Coating of the drug particles with nanoparticles

3.2.1 Preliminary remarks

As was already mentioned, in order to reduce interparticle forces and powder agglomeration the micronised drug particles may be coated with particles in the nanometer range. The nanoparticles act as spacers and intensify the surface roughness thereby reducing the area of contact and declining the cohesion between the drug microparticles. In order to reduce Van der Waals forces effectively, the diameter of the nanoparticles has to be of a larger scale than the surface asperities of the drug particle (Figure 3 a, b). Otherwise the nanoparticles are entrapped within the asperities of the surface and decline the surface roughness again. At the same time, the contact

area between the contacting partners may be increased and the adhesion forces as well (Figure 3 c).

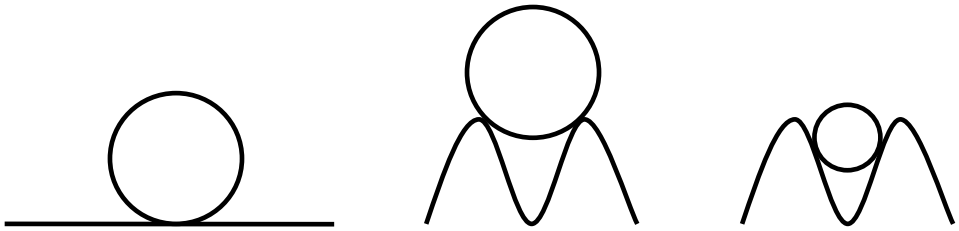

a b c

Figure 3: Interactions between the particle and the plate: spherical particle adhered to smooth planar surface (a), spherical particle adhere to a surface with relatively small asperities (b) and entrapment of a fine particle within the asperities of surface with relatively large asperities (c) (taken from Zeng et al., 2001)

With the help of the Hamaker and Lifschitz approaches, Schubert (Schubert, 1977) was able to calculate the Van der Waals forces between macroscopically bodies, as plate - plate, sphere - plate and sphere - sphere (Table 1). These theoretical approaches, which are described below, are usually used when Van der Waals forces between the interacting partners have to be calculated.

Table 1: Van der Waals forces between plate - plate, sphere - plate and sphere - sphere

Model	Hamaker		Lifschitz	
	$\frac{A_H}{6 \cdot \pi \cdot a^3}$	**Equation 15**	$\frac{\hbar \cdot \varpi}{8 \cdot \pi^2 \cdot a^3}$	**Equation 16**
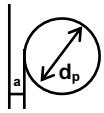	$\frac{A_H \cdot d_p}{12 \cdot a^2}$	**Equation 17**	$\frac{\hbar \cdot \varpi \cdot d_p}{16 \cdot \pi \cdot a^2}$	**Equation 18**
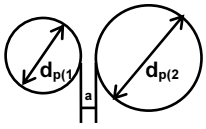	$\frac{A_H \cdot d_p}{24 \cdot a^2}$	**Equation 19**	$\frac{\hbar \cdot \varpi \cdot d_p}{32 \cdot \pi \cdot a^2}$	**Equation 20**

***ħ* is the Planck's constant, ϖ is the mean frequency from the absorption spectrum, d_p, $d_{p(1)}$, $d_{p(2)}$ diameter of the spheres; for the sphere/sphere: $d_p = 2 \cdot d_{p(1)} \cdot d_{p(2)} / (d_{p(1)} + d_{p(2)})$, *a* is a distance between the surfaces of the two interacting partners, A_H is the Hamaker - Van - der - Waals constant**

The above mentioned cases are very important for the theoretical evaluation of the interactions between particles. They are also useful, if interactions between particles in real bulk solids must be calculated. The important question is, whether it is possible to reduce the cohesion forces between two particles. Introduction of small particles (spacers) between two coarse particles leads to increasing of the distance and decreasing of the interactions between the latter. Some authors prepared and characterised powder mixtures, which consisted of coarse particles, for

example starch corn particles (Meyer, 2003; Duenisch, 2005) and particles in the submicron range. In those mixtures the nanoparticles are adhered on the surface of the larger particles and play the role of a flowability enhancer. In this case the amount of the nanoparticles is very important, because they may not only increase the distance between the coarse particles but also increase the amount of the contact points.

3.2.2 Ideal sphere - plate model

Figure 4 shows the influence of the distance on the interparticle forces between a sphere with the diameter of 10 µm and a plate. It is assumed for the calculations that the particles are rigid and do not deform upon the contact. The contact distance must be greater than 0.4 nm (see 2.2), otherwise the calculated forces are much stronger than the real ones. Krupp (Krupp, 1967) introduced the minimum distance $a_0 = 0.4$ nm between two bodies. The strongest attractive forces can be observed if the two interacting partners contact each other at $a_0 = 0.4$ nm. With increasing distance from $a_0 = 0.4$ nm the decreasing of the Van der Waals forces begins. If the distance is around 10^{-5} cm the electrostatic forces begin to dominate (Figure 4). It is important to differentiate between electrical isolators and conductors, because in case of insulators charge decay is not as fast as in case of conductors (Lohrmann, 2005). Liquid bridges are built at very small distances. The attractive forces are very high. By detaching of one of the interacting partner from the other the bridge breaks off at some distance and does not influence the interacting forces any more.

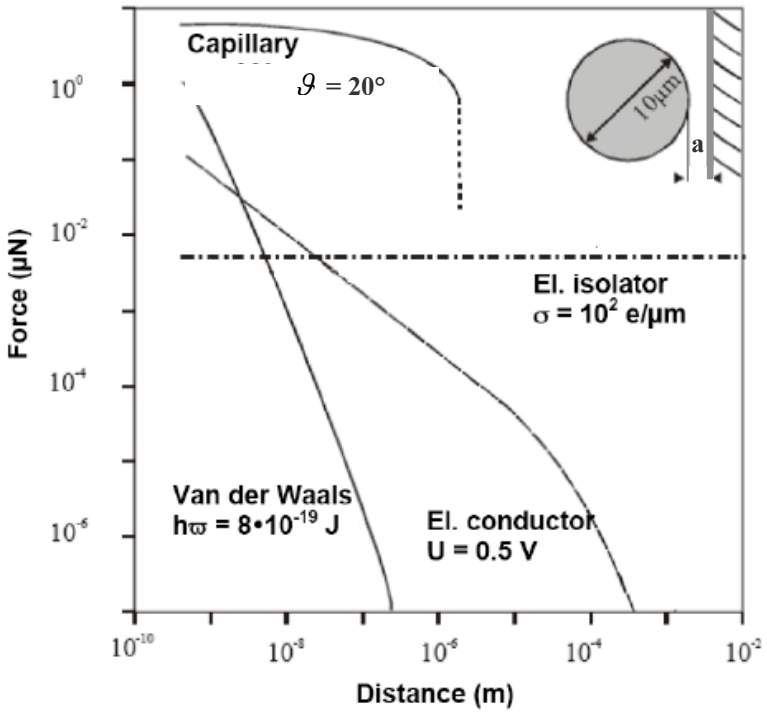

Figure 4: Interactive forces according to the model sphere - plate as a function of the contact distance a = 0.4 nm, $\hbar\varpi$ is the Lifschitz - van - der - Waals constant, U is the contact potential, ϑ is the contact angle, σ is the surface charge density (taken from Schubert, 1977; modified)

3.2.3 Sphere - one roughness - plate model

The surface of real particles is rough. Each roughness increases the distance between the interacting partners. The strength of the Van der Waals forces is dependent on the dimensions of the roughness and the dimensions of the sphere. The diameter, shape and nature of the roughness play an important role for the decreasing of the attractive forces (Schubert, 1977).
On the basis of the sphere - plate model Rumpf was able to show the influence of the roughness with diameter *d* on the Van der Waals forces (Figure 5). The surface roughness in the shape of a hemisphere is attached to the surface of the large sphere.

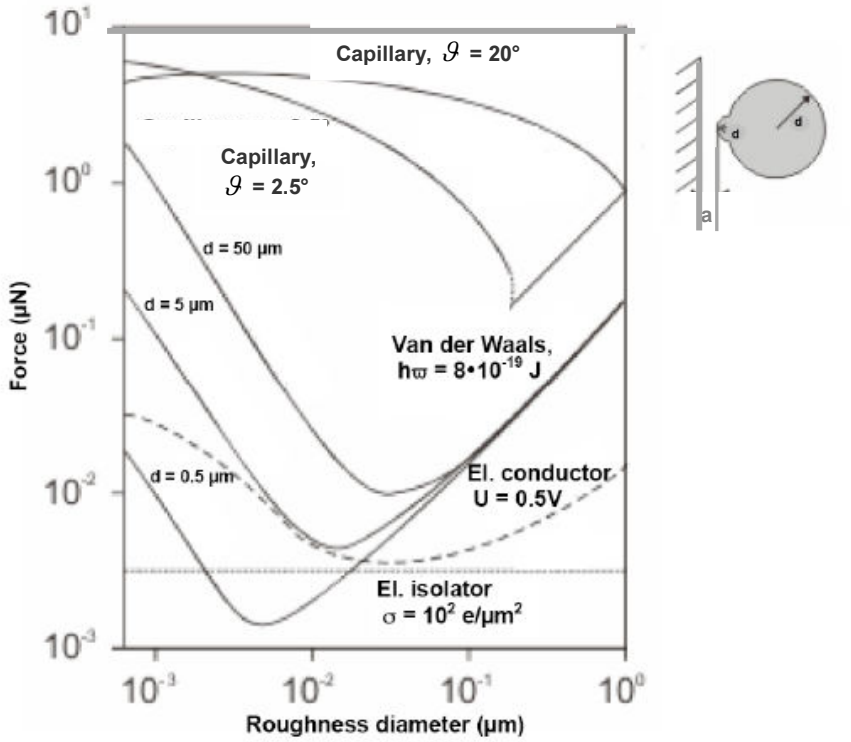

Figure 5: Influence of the diameter of the roughness on the Van der Waals forces, *a* = 0.4 nm is a contact distance, $\hbar\varpi$ is the Lifschitz - van - der - Waals constant, *U* is the contact potential, *d* the diameter of the roughness/sphere, ϑ is the contact angle, σ is the surface charge density (taken from Rumpf, 1977; modified)

According to Rumpf's model the Van der Waals forces between all interacting partners are the sum of the interactions between the roughness and the plate, as well as between the sphere and the plate. Interactions between the roughness and the plate are described by:

$$F_{VdW} = \frac{A_H}{6} \cdot \frac{r}{a^2}$$ **Equation 21**

where F_{VdW} is the Van der Waals force, A_H the Hamaker - Van - der - Waals constant, r the radius of the hemisphere and a the contact distance. Interactions between sphere and plate are calculated according to:

$$F_{VdW} = \frac{A_H}{6} \cdot \frac{R}{(a+r)^2}$$ **Equation 22**

where R is the radius of the large particle.
The sum of both forces results in:

$$F_{VdW} = \frac{A_H}{6} \cdot \left(\frac{r}{a^2} + \frac{R}{(a+r)^2} \right)$$ **Equation 23**

There are three typical cases, which help to describe the run of the interaction curves in Figure 5. The radius of the hemisphere, at which minimum attraction between the partners occurs, is defined as r_{min}. In the first case, the hemisphere radius is smaller than r_{min}, the interactions between the sphere and the plate are still high. The increase of interactions caused by the interactions between the hemisphere and the plate is smaller than the decrease of interactions between the plate and the sphere, which are reduced due to the enlargement of the distance between them. This leads to a decrease of the attractive forces between the sphere and the plate.
In the second case, the Van der Waals forces are minimal. This can be reached when the increase of interactions between the plate and the roughness are of the same order, due to the introduction of the hemisphere, as the decrease of interactions between the sphere and plate.
In the third case, the radius of the hemisphere is larger than r_{min} and the increase of interactions between the roughness and the plate is higher than the decrease of interactions between the sphere and the plate. Here, an increase of the attractive forces takes place (Meyer, 2003).

3.2.4 Sphere - sphere model

Hamaker (Hamaker, 1937) calculated the Van der Waals forces between two large spherical particles:

$$F_{VdW} = \frac{A_H}{6 \cdot a^2} \cdot \frac{R_{(1)} \cdot R_{(2)}}{R_{(1)} + R_{(2)}}$$ **Equation 24**

where $R_{(1)}$ and $R_{(2)}$ are the radii of the two large spherical particles, $A_H = 8 \times 10^{-19}$J is the Hamaker - Van - der - Waals constant, which combines all material constants. a is the distance between the surfaces of the two large spherical particles (Hamaker, 1937). In order to avoid a diverging force upon contact, the distance a cannot become smaller than the so - called contact distance $a = 0.4$ nm (Krupp, 1967).

3.2.5 Sphere - one roughness - sphere model

Rumpf (Rumpf, 1977) was able to show that the introduction of one roughness in the sphere - plate model can help to reduce the Van der Waals forces (Figure 6 a - f). Figure 6 b presents such a model, where the small particle is centrally placed between two spheres and plays the role of a surface roughness. The resulting Van der Waals forces can be calculated according to Derjaguin (Derjaguin et al., 1958, Derjaguin et al., 1975) with the help of the following equation:

$$F_{VDW} = \frac{A_H}{6}\left[\frac{1}{a_{(1)}^2}\cdot\frac{r\cdot R_{(1)}}{\left(r+R_{(1)}\right)}+\frac{1}{a_{(2)}^2}\cdot\frac{r\cdot R_{(2)}}{\left(r+R_{(2)}\right)}+\frac{1}{\left(a_{(1)}+2\cdot r+a_{(2)}\right)^2}\frac{R_{(1)}\cdot R_{(2)}}{R_{(1)}+R_{(2)}}\right] \quad \textbf{Equation 25}$$

where $R_{(1)}$ and $R_{(2)}$ are the radii of the large spherical particles, r is the radius of the roughness, a = 0.4 nm is the contact distance, A_H is the Hamaker - Van - der - Waals constant.

The probability, that the surface of a real particle possesses only one roughness or spacer which is situated exactly between the two large particles is quite low (Figure 6 b, c). Also, in case if two small sized particles are situated between two coarse particles the interaction forces will not be decreased always, but may be rather increased (Figure 6 e). If the amount of the small particles is increased in such a way that the distance between two fine particles is small enough that the two large particles do not contact (Figure 6 d), the attractive forces will be loosing their strength with increasing contact distance. Transporting this to the three dimensional space minimum three fine particles have to be placed between two large particles in order to ensure non - contact of the two large particles (Figure 6 f). In case of the stable three - point contact the large particles have no possibility to contact each other, because at least three small particles are placed between the large ones. In that way the interparticle forces may be reduced.

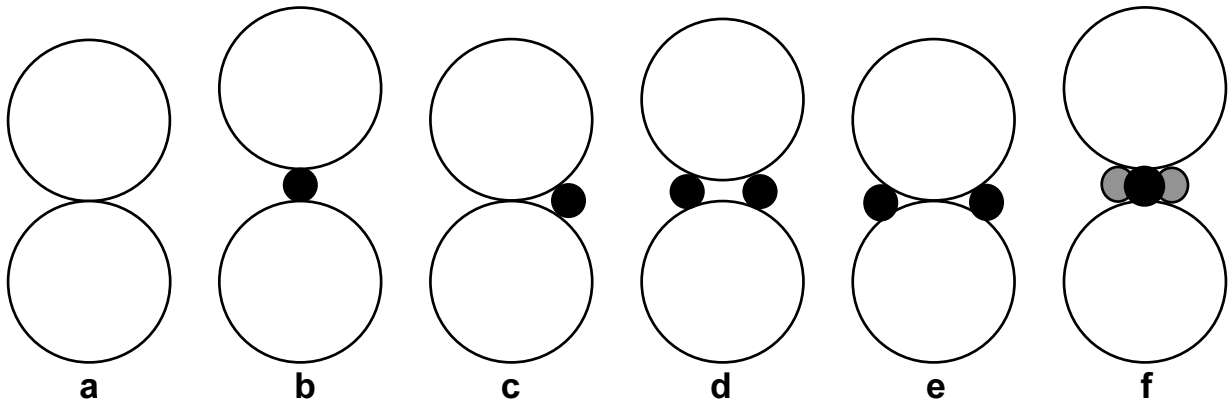

Figure 6: The possible placement of small spheres between large spheres: (a) contact between two large spherical particles, (b) one small particle placed centrally between two large spheres, (c) one small particle placed aside from the point of contact between two large spheres, (d) two small spheres placed between two large spheres providing non - contact conditions, (e) two small spheres placed between two large spheres providing contact conditions, (f) three - point contact configuration (taken from Pahl et al., 1988; modified)

It is important to know the minimum needed of the small particles, the so - called lower coating level, in order to establish the stable three - point contact (Figure 6 f). In this case the reduction of the interparticle interactions may be achieved.

3.2.6 Pahl and Wicke model

Pahl and Wicke (Pahl et al., 1988) used the surface roughness of the particles or the fine powder fraction present on the particles´ surface as a basis for their model. For their calculations, the model, which is presented in Figure 7, was used. It seems quite reasonable to include the number of roughnesses when calculating interparticle forces in real bulk solids. The primary aim of the mentioned model is the calculation of the attractive forces between the interacting partners. This idea may be used as a basis for the improvement of flowability, uniformity of mass and dispersibility in dry powder inhaler formulations. According to the model, where three hemispheres are placed between two large particles, for the calculation of the Van der Waals forces the following equation is used:

$$F_{VdW} = \frac{1}{12} \cdot A_H \left[\frac{R_{(1)} \cdot R_{(2)}}{\left(a_{(0)} + r_{(max)}\right)^2 \cdot \left(R_{(1)} + R_{(2)}\right)} + \sum_{i=1}^{N} \frac{2 \cdot r_{(i)} \cdot R_{(i)}}{a_{(0)}^2 \cdot \left(2r_{(i)} + R_{(i)}\right)} \right] \qquad \textbf{Equation 26}$$

where F_{VdW} are the Van der Waals forces, N the number of hemispheres on the surface of the large particles, $a_{(0)}$ the minimal contact distance between the large particles, $R_{(1)}$, $R_{(2)}$ the radii of the large particles, $r_{(max)}$ and $r_{(i)}$ the radii of the hemispheres on the surface of the large particles, where $r_{(max)}$ is the radius of the largest hemisphere, A_H the Hamaker - Van - der - Waals constant. With the help of the equation the interactions between the large particles with the distance $a_{(0)} + r_{(max)}$ can be calculated. If the large particles possess more hemispheres interparticle interactions are calculated with the help of this equation by adding a further summand.

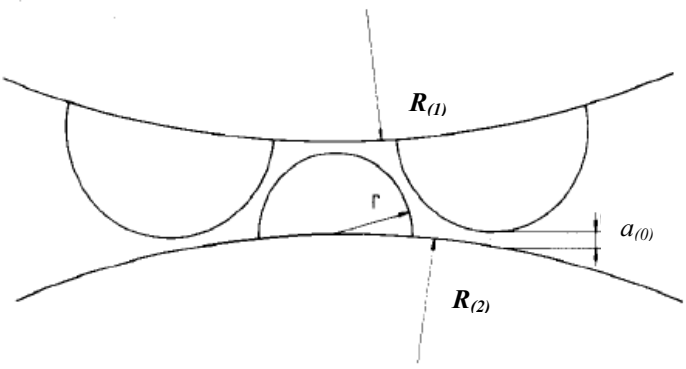

Figure 7: Graphical explanation of the equation according to Pahl and Wicke (taken from Pahl et al., 1988)

3.3 Coating ratio

3.3.1 Preliminary remarks

In order to reduce interparticle interactions, microparticles may be coated with nanoparticles by a mixing procedure. The coating ratio, the ratio of nanoparticles to microparticle plays an important role in flowability enhancement. The flowability is supposed to be enhanced when the coating ratio is in between the so - called lower and upper coating limit (Huber et al., 2003). The lower limit is achieved by mixing microparticles with the minimum amount of nanoparticles needed to prevent direct contact between two microparticles. The upper coating limit is obtained when the microparticulate host particle is covered with a monolayer of nanoparticulate guest particles.

Pahl and Wicke were able to show that with increasing amount of the asperities on the surface of coarse particles the interactions between the latter can be decreased (Pahl et al., 1988). Meyer (Meyer, 2003) used the Pahl and Wicke model in order to calculate the amount of fine powder, which is needed for the declining of the Van der Waals forces in real powder mixtures consisting of guest particles in the submicron range and corn starch particles (host particles). Huber (Huber, 2001) proposed a similar procedure, where spherical triangles, instead of planar triangles were used for the calculation of the amount of the guest particles, which are needed for the reducing of the interparticle interactions. Kurfess (Kurfess et al., 2005) developed a theoretical description of the effect of flow regulating particles on the interparticle forces by simulating the random coverage of the surfaces of the host particles with guest particles. Bresges (Bresges et al., 2008) proposed a detailed analytical method for the theoretical determination of the minimum amount of guest particles needed to ensure the non - contact between the host particles.

3.3.2 Lower coating limit

3.3.2.1 Meyer and Huber models

In these models the flow regulating particles are adsorbed on the surface of the large particles and play the role of the asperities according to the Pahl and Wicke model. The higher the amount of the adsorbed particles is, the higher their number in the zone of contact between the host particles. However, at least three guest particles are needed in the zone of contact in order to prevent contact of two hosts. The minimum number of guest particles, needed to ensure the non - contact of the host particles, was determined by covering the surface of the host particles with equilateral triangles, their vertices being occupied by guest particles (Figure 8). The distance between the guest particles or in other words the circumcircle of any of those triangles was such, that the distance between the host particles became just zero. The triangles were placed tangentially to the surface of the large particles and assumed to be planar in the model proposed by Meyer (Meyer, 2003).

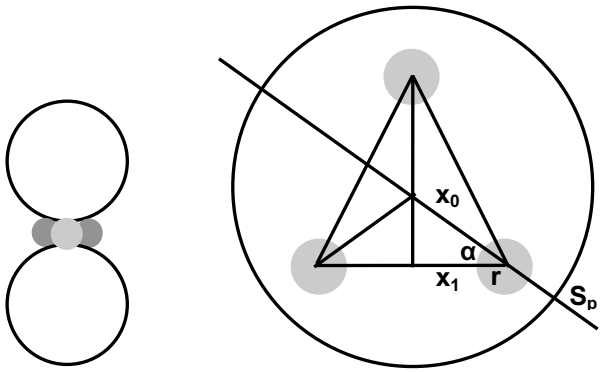

a **b**

Figure 8: Three point contact model, side view (a) and view on the top of the lower particle (b); *r* is the radius of the guest particles, $x = 2x_1$ is the distance between two guest particles, α is the half of the interior angle of the equilateral triangle, $r + x_0$ is the distance of the median line to the intersection of all median lines and S_p the sectional plane (taken from Meyer, 2003; modified)

In order to calculate the distance between two host particles with two guest particles between them (Figure 9) in the 2d - model the following equation can be used:

$$(r + x_1)^2 + (R + y_1)^2 = (R + r)^2 \qquad \textbf{Equation 27}$$

where R is the radius of the host particles, r is the radius of the guest particles. For the calculation of contact distance y between two host particles the following equation is used:

$$y = 2 \cdot y_1 \qquad \textbf{Equation 28}$$

y_1 has to be calculated according to:

$$y_1 = \sqrt{(R + r)^2 - (r + x_1)^2} - R \qquad \textbf{Equation 29}$$

x_1 is the half of the distance between two guest particles:

$$x = 2 \cdot x_1 \qquad \textbf{Equation 30}$$

It can be calculated according to:

$$x_1 = \sqrt{(R + r)^2 - (R + y_1)^2} - r \qquad \textbf{Equation 31}$$

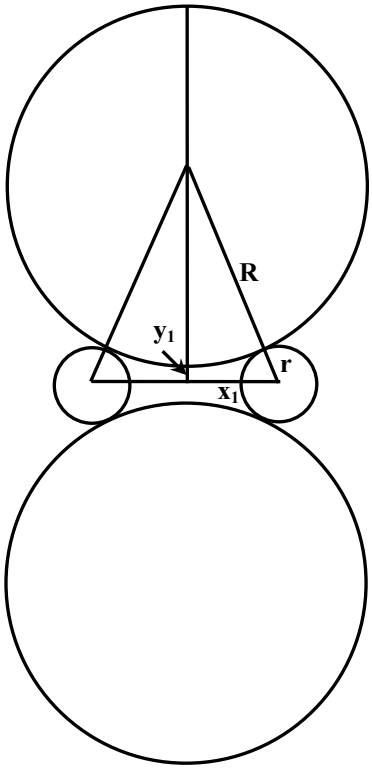

Figure 9: Cross section of the 2d - model; *r* is the radius of the guest particles, *R* is the radius of the host particles, x_1 is the half distance between two guest particles, y_1 is the half distance between two host particles (taken from Meyer, 2003; modified)

With the help of this 2d - model the contact distance between two host particles in dependence on the radii of the guest particles and the distance between them according to the three point contact model (Figure 8) can be calculated. However, in contrast to the 2d - model shown in Figure 9 the second guest particle of the 3d three point contact model is not situated in the sectional plane S_p. The second and also the third particle are placed in front or behind. The distance of the median line to the intersection of the three medians is defined as $r + x_0$. In this case the right angle triangle with the side lengths $(R + r)$, $(r + x_0)$ and $(R + y_1)$ is looked at.
The distance between two host particles $y = 2y_1$ can be calculated using the following equation:

$$y_1 = \sqrt{(R+r)^2 - (r+x_0)^2} - R \qquad \textbf{Equation 32}$$

Using α, the half of the interior angle of the equilateral triangle the side length $(r + x_0)$ can be expressed as:

$$\cos\alpha = \frac{x_1 + r}{x_0 + r} \qquad \textbf{Equation 33}$$

$$x_0 + r = \frac{x_1 + r}{\cos\alpha} \qquad \textbf{Equation 34}$$

With the interior angle $\alpha = 30°$, $cos\ \alpha$ and x_0 is calculated according to:

$$cos\,\alpha = \frac{1}{2}\cdot\sqrt{3} \qquad \textbf{Equation 35}$$

and

$$x_0 = \frac{(x_1 + r)\cdot 2}{\sqrt{3}} - r \qquad \textbf{Equation 36}$$

So, y_1 can be expressed as follows:

$$y_1 = \sqrt{(R+r)^2 - \frac{4}{3}\cdot(x_1 + r)^2} - R \qquad \textbf{Equation 37}$$

and x_1 as follows:

$$x_1 = \frac{1}{2}\cdot\sqrt{3}\cdot\sqrt{(R+r)^2 - (R+y_1)^2} - r \qquad \textbf{Equation 38}$$

Equation 37 and Equation 38 show the dependence of the distance $y = 2y_1$ between two host particles on the distance $x = 2x_1$ between two guest particles and the radius r of the guest particles.
With increasing distance $x = 2x_1$ between two guest particles the distance between two host particles $y = 2y_1$ is reduced till the latter contact each other. In case if $y_1 = 0$ Equation 37 can be expressed as follows:

$$x_{10} = -r + \frac{1}{2}\sqrt{3\cdot r^2 + 6\cdot r\cdot R} \qquad \textbf{Equation 39}$$

As already mentioned, the distance between two host particles is ensured by three guest particles. The surface area A_s of the equilateral triangle built by the guest particles, which occupy the vertices of this equilateral triangle is:

$$A_s = \frac{\sqrt{3}\cdot(x_1 + r)^2}{2} \qquad \textbf{Equation 40}$$

In order to obtain the number of triangles N_t needed to cover the surface of the host particles the total surface area of host particles A_h is divided by the surface area of the equilateral triangle:

$$N_t = \frac{A_h}{A_s}$$ **Equation 41**

If this number is known, the number of guest particles, which is needed to obtain such configuration, where the distance between the host particles just becomes zero, can be calculated.
However, the surface area covered by one triangle is presumed to be too small, because only the centre point of the triangle is tangent to the host sphere, the vertices of the triangle are lying outside the sphere. Nevertheless, this error decreases at higher numbers *N* of guest particles.
According to the Meyer model, the Van der Waals forces were calculated as follows:

$$F_{VdW} = \frac{A_H}{6}\left[2 \cdot \frac{2}{a^2} \cdot \frac{R \cdot r}{(R+r)} + \frac{1}{2y^2} \cdot \frac{R}{2}\right]$$ **Equation 42**

The result of the calculations, which were done by Meyer, defines two states sharply separated by a critical coating ratio *CRc.* If *CR* < *CRc* the host particles contact and attract each other, in the opposite case, the gap between them extends the range of the effective attraction of the adhesive forces.
In order to cover the host particles with guest particles homogeneously, Huber proposed a similar procedure, where spherical triangles instead of planar triangles were used (Huber, 2001). In this case the systematic underestimation of the surface area covered by one triangle is avoided, but still it is not possible to cover the surface of the spherical host particles with equilateral spherical triangles. The surface area of spheres is twice folded, boundless but of limited area, the distribution of guest particles on equidistant positions on the host particle is not possible but in a few cases, when the positions of guest particles are building the vertices of Platonic solids (Bresges et al., 2008). These configurations may be obtained only in the cases of 4, 6 or 12 guest particles and 8 or 20 guest particles.

3.3.2.2 Computer simulating models

3.3.2.2.1 Kurfess model

The aim of the paper, which was published by Kurfess (Kurfess et al., 2005), was to provide a theoretical description of the effect of flow regulating particles on the interparticle forces by simulating a random coverage of the surfaces of the host particles with guest particles and calculating the Van der Waals forces with the help of this model. Spherical host and guest particles were used as a first approximation of reality. The used algorithm consists of three parts:
- Covering of the host particles with guest particles in the nanometer range: the host particle is randomly covered by guest particles, so that a Poisson distribution with respect to the spherical surface area is obtained;
- Checking of contact of two host particles: two particles, one of them is covered with guest particles and another one, which is uncovered, are brought together. The uncovered particle rolls

on the surface of the host particle covered with guest particles until a three - point contact is established. If the three guest particles, which are potentially able to prevent the contact between the host particles are situated far away from each other, the uncovered particle rolls till it contacts the host particle. The characteristics of the contact can be easily calculated and used for the determination of the position of the centre of the uncovered particle relative to the centre of the covered host sphere, which is assumed to be located at the origin;

- Computation of the Van der Waals forces by summation over all resulting interactions. It has to be mentioned, that not only the interactions between the contacting uncoated host particles and the guest particles contacting the host, but also all other guest particles, even if they are not contacting the uncovered particle, are taken into account, although the contributions to the overall interactive force given by them is minor, because they are situated away from the second host particle. However, statistically some of them may come quite close and may give force contributions of significant order of magnitude. Therefore, the complete treatment of all interactions seems to be reasonable.

So, each run of this algorithm gives one set of adhesive forces. Although the computer simulation helps to correlate the averaged Van der Waals forces F_{VdW} with the relative surface coverage ρ, it cannot be used for the estimation of the minimum number of guest particles needed to ensure non - contacting of two host particles, because the statistically random rather then the minimum coverage is simulated with this program. Furthermore, even if all output parameters are kept identical, the calculated forces differ from each other by each run and have to be averaged, which means that the true lowest limit is lower than the averaged one and might be involuntarily skipped.

3.3.2.2.2 Bresges model

Till recently, there were no detailed analytical methods for the theoretical determination of the minimum number of the guest particles needed to ensure non - contact between the host particles. Now, a new model has been proposed by Bresges (Bresges et al., 2008). The model has been created and implemented in MATLAB®. For the simplifying of the theoretical model it was assumed, that the particle shape of both, host and guest particles, is spherical.

- During the first step the positioning of the guest particles is carried out. To ensure the uniform distribution of the guest particles, which are represented by imaginary point charges, on the host particles, Coulomb's Law is used. The distribution of the point charges on the surface of the conducting sphere leads to the configuration with minimum potential energy resulting in stable positioned points. According to Coulomb's Law, these positions are taken up on the sphere by the point charges because of their mutual rejections (Figure 10);

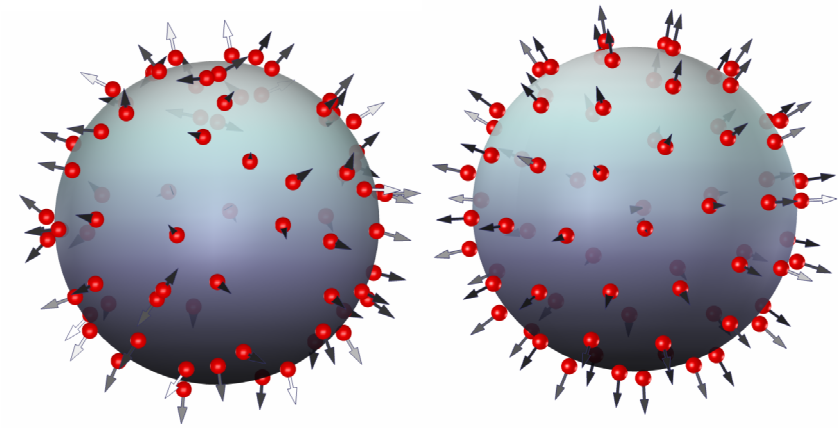

Figure 10: Different states of guest particles distribution on the surface of the host particle: (a) during the distribution process, (b) at the end of the distribution process (Bresges et al., 2008)

- At least three guest particles, which are placed between two host particles, are needed to keep the host particles on distance. During the second step the computation of circumcircles of every three particles is carried out in order to determine the largest of these circumcircles, which represents the site at which contact of the host particles is most likely to occur (Figure 11). The differences in diameters of the circumcircles can be explained by the fact, that only in the few cases of Platonic solids (Figure 12), the equidistance of points on a sphere is achievable (Bresges et al., 2008). For all other cases the most uniform distribution of the guest particles on the surface of the host particles has to be calculated numerically;

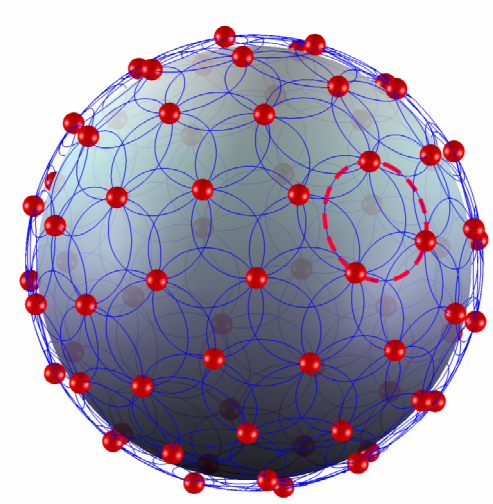

Figure 11: Determination of the circumcircles of every three particles. The largest of the circumcircles is represented by the bold dotted line (taken from Bresges et al., 2008)

- During the last step it is checked, whether the two host particles contact each other at the site of the largest circumcircle. If the distance between the guest particles is too large, the number of guest particles N must be increased. Otherwise, if the number N is high enough to ensure non - contact of the host particles, it has to be checked, whether this number is the minimum needed number indeed. This can be done by decreasing the number stepwise until contact

between the host particles is obtained. So, the highest number N of the guest particles, for which contact has been found plus one particle is the minimum needed number.

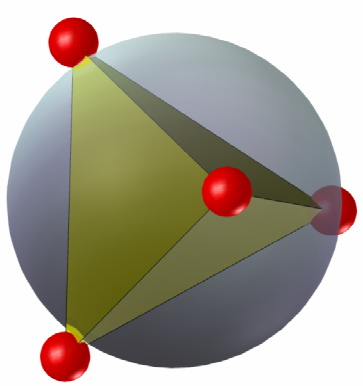

Figure 12: Example of a Platonic solid (taken from Bresges et al., 2008)

The goal of the estimation of the lower coating limit is the successful reducing of the Van der Waals interactions between the microparticles. So apart from and additionally to the calculations of the number of the nanoparticles needed according to the Bresges model the Van der Waals forces in dependence on the distance between the host particles will be calculated in the present study. The Van der Waals forces between two host particles are calculated as follows:

$$F_{VdW} = \frac{A_H \cdot R}{12 \cdot a^2}$$ **Equation 43**

where a is the distance between the two surfaces of the host particles, $A_H = 8 \cdot 10^{-19}$ J is the Hamaker - Van - der - Waals constant (see 3.2.3) and R is the radius of the host microparticles. Furthermore, the Van der Waals forces between the guest particles, which are placed on the surface of the host particles and a second host particle, which is not coated with the guest particles, assuming that the contact happens at the site of the critical circumcircle, is estimated using the following equation:

$$F_{VdW} = \sum_{i=1}^{n} \frac{A_H \cdot R \cdot r}{6 \cdot a_{(g/h)}(i)^2 \cdot (R + r)} \cos(\text{angle to principal axis (i)})$$ **Equation 44**

where r is the radius of the guest particles, $a_{(g/h)}\ (i)$ is the distance between the surface of each of the guest particles placed on the surface of the first host particle and the surface of the second host particle. Here it is also assumed, that the contact happens at the site of the critical circumcircle. The *angle to the principal axis (i)* differs for each guest particle i. The angle must be calculated for the each of the nanoparticles, because the distance $a_{(g/h)}\ (i)$ is not parallel to the principal axis.

In case if both host particles are covered with guest particles in such a way, that the contact happens at the site of the critical circumcircle, the total forces, which act between the *host - host*, *second host particle - all guest particles*, which are placed on the surface of the first host particle, and *first host particle - all guest particles*, which are placed on the surface of the second host particle may be estimated by adding the results of Equation 43 and twofold the results of Equation 44. It is not possible to calculate the Van der Waals forces, which act between the guest particles placed on the surface of the two host particles, because the precise positions of the guest particles relative to each other is not known.

3.3.3 Upper coating limit

The upper coating limit is reached, when one host particle is completely covered with a single layer of guest particles. The densest arrangement of spherical guest particles on a surface is the hexagonal arrangement, where one particle takes the area of one hexagon (Figure 13).

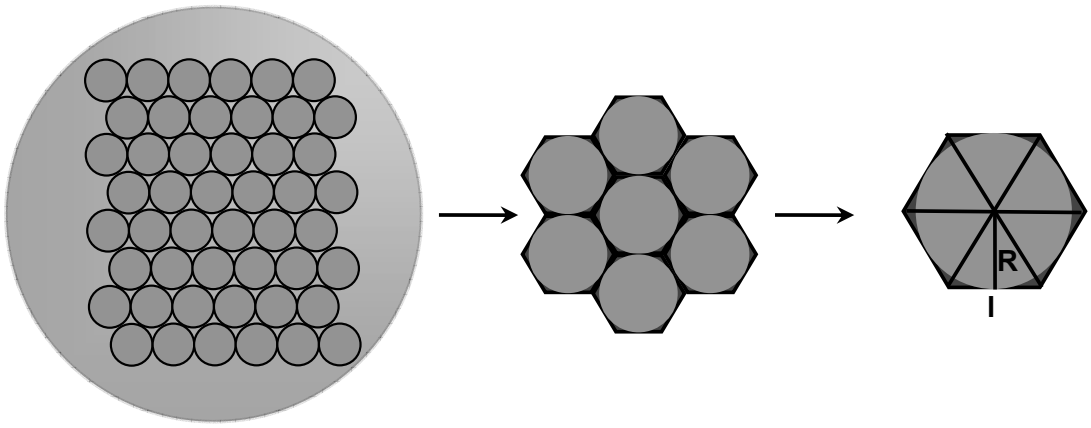

Figure 13: Arrangement of spherical particles according to the hexagon model (taken from Meyer, 2003; modified)

The required area A_{hex} for one particle in the hexagon model can be calculated as follows:

$$A_{hex} = 6\left(\frac{1}{2} \cdot l \cdot r\right) \qquad \textbf{Equation 45}$$

$$l = \frac{2}{3} \cdot \sqrt{3} \cdot r \qquad \textbf{Equation 46}$$

$$R_{hex} = 2 \cdot \sqrt{3} \cdot r^2 \qquad \textbf{Equation 47}$$

where l is the edge length of the hexagon and r the radius of the guest particle.

3.3.4 Concluding remarks

In this work the Bresges model was used for the theoretical determination of the lower coating limit and the hexagon model for the calculation of the upper coating limit. Speaking about preparing a powder formulation by mixing under real conditions the theoretical models may only approach but never represent reality. For the calculations it is assumed that all guest particles are smooth and spherical and that each single guest particle is adhered on the surface of the host particle. However, this is not true for real particles and real particle mixing. For example, agglomerates of the fine - grained powder may be not properly dispersed and the surface of the particles is not smooth and spherical at all. These and other factors may influence the mixing process and the coverage of the host particles with guest particles. Therefore, the calculations may be taken as an approximation for the estimation of the coating limits, but may never be taken as totally reflecting reality.

4. Aim of the work

The most important requirement for a powder, which is intended for the use in dry powder inhalers, is the particle size of the drug. To ensure that the drug will be presented to the lower respiratory tract, especially the alveolar region, the aerodynamic diameter of the particles has to be between 1 µm and 5 µm. It is known that with decreasing size of the powder Van der Waals forces become more important in comparison to gravitation. This impacts flowability dosing and dispersibility of the powder because of agglomeration processes.

Goal of the study is the evaluation of an alternative DPI formulation approach, designed to work without coarse carriers, using drug particles coated with particles in the nanometer range. Nanoparticles are used as spacers between drug particles reducing the interparticle interactions.

To prove the viability of this concept, models were chosen consisting of α - lactose - monohydrate, salbutamol base and salbutamol sulphate as the model substances for the active ingredient and colloidal silicon dioxide (Aerosil® R972) as the model substance for the nanoparticles covering the drug particles. Mixtures of drug microparticles and nanoparticles were prepared by conventional mixing using the TURBULA® shaker mixer or by electrostatically supported mixing using the high speed homogenator ULTRA - TURRAX®. Furthermore, the amount of nanoparticles, needed to reduce interparticle interactions effectively, was calculated using different calculation models. Mixtures with different nanoparticle concentrations were prepared. In order to investigate the influence of drug particle geometry on the performance of the dry powder inhaler, spray - dried, usually spherical particles as well as micronised irregular shaped powders were used.

The amount of active ingredient presumably reaching the respiratory tract was determined by measuring the fine particle fraction in vitro using the Next Generation Pharmaceutical Impactor. Different methods to characterise the flowability of the mixtures by ring shear testing and by measuring the angle of repose, flow rate and Hausner ratio were evaluated. Uniformity of mass was evaluated by repeatedly discharging the formulations from a multidose reservoir. The obtained results were compared with results obtained using the corresponding untreated powders.

C. Materials and methods

1. Materials

1.1 Models for the active ingredient

1.1.1 α - Lactose - monohydrate

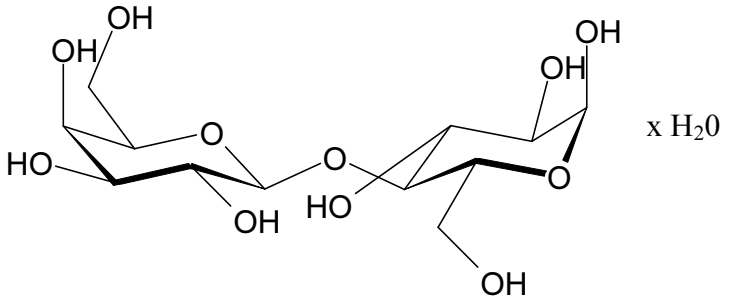

Figure 14: Structural formula of α - lactose - monohydrate

The drug active ingredients are quite expensive, that is why for the development of the powder formulations and some flowability measurements requesting 100 ml or more of the formulation, α - lactose monohydrate (Figure 14) as a model for the active ingredient was chosen.

For the recovery of α - lactose - monohydrate cow milk is used. Lactose is a disaccharide, which consists of glucose and galactose, both existing in the form of a pyranose. Lactose has two optical isomers, α - and β - lactose. If the powder is dissolved in a liquid medium, the equilibrium between the isomers will be obtained. In the solid state different crystalline forms of lactose are found. α - Lactose - monohydrate is obtained when crystallised from an aqueous solution at temperatures below 93° C. If the temperature is higher than 93° C, the powder crystallises as anhydrous β - lactose. Also anhydrous α - lactose exists. The stable form of anhydrous α - lactose is obtained by drying of the monohydrate in organic fluids, like methanol. The second non - stable form of anhydrous α - lactose is produced by the heating of α - lactose - monohydrate under vacuum (Lerk, 1984; Saint - Lorant et al., 2007). After the production of α - lactose - monohydrate, the powder may possess a residual content of amorphous material. The amorphous part of the powder may re - crystallise during storage. The recrystallisation is water mediated and may induce changes of the powder properties, such as changes of the flow behaviour, agglomeration or even building of solid bridges.

Crystalline α - lactose - monohydrate is little hygroscopic, the powder begins to take up considerable amounts of water at the critical hygroscopicity, which is above 93 % RH. α - Lactose - monohydrate is a white crystalline powder with a wide range of particle size distributions, which can be used for such purposes as production of tablets, compactions and preparation of interactive mixtures for dry powder inhalers (Steckel, 2003 (a)). Lactose is approved for pulmonary delivery (Zeng et al., 2002).

1.1.2 Salbutamol base and sabutamol sulphate

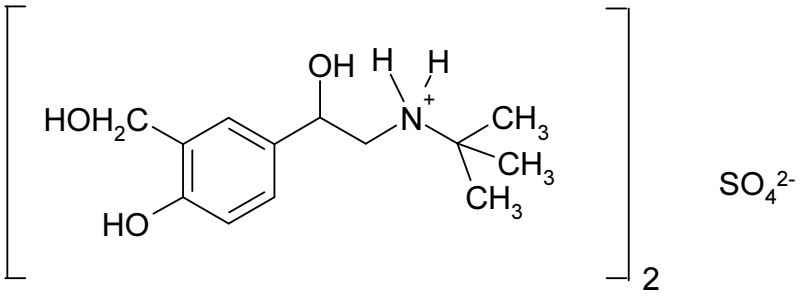

Figure 15: Structural formula of salbutamol sulphate

Both substances salbutamol and salbutamol sulphate (Figure 15) are listed in the European Pharmacopoeia. The aqueous solubility of salbutamol sulphate is higher than the solubility of the base, therefore the salt is applied more frequently. One part of salbutamol base can be dissolved in 70 parts of water or in 25 parts of ethanol. Salbutamol crystallises from ethanol/ethyl acetate in the form of fine odourless and flavourless crystals.

Salbutamol is a direct β_2 - sympathomimetic drug with typical phenylethylamine basic structure. The substitution on the nitrogen increases the affinity of the substance to β - receptors. The substitution of the phenyl ring protects against the reduction by the catechol - O - methyl - transferase (COMT). Salbutamol stimulates preferably the β_2 - receptors and causes the atony of the smooth muscles, in particular of the bronchi, blood vessels in skeletal muscles and uterus (tocolysis). By the atony of the bronchial muscles the dilatation of the bronchi (bronchodilation) takes place. The drug is used for the treatment of the chronic obstructive pulmonary disease (COPD) and may be delivered to the lung by inhalation or may be taken orally or parenterally. Salbutamol enchases the mucociliary clearance and inhibits the deliberation of the bronchial constrictor mediators.

1.2 Nanoparticle model

Hydrophobic colloidal silicon dioxide Aerosil® R972 is a pyrogenically obtained, highly dispersed, amorphous powder. In this work it was used as a nanoparticle model. Although it is not suited for pulmonary delivery from a physiological standpoint, from a technological point of view it matches all the requirements for the use as spacer, such as size in the nanometer range and chemical non - reactivity. Hydrophilic Aerosil® is manufactured by the hydrolysis of chlorosilanes in a hydrogen/oxygen flame.

$2H_2 + O_2 \rightarrow 2H_2O$

$SiCl_4 + 2H_2O \rightarrow SiO_2 + 4HCl$

$2H_2 + O_2 + SiCl_4 \rightarrow SiO_2 + 4HCl$

Directly after production, silicon dioxide is hydrophilic and contains silanol (-Si-OH) and siloxane, (-Si-O-Si-) groups on its surface. The silanol groups of the initially hydrophilic Aerosil® reacts with organosilicon compounds to form hydrophobic Aerosil®. Freshly prepared hydrophilic Aerosil® is treated immediately after the deacidification step to form the hydrophobic Aerosil®. Through hydrophobic treatment the density of silanol groups per nm^2 decreases from approximately 2 for hydrophilic to approximately 0.75 for the hydrophobic types. The different hydrophobic Aerosil® types differ by particle size (10 nm to 40 nm), but also by active surface groups, such as non - polar $-CH_3$ or $-C_8H_{17}$. That is why they possess different chemical and physical properties. Degussa designed a series of hydrophobic Aerosil® types, so - called Aerosil® R types. The addition of the "R" means that the material is "water - repellent". Aerosil® R types are fine, light, white and amorphous powders, which consist of primary particles in the nanometer range (between 10 nm and 40 nm), with very large specific surface area (between 50 m^2/g and 400 m^2/g). The primary particles are not isolated, they are agglomerated in stable chain - like aggregates in the low micrometer range. In this study the hydrophobic Aerosil® R972 with the following characteristics was used:

- Primary particle size: 16 nm;
- x_{50} of Aerosil® R972 agglomerates: 0.2 µm;
- Specific surface area: 110 $m^2/g \pm 20$ m^2/g;
- Density of the primary particles: 2.2 g/cm^3.

2. Characterisation of the materials

2.1 Particle size

As particle size of the drug is crucial for the performance of any dry powder inhaler (Buckton, 1995), particle size distributions of the model drugs were determined using laser light diffractometry. The principle of this method is the diffraction of laser light by particles. The diffraction patterns depend on the size and the shape of the particles. In case of spherical particles radial - symmetrical patterns are obtained on the concentric rings of the detector. The radius of the diffraction ring is reciprocally related to the size of the particle, small particles diffract the light with large diffraction angles, and large particles with small diffraction angles. The patterns can be evaluated with the help of mathematical theories, the so - called Fraunhofer or Mie theory (Mueller et al., 1996). The intensity of the diffracted light, which is a measure of the amount of particles of a certain size present in the sample, is registered by the detector. For the measurement, the samples are dispersed in a liquid or in a gas stream using a Venturi nozzle. The particle size distribution is plotted as the volume quotient of the single particle size classes in relation to the total volume. The particle size is calculated as the diameter equivalent to a sphere with the same diffraction pattern as the particles under investigation. Laser light diffraction works ideally for the measurement of spherical particles. The higher is the deviation from sphericity, the higher the possibility of errors is.

2.2 Particle shape

In order to estimate the particle shape but also size and surface of the particles, the powders were examined using scanning electron microscopy (SEM). The object has to conduct the electron current, therefore, before the examination, the samples must be sputtered with a thin layer of gold. To generate the image of the gold sputtered particle surface, the sample is scanned with an electron beam. The electrons impinge on the surface of the object and induce secondary electrons. These secondary electrons are accelerated in an electrical field and gathered on a scintillator, inducing there a light flash. The photomultiplier counts those light flashes. Each scanned spot corresponds to one pixel on the monitor. The higher the amount of the electrons, the brighter is the pixel. In that way, it is possible to examine the surface of the material. The emerging image is displayed on the cathode ray tube screen without aberration. Due to the minor wave length of the electrons, which is considerably smaller than the De - Broglie - Wave length, the resolution by this method is better than by light microscopy and the images of the objects under examination can be viewed by over 30000 - times magnification.

2.3 Particle density

With the help of a helium pycnometer the particle density of solid objects, which is also a parameter influencing the aerodynamic behaviour, can be measured without damaging of the samples. This technique works on the principle, that a sample displaces an amount of fluid equal to its volume. The helium pycnometer method uses helium as a fluid. Because of the small size of the helium atoms, they are able to penetrate all the cracks and holes in the powder to the minimal size of ca. 0.1 nm, but are not able to get inside the closed pores. The pycnometer consists of two chambers, connected by a tube with a valve in it. The volumes of the two

chambers are known precisely (V_{SC}, V_{REF}). The presence of the sample causes a difference in volume available to the gas. At the beginning of the measurement the air is eliminated from the chamber with the sample and it is filled with the helium gas till a defined pressure ($P_{(1)}$). Afterwards the valve in the connection tube is opened and the total pressure $P_{(2)}$ can be measured. The volume of the sample can be calculated as follows:

$$V_S = V_{SC} - V_{REF} \frac{P_{(2)}}{P_{(1)} - P_{(2)}}$$ **Equation 48**

If the mass of the sample is known, the density of the sample can be calculated.

2.4 Crystallinity/amorphicity

2.4.1 Preliminary remarks

It is widely accepted, that solid dosage forms are mostly formulated using crystalline materials, possessing an ordered crystalline structure. Apart from unstable polymorphs, this state is regarded to be thermodynamically stable. It ensures high purity and reproducibility of the material properties, even when different batches are used.

However, there are many processes, such as mechanical activation of a crystalline material by milling or rapid precipitation from solutions by spray or freeze - drying, which may transform particles or parts of them to the disordered, thermodynamically unstable amorphous state with a higher energy level. The presence of amorphous structures may affect the stability of the formulations, because the disordered state may spontaneously convert back to the ordered state during processing or storage, it may crystallise. This is especially true when exposed to high relative humidity and/or temperature conditions. Crystallisation can be described as a deactivation process, because it arranges the molecules thereby reducing the total energy of the system. It is known, that powder characteristics like dissolution and bioavailability may be affected.

Amorphicity and recrystallisation of pharmaceutical powders may have an impact on many types of dosage forms. It is especially critical for dry powder inhalation formulations. During milling processes crystalline structures may be destroyed. Generated amorphous areas are mainly located at the surface of the particles, so - called “frictional hot spots”. Although the amorphous content may be very low compared to the total mass, it may greatly affect interfacial interactions altering dispersibility, flowability and fluidization of the powder used for powder inhalation. Consequently, there is a growing interest not only in distinguishing between crystalline and amorphous states of the material, but also in the ability to quantify the amount of the one state in the presence of the other.

2.4.2 Moisture sorption

In comparison to crystalline materials, the amorphous state is characterised by a higher potential to absorb moisture. This leads to a higher water uptake at a defined relative humidity in comparison to the crystalline material. Due to the instability of the amorphous state, the powder

tends to recrystallise upon exposure to moisture. This can be explained by the fact that the absorbed water acts as a plasticizer. Below the glass transition temperature (*Tg*) recrystallisation occurs spontaneously but slowly. When the temperature is higher than the *Tg*, the process proceeds faster. Recrystallisation is accompanied by the expulsion of water from the just - formed crystal lattice and consequently by a mass decrease. The increase and decrease of mass can be gravimetrically detected (Buckton et al., 1995 (c)) and may be used to quantify the amount of amorphous material in the sample.

In this study, water vapour sorption is performed in humidity and temperature controlled chamber. A balance measures weight changes of the samples exposed to a defined humidity program. So, it is possible to determine the water uptake and the recrystallisation of the sample in dependence on the relative humidity. Sorption isotherms are obtained by plotting the mass change at equilibrium against the relative humidity (Gorny et al., 2007).

The advantages of the technique are its sensitivity and fast automatic acquisition of data with little sample preparation. Fast data generation applies especially when using instruments being able to record the weight of several samples simultaneously (Gorny et al., 2007). Water vapour sorption is reported to be a very useful technique for measurements of amounts of disorder as low as 0.125 % (Buckton et al., 1995 (c)). Moisture sorption is a dynamical method, and it is possible to monitor the changes in the degree of disorder of the powders upon exposure to moisture. However, it is not possible to directly examine the original state of the powder prior to the subjection to moisture.

2.4.3 Differential Scanning Calorimetry

This thermal technique is used for the measuring of the physical and chemical properties of substances or mixtures of different materials subjected to a temperature program (Itoh et al., 1977). The measurement of the heat absorption or emission as a function of the temperature program allows the monitoring of such features as evaporating and melting as well as recrystallisation or changes of crystal modifications. Furthermore, changes of the heat capacity may be detected caused for example by the glass transition of amorphous material present in the sample.

It is differentiated between power - compensation and heat - flux differential scanning calorimetry (DSC). In the first case a sample and a reference are placed in separate ovens. In order keep the temperature of the sample and the reference the same during the phase transition of the sample, an additional positive or negative energy for the latter is required.

In the second case the sample and the reference are put inside the same oven and the difference in temperature between both is determined. With the help of the thermal resistance of the measuring cell and the temperature difference, the heat flux can be calculated. The temperature difference is constant, if no phase transition in the sample takes place, and depends on the heat capacity of the sample. During a phase transition the temperature difference changes till the end of the transition. The temperature difference between the sample and the reference during the change of state in the sample is directly related to the energy released or used for the phase transition.

In the DSC - thermogram the differential heat flow is plotted versus the temperature. A positive heat flow means a higher absorption of energy by the sample in comparison to the reference. In case of negative heat flow, the sample releases energy.
Saleki - Gerhardt (Saleki - Gerhardt et al., 1994) determined the amount of amorphous material with a quantification limit of 10 % using sucrose as a model compound. As mechanically induced surface effects are mainly manifested at the particle surface and the overall amorphous content may be a small percentage of the total mass only, DSC often fails to quantify low amorphous amounts. DSC is a dynamical method and it is possible to determine the changes in the degree of disorder of the powders upon heating or cooling. However, it is not possible to directly assess the original condition of the powder prior to the subjection to heat. This always holds the risk of artefacts.

2.4.4 X - ray powder diffraction

X - ray powder diffraction (XRD) is an instrumental technique, that is used to identify phases by comparison with data from known structures, to quantify changes in the parameters of the crystals, orientation, size and other structural parameters. Other information obtained includes information about the degree of crystallinity of a powder and possible deviations of mixtures from their ideal compositions.
X - ray radiation is an electromagnetic radiation with wavelengths between roughly 0.1 Å and 100 Å. For diffraction applications X - rays of a short wavelength in the range of a few Angstroms to 0.1 Angstrom are used. For most experiments, a single characteristic radiation is selected using a filter or monochromator. This range of the wavelengths of X - rays is similar to the size of atoms and molecules, therefore suited for probing the structural arrangement of atoms and molecules in a wide range of materials. X - rays penetrate into the material and provide information about the bulk structure.
The three - dimensional structure of crystalline materials is defined by regular, repeating planes of atoms or molecules that form a crystal lattice. When a focused X - ray beam interacts with these planes, part of the beam is transmitted, part is absorbed by the sample, part is refracted and scattered and part is diffracted. X - rays are diffracted depending on what atoms or molecules make up the crystal lattice and how these are arranged. The integral intensity of the crystalline reflexes characterises the crystalline parts. The amorphous regions show one or more halos in the diffraction diagram, their integral intensity characterises the amorphous phase. The detection limit of X - ray powder diffraction for amorphous materials is about 10 %. As mechanically induced surface effects are mainly manifested at the particle surface and the overall amorphous content might be only a small percentage of the total mass, powder X - ray often fails to quantify low amorphous amounts.

3. Preparation of the interactive formulations

3.1 Comminution of the drug substance

3.1.1 Micronisation

In order to obtain powders with particle diameters between 1 µm and 5 µm micronisation in a jet mill has been carried out in this study. The drug particles are fed into a milling chamber, where two airstreams meet at high velocity and micronisation results from the collision of drug particles. Due to the centrifugal force the coarse material circulates in the peripheral part of the mill, the fine particles follow the air stream through the opening in the centre of the mill into a filter bag, where the particles are separated from the air stream. The energy for the milling process is provided by compressed air. The drug substance is not warmed up during the process, because there are no grinding parts in the mill, therefore heat - sensitive materials may be micronised without decomposition.

3.1.2 Spray - drying

Another means applied in this study to obtain particles in the low micrometer range is spray - drying. Spray - drying generates solid powders from solution or suspension. It represents a single step process that involves the atomisation of the liquid feed, the forming of a fine mist of droplets and injection of the droplets into a drying chamber containing hot air or nitrogen. The droplets instantly are dried to form solid, usually spherical particles that are then separated from the drying gas and subsequently collected in the drying chamber. Two factors influencing the properties of the output material are the composition of the liquid feed and the spray - drying parameters.

3.2 Conventional mixing

The coverage of the microparticulate drug with the nanoparticulate spacers is a procedural process including the deagglomeration of the agglomerates of the particles of the same species preferably up to the primary particles, mixing and bonding of the nanoparticles on the surface of the microparticles with the aim of achieving a homogeneous distribution of the nanoparticles on the microparticle surface. One method of mixing is the conventional turbulent mixing process. Mixtures of microparticles, which were produced either by spray - drying or milling, and Aerosil® R972 in different concentrations, were prepared by mixing the components in a glass vial using a TURBULA® shaker mixer in this study.

For the preparation of binary mixtures not only mixing parameters such as mixing duration, but also the model of the mixer is important (Jonat et al., 2004). For the classification of different models of mixers into categories, Rumpf introduced a factor, which is called Froude - Number *Fr*. This number specifies the relation between centrifugal acceleration and acceleration due to gravity and can be calculated as follows:

$$Fr = \frac{r_c \cdot \omega^2}{g}$$ **Equation 49**

where r_c is the radius of the mixing cylinder, g the acceleration due to gravity, ω the angular speed. The Froude - Number of the TURBULA® shaker mixer, which was used in this work is $Fr < 1$. Due to the low Froude - Number the shear forces during the mixing process were quite low, which means that the deagglomeration of like particles is poor (Degussa, 2002).
The TURBULA® blender mixes the particle fractions in a three dimensional movement of the mixing container producing directly the nanoparticle coated microparticles. These movements are based on the eversion theory according to Schatz and are composed of translation, rotation and inversion. Translation can be determined from the free length of path and rotation of the circular motions of the mixing cylinder. The movements of both rotating arms are not dependent on each other, therefore the mixing cylinder has paths, which are very complicated to describe. Translation and rotation movements cause the additional inversion movements. As a result of the complexity of movements there is no model existing, describing the movements of the particles inside the rotating cylinder (Duenisch, 2005).

3.3 Electrostatically supported mixing

3.3.1 Preliminary remarks

Another way to control the mixing process is to charge the particle fractions using electrostatically supported mixing. Electrostatically supported mixing provides charging and dispersion of the nano - and the microparticle fraction and subsequent attraction between nano - and microparticles, caused by the differences of the charge acquired by the nanoparticles and the one acquired by the microparticles, which in turn is caused by the differences of their electrostatic properties. Because of these effects, the nanoparticles can be homogeneously distributed on the microparticles´ surface.
When two electrically neutral materials with different electrostatic properties make and then break contact, charge transfer from one of the materials to the other may occur (Bailey, 2003). In order to transfer a measurable charge, it is often only necessary to bring the surfaces of the particles together and then separate them (Cross, 1987). In case of insulators the charge remains at the points of contact. Repeated collisions are causing further charge transfer between the particles (Figure 16) (Zeng et al., 2001).

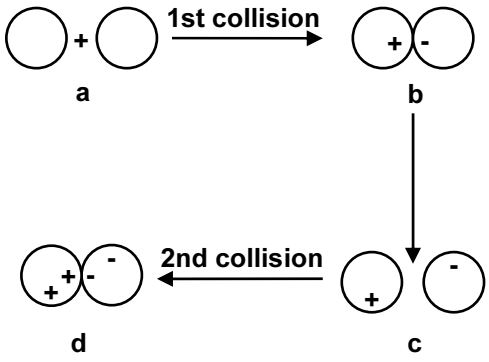

Figure 16: Scheme of the acquisition of electrical charge: (a) two uncharged particles; (b) first collision and electron transfer; (c) two charged particles; (d) second collision and further electron transfer (taken from Zeng et al.; modified)

Compared to the frequency of collision, the rate of charge distribution on an insulator particle surface is negligible (Zeng et al., 2001). New charges may be continuously created causing the rise of the charge density until further collisions occur on previously charged spots, without charge transfer.
The molecules of an amorphous material exhibit higher mobility than molecules arranged in a crystal lattice. In case of the insulators, the charge on amorphous particles usually distributes faster than on crystalline particles. Therefore, the crystallinity also has an effect on the charge distribution. Figure 17 a shows the relatively homogeneous distribution of the electrical charges on a spherical amorphous particle. In case of crystalline particles charges may concentrate on the tips of the pointed edges, because contact occurs more often on the edges, than on the planar surfaces.

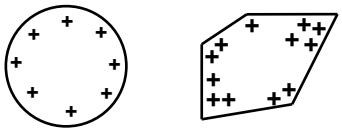

a b

Figure 17: Charge distribution on amorphous spherical (a) and crystalline irregular particles (b) (taken from Zeng et al., 2001)

Such surface phenomenon as the charge transfer involves not more than eight out of every million surface atoms (Vercoulen, 1995). Electrostatic charging of the particles can be done by transferring electrons or inducing electron vacancies, both may be done by simple contact or friction between two materials. Both types of charging, by contact and by friction, are called triboelectrical charging. Actually, no model exists, which is capable to describe both types of charging satisfactorily. The available models are always valid for one of these two mechanisms. However in practice, charging by contact and charging by friction can be hardly separated.
Furthermore, a powder may be charged by applying high voltage and corona - charging, X - ray and UV - radiation. In the following, only the basic ideas concerning the experiments of electrostatically supported mixing will be described.

3.3.2 Work function model

A work function model is frequently used to describe tribocharging. It is based on the energetically favourable transfer of electrons from one material to another material if contact is made. The work function is the difference between the vacuum potential and the Fermi energy of the material and represents the minimum energy required to extract the weakest bound electron from a particle surface and to move it to infinity (Cross, 1987; Vercoulen, 1995; Linsenbuehler, 2005). By the contact of two unlike materials, the material with the minor work function gives electrons off to the material with the higher work function. During the encounter of the materials thermodynamical equilibrium is obtained in the way that the Fermi levels are equalled. However,

surfaces of insulators, which are triboelectrically charged, may possess, depending on the chemical structure, positively and negatively charged areas at the same time, the predominating polarity determines the net charge of the surface (Cross, 1987).
The number and the speed of the electron migration are dependent on environmental and process conditions, such as relative humidity, intensity of the contact and friction velocity. The nature of the electron migration also depends on the type of materials. It depends on whether the material is a conductor or insulator (non - conductor), because the positions of the energy levels of those materials differ.
With the help of the simple band model the difference in electrical conductivity between metals and insulators can be explained. If the outer electrons are located in an energy band which is partially empty, the material is able to conduct. According to the quantum mechanical rules only two electrons can occupy the band. If the band is full, no electron can increase its energy and can be accelerated by an electric field. In this case the material is an insulator.
The surface - state - model describes the surface charge on an insulating material after a three step sequence: approach of the insulator to a conducting material, physical contact of the two materials and separation of the two bodies. It is presumed that the final charge is determined by equilibrium considerations at some small distance of molecular dimensions between the two surfaces during the third step, the separation (Vercoulen, 1995).

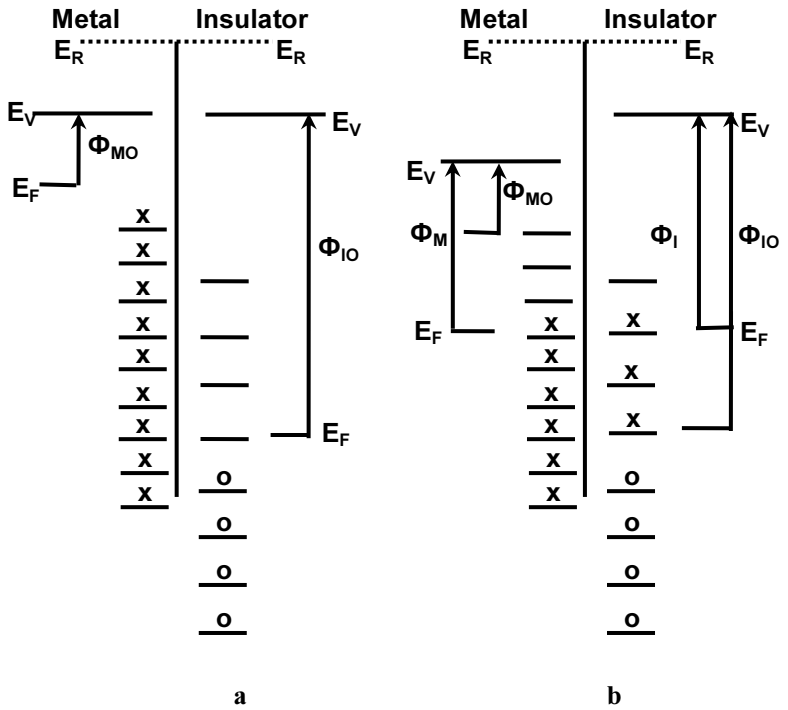

Figure 18: Metal - insulator electron potential energy diagram before (a) and after (b) the contact of the metal and the insulator (taken from Vercoulen, 1995; modified)

Figure 18 shows the electron energy diagrams and their differences before and after the contact of the metal and the insulator schematically. Each diagram is divided vertically into two parts, the left hand side represents the metal, the right hand side the insulator. Figure 18 a, describes

both solids before the charge exchange has taken place, Figure 18 b after the contact and following separation of the metal and the insulator. For the comparison of both materials with respect to their electrostatic potential E_R, the energy levels are given relative to some fixed reference.

The Fermi level E_F describes the distribution of the electrons in the surface of the solid as a function of energy. The occupation of this level is dependent on temperature. It is empty at the temperature of absolute zero. By increasing temperature and therefore energy the probability of occupation increases. The vacuum level E_V represents the energy an electron from a given solid would have just outside the solid, in space, and may be considered as a structural feature of the surface. The Coulomb work which is needed to remove the electron from the charged surface to the reference level is represented by the difference between the E_V and E_R. Here the difference between the energies E_V and E_F is the work function Φ^M. The surface states, which are the structural levels that can be occupied by an electron at the surface, are indicated by the horizontal line when vacant and by *x* (metal) or *o* (insulator) when occupied. The energy density, which is high for a metal and may be many orders of magnitude lower for an insulator, is indicated by a vertical spacing.

According to this model there is no electrical communication between the surface state and the interior of the insulator, so that the indicated Fermi level of the insulator only describes the electron distribution at the surface. The two main points of this model are that the two Fermi levels of the different surfaces are equalized during the physical contact and that the electrostatic potential between the two solids is given by the difference in the values of the vacuum levels. It is also assumed that no charge can be transferred through the interior of the insulator. In case when both solids have an equal charge or no charge, the vacuum energy levels are the same. During the contact the electrons are transferred from the metal to the surface states of the insulator.

The difference in energy between the two levels is larger for the insulator, therefore the work function of the latter changes more than that of the metal. This is indicated by the values of W, the work functions after the charge transfer:

$$\phi^M = \phi^{MO} - W^M \qquad \textbf{Equation 50}$$

$$\phi^I = \phi^{IO} - W^I \qquad \textbf{Equation 51}$$

where the M and I denote metal and insulator respectively and O means uncharged. When the solid is negatively charged the value W is positive. The absolute value of W^M usually is very much smaller than that of W^I. The electrostatic potential of the metal surface relative to the insulator at equilibrium V can be calculated as follows:

$$V = \frac{\phi^I}{e} - \frac{\phi^M}{e} = \frac{\Delta\phi - W}{e} \qquad \textbf{Equation 52}$$

here:

$$\Delta\phi = \phi^{IO} - \phi^{MO}$$ **Equation 53**

and

$$W = W^{I} - W^{M}$$ **Equation 54**

Since W^M is very small compared to W^I and if the surface charge density of the insulator σ is not a function of energy, W can be calculated according to:

$$W = \frac{\sigma}{N_s}$$ **Equation 55**

here N_s is the density of the surface states of the insulator and can be rewritten:

$$V = \frac{\Delta\phi}{e} - \frac{\sigma}{e \cdot N_s}$$ **Equation 56**

The potential difference and therefore the charge transfer between two surfaces depend on the material properties $\Delta\Phi$ and N_s (Vercoulen, 1995).
Greason mentioned that the amount of charge transferred is a function of the difference in work function and of the true contact area (Greason, 1992). It is quite difficult to generate experimental conditions, which make triboelectrical charging the only phenomenon involved, therefore the usefulness of the work function concept is limited.

3.3.3 Types of tribocharging

Often, the attempt is made to divide tribocharging into contact and frictional charging (Poppe, 1999). Contact charging was introduced because charging also occurs if no rubbing is involved, for example during contact of liquid mercury with insulating materials (Cross, 1987). Frictional charging is responsible if two objects are charged by rubbing. However, almost always both types of charging occur during surface contact and cannot be easily attributed to the one or the other type.
Reproducible experimental results on tribocharging are difficult to obtain, because charging of surfaces is very sensitive to numerous parameters that are hard to identify or to control. Harper mentioned that during charging experiments, the polarity of the obtained charge may reverse to the opposite without obvious reason (Harper, 1967). Among the parameters, which may influence the charging procedure are the surface material, the crystalline structure, the roughness,

the contact pressure, the temperature, the size of the object and the rubbing or gliding velocity between the surfaces (Poppe, 1999).
In practice, frictional charging is carried out by rubbing surfaces together without applying high voltage. The charge transfer between the interacting surfaces further depends on which sample is rubbed and which is doing rubbing. The probable explanation to that fact is that the temperature of the contact point may affect the charge transfer. This transfer mechanism is based on "hot spots". If two materials are rubbed against each other, the contacting parts are heated. The electrons on the heated surface may have a higher mobility and move to colder spots changing the surface charge (Harper, 1967). Generally, there is an increase in charge with rubbing velocity. Till now, the accurate prediction of the polarity induced by frictional charging is not possible. However, there are different triboelectric series published by several authors: Davies, 1976, Strella, 1970 (Cross, 1987). These series may help in estimating the polarity of the contacting materials. The series are based on the results of experiments. The materials at the top of the series are charged positively relative to the materials at the bottom (Table 2).

Table 2: Triboelectric series according to Davies, 1976; Strella, 1970 and Huber 2001

Polarity	Material	Work function
		Low work function
-	PVC	
	PTFE	
	PE	
	Hydrophilic Aerosil®	
	Hydrophobic Aerosil®	
	Lactose	
	Nylon 66	
+	Polyethylene oxid	
		High work function

Coste (Coste et al., 1977) observed three different charging modi during the charging of polymers (Figure 19). The polymer films were passed over metal rollers, one of the roller moved faster than the polymer film fixed on the other roller. In that way friction was provided.
1. The charge density grows to a constant value till a saturation value is reached. This type of curve can be obtained during the charging with little friction;
2. The charge density passes through a maximum then decreases and changes polarity to reach a new equilibrium state;
3. The charge density reaches a maximum then decreases to a new steady state without changing polarity.

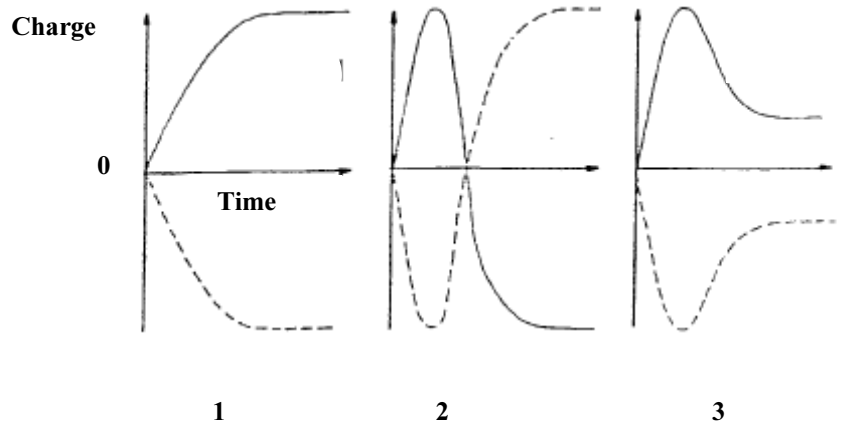

Figure 19: Different types of charging modi (taken from Coste et al., 1977; modified)

Which type of behaviour is observed with the material is depending on the physical and chemical properties of the materials involved, the speed of the rubbing, the force and duration of the contact and the relative humidity (Cross, 1987). However, the charge of a particle cannot exceed a certain maximum (Vercoulen, 1995). Frictional charging of insulating surfaces of solids in the air enables the charge density to reach the Gaussian limit of 2.64 x 10^{-5} Cm^{-2}, when the electric field above the surfaces reaches the level at which the air ionises. The charge on the surface of dispersed particles may be even lower than this value if the electric field due to the total volume of charge reaches the breakdown limit of air.
The correlation between the specific surface charge of the spherical particle σ and the electric field strength E_f can be described with the help of the following equation (Linsenbuehler, 2005):

$$E_f = \frac{\sigma}{\varepsilon_r \cdot \varepsilon_f} \qquad \textbf{Equation 57}$$

where ε_r is the relative dielectricity constant and ε_f the electric field constant ($\varepsilon_0 = 8.85 \times 10^{-12}$ *As/Vm).*
The higher the breakdown limit, the higher the amount of charge, which can be situated on the particles´ surface. Generally, the smaller the size of the particles is, the fewer the number of charges that can be placed on the surface. According to Equation 57 a particle with the diameter $d = 5.3$ nm represents the case of the minimal limit charge and possesses accurately one elementary charge (Linsenbuehler, 2005).

3.3.4 Mixing and coating of microparticles and nanoparticles

For the targeted placing of the nanoparticles on the surface of drug microparticles the procedure of electrostatically supported mixing was introduced (Huber, 2001). This type of mixing was applied in order to positively influence the result of mixing by purposeful increasing of the homogeneity of the mixture. Electrostatically supported mixing provides charging and dispersion of nano - and microparticles, but also attraction between nano - and microparticles, caused by the

differences of the acquired charge, which is caused by the differences of their work functions. Due to these effects, the nanometric powder fraction can be homogeneously distributed on the micrometric second powder fraction.

One of the most important prerequisites for a successful mixing result is the proper dispersion of the educts. Therefore it is reasonable to choose such dispersion media and dispersion tools, which provide satisfactory dispersion of undesired agglomerates into single particles as far as possible. In order to reduce the cohesion forces between the particles and to enhance dispersion a liquid media may be used. In liquids the Van der Waals forces are usually less strong than in gaseous media and therefore undesired agglomerates can be easily dispersed.

To enable the particles to retain their, during electrostatically supported mixing, acquired charge, the dispersion medium has to be electrically non - conducting. Characteristics as low surface tension and vaporisation heat, chemical inertness and environmental compatibility are also of great advantage. Usually, most organic fluids are chemically not inert and environmentally non - friendly. In order to carry out electrostatically supported mixing liquid nitrogen can be used (Huber et al., 2003; Linsenbuehler et al., 2004). This fluid gas possesses all the above requested characteristics. Furthermore, liquid nitrogen evaporates easily at the end of the experiment leaving behind the dry powder mixture, which is ready for use.

Huber (2001) introduced a two step mixing procedure in liquid nitrogen (Figure 20). At the beginning of the experiment the two components of the mixture are separately dispersed and triboelectrically charged. In the second step the mixing of the two particle fractions takes place. After the evaporation of the liquid nitrogen the dry product is obtained.

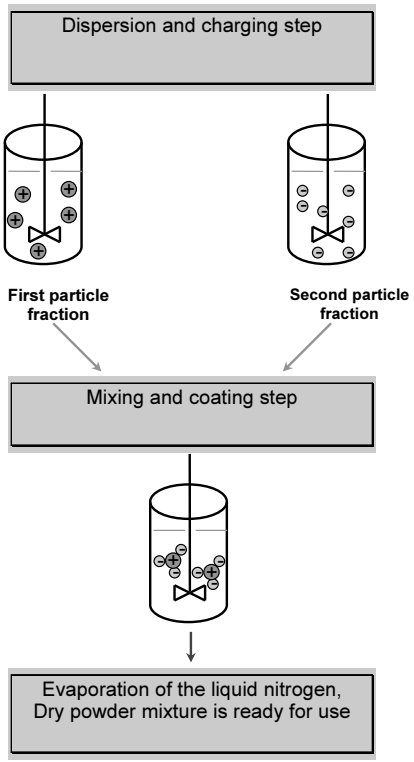

Figure 20: Two step dispersion and mixing procedure introduced by Huber (taken from Huber, 2001; modified)

Further, this procedure was transformed into a one step procedure (Linsenbuehler, 2005). Here dispersion and mixing takes place in one step (Figure 21).

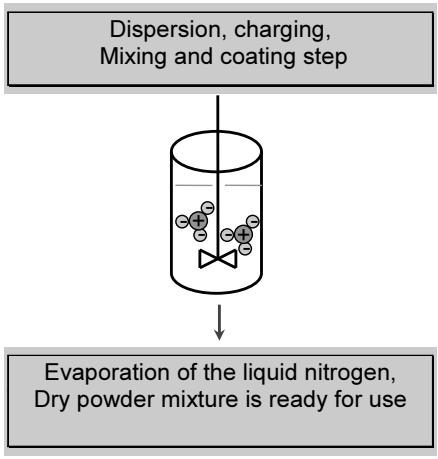

Figure 21: One step dispersion and mixing procedure introduced by Linsenbuehler (taken from Linsenbuehler, 2005; modified)

In this study, the one step procedure was further modified. Due to the differences in sizes, the specific surface of the nanoparticle fraction is larger than that of the microparticles. Therefore the time, which is needed for the charging of the surface of the nanoparticles, is longer in comparison to the microparticles. At the beginning of the experiment, the nanoparticle fraction was suspended in liquid nitrogen. The nanoparticle dispersion was stirred with a high - speed homogenator. Due to the intensive contact between the particles and the homogenator triboelectrical charging of the particles takes place. For the measuring of the acquired charge an electrometer was used. Further, the microparticle fraction was given to the nanoparticle suspension. At that point not only charging and dispersion of like particles, but also charge diffusion and attraction between unlike charged micro - and nanoparticles and therefore the coating of microparticles with nanoparticles takes place.
For the dispersion and charging of the particles in liquid nitrogen the high - speed homogenator ULTRA - TURRAX® T25 basic was used. The stator of the ULTRA - TURRAX® is an ideal flow breaker and therefore is able to prevent the rotation of the fluid. In this device the velocity of the rotor could be controlled between 6200 rpm and 20500 rpm, thus the energy introduced into the dispersing process. During the dispersion, the particles repeatedly pass the rotor - stator system and get repeatedly speeded up and slowed down. The shear flows and collisions of the agglomerates with the wall play an important role in deagglomeration.
Degussa (Degussa, 1993) described schematically the behaviour of fine scaled particles using silicon dioxide Aerosil®. Synthesised primary particles tend to build aggregates during the production, because of sintering processes (Figure 22). These aggregates attach to each other and build loose three - dimensional networks. At rest the aggregates begin to agglomerate. This happens because of the Brownian movement and the Van der Waals attraction and/or capillary

forces. The loose agglomerates can be broken by applying shear forces. The aggregates cannot be separated into the primary particles again (Jonat et al., 2004).

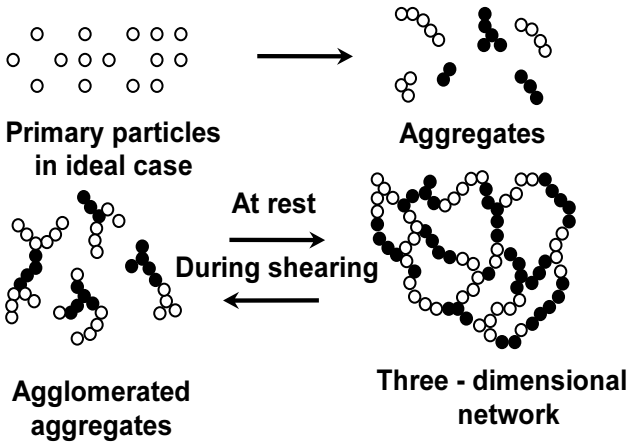

Figure 22: Scheme of the aggregation and agglomeration behaviour of fine scaled particles exemplified by silicon dioxide (taken from Linsenbuehler, 2005; modified)

Pohl and Schubert (Pohl et al., 2004) investigated the dispersion of Aerosil® 90 and Aerosil® 200V with the help of an ultrasound generator and an ULTRA - TURRAX® S25KV (IKA - Werke, Staufen, Germany). A correlation between the mean agglomerate size and the energy introduced into the system has been found. For Aerosil® 200V (5 % (m/m)) the lowest mean agglomerate diameter obtained was ca. 130 nm during the dispersion of the powder using ultrasound. With the help of the ULTRA - TURRAX® the agglomerates were dispersed down to 200 nm. For this work, the mean diameter of the agglomerates around 200 nm is considered as appropriate and therefore the dispersion of the particles was carried out with the ULTRA - TURRAX® in this study.

The most important parameters for the successful dispersion of the powder in a fluid medium are the concentration of the solid particles in the medium, the size of the particles and the amount of the electrostatic charge. Generally, the higher the concentration of the solid particles in the dispersion, the higher must be the number of charges on the surface of the particles in order to prevent agglomeration (Linsenbuehler, 2005).

3.3.5 Charge measurements

According to the above mentioned points, it is important to examine the charging properties of the powder fractions. Therefore, the influence of different rotation velocities of the ULTRA - TURRAX® and concentrations of the solid particles in the fluid medium on the charging process was investigated. For the measurement of the particle charge a Faraday cup was used. The Faraday cup is a double - walled vessel of any suitable shape. It consists of a measuring inner cup and an outer cup. The inner cup is isolated from the ground and from the outer cup. The inner cup is connected to a high - resistant electrometer, which measures the charge by detecting the voltage built up across a known capacitance (Cross, 1987). The outer cup

is grounded, forms an electrical screen for the inner cup and prevents the measurement of external charges. If a charged object of any shape or conductivity is placed in the container, an equal but opposite charge will be induced on the inner cup (Figure 23). This charge leaves behind an equal and opposite charge on the capacitor of the electrometer. So in that way it is possible to measure the charge inside the inner cup.

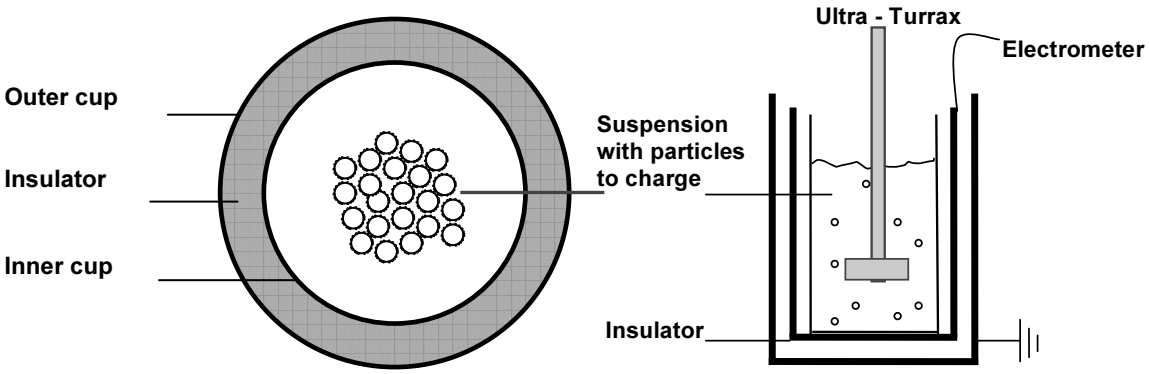

Figure 23: Charge measuring principle during electrostatically supported mixing with an ULTRA - TURRAX® in a Faraday cup: (a) view from the top of the Faraday cup and (b) side view

Care must be taken, that the means by which the liquid or powder is introduced into the cup does not produce additional charge. The powder sample has to enter the cup directly without the help of a funnel or tube, which is not part of the inner container. The insulation between the inner and the outer cup must be extremely high. There should be no decay of charge when charged articles are left in the cup. Therefore during the charge measurements both cups are isolated from each other by a Teflon cylinder. To ensure the volume of the fluid medium to be constant the suspension was introduced into the glass vessel and the evaporation of the liquid nitrogen from the not hermetically sealed inner measuring cup was compensated with a new corresponding portion of liquid nitrogen.

4. Characterisation of the powder mixtures

4.1 Flowability measurements

The flowability of the powder for the use in dry powder inhalers is a very important factor and plays a crucial role in mixing, dosing and fluidization. Flowability of the powder cannot be expressed as a single index or value. For the evaluation of the flow behaviour of single fractions and powder mixtures, techniques like shear cell tests and parameters like the Hausner ratio, the angle of repose and the flow rate may be used (Zeng et al., 2001; Markefka et al., 2005). Flow behaviour is a function of parameters like particle size and distribution, particle shape, surface morphology, moisture and temperature, all of them affecting interparticle interactions (Neumann, 1967; Schulze, 1996).

4.1.1 Ring shear tester

In order to measure the flow properties of fine - grained solids a ring shear tester may be used to measure the yield limit of a consolidated powder (Schulze, 2003). Flowability ff_c is defined as the ratio of the consolidation stress σ_1 to the unconfined yield strength σ_c:

$$ff_c = \frac{\sigma_1}{\sigma_c}$$ **Equation 58**

The higher the ff_c value the better the powder flows. Flow properties of different bulk solids can be compared by their ff_c values, if all measurements are made at the same consolidation stress.
Jenicke (Jenicke, 1964) classified the flowability of solids according to the ff_c values:

$ff_c < 2$ very cohesive and non - flowing powder
$2 < ff_c < 4$ cohesive powder
$4 < ff_c < 10$ easy - flowing powder
$10 < ff_c$ free - flowing powder

Schulze modified the classification by fine - tuning of the low limit:

$ff_c < 1$ non - flowing powder
$1 < ff_c < 2$ very cohesive powder

Figure 24 presents the flow function A and limits of the ff_c values. The boundaries of the ranges are shown as straight lines and represent a constant value of flowability. The ff_c value is dependent on the consolidation stress σ_1 therefore, on the stress level at which it is measured. Because of this dependence of the flowability on σ_1, the flowability cannot be described with only one numerical value.

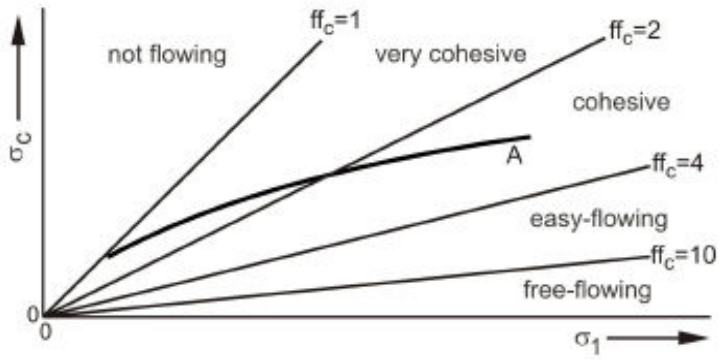

Figure 24: Flow function and lines of constant flowability (taken from Schulze, 1994)

4.1.2 Hausner ratio

The Hausner ratio is the ratio of the loose bulk volume and the tapped bulk volume. At the beginning of the experiment 100 g of the powder are loosly poured into a specified glass cylinder and the volume V_{beg} is read. The number of tappings which are needed to be performed according to the procedure in order to measure the changed volume are described in the Monograph "Apparent and tapped volume" of the European Pharmacopoeia 6.0. At the end of the test the volume of the tapped powder V_{end} is read. A high Hausner ratio means poor flowability. The lower the Hausner ratio and therefore the difference between the volume of the loosely poured powder at the beginning of the experiment and after tapping it a defined number of taps, the better the flowability of the powder. This can be explained by the fact, that poorly flowing powders need some additional energy input by tapping in order to overcome internal friction and to arrange themselves at the final position, whereas well flowing powders take up this position already when pouring them into the glass cylinder without additional energy input. With the help of this measurement also the behaviour of powders inside the powder reservoir of dry powder inhalers can be imitated.

4.1.3 Angle of repose

The measurements of the angle of repose were carried out using the equipment as described in the German Industry Norm DIN 53916: "Surface active agents - Powders and granules - Measurement of the angle of repose; Proceeding according Pfrengle". According to DIN 53916 the powder flows out of a specified funnel and settles as a cone on a plastic plate of the diameter of 100 mm. For the measurement of the angle of repose of powders showing poor flow properties a stirring device is used. The stirring device ensures that non - flowing powders may be measured as well. For comparing different powders, the same volume of the powders has to be tested. The angle of repose φ is the angle between the sloping surface of the sample pile of the height h and the horizontal. A freely flowable powder, forming a relatively flat pile has a low angle of repose. A poorly flowable powder with a relatively tall pile has a high angle of repose.

$$\tan\varphi = \frac{2h}{100} = \frac{h}{50}$$ **Equation 59**

4.1.4 Flow rate

The flow rate is defined by the time, which 100 ml of the powder need to pass the outlet of a funnel. With this experiment the flow behaviour of the powder under the influence of gravity is determined. The samples under investigation are allowed to flow through the orifice of a specific diameter. The higher the flow rate the better the flowability of the powder. The flow rate is a function of the diameter of the orifice, and powder properties like particle diameter, particle shape and density (Neumann, 1967). All measurements of the flow rate, which were carried out in this work were performed according to the Monograph "Flow behaviour" of the European Pharmacopoeia 6.0. As was already mentioned, the results of the flow rate are dependent on the geometry of the funnel but also on its material. Therefore all measurements must be carried out under the same conditions in order to be compared.

4.2 Uniformity of mass

Uniformity of mass is one of the functional factors for the performance of any multi dose dry powder inhaler (Mykhaylova et al., 2006). Measurements are performed together with the aerodynamic assessment of fine particles. The multiple - unit reservoir containing the mixture is weighed before and after each dose discharge. The mass of each dose is calculated by subtracting the weight of the multi dose reservoir after discharge from the weight before discharge.

4.3 Aerodynamic assessment of fine particles

The aerodynamic assessment of fine particles provides in vitro information about how much of the dry powder inhalate released from the inhaler presumably will be reaching the deep parts of the lung. Thereby the aerodynamic diameter is a key parameter influencing the transport of the drug along the airways. The aerodynamic diameter is defined as the diameter of a unit density sphere, which has the same settling velocity in air as the particle. The aerodynamic diameter is dependent on the geometric particle diameter, particle shape and density. Particles of aerodynamic diameters between 1 µm and 5 µm are supposed to reach the deep parts of the lung.
Usually, for the determination of the aerodynamic particle size impactors are used. The principle of inertial impaction is presented in Figure 25. At the top of a jet the air flows towards a collection surface and the airborne particles follow the air stream. When the air flow approaches the collection plate it changes direction and goes around a bend. Small particles follow the streamline, but larger ones impact on the collection surface. They are not able to follow the air flow because of their inertia.
The operation principle of the cascade impactor is inertial impaction. Each stage of the impactor comprises a single or series of nozzles or jets through which the sample laden air stream is drawn directing any airborne particle towards the collection plate for that particular stage. Whether a particular particle impacts on that stage is dependent on its aerodynamic size. Particles having sufficient inertia will impact on that particular stage collection plate, whilst smaller particles with insufficient inertia will remain entrained in the air stream and pass to the next stage, where the process is repeated. The stages are assembled in a stack, in the order of decreasing particle size. As the jets get smaller, the air velocity increases and finer particles are collected. At the end of

the test, the particle mass relating to each stage collection plate is recovered using a suitable solvent and then analysed usually using HPLC to determine the amount of active drug actually present.
By analysing the amount of drug deposited on the various stages, it is possible to calculate the Fine Particle Dose (FPD) and Fine Particle Fraction (FPF) of the active drug particles collected. The Fine Particle Dose (FPD) is defined as the quantity of drug that is generally considered to be of a size capable of penetrating the low part of the lung during inhalation. The Fine Particle Fraction (FPF) is the FPD expressed as the percentage of the delivered dose (the dose that leaves the inhaler device and is available to the patient). However, in this work, the FPF was calculated as percentage of the mass of particles smaller than 5 µm and the total mass of the powder delivered (in case of the spray - dried and micronised lactose) and total drug mass of the powder delivered (in case of the spray - dried and micronised salbutamol base and salbutamol sulphate).

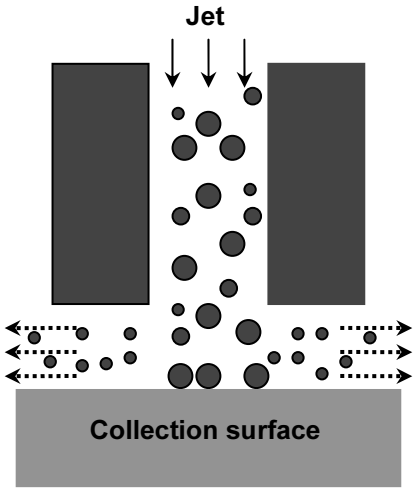

Figure 25: Schematic illustration of the principle of inertial impaction

The selection of an impactor depends largely on the product to be tested and the data that is required. In this work the Next Generation Impactor was used (Figure 26). This impactor was designed for testing pharmaceutical inhalers using the very latest design theory. The NGI is a high performance, precision particle classifying cascade impactor. It has seven stages (at least five with cut - offs between 0.5 µm and 6.6 µm at all flow rates) plus a micro - orifice collector (MOC), which, in most cases, eliminates the need for a final particle filter.
The design of the NGI allows the operation between a calibrated flow rate in a range from 30 litres to 100 litres per minute. The flow rate, that has to be chosen, depends on the resistance of the used dry powder inhaler.

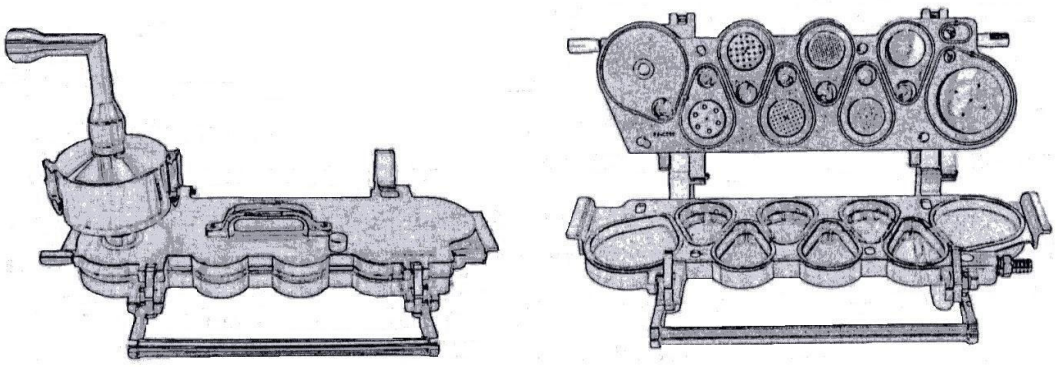

Figure 26: Next Generation Impactor (taken from Marple, 2003)

The air flow passes through the impactor in a saw - tooth pattern. Particle separation and sizing is achieved by successively increasing the velocity of the air stream as it passes through each stage by forcing it through a series of nozzles containing progressively reduced jet sizes. Apart from the first stage all further stages possess multiple nozzles:

The impactor itself comprises just three main parts: bottom frame with cup tray for eight collection cups, the seal body that holds the nozzles in place and the lid that contains the inter - stage passageways. During the operation the three parts are held together using the handle clamping mechanism. The NGI also requires the use of a preseparator with the sharp cut - point of between 10 µm and 15 µm, depending on the flow rate used, in order to collect any powder boluses and large non - inhalable particles.

D. Results and discussion

1. Coating ratio

1.1 Preliminary remarks

In this study microparticles (host particles) were coated with nanoparticles (guest particles) during a mixing procedure in order to decrease interparticle interactions. The number of nanoparticles present in the nanoparticle - microparticle mixture plays an important role in flowability enhancement. The flowability is supposed to be enhanced, when the coating ratio is in between the so - called upper and lower coating limit (Huber et al., 2003) (see B.3.3).

As was mentioned in B.3.3.2, the lower coating limit is reached, when the microparticle is coated with such a number of nanoparticles that the contact between the microparticles is not possible anymore and abrupt decreasing of the Van der Waals forces can be observed. The upper coating limit is reached when the microparticle is completely covered by a monolayer of nanoparticles (see B.3.3.3).

When the particle diameter and the particle shape of both fractions are known, the upper and lower coating limit can be estimated. Different models were developed in order to calculate both coating limits (see B.3.3). All of these approaches assume host and guest particles to be spherical. In this study spray - dried and micronised microparticles of lactose, salbutamol base and salbutamol sulphate were used as model drugs. Although the spray - dried powders usually have a spherical shape, the micronised powders are far away from the desired configuration. The micronised particles are usually of non - spherical, irregular shape, therefore calculation models assuming sphericity are not perfectly adequate.

As a model nanoparticle Aerosil® R972 was chosen. Aerosil® R972 is not provided as a powder consisting of primary particles, but of agglomerates, which are usually formed during the manufacturing process (see C.1.2). Deviation of the agglomerates' geometry from sphericity may cause errors when calculating the number of the nanoparticles for the estimation of both, lower and upper coating limits. However, to the author's best knowledge there is no calculation model with the help of which the proper lower coating level for non - spherical particles, neither for host nor for guest particles, can be calculated. After having taken into account the above mentioned considerations, it was decided to carry out the calculation of the lower and upper coating limit only for the spray - dried microparticles, which are fairly spherical and the Aerosil® R972 agglomerates although they deviate from sphericity admittedly.

To transform the number of nanoparticles needed to cover the microparticles into the mass ratio of nanoparticles to microparticles, the density of the particles must be known. The spray - dried particles are usually hollow inside and may have an orifice in their surface, therefore difficulties in measuring the density of the particles may arise (see 2.4). Another possibility of determining the density is to calculate the density of the spray - dried particles. Assuming that the spray - dried particles are of the same diameter than the sprayed droplets and knowing the diameter of the sprayed droplets and the concentration of the sprayed solution, density can be calculated (see 2.4). So, the calculations of the percentage (w/w) of the nanoparticles in the mixtures were done assuming different densities for the spray - dried microparticles, either measured or calculated.

Though the density of the primary particles of Aerosil® R972 is known (see 2.4), the density of Aerosil® R972 agglomerates is not. For calculations of the lower and upper coating limit two different densities were assumed, a tapped density of the nanoparticle agglomerates and a density of the primary particles. The first one underestimates the true value probably, whereas the second one overestimates it.
In this chapter for the theoretical calculation of the lower coating limit the Bresges model (see B.3.3.2.2.2) and for the calculation of the upper coating limit the hexagon model was used (see B.3.3.3). The calculated coating limit values are considered as an approximation for the real nanoparticle/microparticle ratio.

1.2 Lower coating level according to Bresges model

To calculate the lower coating limit Bresges (Bresges et al., 2008) developed a new computation model (see B.3.3.2.2.2). With the help of the program the theoretical lowest number of guest particles, needed to keep two host particles on distance, was calculated in this study. The calculations were performed for spray - dried lactose, salbutamol sulphate and base as microparticles and Aerosil® R972 as nanoparticles.
Figure 27 shows the results of the calculation of the minimum needed number of guest particles (x_{50} of Aerosil® R972 agglomerates is assumed to be approximately 0.2 µm (see C.1.2 and 2.4) for spray - dried lactose (x_{50} = 8.37 µm ± 0.15 µm) (see 2.2) ensuring the non - contact of two lactose particles. If the number of guest particles is lower than 112, the host particles are able to contact each other and the distance between them is the shortest distance that can be taken up by two particles. In order to avoid a diverging force upon contact, the shortest distance cannot become smaller than the so - called contact distance a = 0.4 nm (see B.2.2).
The goal of the estimation of the lower coating limit is the successful reducing of the Van der Waals interactions between the microparticles. Apart from the calculations according to the Bresges model, the Van der Waals forces in dependence on the distance between the host particles at the site of the largest circumcircle (see B.3.3.2.2.2) were calculated.
If the host particles contact each other, the Van der Waals forces are quite strong (Figure 28), possibly leading to poor flowability and dispersion characteristics of the powder sample. If the spray - dried lactose host particle is covered with exactly 112 guest particles, the distance between the host particles is slightly increased (Figure 27), leading to an enormous decrease of the Van der Waals forces. Further increasing of the number of the guest particles results in a decrease of the distance between two host particles again and therefore, in an increase of the Van der Waals forces. So, it can be said, that though 112 is the number at which the first non - contact between host particles occurs, this number is still critical in terms of ensuring permanent non - contact conditions, because further increasing the number of guest particles may lead to contact between the host particles again. This phenomenon can be explained by differences of the local energy state and therefore of the total energy state, which are dependent on the symmetry of the placement of the guest particles on the surface of the host particles (Bresges et al., 2008). Increasing of the number of guest particles doesn't necessarily lead to non - contact of the host particles.

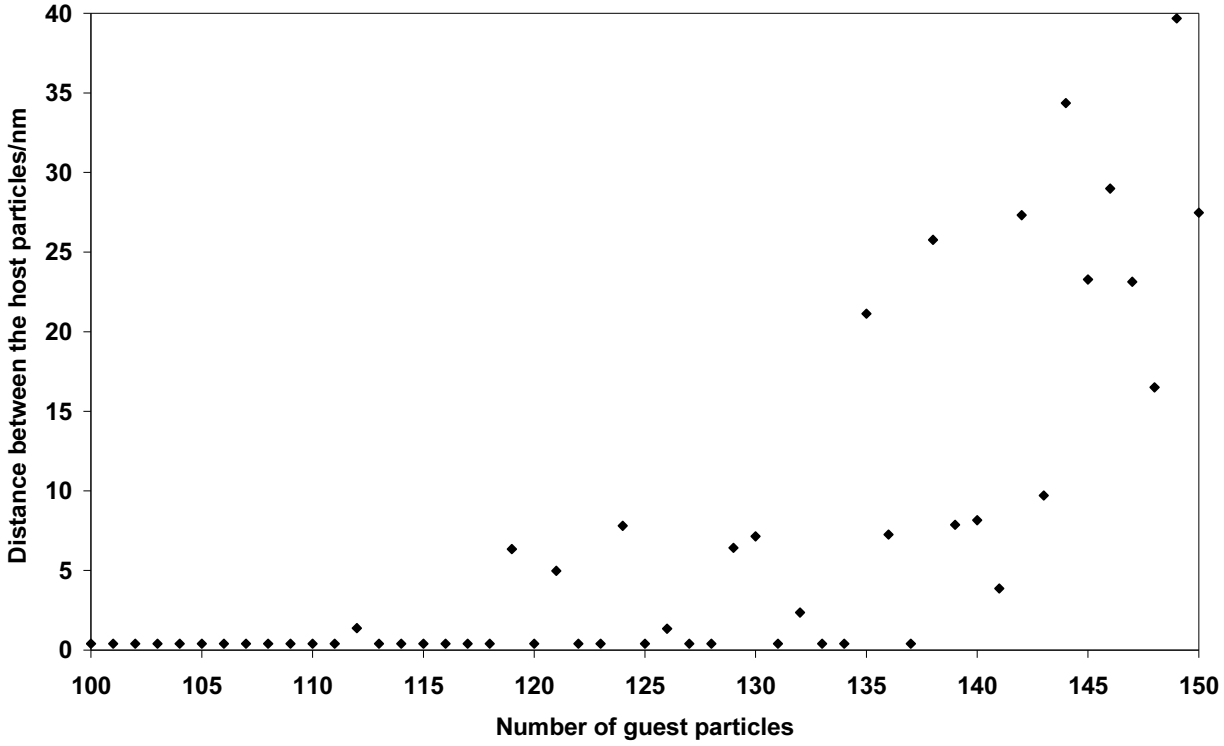

Figure 27: Dependence of the distance between the spray - dried lactose host particles on the number of the guest particles (Aerosil® R972)

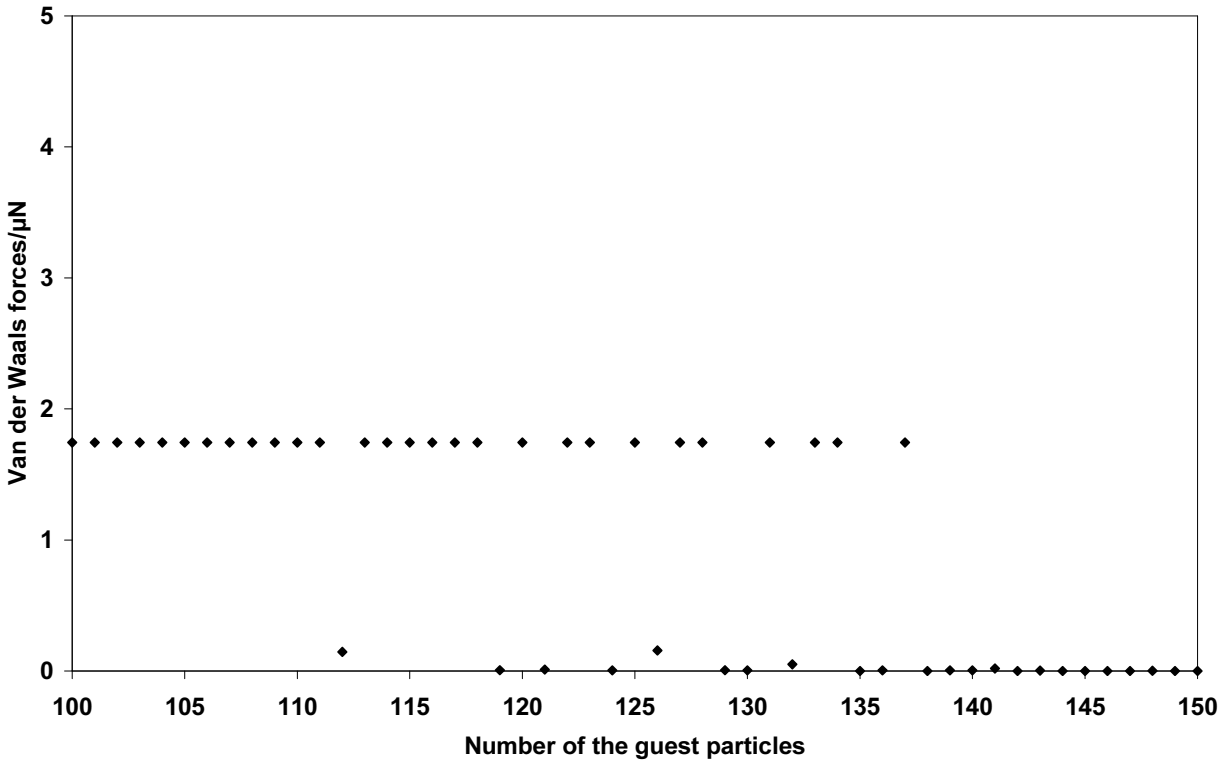

Figure 28: Dependence of the strength of the Van der Waals forces between the spray - dried lactose host particles on the number of the guest particles (Aerosil® R972)

Only covering of the host particles with 138 guest particles or more leads to permanent non - contact conditions. The number of 138 is the proper theoretical number, which ensures permanent non - contact conditions between the host particles and continuously decreased Van der Waals forces.

As was already mentioned in the preliminary remarks at the beginning of this chapter, different calculated and pycnometrically determined densities were used (see 2.4) for the calculation of the mass of the guest particles needed to cover the spray - dried lactose particles. Table 3 presents the results of these calculations. The calculations were carried out using the proper theoretical number (138) of nanoparticles.

According to the Bresges model, it can be seen, that depending on the densities assumed for Aerosil® R972 and lactose the concentration of Aerosil® R972 in the mixture with spray - dried lactose varies from 0.01 % to 4.26 %. The concentration of Aerosil® R972 actually needed to obtain the state of the lower coating limit will be probably laying in between the mentioned values.

Table 3: Concentration of Aerosil® R972 needed to cover spray - dried lactose at the lower coating limit according to the Bresges model. Values are calculated using particle density (helium) and calculated density values of lactose and tapped and primary particle density values of Aerosil® R972

	Concentration of Aerosil® R972 in the mixture/% (w/w)			
Lactose, x_{50} = 8.37 µm	x	x	x	x
Aerosil® R972, x_{50} = 0.2 µm	x	x	x	x
Lactose, $\rho_{measured}$ = 1.36 g/cm^3	x	x		
Lactose, $\rho_{calculated}$ = 0.0931 g/cm^3			x	x
Aerosil® R972, $\rho_{primary\ particle}$ = 2.2 g/cm^3	x		x	
Aerosil® R972, ρ_{tapped} = 0.05 g/cm^3		x		x
	0.30	**0.01**	**4.26**	**0.10**

In case of spray - dried salbutamol base differences in the minimum and proper theoretical number of nanoparticles can be detected also (Figure 29 and Figure 30). The calculated minimum number, which ensures the first non - contact and therefore the decreasing of the Van der Waals forces, in this case is 57 and the proper theoretical number, at and above which no contact between two host particles can be detected anymore, is 66.

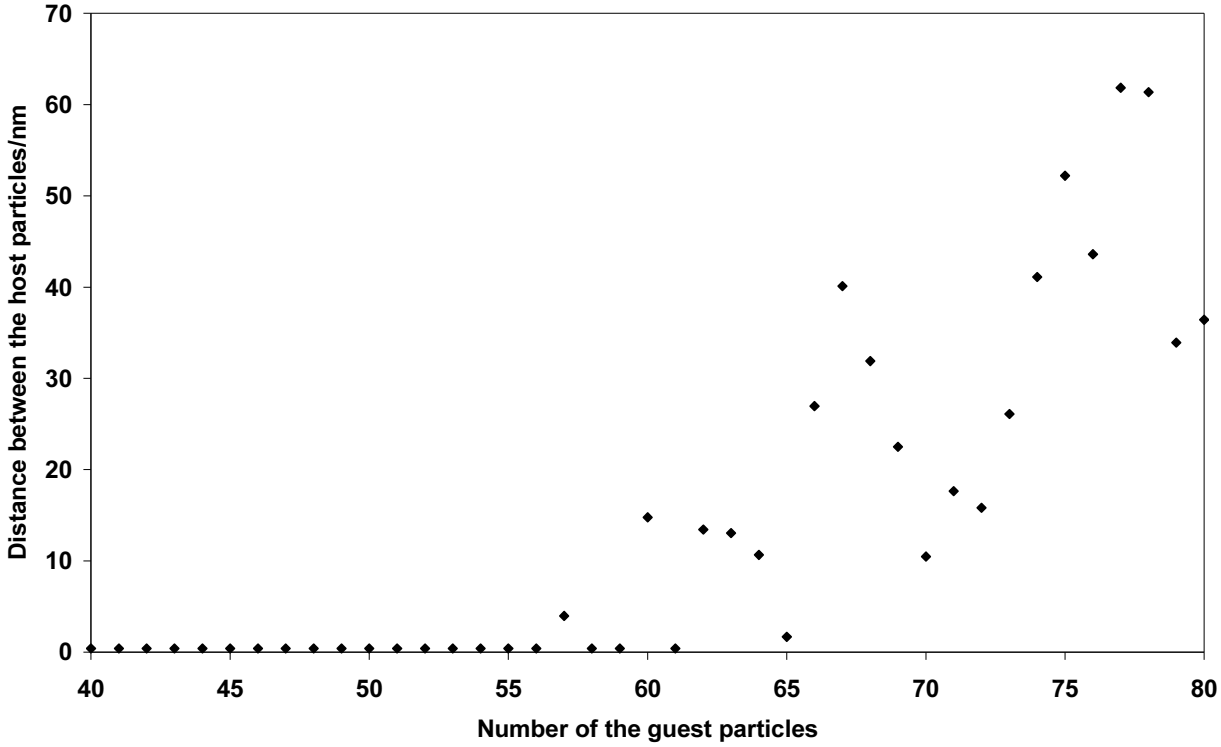

Figure 29: Dependence of the distance between the spray - dried salbutamol base host particles on the number of the guest particles (Aerosil® R972)

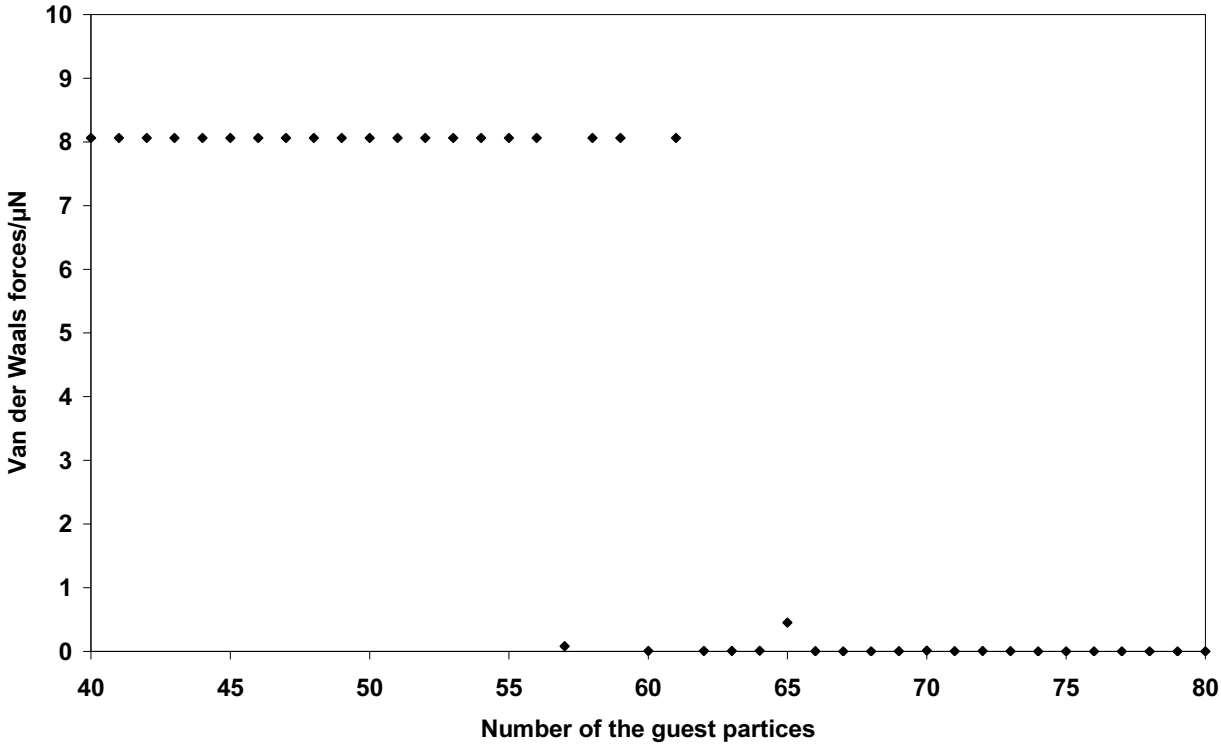

Figure 30: Dependence of the strength of the Van der Waals forces between the spray - dried salbutamol base host particles on the number of the guest particles (Aerosil® R972)

According the calculations the amount of Aerosil® R972 needed to cover spray - dried salbutamol base particles varies between 0.04 % and 17.71 % (Table 4).

Table 4: Concentration of Aerosil® R972 needed to cover spray - dried salbutamol base at the lower coating limit according to the Bresges model. Values are calculated using particle density (helium) and calculated density of salbutamol base and tapped and primary particles density values of Aerosil® R972

	Concentration of Aerosil® R972 in the mixture/% (w/w)			
Salbutamol base, x_{50} = 3.87 μm	x	x	x	x
Aerosil® R972, x_{50} = 0.2 μm	x	x	x	x
Salbutamol base, $\rho_{measured}$ = 1.16 g/cm^3	x	x		
Salbutamol base, $\rho_{calculated}$ = 0.0931 g/cm^3			x	x
Aerosil® R972, $\rho_{primary\ partcile}$ = 2.2 g/cm^3	x		x	
Aerosil® R972, ρ_{tapped} = 0.05 g/cm^3		x		x
	1.70	**0.04**	**17.71**	**0.49**

According to the calculations done for spray - dried salbutamol sulphate, the lower minimum number of the guest particles is 46 and the proper number is 54 (Figure 31 and Figure 32).

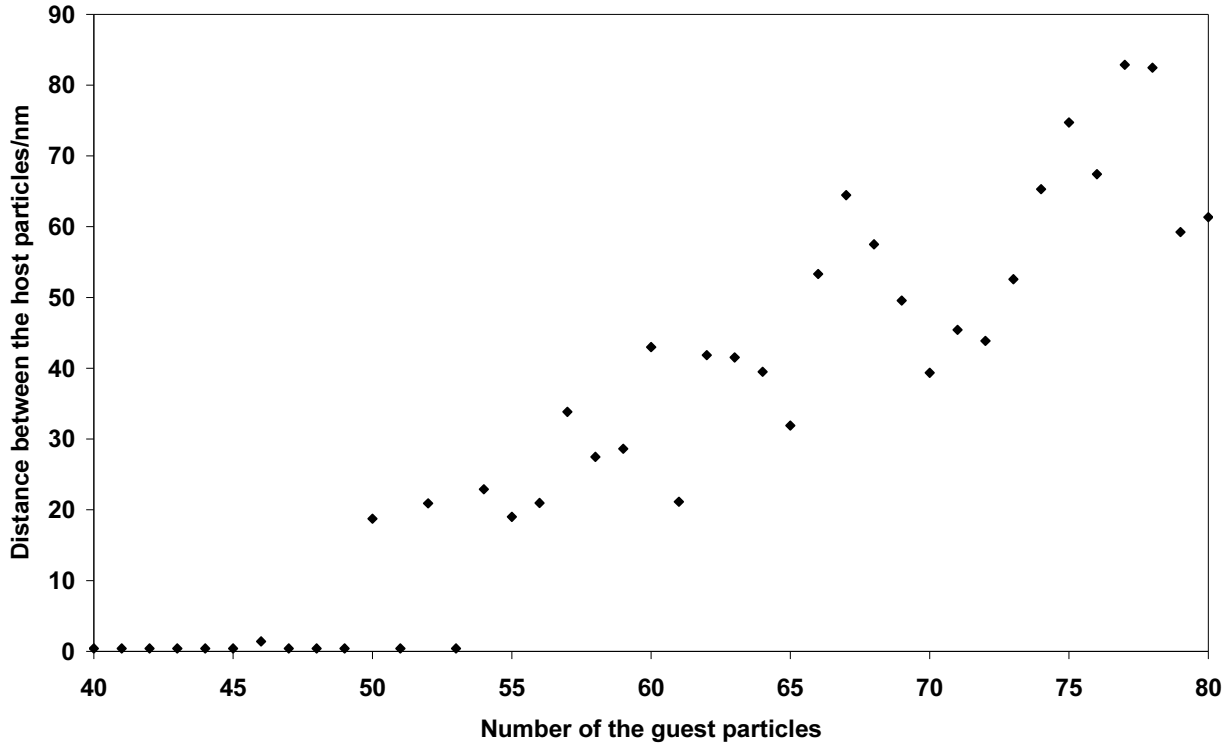

Figure 31: Dependence of the distance between the spray - dried salbutamol sulphate host particles on the number of the guest particles (Aerosil® R972)

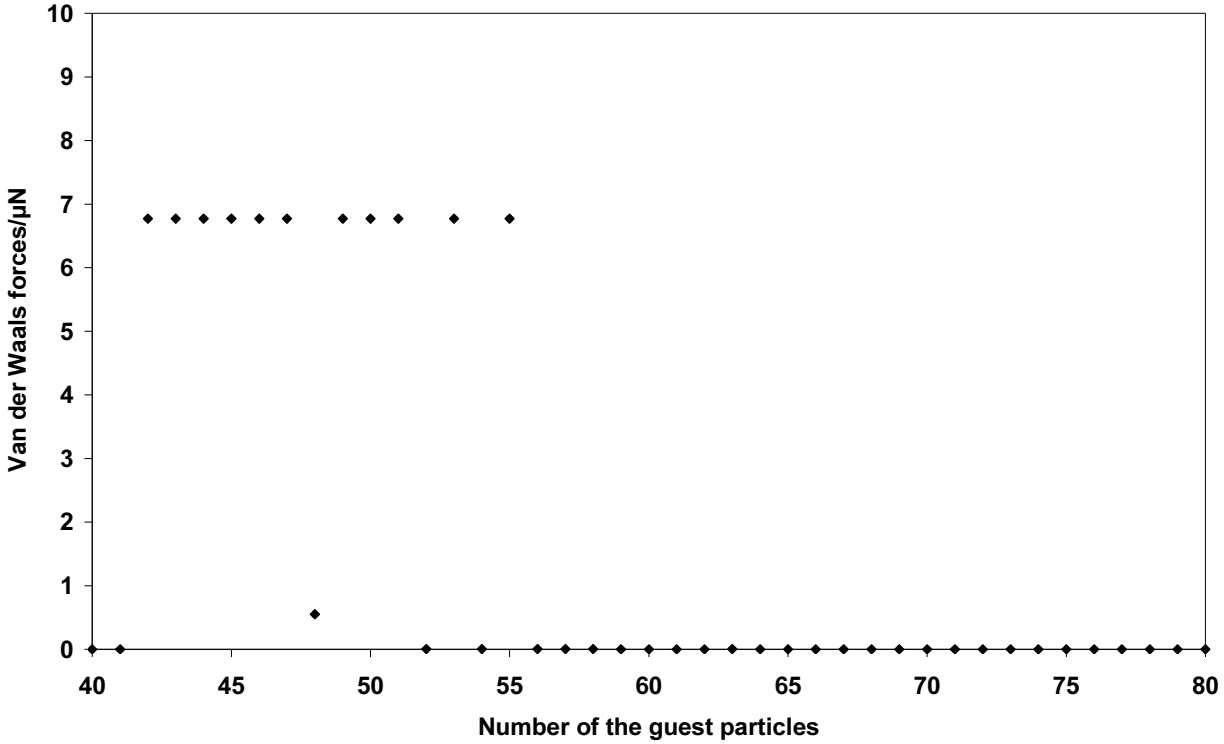

Figure 32: Dependence of the strength of the Van der Waals forces between the spray - dried salbutamol sulphate host particles on the number of the guest particles (Aerosil® R972)

The calculated lower amount of the guest particles in the mixtures containing spray - dried salbutamol sulphate and Aerosil® R972 ranges between 0.05 % and 22.78 % (Table 5).

Table 5: Concentration of Aerosil® R972 needed to cover spray - dried salbutamol sulphate at the lower coating limit according to the Bresges model. Values are calculated using particle density (helium) and calculated density of salbutamol sulphate and tapped and primary particles density values of Aerosil® R972

	Concentration of Aerosil® R972 in the mixture/% (w/w)			
Salbutamol sulphate, x_{50} = 3.25 µm	x	x	x	x
Aerosil® R972, x_{50} = 0.2 µm	x	x	x	x
Salbutamol sulphate, $\rho_{measured}$ = 3.25 g/cm^3	x	x		
Salbutamol sulphate, $\rho_{calculated}$ = 0.093 g/cm^3			x	x
Aerosil® R972, $\rho_{primary\ particle}$ = 2.2 g/cm^3	x		x	
Aerosil® R972, ρ_{tapped} = 0.05 g/cm^3		x		x
	2.05	**0.05**	**22.78**	**0.67**

As the minimal number of guest particles ensuring non - contact of the host particles depends on the particle sizes of the host and the guest particles, it can be seen, that the larger the diameter of the host particles, the higher the number of the nanoparticles needed to ensure non - contact of the host particles. In this study the particles of spray - dried lactose possess the greatest particle diameter x_{50} = 8.73 µm. The lowest particle diameter x_{50} = 3.25 µm was measured for salbutamol sulphate particles. Therefore, the calculated number of Aerosil® R972 was 138 for the spray - dried lactose, and for salbutamol sulphate 54. Nevertheless, because of decreasing of the specific surface with increasing particle size, the concentration (w/w) of the nanoparticles,

needed to obtain lower coating limit, decreases. So, in case of spray - dried lactose the amount of nanoparticles in the mixture is lower than in case of salbutamol sulphate.

1.3 Upper coating level

The upper coating limit is defined as the densest monolayer of guest particles on the surface of the host particles. To cover the surface of spherical host particle with spherical guest particles, the hexagon model, where one guest particle claims the surface of a hexagon, may be used (see B.3.3.3).

In the following tables (Table 6 - Table 8) the amount of nanoparticles needed to obtain upper coating limit conditions for spray - dried lactose, salbutamol base and salbutamol sulphate are shown. Here again, the coating ratios obtained using different measured and calculated densities of microparticles and tapped and primary particle densities of nanoparticles are presented. Particle sizes and densities are described in chapter 2.

Table 6: Concentration of Aerosil® R972 needed to cover spray - dried lactose at the upper coating limit according to the hexagon model. Values are calculated using particle density (helium) and calculated density of lactose and tapped and primary particle density values of Aerosil® R972

	Concentration of Aerosil® R972 in the mixture/% (w/w)			
Lactose, x_{50} = 8.37µm	x	x	x	x
Aerosil® R972, x_{50} = 0.2 µm	x	x	x	x
Lactose, $\rho_{measured}$ = 1.36 g/cm^3	x	x		
Lactose, $\rho_{calculated}$ = 0.0931 g/cm^3			x	x
Aerosil® R972, $\rho_{primary\ particle}$ = 2.2 g/cm^3	x		x	
Aerosil® R972, ρ_{tapped} = 0.05 g/cm^3		x		x
	12.33	**0.37**	**67.18**	**4.45**

Table 7: Concentration of Aerosil® R972 needed to cover spray - dried salbutamol base at the upper coating limit according to the hexagon model. Values are calculated using particle density (helium) and calculated density of salbutamol base and tapped and primary particles density values of Aerosil® R972

	Concentration of Aerosil® R972 in the mixture/% (w/w)			
Salbutamol base, x_{50} = 3.87µm	x	x	x	x
Aerosil® R972, x_{50} = 0.2 µm	x	x	x	x
Salbutamol base, $\rho_{measured}$ = 1.16 g/cm^3	x	x		
Salbutamol base, $\rho_{calculated}$ = 0.0931 g/cm^3			x	x
Aerosil® R972, $\rho_{primary\ partcile}$ = 2.2 g/cm^3	x		x	
Aerosil® R972, ρ_{tapped} = 0.05 g/cm^3		x		x
	26.22	**0.80**	**81.58**	**9.14**

Table 8: Concentration of Aerosil® R972 needed to cover spray - dried salbutamol sulphate at the upper coating limit according to the hexagon model. Values are calculated using particle density (helium) and calculated density of salbutamol sulphate and tapped and primary particles density values of Aerosil® R972

	Concentration of Aerosil® R972 in the mixture/% (w/w)			
Salbutamol sulphate x_{50} = 3.25 µm	x	x	x	x
Aerosil® R972, x_{50} = 0.2 µm	x	x	x	x
Salbutamol sulphate, $\rho_{measured}$ = 3.25 g/cm^3	x	x		
Salbutamol sulphate, $\rho_{calculated}$ = 0.093 g/cm^3			x	x
Aerosil® R972, $\rho_{primary\ particle}$ = 2.2 g/cm^3	x		x	
Aerosil® R972, ρ_{tapped} = 0.05 g/cm^3		x		x
	27.20	**0.84**	**84.03**	**10.68**

According to the calculations the highest upper coating limit varies from 0.37 % to 67.18 % in case of spray - dried lactose, in case of spray - dried salbutamol base from 0.80 % to 81.58 % and in case of salbutamol sulphate from 0.84 % to 84.03 %, depending on the densities, which were used for the calculations.

1.4 Concluding remarks

In conclusion it has to be stated, that even though calculations of the lower and upper coating limits have been carried out for spray - dried lactose, salbutamol base and salbutamol sulphate host particles and Aerosil® R972 as guest particle fraction, the results obtained for each limit and each host - guest pair cover the range of several decimal powers. This is due to the already mentioned difficulties in the estimation of the densities probably resulting in the deviation of the calculated values from the true values. Another factor causing differences between calculated and true values is the assumption, that all guest particles take part on the coverage of the surface of the host particles. However, this is not reality. The guest particles may stick to each other rather than to the host particles and form agglomerates, leading to a lower number of discrete particles actually taking part in the coverage of the host particles surface. It was assumed for the calculations, that both particle fractions, the host as well as the guest particle fraction, are spherical. Although the shape of the spray - dried host particles is fairly spherical, the shape of Aerosil® R972 guest particle agglomerates is not, also possibly causing deviation of the calculated values from the true ones.

After all theoretical calculations and considerations, it was decided to prepare powder mixtures with Aerosil® R972 concentrations ranging from the lowest value of the lower coating limit to the highest value of the upper coating limit for the guest/host pair Aerosil® R972/spray - dried lactose and to double check the coverage of the host particles by the guest particles using SEM (Figure 33) first. The lowest value determined for the lower coating limit is 0.01 % and the highest value of the upper coating limit is 67.18 %, so a range of different concentrations of guest particles, namely 0 %, 0.5 %, 2.5 %, 12.5 % and 67.5 % were prepared by mixing both fractions in a TURBULA® mixer. According to the SEM photographs of spray - dried lactose covered by 12.5 % (Figure 33 c) and 67.5 % of Aerosil® R972 (Figure 33 d), the host particle is coated by far more than one layer of guest particles, which means, that both concentrations lay

beyond the upper coating limit. In this case mechanical interlocking is likely to occur, leading to the deterioration of the powder characteristics in terms of flowability and dispersion. So, it was decided not to prepare two mixtures with guest particle numbers above the upper coating limit and to skip the mixtures containing 67.5 % Aerosil® R972. Finally, the highest guest particle concentration was chosen to be 12.5 %.

In the mixture, which contains 0 % Aerosil® R972, the amount of guest particles lays definitely below the lower coating limit. As for the mixtures with 0.5 % (Figure 33 a) and 2.5 % (Figure 33 b), it is not possible to decide from an SEM photograph whether these concentrations will be between the lower and the upper coating limit or below the lower coating limit. Anyway, these concentrations of Aerosil® R972 lay definitely below the upper coating limit, because in both cases, the host particles are not completely covered with a monolayer of guest particles. Where the precise values of the upper and the lower coating limit, and - even more important - the precise value ensuring minimum interparticle interactions lay in fact, may only be decided with the help of investigations on flowability, mass uniformity and respirable fraction. Thus the fine tuning in the range between 0 % and 12.5 % would have to be done depending on the results obtained by these studies. It is also important to keep in mind, that the calculated values of the lower and upper coating limits are only approximations to the values, at which interparticle interactions are minimum and flowability, mass uniformity and respirable fraction are maximum. In reality, improvement of flowability may be achieved with much less spacers situated on the surface of the host particles than calculated for the theoretical values, because the contact between two host particles may be already prevented below the calculated coating level as contact may not necessarily take place at the site of the largest circumcircle. However, this was assumed for the above calculations of the interparticle interactions (see 1.2).

To be able to compare the results obtained using different spray - dried host particles, namely lactose, salbutamol base and salbutamol sulphate, and to compare the results of spray - dried and micronised host particles, the same concentrations of Aerosil® R972 calculated for spray – dried lactose were used for all host particles irrespective of their chemical identity, particle size and mode of preparation.

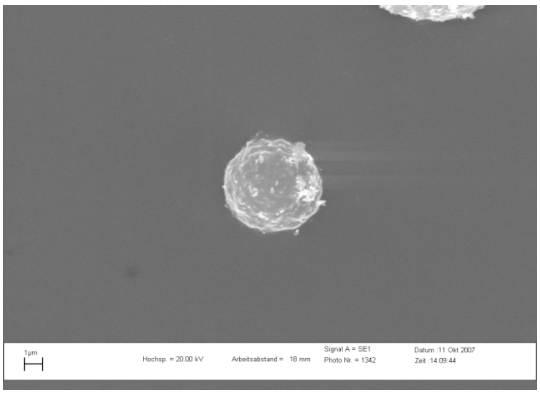

a: Mixture of lactose (sd) and 0.5% Aerosil® R97, TM 90 min

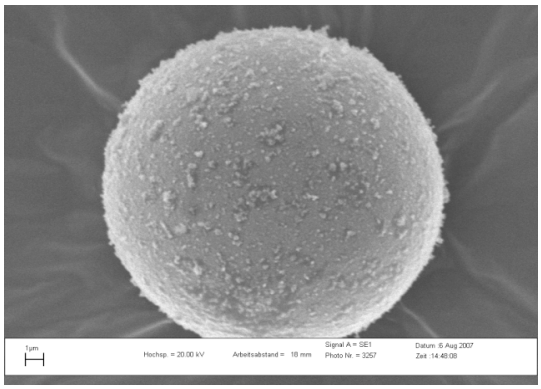

b: Mixture of lactose (sd) and 2.5% Aerosil® R972, TM 90 min

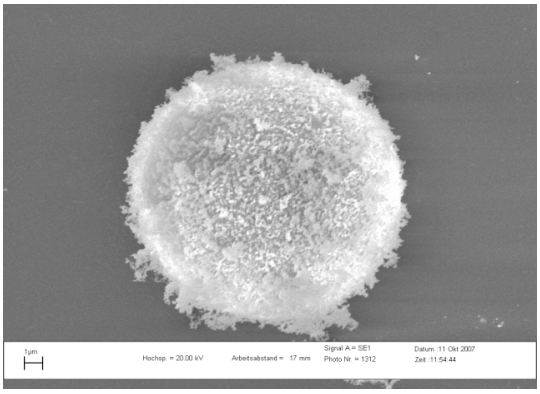

c: Mixture of lactose (sd) and 12.5% Aerosil® R972, TM 90 min

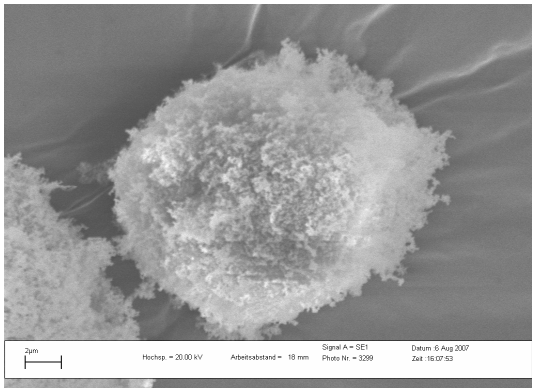

d: Mixture of lactose (sd) and 67.5% Aerosil® R972, TM 90 min

Figure 33 a - d: Scanning electron micrograph (magnification: 4000x) of the mixtures containing spray - dried (sd) lactose and 0.5 %, 2.5 %, 12.5 % and 67.5 % Aerosil® R972 prepared using conventional mixing (TM 90 min)

2. Characterisation of the particle size, shape and density

2.1 Preliminary remarks

In the following experiments spray - dried (sd) and micronised (m) α - lactose - monohydrate (lactose), salbutamol base (SB) and salbutamol sulphate (SS) were used as active ingredient models. As nanoparticle model hydrophobic silicon dioxide (Aerosil® R972) was employed.

2.2 Laser diffraction

The determination of the particle size distribution of the active ingredient models was carried out using laser diffraction (see C.2.1 and E.3.1). The median of the particle size distribution for each drug model is presented in Table 9. It is lowest for spray - dried salbutamol sulphate (x_{50} = 3.25 µm) and highest for spray - dried lactose (x_{50} = 8.37 µm). The particle size of spray - dried lactose is high with respect to the respirable particle size. Nevertheless, the experiments were still carried out in order to investigate the performance of the different formulations and mixing procedures.

In case of the micronised products, salbutamol base was used as received. Salbutamol sulphate and lactose were milled in an air jet mill. The median of the micronised products is below 5 µm. However, the median of the lactose particles is highest again. The differences in size may be explained by the fact that the output size depends on the individual milling characteristics of each material.

Table 9: Median ± s.d. of the particle size of spray - dried and micronised materials (n = 3)

Substance	Median/µm	Standard deviation/µm
Lactose, spray - dried	8.37	± 0.16
Salbutamol base, spray - dried	3.87	± 0.13
Salbutamol sulphate, spray - dried	3.25	± 0.08
Lactose, micronised	4.95	± 0.41
Salbutamol base, micronised	1.95	± 0.16
Salbutamol sulphate, micronised	2.11	± 0.20

2.3 Scanning electron microscopy

Scanning electron micrographs (SEM) (see C.2.2 and E.3.2) were used for the illustration of shape, surface topography (e.g. asperities) and also size of the active ingredient models, which were further used for the production of the host - guest formulations. The following images (Figure 34 a - f) show the SEM pictures of spray - dried and micronised lactose, salbutamol base and salbutamol sulphate, respectively.

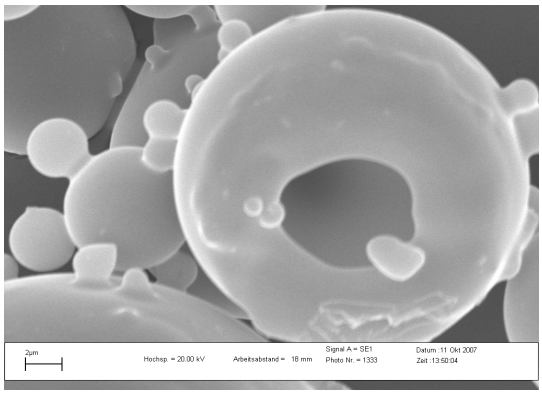

a: Spray - dried lactose

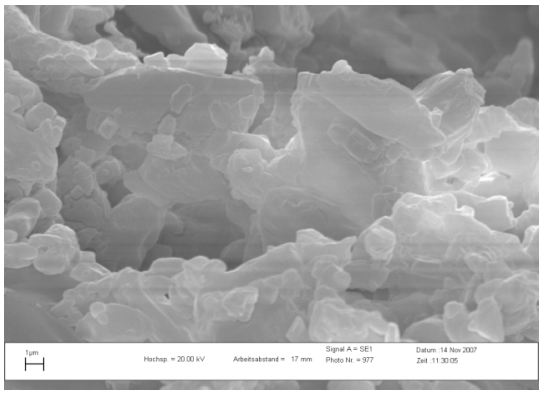

b: Micronised lactose

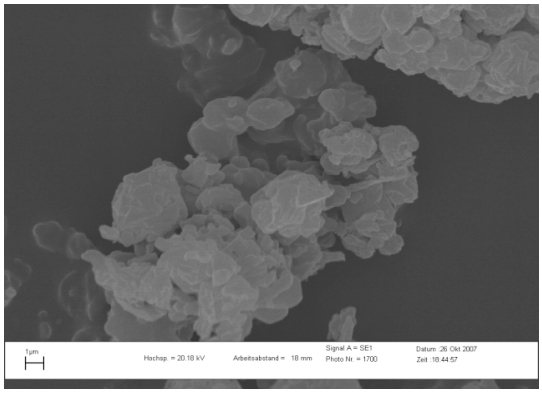

c: Spray -dried salbutamol base

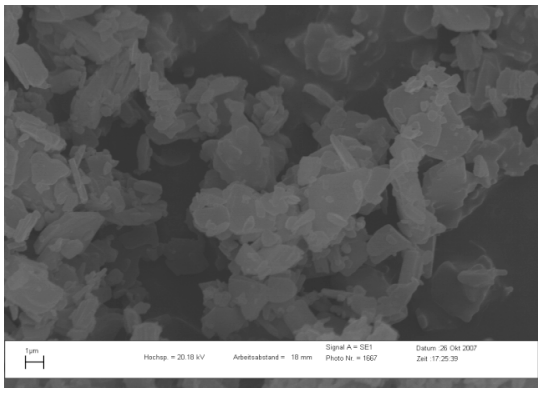

d: Micronised salbutamol base

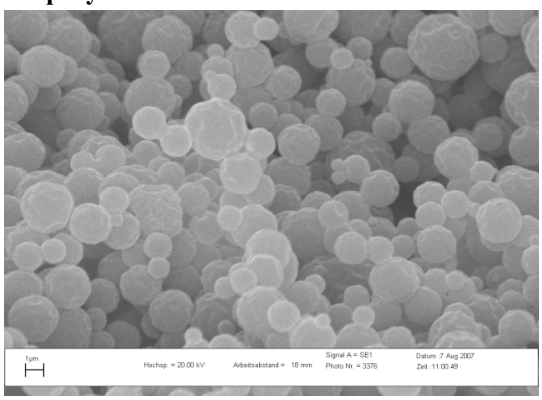

e: Spray - dried salbutamol sulphate

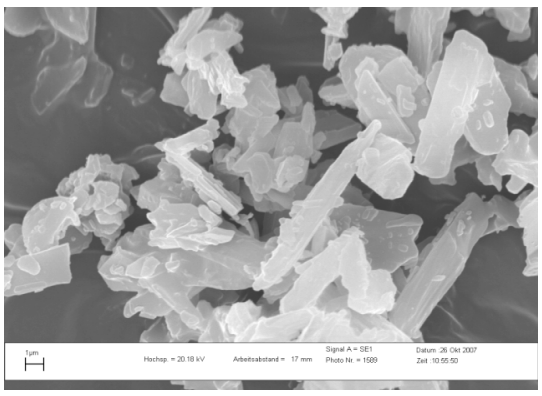

f: Micronised salbutamol sulphate

Figure 34 a - f: Scanning electron micrographs (magnification: 4000x) of spray - dried and micronised active ingredient models

According Figure 34 a the spray - dried lactose particles are of spherical shape. An orifice in the wall of the particles, which is generated during the drying process, is observed. The particle

surface is smooth, though curvilinear. Spray - dried lactose and salbutamol sulphate (Figure 34 a, e) are known to be obtained in the amorphous form usually, whereas salbutamol base (see Figure 34 c) is crystalline. It might be expected, that the crystallinity/amorphicity of the particles may influence the shape of it. Probably, because of the crystallisation during the spray - drying procedure, salbutamol base particles appear irregular, in contrast to the products which stay amorphous. The shape of the spray - dried salbutamol sulphate is spherical, though the surface of the particles is not as smooth as the surface of spray - dried lactose. Spray - dried lactose and salbutamol sulphate will be shown to be amorphous later on in this section, whereas salbutamol base will turn out to be crystalline (see 3).

Figure 34 b, d and f show the micrographs of micronised lactose, salbutamol base and salbutamol sulphate, respectively. In contrast to spray - dried spherical particles, micronised particles show an irregular shape. Because of this shape with numerous edges, particles might be prevented from getting into close contact. Also, the presence of fines in the samples of micronised lactose, salbutamol base and salbutamol sulphate is striking. The fines may play the role of spacers, when adhered on the surface of the larger particles, decreasing thereby the interparticle interactions between the latter. It is also one of the major points of interest in this work, to find out, whether the coating of micronised host particles with nanoparticulate guest particles leads to an enhancement of the flowability, dosing and respirable fraction or whether the addition of nanoparticles may even deteriorate these important characteristics by filling of the cavities on the surface of the microparticles resulting in surface smoothening.

2.4 Density

2.4.1 Active ingredient models

The densities of lactose, salbutamol base and salbutamol sulphate were determined using helium pycnometry (see C.2.3 and E.3.3). Determined values of the particle density (helium) were further used for the calculation of the lower and upper coating limits (see B.3.3 and 1). According to Table 10, the density of micronised lactose particles is significantly higher than the one of spray - dried particles. This may be attributed to the high density of the predominantly crystalline micronised product in comparison to the predominantly amorphous spray - dried material (see 3.1.2). The same applies for salbutamol sulphate (see 3.1.4). On the contrary, the densities of micronised and spray - dried salbutamol base do not differ, because salbutamol base is crystalline also after spray - drying.

Table 10: Mean ± s.d. of the particle density (helium) of the spray - dried and micronised active ingredient models, (n = 5)

Substance	Spray - dried powder/g/cm^3	Micronised powder/g/cm^3
Lactose	1.36 ± 0,0001	1.57 ± 0.0070
Salbutamol base	1.15 ± 0,0037	1.16 ± 0.0105
Salbutamol sulphate	1.31 ± 0,0078	1.34 ± 0.0061

The spray - dried particles are spherical and usually hollow inside. Furthermore, they may have a hole in their surface, due to the evaporation of the solvent from inside the particle in outside direction during the drying process (Figure 35):

Figure 35: Scheme of spray - dried particles, hollow inside (a), with additional orifice in the particle wall (b)

The density determination of the spray - dried products exhibiting an orifice in the wall by helium pycnometry actually gives the density of the wall. For the calculation of the coating limit, apart from the radius, the average density of the hollow particles is needed in order to be able to calculate the surface area of a given mass of particles. Equation 60 represents the term for the calculation of the mass of one particle:

$$m_p = \frac{4}{3} \cdot \pi \cdot r_p^3 \rho_p \qquad \textbf{Equation 60}$$

where r_p is the particle radius and ρ_p the density of the particle. Knowing the mass of one particle and the total mass of the sample $m_{p\ total}$ the number $N_{p\ total}$ of the particles in the sample can be estimated:

$$N_{p\ total} = \frac{m_{p\ total}}{m_p} \qquad \textbf{Equation 61}$$

Knowing the number of the particles in the sample, the total area of the particles $A_{p\ total}$, which is needed to be covered with nanoparticles, may be calculated according to the following equation:

$$A_{p\ total} = N_p \cdot \frac{3}{4} \cdot \pi \cdot r_p^2 \qquad \textbf{Equation 62}$$

This means, that the higher the density the lower is the total surface area of a given mass of the sample, which must be coated with nanoparticles. Given the presence of a hole in the wall of the spray – dried microparticulate powder, the density of the particle determined by helium pycnometry is higher than the one needed to calculate the required particle surface area, finally resulting in an underestimation of the amount of nanoparticles, needed to cover the microparticles.

Due to the impossibility of the experimental determination of the appropriate density, the density of the spray - dried particles was calculated approximately. Mass, volume and density of a spherical spray - dried particle were calculated using Equation 63 - Equation 66.
The volume of one spray - dried particle with radius r_p can be determined using the following equation:

$$V_p = \frac{4}{3}\pi \cdot r_p^3 \qquad \textbf{Equation 63}$$

Given the assumption that the volume of the spray - dried particle equals the volume of the sprayed droplet, the mass of one droplet m_d may be calculated according the next equation:

$$m_d = \rho_d \cdot V_p \qquad \textbf{Equation 64}$$

where ρ_d is the density of the droplet which roughly equals the density of water in case of a dilute solution. Knowing the concentration c of the active ingredient in the solution, the mass of the spray - dried particle may be calculated according to the following equation:

$$m_p = m_d \cdot c \qquad \textbf{Equation 65}$$

Finally, the density of the particle can be determined as follows:

$$\rho_p = \frac{m_p}{V_p} \qquad \textbf{Equation 66}$$

The calculated particle densities of spray - dried lactose, salbutamol base and salbutamol sulphate are listed in Table 11. The calculations of the lower and upper coating limits were done using both, the measured and theoretically calculated densities.

Table 11: Calculated particle densities of the spray - dried active ingredient models

Substance	**Density/g/cm^3**
Lactose	0.0931
Salbutamol base	0.0931
Salbutamol sulphate	0.0930

2.4.2 Aerosil® R972

The density of the primary particles of Aerosil® R972 is 2.2 g/cm^3 (Degussa, 2001). As already mentioned, it is impossible to disperse Aerosil® R972 agglomerates till the size of primary particles. The lowest size of the agglomerates after dispersion in liquid nitrogen with the high - speed homogenator ULTRA - TURRAX® is approximately 200 nm (Linsenbuehler, 2005). The tapped density of Aerosil® R972 is 0.05 g/ml (Degussa, 2001), which might be closer to the density of the agglomerates than the density of the primary particles. Therefore, for the calculations of the lower and upper coating limits (see 1) both, tapped density and the density of the primary particles, were used.

3. Impact of mixing on crystallinity

3.1 Moisture sorption

3.1.1 Preliminary remarks

The samples of the untreated spray - dried and micronised powders, as well as the ones treated by conventional and electrostatically supported mixing, were examined by moisture sorption (see C.2.4.2 and E.3.4). The experiments were carried out in humidity and temperature controlled chamber. Every six minutes a balance measured the weight of the samples exposed to a defined humidity program. Sorption isotherms were obtained by plotting the mass change at equilibrium against the relative humidity. Both, sorption and desorption were registered. After the completing of the first cycle a second cycle was carried out in order to check, whether recrystallisation processes of amorphous material, possibly present in the sample, had been completed during the first cycle (Gorny et al., 2007).

3.1.2 Lactose

Figure 36 displays the moisture induced mass change of crystalline α - lactose monohydrate over time. At first a mass loss at 0 % RH is detectable. This is caused by the loss of water, which has not been removed completely during storage over silica gel prior to analysis. Raising the relative humidity is associated with an increase of mass. The higher the humidity raises, the higher the mass gain. Despite its good solubility in aqueous media, α - lactose monohydrate is not hygroscopic (Buckton et al., 1995 (c)). Up to 95 % RH the registered weight increase is below 0.4 %. Upon increase of the relative humidity the water is adsorbed on the surface of the crystalline sample (Buckton et al., 1995 (c)). The results documented in the literature are confirmed by the present experiments. Decreasing the relative humidity, after having reached 95 % RH, leads to a decrease of mass.

The mass, which has been measured at 0 % RH at the beginning of the first cycle, was not achieved again at the end of the first cycle. The weight of the lactose at the end of the first cycle is 0.046 % higher than at the beginning. The differences between the mass at the beginning and at the end of the first cycle may be explained by the fact that equilibrium conditions for the micronised powder were not appropriate and the sample was not completely dry at the end of the first cycle at 0 % RH. Probably, by modifying the equilibrium conditions it may be possible to achieve the same sample weight at the beginning and the end of the first cycle. This applies especially if agglomerates that might have been formed at higher relative humidity cause the incorporated water to be entrapped within the agglomerates and not to be given off slowly. Another possible explanation for the fact that not all of water is given off, could be, that at the beginning of the test not all lactose crystals were crystals of α - lactose monohydrate, but of an unstable modification of anhydrous α - lactose, which can be rapidly transformed into α - lactose monohydrate even at ambient humidity (Lerk, 1987; Kirk et al., 2007). Therefore, the water is not expelled from the material after the lowering of the relative humidity completely, but remains as crystal water, because of the formation of α - lactose monohydrate. Another explanation might be that surface defects or minor amorphous parts heal or recrystallise to form α - lactose monohydrate causing an increase of the water content at 0 % RH at the end of the first cycle.

Furthermore, the mass change over time of the second cycle is not equal to the first cycle. During the second cycle the measured water uptake at 95 % RH is lower than during the first cycle. This may be due to the fact that α - lactose monohydrate takes up less water than anhydrous α - lactose. Another explanation could be that the amount of the surface defects during the second cycle is lower than in the first cycle, because of the recrystallisation of the voids, the energy state of the powder during the second cycle is lower, leading to a diminished possibility of water uptake. Another probable explanation may be that during the increasing of the relative humidity up to 95 % RH, local dissolution phenomena on the particle surface may have taken place leading to the formation of agglomerates and to the decrease of the specific surface of the powder sample. If the specific surface of the powder sample during the second cycle is smaller than during the first cycle, a lower amount of water will be adsorbed on the surface, leading to a difference of the mass gain between the two sorption cycles.

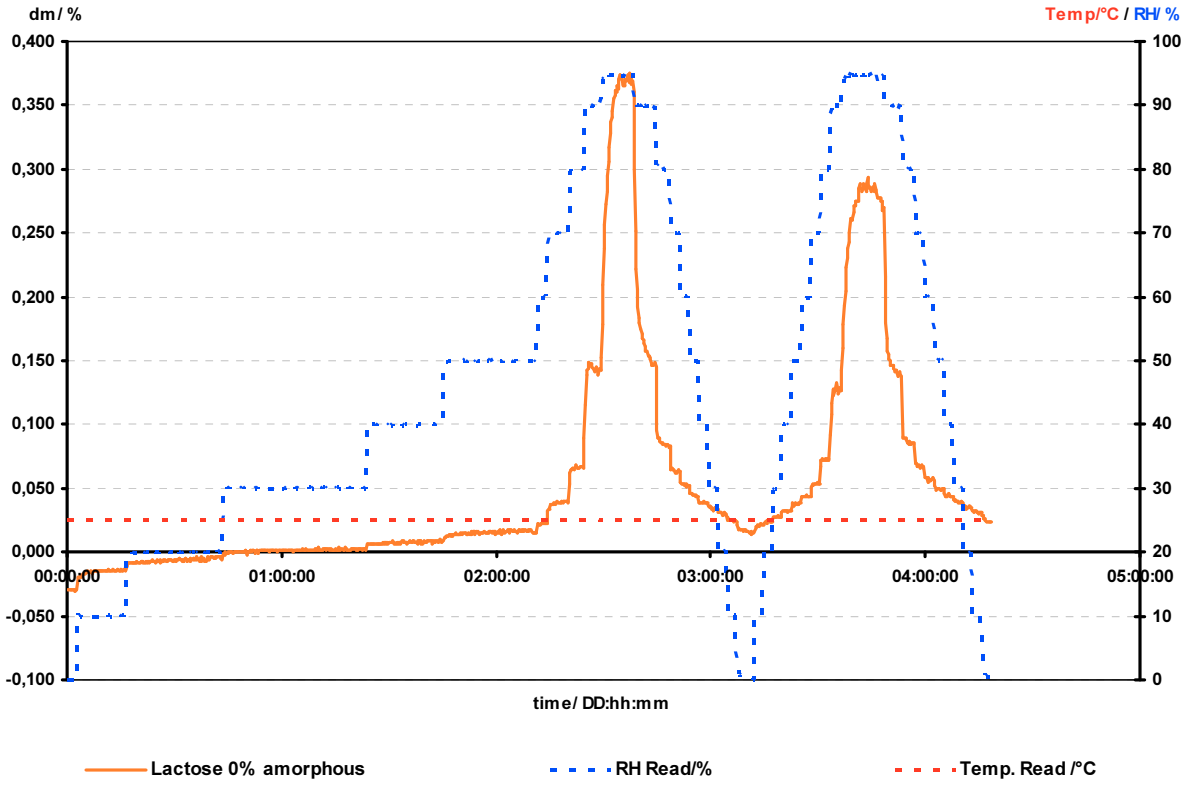

Figure 36: Mass change of crystalline α - lactose monohydrate over time, 0 % RH - 95 % RH, 25°C, the curve of the first of two measurements is presented

Figure 37 shows the mass change over time of amorphous lactose. In order to produce the amorphous powder an aqueous solution of lactose was spray - dried using the spray - drying parameters described in E.2.2. Initially, up to 50 % RH, this sample shows a higher mass increase than the crystalline sample at the same relative humidity. In contrast to the mass increase of the crystalline sample, a mass decrease is detectable at 50 % RH, which is ascribed to recrystallisation. Upon crystallisation the absorbed water is expelled from the just - forming crystal lattice, which is accompanied by the weight loss. At higher relative humidities, the curves

of the amorphous and the crystalline samples are similar. Also, the curve of the second cycle is similar to that of the crystalline sample.

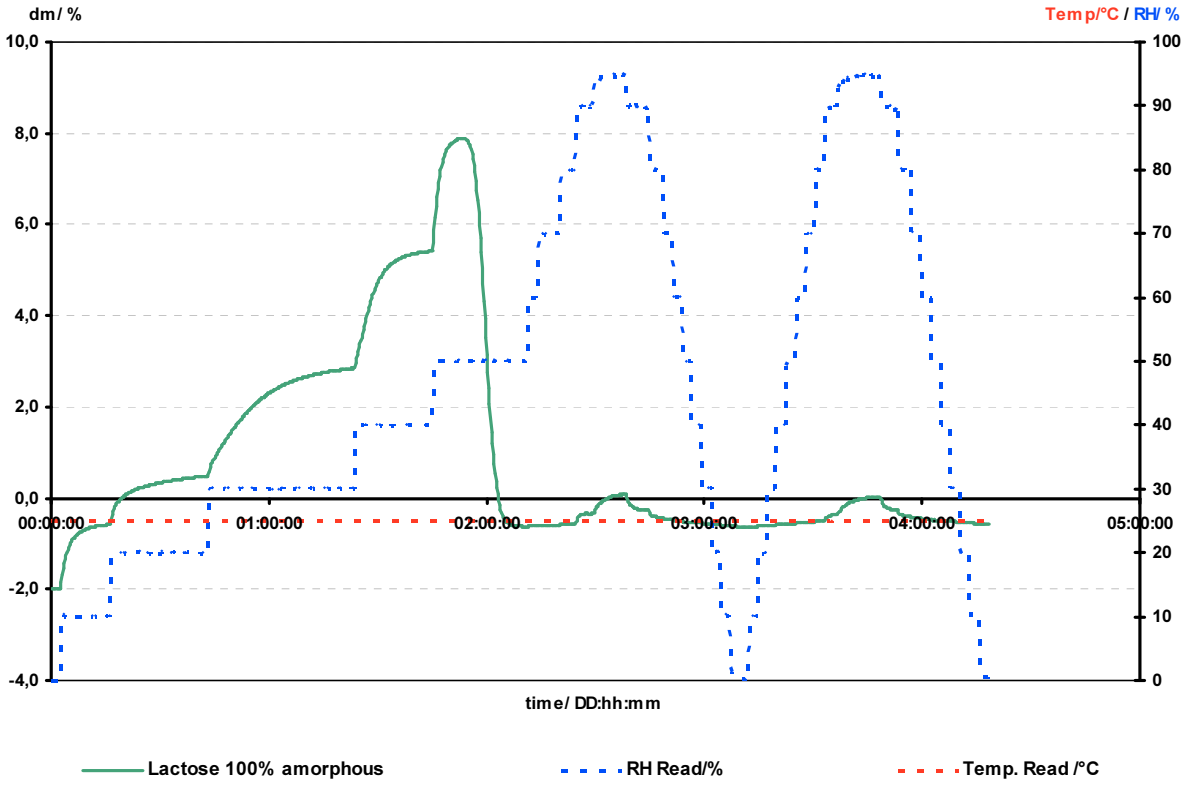

Figure 37: Mass change of amorphous spray - dried lactose over time 0 % RH - 95 % RH, 25 °C, the curve of the first of two measurements is presented

As expected, the weight at 0 % RH at the end of the first cycle is higher than the corresponding value at the beginning of the first cycle. The reason for this is that during the first cycle the sorbed water caused the amorphous material to recrystallise and to form the monohydrate (Buckton et al., 1995 (c)). The weight of the powder at the beginning of the first sorption cycle is lower than at the end. Knowing the mass of the amorphous sample at 0 % RH and the molecular weight of α - lactose monohydrate (360.29 g/mol) and of amorphous lactose (342.29 g/mol) the theoretical weight gain after the recrystallisation of the totally amorphous sample can be calculated. If the sample of the amorphous lactose would had recrystallised completely to form the monohydrate, the theoretical weight gain at 0 % RH at the end of the first sorption cycle would have been 5.26 %. In case of the investigated spray - dried lactose the mass gain is about 1.5 %, corresponding to a water content less than the crystal water content of α - lactose monohydrate. Similar results were reported by Elamin (Elamin et al., 1995). An explanation could be that during the recrystallisation a mixture of α - lactose monohydrate and the stable modification of anhydrous lactose is formed (Elamin et al., 1995). Another explanation could be the formation of β - lactose during recrystallisation. Steckel (Steckel et al., 1997) reported that recrystallisation at 100 % RH led to the formation of α - lactose monohydrate, but recrystallisation at lower relative humidities led to the increasing of the amount of β - lactose.

During the investigations of the recrystallisation behaviour of the powder samples the relative humidity was raised in 10 % RH steps beginning from 0 % RH and ending at 95 % RH. This means that part of the formed crystalline lactose could be β - lactose. Another possibility might be, that the amorphous sample recrystallises only at the surface of the powder, preventing the water molecules from further penetration into the sample and leaving amorphous areas inside. One more explanation is, that the spray - dried lactose sample was not fully amorphous. However, this assuming is not confirmed by differential scanning calorimetry and X - ray diffractometry investigations, that will be shown later (see 3.2.2 and 3.3.2).
The sorption isotherms (Figure 38 a, b) of samples containing 100 % crystalline and 100 % amorphous lactose are constructed using the mass change of lactose at equilibrium at different relative humidities. Figure 38 a shows, that the crystalline sample of lactose behaves in a different way than the amorphous sample (Figure 38 b). There is no mass decrease at 50 % RH, when increasing the relative humidity in the first cycle. The maximal water uptake of the crystalline sample is below 0.4 %, though the water uptake in the amorphous sample is more than 5 %. Due to the formation of α - lactose monohydrate the mass of the amorphous sample at the end of the first cycle is considerably higher than at the beginning of the first cycle.

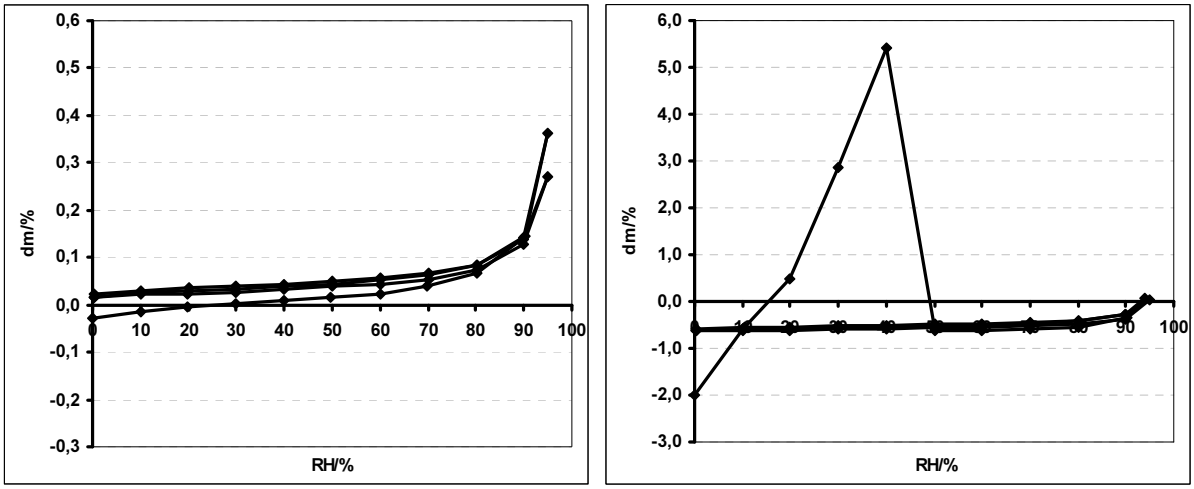

a b

Figure 38: Sorption isotherms of samples of 0 % (a) and 100 % (b) amorphous lactose

Aim of the following investigations was to find out whether the crystallinity/amorphicity of the powder samples was changed by the treatment of the amorphous spray - dried lactose using electrostatically supported and conventional mixing. It is known, that amorphous powders tend to recrystallisation when exposed to unfavourable conditions during processing or storage.
Figure 39 presents the mass increase of the untreated spray - dried lactose sample and the ones treated by conventional and electrostatically supported mixing upon exposure to the humidity program over time. All samples experience a mass gain with the increasing of the relative humidity up to 40 % RH. At 50 % RH the typical mass decrease of the amorphous powder takes place. Generally, the run of the curves of the two samples treated by conventional and

electrostatically supported mixing are similar to the run of the curve of the untreated spray - dried amorphous sample.

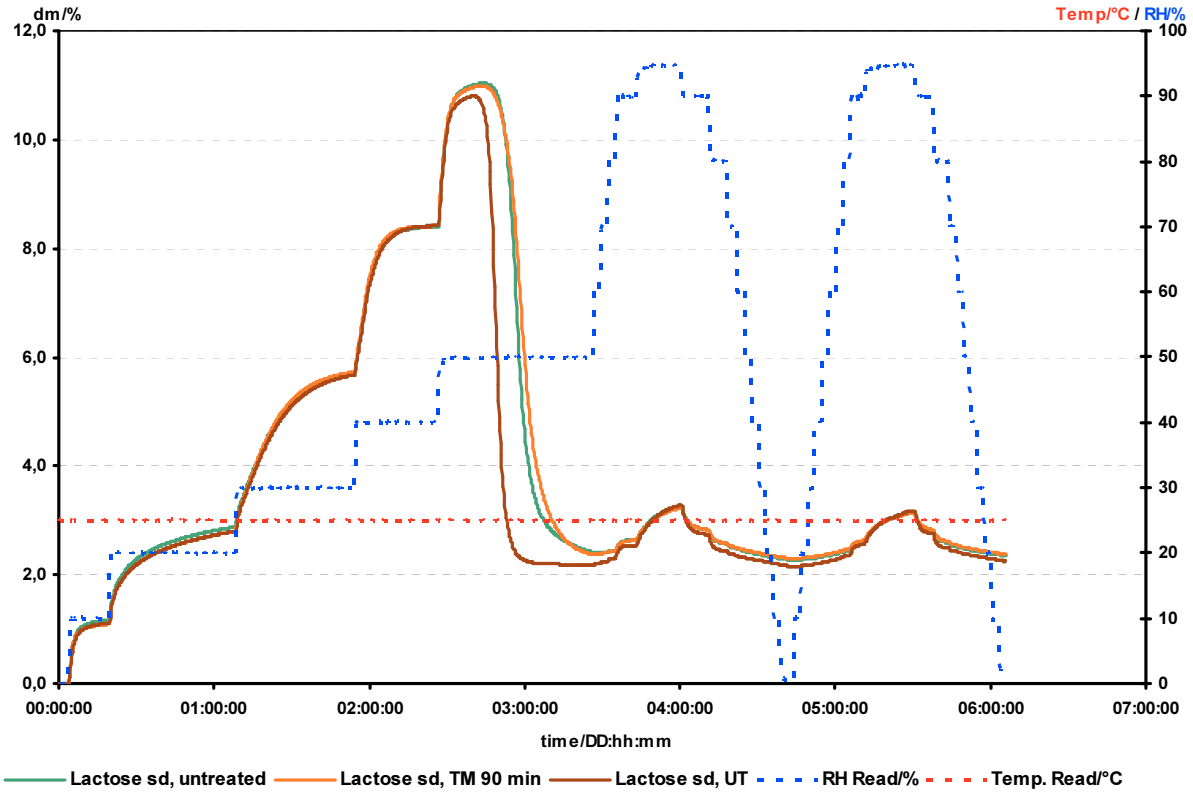

Figure 39: Mass change of spray - dried (sd) lactose, untreated and treated by electrostatically supported (UT) and by conventional (TM 90 min) mixing, 0 % RH - 95 % RH, 25 °C, the curve of the first of two measurements is presented

Table 12 presents the weight differences of the spray - dried samples before and after recrystallisation at 0 % RH at the beginning and at the end of the first cycle. It is not possible to estimate the amorphous content of the analysed samples precisely, because of the reasons mentioned before in this chapter for the spray - dried 100 % amorphous sample. Nevertheless, there is not much of a difference between untreated spray - dried lactose and samples treated by conventional and electrostatically supported mixing.

Table 12: Mass gain of spray - dried (sd) lactose, untreated and treated by electrostatically supported (UT) and conventional (TM 90 min) mixing, 0 % - 95 % RH, 25 °C

Powder sample	Mass gain/%
Spray - dried lactose (sd), untreated	2.25
Spray - dried lactose (sd), UT	2.15
Spray - dried lactose (sd), TM 90 min	2.28

Summarising the results of the water vapour sorption measurements of spray - dried lactose, it has to be pointed out, that there is no difference between the untreated sample and the samples

treated using conventional and electrostatically supported mixing. Both, conventional and electrostatically supported mixing methods, do not influence the amorphicity/crystallinity grade of the powder samples, which is important in respect on the stability of the powder samples upon processing.

Figure 40 presents the mass change of the micronised lactose samples over time upon exposure to different humidities. In order to micronise the powder, lactose particles were milled in an air jet mill using the milling parameters described in E.2.1. The mass of micronised lactose samples over time increases with the relative humidity. At 70 %, 80 %, 90 % and 95 % RH a mass decrease after the initial increase of mass is observed, indicating the presence of amorphous parts, which could have been induced during the milling of the powder (Hancock et al., 1997). The desorption curve of the first cycle and the second cycle are similar to the 100 % crystalline sample (Figure 36). The difference of the mass between the beginning and the end of the first cycle is attributed to the transformation of the amorphous parts into the monohydrate during the first cycle (Buckton et al., 1995 (c)). Further reasons, already encountered, for causing the difference of mass of the unmilled crystalline sample are inappropriate equilibrium conditions, the presence of unstable modifications of anhydrous α - lactose and formation of agglomerates entrapping water. Therefore, the weight of the powder at the beginning of the first sorption cycle is lower than at the end.

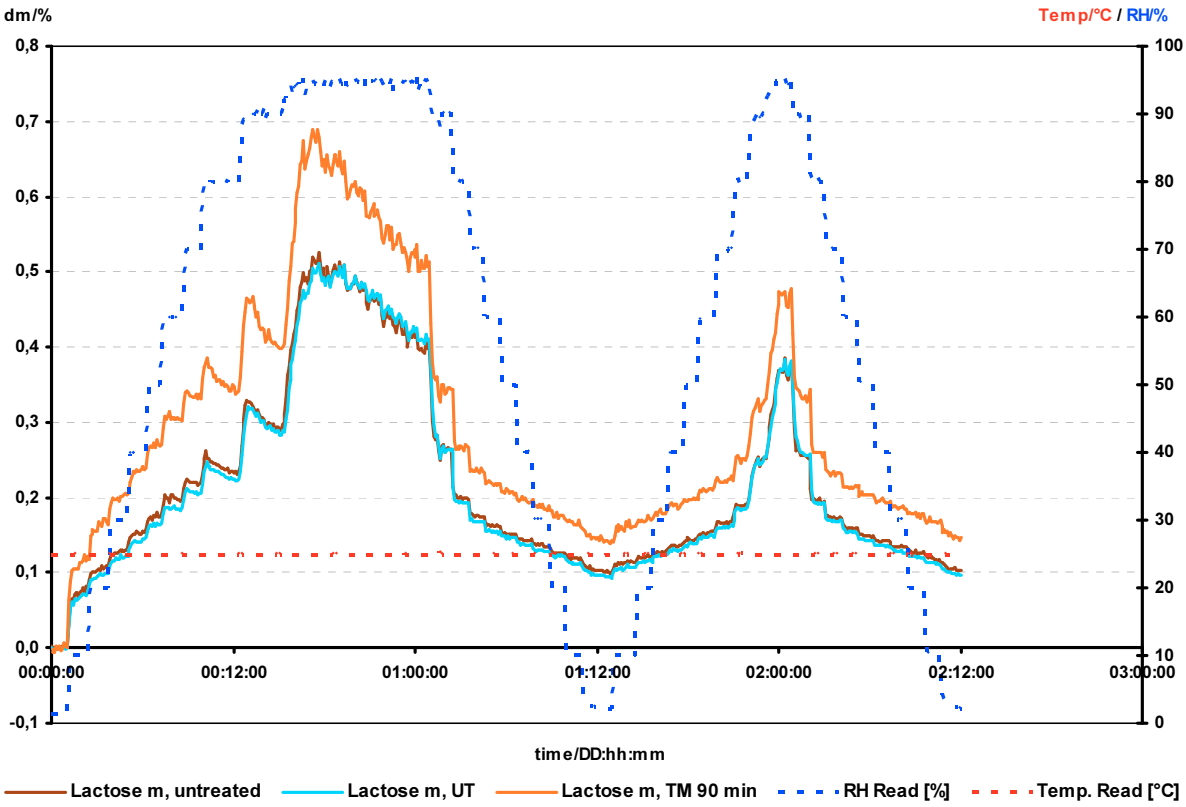

Figure 40: Mass change of micronised (m) lactose, untreated and treated by electrostatically supported (UT) and by conventional (TM 90 min) mixing, 0 % RH - 95 % RH, 25 °C, the curve of the first of two measurements is presented

Table 13 presents the results of the mass gain of untreated micronised lactose and the samples treated by conventional and electrostatically supported mixing before and after recrystallisation at 0 % RH at the end of the first cycle. Even there is not much of a difference between the samples, the mass gain is considerably lower compared to the spray - dried samples (Table 12). The reason for the difference between micronised and spray - dried products is attributed to the fact that micronisation may induce the emergence of so - called “frictional hot spots (see C.2.4.1), representing amorphous areas, usually formed on the surface of the particles, whereas spray - drying affects the crystallinity of the whole particle (bulk). So, crystallisation of the micronised particles takes place at these spots, whereas crystallisation of the spray - dried products affects the whole powder (bulk) leading to a much higher amount of amorphous material in the powder, which may recrystallise upon exposure to humidity. Finally, as well as in the case of the spray - dried lactose, there is no major difference, considering the scale, between untreated sample and those, which were treated by conventional and electrostatically supported mixing. This means, that neither electrostatically supported mixing nor conventional mixing affects the crystallinity/amorphicity of the micronised lactose.

Table 13: Mass gain of micronised (m) lactose untreated and treated by electrostatically supported (UT) and conventional (TM 90 min) mixing, 0 % - 95 % RH, 25 °C

Powder sample	Mass gain/%
Micronised lactose (m), untreated	0.10
Micronised lactose (m), UT	0.10
Micronised lactose (m), TM 90 min	0.14

Concluding the discussion of the results of the water vapour sorption analyses of the lactose samples it has been shown that after spray - drying lactose contains considerable amounts of amorphous material and shows a behaviour characteristic for amorphous lactose, such as high water gain upon exposure to humidity and water expel from the particles due to the recrystallisation after having achieved the critical humidity. On the contrary, micronised lactose particles show the behaviour of a predominantly crystalline powder. With the increase of the relative humidity the measured water gain is lower in comparison to the amorphous samples.
It also has been shown, that exertion of mechanical stress by mixing, either by conventional or electrostatically supported mixing, causes no major changes of crystallinity/amorphicity neither in spray - dried nor in micronised powders. This indicates that mixing induced changes of lactose are not an issue.

3.1.3 Salbutamol base

Figure 41 illustrates the mass change of a sample consisting of crystalline salbutamol base. Raising of the relative humidity leads to an increasing of the mass of the sample. After having achieved 95 % RH, the relative humidity was then decreased, leading to a decrease of mass. However, the initial mass is not reached at the end of the first cycle. The differences between the mass at the beginning and at the end of the first cycle may be explained by the fact that

equilibrium conditions were not fully appropriate. So, it might happen that the water molecules, which are entrapped inside the particles, do not have enough time to leave the particles, leading to a higher mass at the end of the first cycle than at the beginning. Probably, by modifying the equilibrium conditions, clearly spoken by reducing the mass change allowed per time or by prolonging the time, a given mass change is allowed to happen, it should be possible to achieve the same sample weight at the beginning and the end of the experiment. There is no evidence of other reasons like the presence of amorphous parts or unstable modifications, which might have caused the mass difference between the beginning and the end of the first cycle.

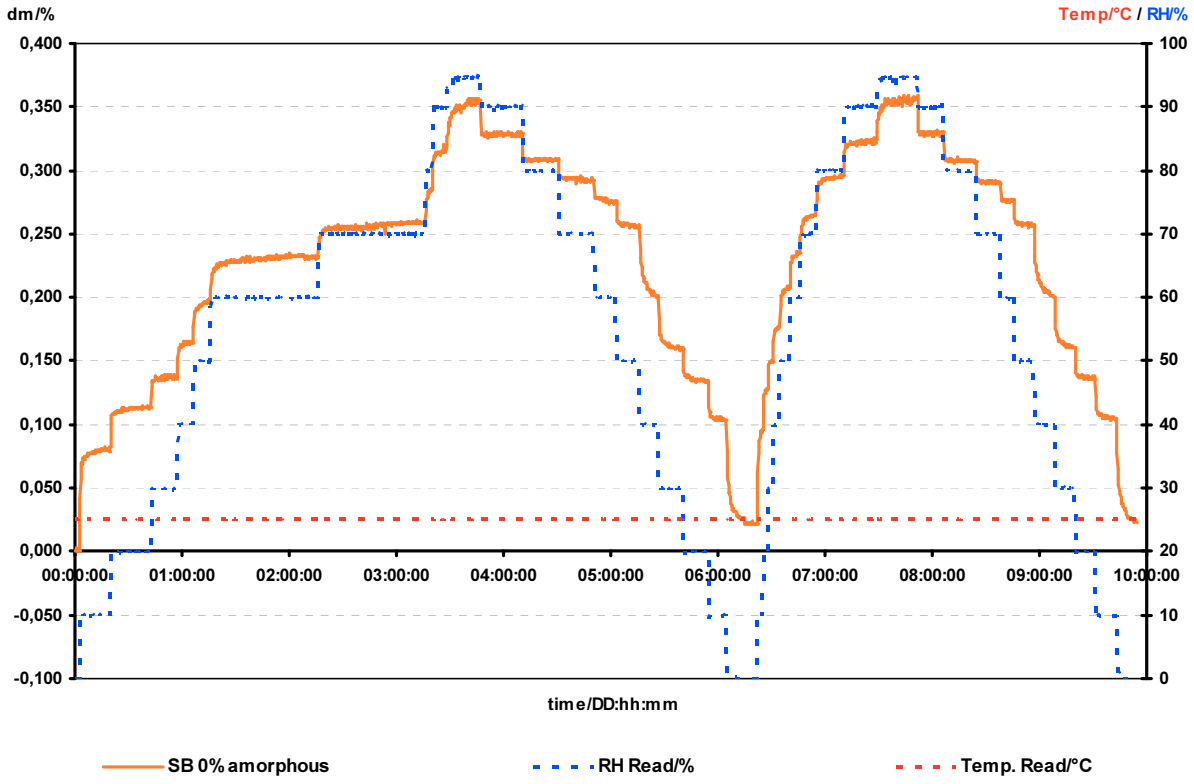

Figure 41: Mass change of crystalline salbutamol base (SB) over time, 0 % RH - 95 % RH, 25 °C, the curve of the first of two measurements is presented

In Figure 42 the moisture induced mass change of amorphous salbutamol base over time is shown. In order to prepare the amorphous powder an aqueous solution was freeze - dried, using the parameters described in E.2.3. Amorphous salbutamol base shows a higher mass increase than the crystalline sample at the same relative humidity during the first sorption cycle. Up to 60 % RH the mass of the samples is growing with increasing relative humidity. Furthermore, a mass decrease is detectable beginning at 60 % RH and proceeding at 70 % RH, indicating recrystallisation. Further increasing the relative humidity again results in mass gain at higher relative humidities. Lowering the relative humidity, after having reached 95 % RH, leads to a decrease of mass. The mass, which is measured at 0 % RH at the beginning of the first cycle, is not achieved again at the end of the first cycle, probably because desorption time was not adequate to remove all the sorbed water from the recrystallised salbutamol base samples.

Presumably, the formation of a macroscopically observed crystalline crust on the surface of the bulk powder impeded the water molecules, which were entrapped inside the sample, from to be removed from the sample completely. Also during the second cycle with increasing relative humidity a mass gain is detected. However, during this cycle no recrystallisation at 60 % RH and 70 % RH takes place, indicating, that the recrystallisation was already accomplished before the start of the second cycle. The phenomenon, that the mass of the sample at all relative humidities above the one following recrystallisation is somewhat higher in the first cycle than in the second cycle, may be attributed to the entrapment of water within the crystal lattice, which is not expelled. Run of the curve during the second cycle is similar to the run of the crystalline sample presented in Figure 41. A difference of the mass gain between the crystalline and the recrystallised freeze - dried samples is observed. This difference in water gain is attributed to the difference in the specific surfaces of the two samples, freeze - dried products typically having a high specific surface area.

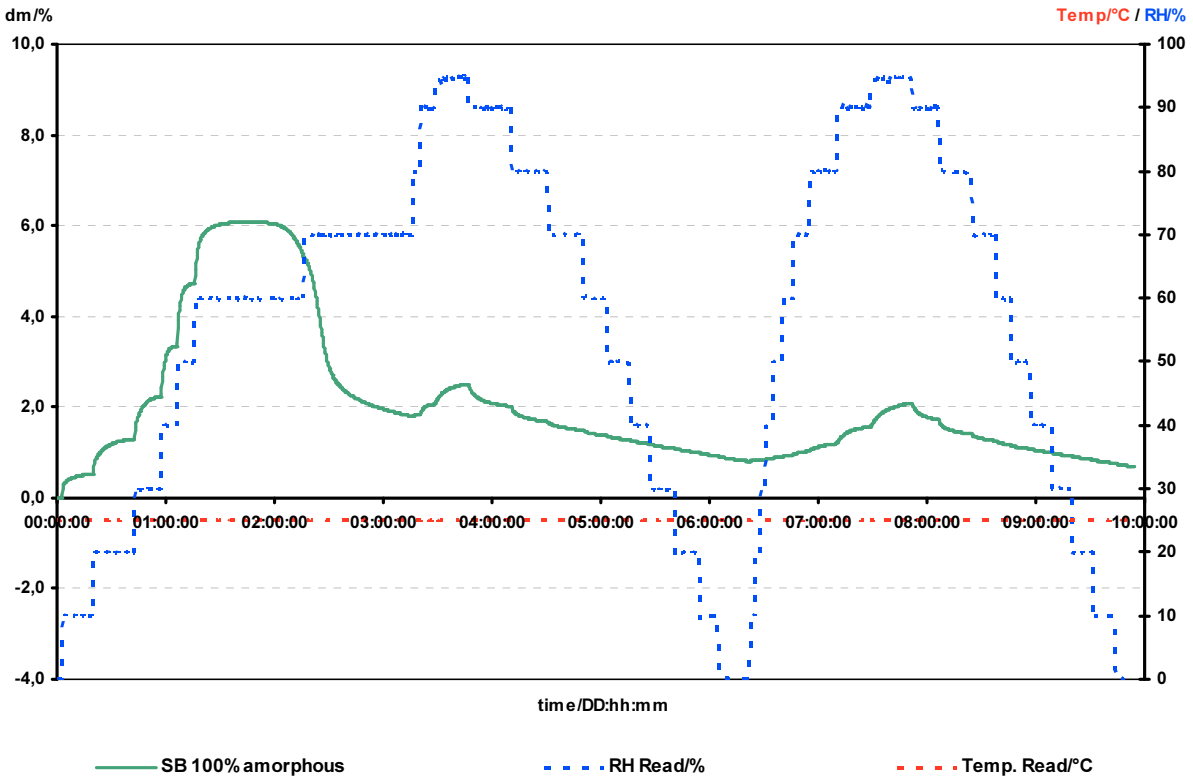

Figure 42: Mass change of amorphous freeze - dried salbutamol base over time, 0 % RH - 95 % RH, 25 °C, the curve of the first of two measurements is presented

The sorption isotherms (Figure 43 a, b) of samples consisting of 100 % crystalline and 100 % amorphous salbutamol base are constructed using the mass change of salbutamol base at equilibrium. Figure 43 shows, that the amorphous sample (Figure 43 b) of salbutamol base behaves in a different way than the crystalline sample (Figure 43 a). Most striking is the mass decrease at 70 % RH when increasing the relative humidity in the first cycle. Furthermore, as desorption time was not adequate to remove all the sorbed water from the recrystallised

salbutamol base samples the initial mass is not reached at the end of desorption cycle. This is also true to a less extent for the crystalline sample.

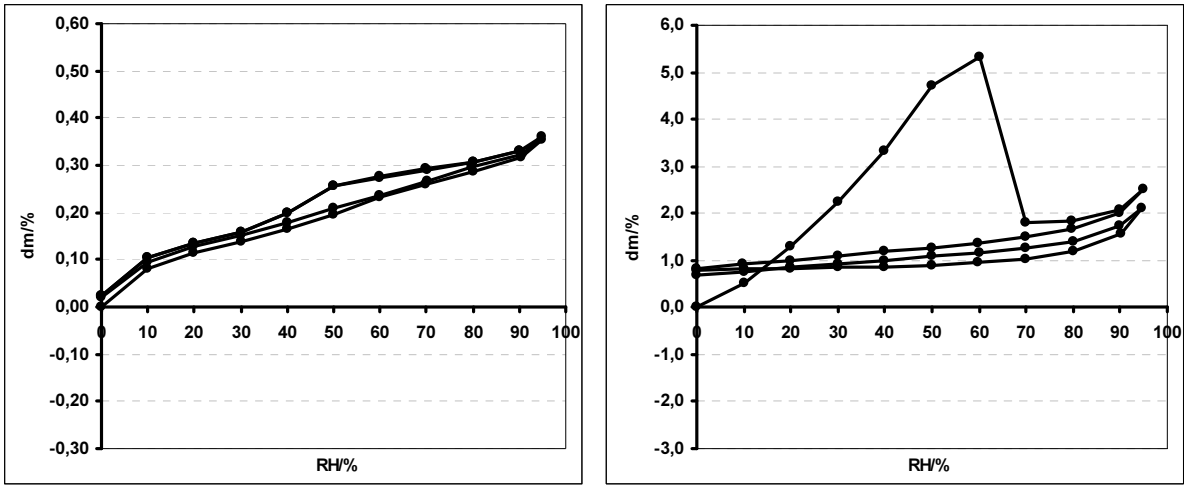

a **b**

Figure 43: Sorption isotherms of 0% (a) and 100 % (b) amorphous salbutamol base

Goal of the following measurements was to find out whether the crystallinity/amorphicity of the powder samples is changed by treating the spray - dried and micronised salbutamol base samples using electrostatically supported and conventional mixing methods. In order to produce the spray - dried powder an aqueous solution of salbutamol base was spray - dried using the parameters described in E.2.2. The micronised salbutamol base was used as received.

The mass gain of all samples is relatively low, indicating a low amorphous amount if any at all (Figure 44). Both, spray - dried and micronised samples, show the characteristics of crystalline salbutamol base (Figure 41). As already observed in Figure 41, the mass of the micronised samples at the beginning of the first cycle at 0 % RH differs from the mass of the samples at the end of the first cycle at 0 % RH. It seems, that in case of the micronised salbutamol base the equilibrium conditions, which ensure complete drying at 0 % RH at the end of the first cycle, were not sufficient to ensure the removal of all water molecules, which are sorbed by the micronised particles, leading to the mentioned difference in weight. However, no mass difference between the beginning and the end of the first cycle in case of spray - dried samples is observed. Probably, the morphology of the spray - dried salbutamol base particles differs from that of the micronised particles, therefore the time needed in order to allow all water molecules to leave the particles differ. So, water vapour sorption investigations of spray - dried and micronised samples would have to be carried out using different equilibrium conditions, suitable for each type of the powder, to ensure the complete drying of the powder at 0 % RH. However, the moisture induced weight changes of spray - dried and micronised products, which were mixed using conventional and electrostatically supported mixing do not differ considerably from the corresponding untreated sample, which is important in terms of stability of the mixtures upon processing.

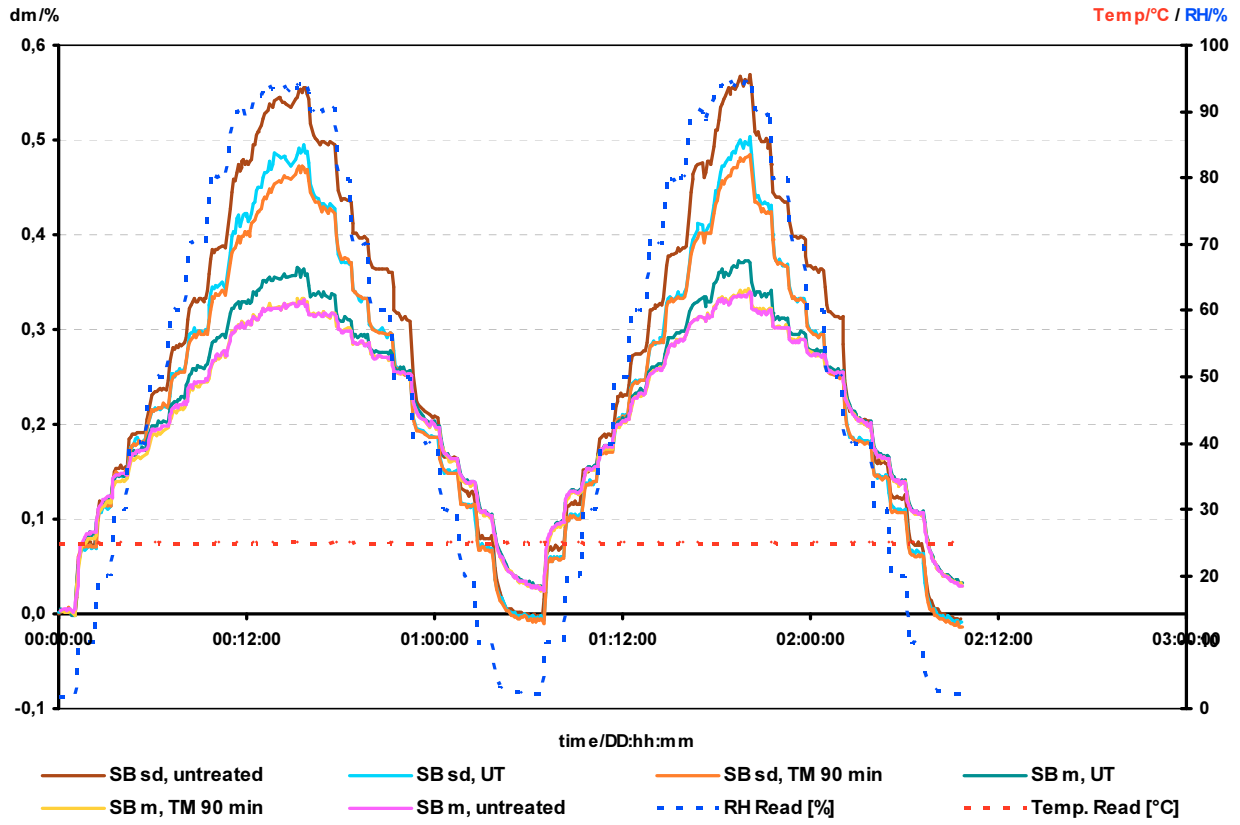

Figure 44: Mass change of spray - dried (sd) and micronised (m) salbutamol base (SB) untreated and treated by electrostatically supported (UT) and conventional (TM 90 min) mixing, 0 % RH - 95 % RH, 25 °C, the curve of the first of two measurements is presented

In summary, the results of the water vapour sorption measurements of salbutamol base indicate that micronised and spray - dried salbutamol base show the behaviour, which is typical for the crystalline powder. Despite the rapid evaporation of the water during spray - drying and therefore the fast solidification, the material still has the opportunity to crystallise, which is advantageous in terms of stability of the powder not only during the preparation of the mixtures, but also during the storage of the formulations for the use in DPIs.
Furthermore, no considerable difference between the mass gain of the untreated samples and the samples treated by conventional and electrostatically supported mixing is detected. Handling of the powder using the TURBULA® mixer or ULTRA - TURRAX® does not influence the crystallinity/amorphicity grade of spray - dried and micronised salbutamol base, which is advantageous in terms of stability of the mixtures upon processing and storage.

3.1.4 Salbutamol sulphate

In Figure 45 the moisture induced mass change of crystalline salbutamol sulphate over time is shown. At first a mass loss at 0 % RH is detectable. This is caused by the loss of water, which has not been removed during storage over silica gel prior to analysis. Raising the relative humidity is associated with an increase of mass. The higher the humidity increases, the higher the mass gain observed. Decreasing the relative humidity, after having reached 95 % RH, leads

to a decrease of mass. The initial value at 0 % RH at the beginning of the first cycle is not reached anymore. Probably, analogous to the salbutamol base samples, the equilibrium conditions have to be modified in order to ensure the complete emersion of the water molecules from the powder sample. There is no evidence of other reasons like the presence of amorphous parts or unstable modifications which might cause the mass difference between the beginning and the end of the first cycle.

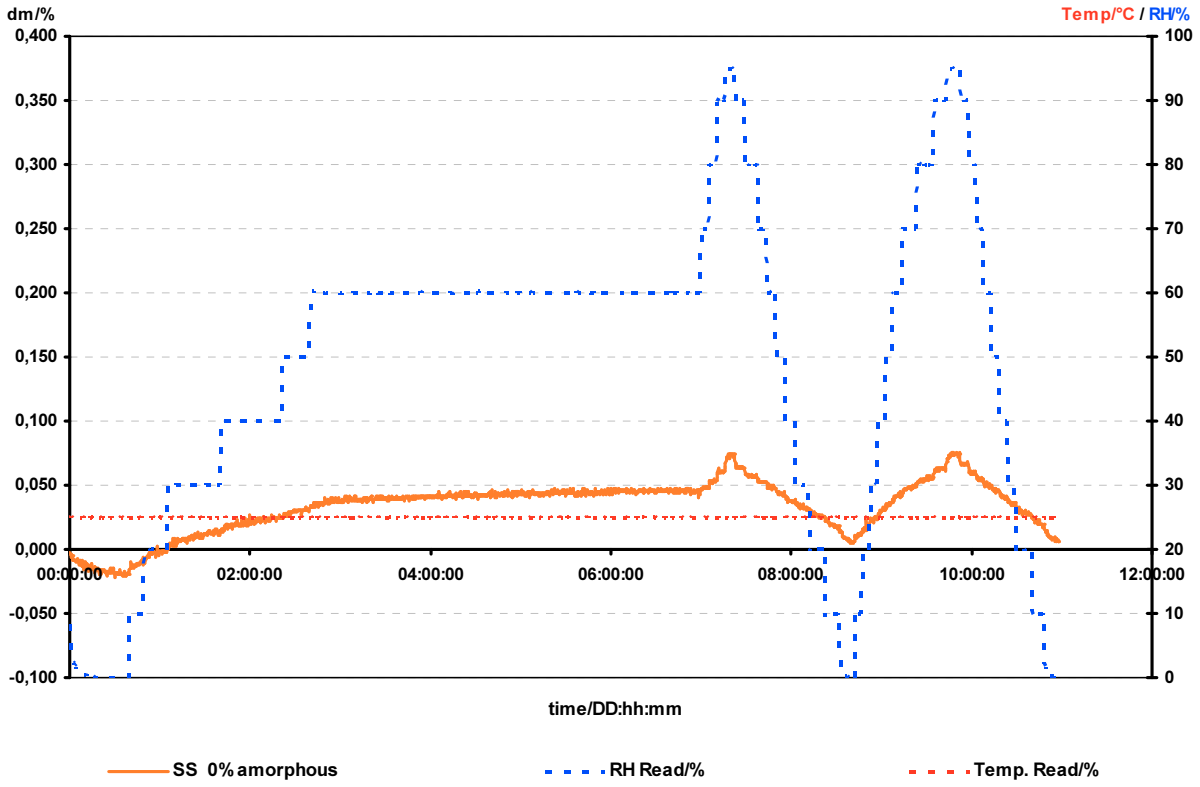

Figure 45: Mass change of crystalline salbutamol sulphate (SS) over time, 0 % RH - 95 % RH, 25 °C, the curve of the first of two measurements is presented

In Figure 46 the mass change over time of the amorphous salbutamol sulphate sample is displayed. In order to produce the amorphous powder an aqueous solution of salbutamol sulphate was spray - dried using the spray - drying parameters described in E.2.2. This sample shows a higher mass increase than the crystalline sample upon increasing the relative humidity. Furthermore, in contrast to the continuous mass increase of the crystalline sample with increasing relative humidity, a mass decrease is detectable at 60 % RH, which is ascribed to recrystallisation. Further increasing of the relative humidity again, results in a mass gain at higher relative humidities. Lowering the relative humidity, after having reached 95 % RH, leads to a decrease of mass. In contrast to the amorphous salbutamol base sample, there is no difference between the mass of salbutamol sulphate at 0 % RH at the beginning and at the end of the first cycle. Probably, in case of salbutamol sulphate, the equilibrium conditions were able to ensure complete drying of the powder at 0 % RH. Also during the second cycle with increasing relative humidity a mass gain is detected. However, during this cycle no recrystallisation at

60 % RH takes place, indicating, that recrystallisation was already accomplished before the start of the second cycle. The phenomenon, that the mass of the sample at all relative humidities above the one following recrystallisation is somewhat higher in the first cycle than in the second cycle may be attributed to the entrapment of water within the crystal lattice, which is not expelled. The run of the curve during the second cycle is similar to the run of the crystalline sample presented in Figure 45.

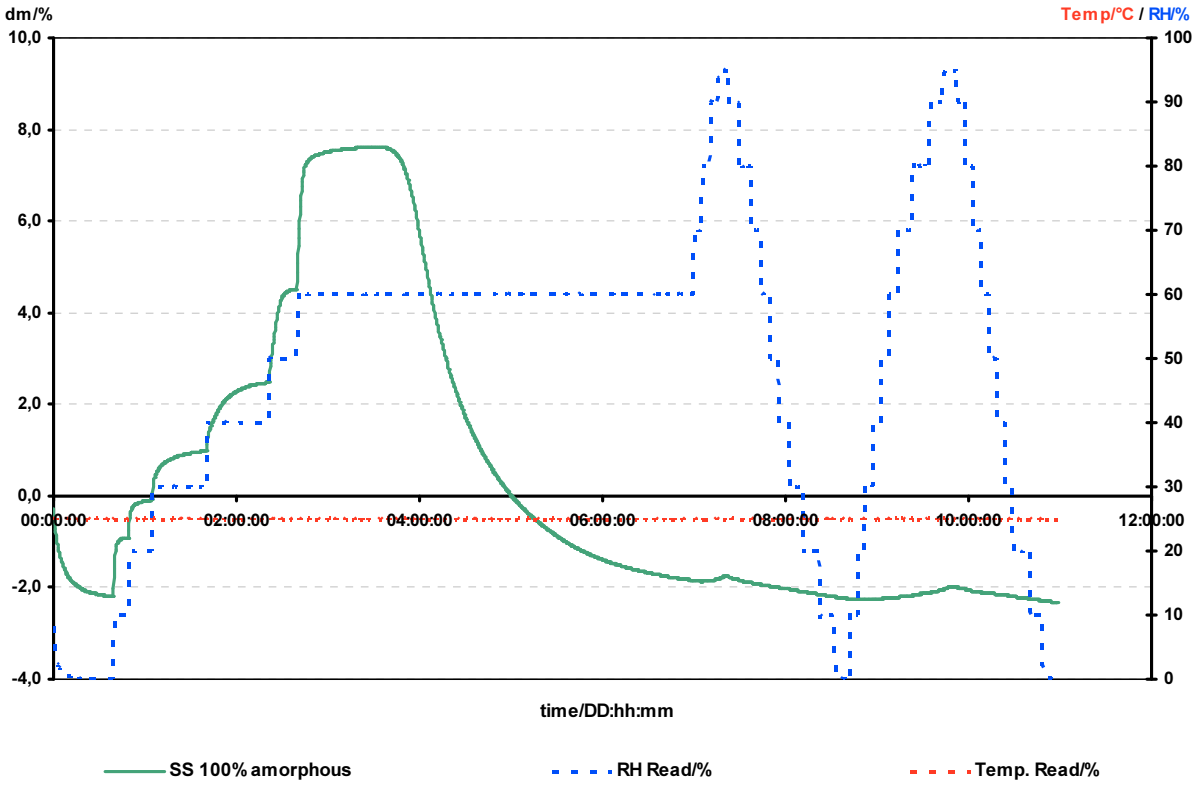

Figure 46: Mass change of amorphous spray - dried salbutamol sulphate over time, 0 % RH - 95 % RH, 25 °C, the curve of the first of two measurements is presented

The sorption isotherms (Figure 47 a, b) of samples consisting of 100 % crystalline and 100 % amorphous salbutamol sulphate are constructed using the mass change of salbutamol sulphate at equilibrium. Figure 47 a shows, that the crystalline sample of salbutamol sulphate behaves in a different way than the amorphous sample (Figure 47 b). There is no mass decrease at 60 % RH when increasing the relative humidity in the first cycle. The results are similar to the ones of the salbutamol base samples, with the exception, that there is no difference between the values of spray - dried salbutamol sulphate samples at the beginning and the end of the first cycle at 0 % RH.

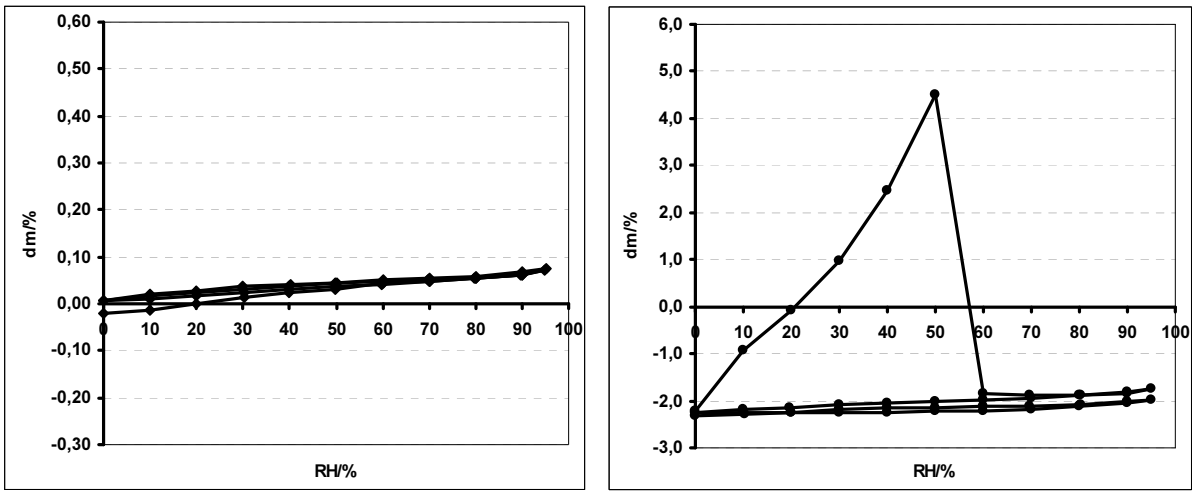

a **b**

Figure 47: Sorption isotherms of 0% (a) and 100 % (b) amorphous salbutamol sulphate

In order to find out, whether the mixing and the mixing mode may influence the crystallinity/amorphicity of the spray - dried and micronised powders, different salbutamol sulphate samples were investigated using water vapour sorption. For that purpose both spray - dried and micronised powder samples were treated using conventional and electrostatically supported mixing. Spray - dried salbutamol sulphate was prepared using the spray - drying parameters described in chapter E.2.2. Micronised salbutamol sulphate was prepared by milling in an air jet mill (see E.2.1) (Brodka - Pfeiffer et al., 2003). The run of the untreated spray - dried sample presented in Figure 48 differs from the run of the spray - dried sample in Figure 46. The point, at which recrystallisation starts, differs. Recrystallisation of the untreated spray - dried sample presented in Figure 48 happens at 70 % RH whereas it happens at 60 % RH with the sample presented in Figure 46. Comparing the runs of these curves a difference of the time period during which the samples were exposed to the relative humidity of 60 % is observed. This difference arises because eleven different samples were investigated in the moisture sorption chamber at the same time. As the different samples, amorphous or crystalline, need different time periods to reach equilibrium, the relative humidity will not be increased till the equilibrium of all samples is obtained even if only one sample out of eleven needs more time to achieve the equilibrium than the other ten. Due to the much longer exposition of the spray - dried sample presented in Figure 46 to 60 % RH the recrystallisation starts at this humidity value already. In case of the untreated spray - dried sample presented in Figure 48, the time during which the sample was exposed to 60 % RH is much shorter. Shortly after the increase of the relative humidity to 70 % RH, recrystallisation starts. After the decrease of the relative humidity till 0 % RH the mass of the sample does not reach the mass value at the beginning of the first cycle. This may be attributed to the fact, that the sample presented in Figure 46, which recrystallised at 60 % RH had much lower water content than the one presented in Figure 48, which had higher water content. Apparently, equilibrium conditions were not appropriate in the latter case to remove all water molecules from the powder sample at the end of

the first cycle at 0 % RH. By modifying the equilibrium conditions complete drying of the sample presented in Figure 48 should be achieved.

The sample of the untreated spray - dried salbutamol sulphate and the one treated using conventional mixing show no major difference in the run of the curves at the beginning of the first sorption cycle. After recrystallisation has taken place a slight difference in the run of the curves can be seen. The sample treated using conventional mixing method expels the water faster than the untreated spray - dried sample causing in the case of the untreated sample more water molecules being entrapped inside the particles. This is due to the difference in the rate of recrystallisation which cannot be controlled. The formation of a crystal layer on the surface of the sample may hinder the expulsion of water.

The moisture induced weight change of the spray - dried sample, which was treated by electrostatically supported mixing, differs from the untreated spray - dried sample and the one treated by conventional mixing. The water sorption characteristic of this sample is similar to that of the crystalline sample (Figure 45). Probably, recrystallisation had taken already place during the preparing procedure or during sample preparation before the water vapour sorption analysis. Most probably, recrystallisation will adversely affect flowability, reproducibility of the single dose and the respirable fraction. This will be shown later on in chapters 5.2.4 for the mass uniformity and 5.3.4 for the respirable fraction.

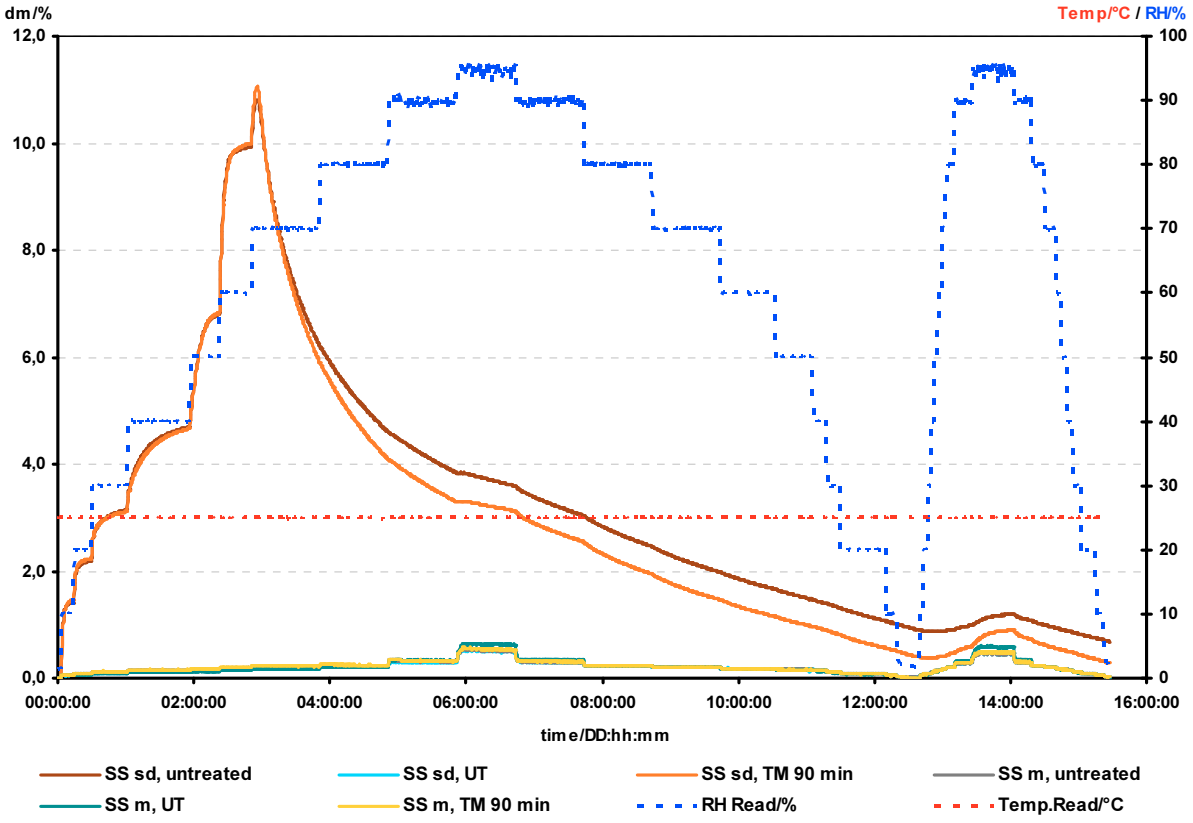

Figure 48: Mass change of spray - dried (sd) and micronised (m) salbutamol sulphate (SS) untreated and treated by electrostatically supported (UT) and conventional (TM 90 min) mixing, 0 % RH - 95 % RH, 25 °C, the curve of the first of two measurements is presented

The mass gain in the micronised salbutamol sulphate samples, untreated and treated using conventional mixing and electrostatically supported mixing do not differ. The run of the three curves is similar to the run of the curve of the crystalline sample presented in Figure 45. Generally, the obtained results indicate good stability of the micronised salbutamol sulphate samples upon processing. This fact is very important in regard to the stability of the powder samples during the handling and the storage of the mixtures.
Summarising the results of the water vapour sorption measurements of salbutamol sulphate it was found out that the untreated spray - dried sample and the one treated by conventional mixing show the behaviour, which is characteristic for the amorphous powder. Run of the curve of the sample treated by electrostatically supported mixing is typical for the crystalline powder. Probably, during the handling of the amorphous spray - dried powder either during mixing or during sample preparation, due to the non - stability of the amorphous state, the sample had the possibility to recrystallise. Especially in this case the importance of the careful handling of amorphous powder samples is illustrated. Recrystallisation may lead to deteriorations in terms of flowability, uniformity of the single dose and respirable fraction.
On the contrary, the untreated micronised samples behave like the crystalline powder and crystallinity was not affected by mixing.

3.1.5 Concluding remarks

Based on the results of the experiments it has been found out that spray - drying of lactose and salbutamol sulphate leads to the emergence of amorphous material, whereas spray - dried salbutamol base exhibits the characteristics of a crystalline powder. Micronised salbutamol base and salbutamol sulphate samples show the thermodynamic behaviour typical for the crystalline powder. However, micronisation of lactose induces amorphous parts.
Furthermore, according to the moisture sorption results no influence of the mixing mode on the amorphicity/crystallinity of the powder samples is detected, with the exception of the salbutamol sulphate spray - dried sample treated by electrostatically supported mixing. The recrystallisation of this sample happened before the start of the moisture sorption measurements, probably after spray - drying or during further handling of the powder, such as treating by electrostatically supported mixing or preparing the sample for the moisture sorption analysis.
The thermodynamic stability of the powder, which can be ensured by using the stable crystalline state, is advantageous if the powder is intended for the use in DPIs. Therefore spray - dried salbutamol base and micronised salbutamol base and salbutamol sulphate, due to the crystallinity of the powder may be preferred over amorphous samples. The recrystallisation due to the instability of the amorphous state may deteriorate flowability, uniformity of dosage and respirable fraction of the powder, which is intended for the use in DPIs.

3.2 Differential Scanning Calorimetry

3.2.1 Preliminary remarks

In order to investigate the influence of the mixing mode on crystallinity/amorphicity samples of spray - dried lactose, salbutamol base and sulphate, the untreated as well as the samples treated by mixing, were examined using differential scanning calorimetry (DSC) (see C.2.4.3 and E.3.5).

As the detection limit of amorphous material by DSC is about 10 % (Brodka - Pfeiffer et al., 2003) and as the amorphous amount in micronised samples is negligible (see 3.1), these samples were not investigated using DSC. All DCS curves presented in the following chapter are standardised by the weight of the samples.

3.2.2 Lactose

Figure 49 presents the thermogram of crystalline α - lactose monohydrate. The endothermic peak at 148 °C is due to the loss of the crystal water. This is a typical temperature, which is described in literature (Lohrmann, 2005; Elamin et al., 1995; Chidavaenzi et al., 1997). The following exothermic peak at 173 °C is ascribed to the relaxation of lattice distortions, caused by the loss of the water previously (Figura, 1993). The endothermic peak at 218 °C represents the melting point of α - lactose. At 223 °C the melting of β - lactose is observed (Lerk, 1987). Upon further heating of the sample decomposition takes place.

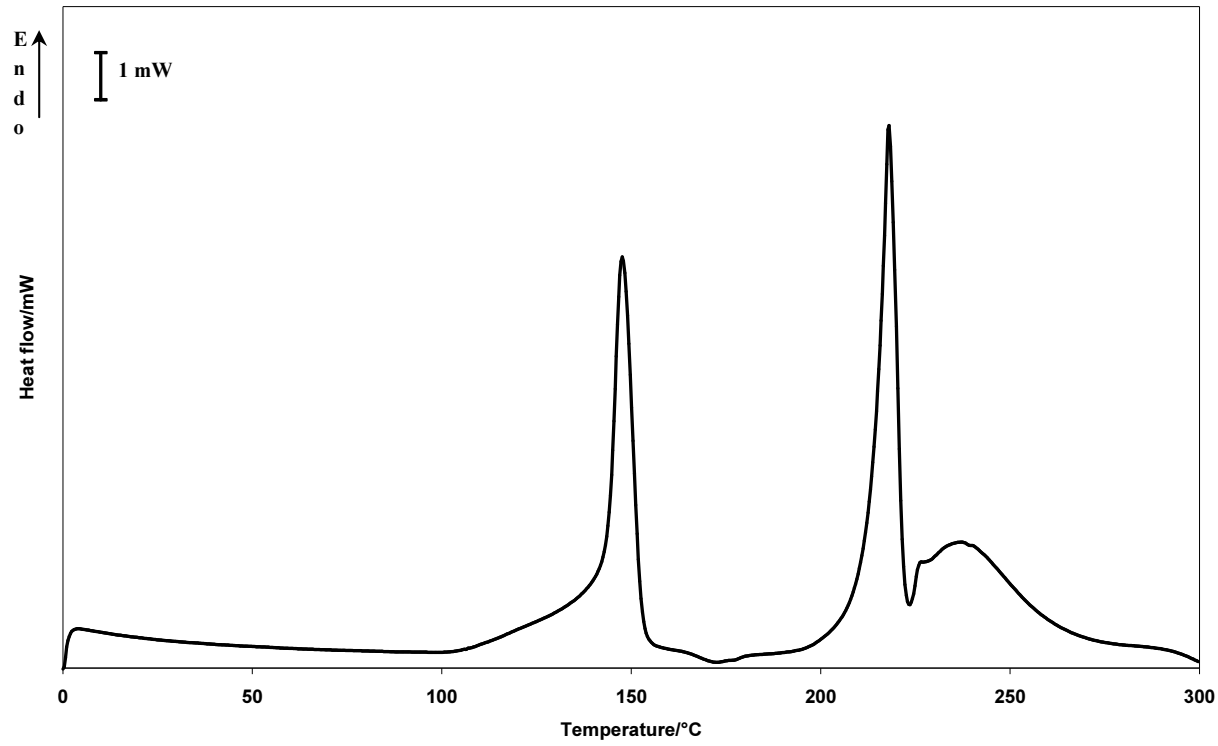

Figure 49: DSC curve of crystalline α - lactose monohydrate, the curve of the first of two measurements is presented

Figure 50 presents the thermograms of untreated spray - dried lactose and spray - dried lactose treated using conventional and electrostatically supported mixing. Lactose was spray - dried using the conditions described in E.2.2. Although the curves of the treated samples, especially the one of the sample treated by electrostatically supported mixing, differ from the one of the untreated sample slightly, they still show the run, which is typical for amorphous lactose. The signal detected at 118 °C with all samples is attributed to a desorption of loosely sorbed water, which is typical for partly dehydrated and then re - humidified amorphous lactose (Lerk, 1984).

During further heating an exothermic peak arises at 190 °C in case of untreated spray - dried lactose and spray - dried lactose treated by conventional mixing, and at 183 °C in case of lactose treated using electrostatically supported mixing. These peaks are ascribed to the transformation from amorphous to crystalline material, which is a typical attribute of amorphous lactose (Gombas et al., 2002). Further on, the endothermic melting peaks of crystalline α - lactose at 218 °C and of crystalline β - lactose at 223 °C of the previously crystallised amount of lactose are detected, followed by decomposition. In case of the sample treated with the ULTRA - TURRAX® the exothermic peak is greater than in case of the untreated and TURBULA® mixer treated samples and in turn, the subsequent endothermic melting peaks are greater also. However, this does not mean that the sample treated by electrostatically supported mixing contained a higher amount of recrystallised material before the start of the DSC experiment. If so, the melting enthalpy would have had to be greater than the enthalpy of recrystallisation before. This is not the case. According to the thermogram of these samples the enthalpy of crystallisation of the amorphous lactose, which recrystallises at 183 °C to form α - lactose and β - lactose is approximately the same as the sum of the melting enthalpies of crystalline α - lactose, which melts at 218 °C and crystalline β - lactose, which melts at 223 °C (Lerk, 1984). The enhanced enthalpy of recrystallisation of the sample treated by electrostatically supported mixing might be due to the spontaneous happening of recrystallisation, which by chance has not taken place in the other two samples. Anyway, this phenomenon recalls the problems associated with the instability of amorphous powders and reminds to take special care when handling amorphous materials.

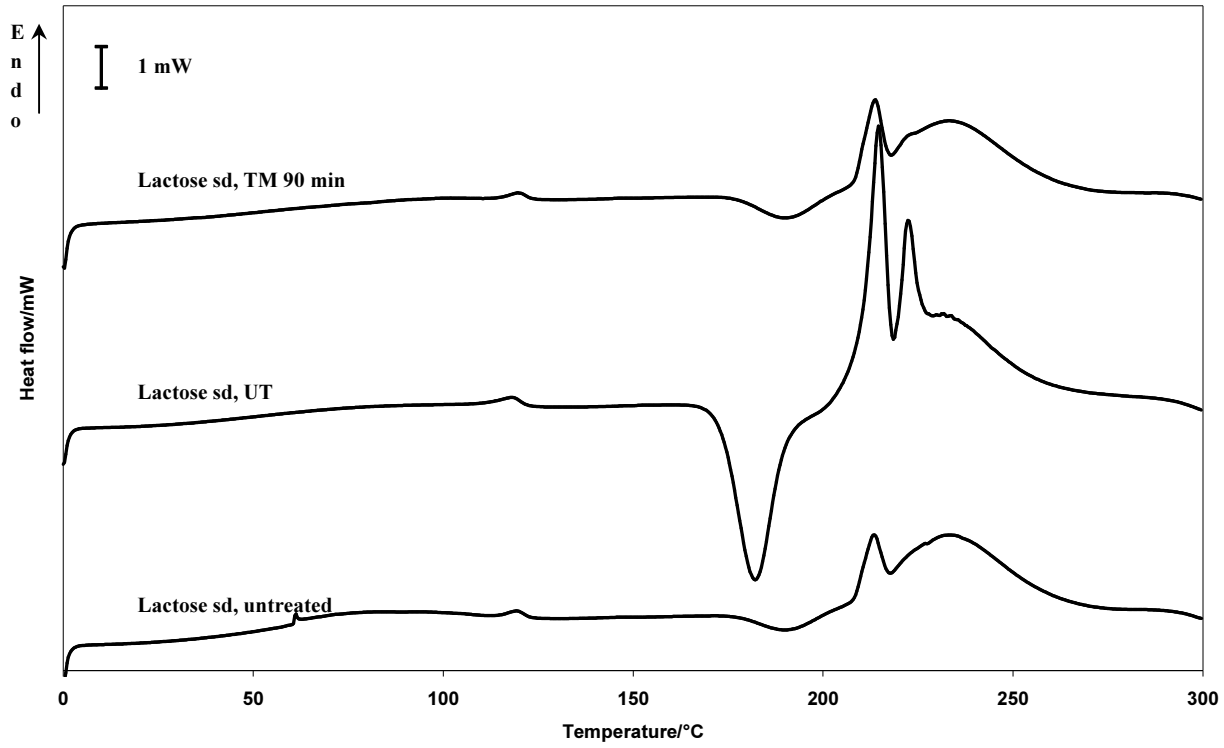

Figure 50: DSC curves of spray - dried (sd) lactose, untreated and treated using electrostatically supported (UT) and conventional mixing (TM 90 min), the curve of the first of two measurements is presented

3.2.3 Salbutamol base

The thermograms of samples of crystalline salbutamol base and spray - dried salbutamol base untreated as well as treated using conventional mixing and electrostatically supported mixing are presented in Figure 51. According to the European Pharmacopea, the melting point of crystalline salbutamol base is between 157 °C and 158 °C. This melting peak is found not only for the crystalline sample, but also for the three spray - dried samples, indicating the crystallinity of the samples (Figure 51). No dependence of the amorphicity/crystallinity grade on the mixing method is detected. These results of the DSC measurements with respect to the crystallinity of spray - dried salbutamol base are consistent with the results of the moisture sorption measurements (see 3.1.3).

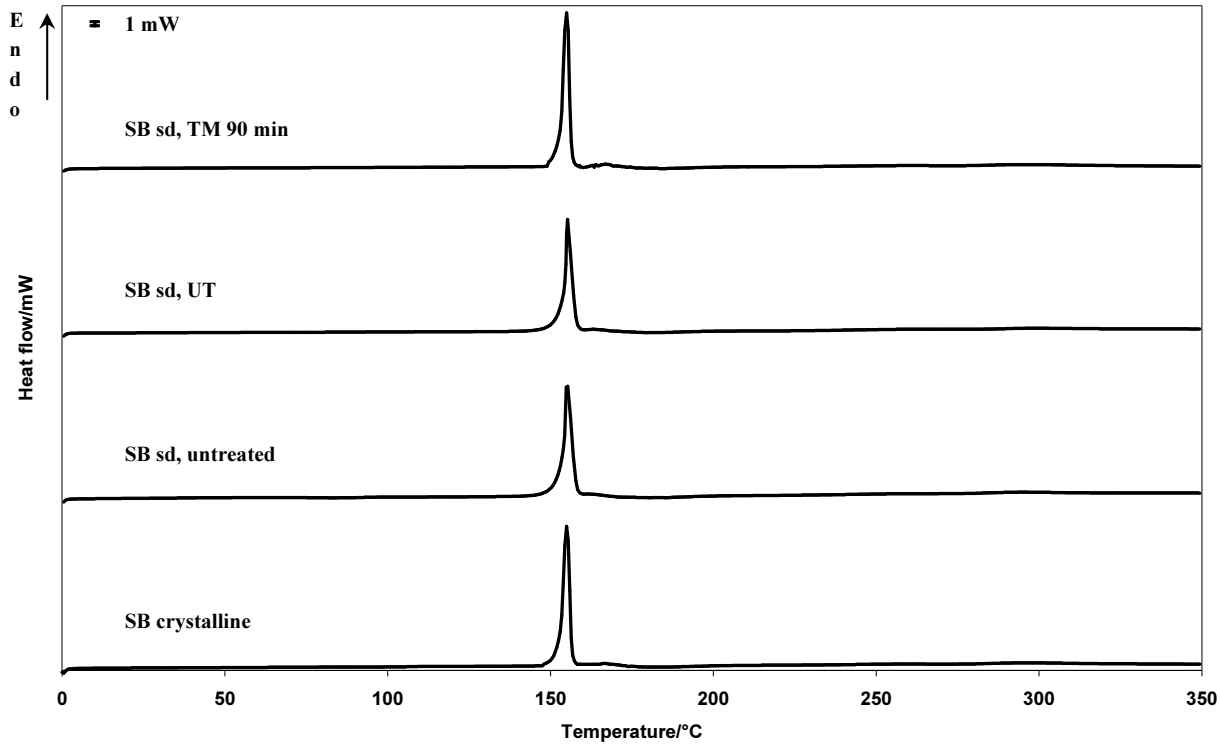

Figure 51: DSC curves of crystalline salbutamol base (SB) and spray - dried (sd) salbutamol base, untreated and treated using conventional (TM 90 min) and electrostatically supported (UT) mixing, the curve of the first of two measurements is presented

3.2.4 Salbutamol sulphate

The DSC scan of crystalline salbutamol sulphate is presented in Figure 52. The sharp peak at 206 °C is associated with the melting of the material and is followed by decomposition (Figure 52). The DSC profiles of the spray - dried salbutamol sulphate samples (Figure 53) differ from the DSC profile of the crystalline sample. The DSC responses of the untreated spray - dried material and samples, which were further treated using conventional and electrostatically supported mixing show a broad endotherm between 50 °C and 100 °C, which is likely to correspond to the evaporation of water, which was not removed from the sample during the

storage of the powder over the silica gel prior the experiments, followed by a diffuse melting endotherm at 180 °C, indicating the melting of that part of salbutamol sulphate which is present in the crystalline state (Columbano et al., 2002). There is no evidence of a crystallisation exotherm. The difference in the melting enthalpy between the crystalline and spray - dried samples are caused by the fact, that the spray - dried samples are mostly amorphous. This is in good agreement with the results obtained by water sorption measurements, except for the sample treated by the ULTRA - TURRAX®, which had been proven to be crystalline according to the results of the water vapour sorption. As already discussed in 3.1.4, the sample treated using electrostatically supported mixing recrystallised before the start of the experiments, most probably during the sample preparation procedure for moisture sorption analysis or during improper treatment, such as short exposition of the sample to ambient relative humidity and temperature before placing it inside the humidity chamber. However, treating by electrostatically supported mixing (see 3.1.4) is unlikely to have caused recrystallisation. If so, not only the sample investigated by moisture sorption but also the sample examined by DSC would have indicated crystallinity.

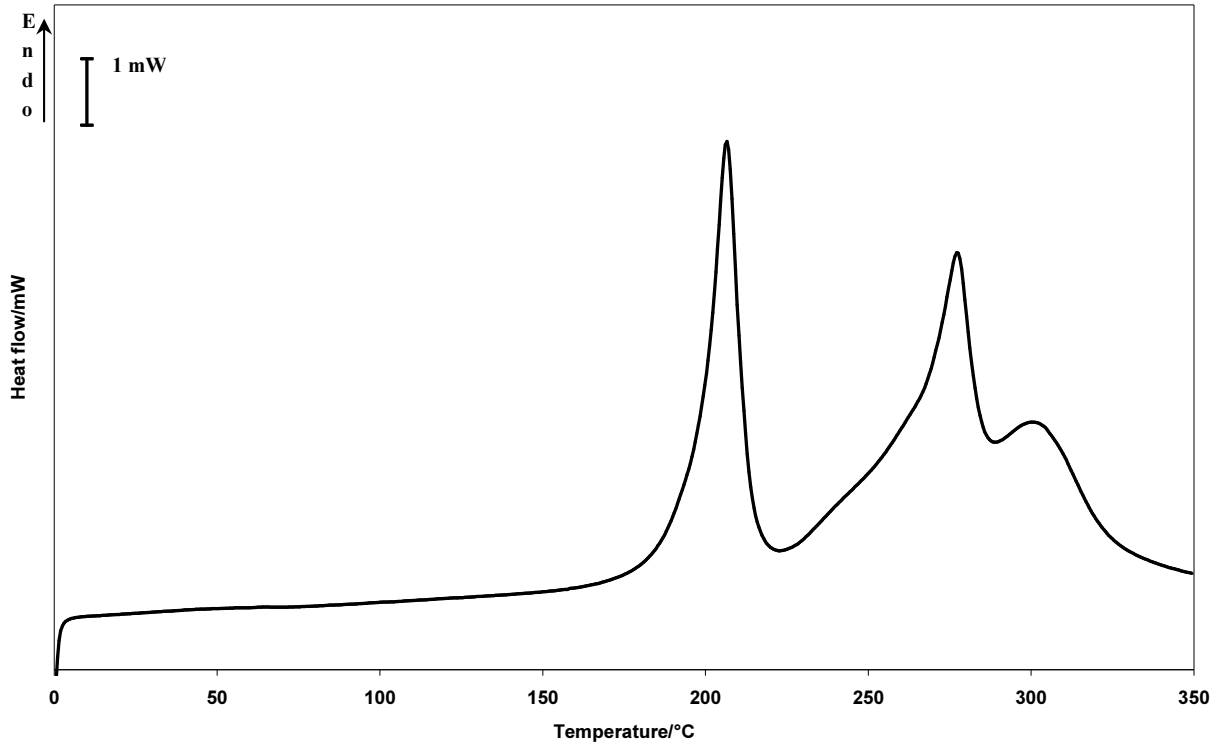

Figure 52: DSC curve of crystalline salbutamol sulphate, the curve of the first of two measurements is presented

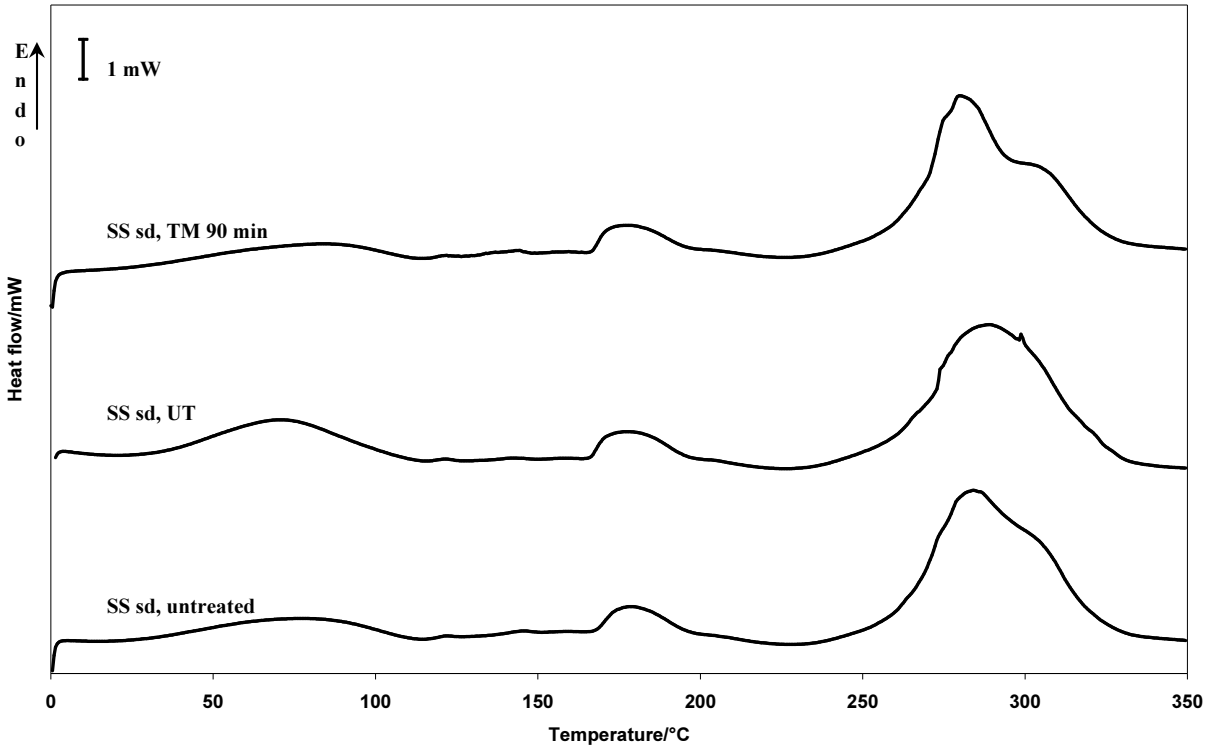

Figure 53: DSC curves of untreated spray - dried (sd) salbutamol sulphate (SS) and samples treated using electrostatically supported (UT) and conventional mixing (TM 90 min), the curve of the first of two measurements is presented

3.2.5 Concluding remarks

DSC was used in addition to moisture sorption for the identification of amorphous parts in spray - dried lactose, salbutamol base and salbutamol sulphate samples, which were either untreated or treated using different mixing methods. Untreated spray - dried lactose and salbutamol sulphate are found to be amorphous. Spray - dried salbutamol base, in contrast, is crystalline. These results are in good accordance with the results obtained by water vapour sorption (see 3.1).

Comparing the samples in dependence on the mixing mode, no differences between the samples, which were untreated or treated by electrostatically supported and conventional mixing are detected, with the exception of spray - dried lactose treated by electrostatically supported mixing. In spray - dried lactose treated by electrostatically supported mixing spontaneous crystallisation during heating took place to a higher extent than in untreated samples and samples treated by conventional mixing. This is indicated by the exothermic recrystallisation peak at 183° C of amorphous lactose forming α - and β - lactose, (Lerk, 1984; Figura, 1993). The recrystallisation peak is followed by the melting peaks of both α - and β - lactose, α - lactose melts at 218° C and β - lactose at 223° C. As the enthalpies determined for the recrystallisation and the melting of α - lactose are similar, it may be assumed that spontaneous recrystallisation of the sample takes place during heating, but not before the start of the investigations. Otherwise, the melting enthalpy of α - lactose would be much higher than the recrystallisation enthalpy.

In contrary to water vapour sorption no difference between spray - dried salbutamol sulphate samples, which were untreated and the ones which were treated by conventional and

electrostatically supported mixing is detected. They exhibit the behaviour characteristic for amorphous salbutamol sulphate. According to the results of moisture sorption analysis, the sample treated by electrostatically supported mixing was identified as crystalline. The difference in results obtained by the two different investigation techniques may be caused by recrystallisation of the sample either after the treatment by electrostatically supported mixing or during sample preparation for the measurements of water vapour sorption. Otherwise, if electrostatically supported mixing itself had caused recrystallisation, both techniques would have identified the sample to be crystalline.

3.3 X - ray powder diffraction

3.3.1 Preliminary remarks

X - ray powder diffraction (see C.2.4.4 and E.3.6), one of the most widely used methods for amorphicity/crystallinity determination, doesn't have the sensitivity required to detect the low amounts of the amorphous material present in the micronised samples. Therefore, only spray - dried samples of lactose, salbutamol base and salbutamol sulphate, untreated and treated by conventional and electrostatically supported mixing were investigated using powder X - ray diffraction. In some diagrams, the peaks are not presented in full height, because of the disadvantageous scale for small peaks in the opposite case.

3.3.2 Lactose

The X - ray powder diffraction peaks of crystalline α - lactose monohydrate (Figure 54) are sharp and defined. The patterns of the spray - dried untreated lactose and lactose samples, which were treated using conventional and electrostatically supported mixing, show broad and diffuse halos due to a random arrangement of the constituent molecules in the amorphous state, which produces poor, coherent scatters (Figure 55). These patterns are quite distinguishable from those produced by crystalline lactose. The lack of crystalline long - range order diffraction peaks suggests the amorphous nature (Young et al., 2007). There is no dependence of the amorphicity/crystallinity grade of the spray - dried lactose sample on the mixing mode, which is in good accordance with the results of the moisture sorption analysis. So, the hypothesis that the difference of the thermogram of the sample treated by electrostatically supported mixing (see 3.2.2) and the one treated by conventional mixing as well as the untreated sample is caused by a spontaneous recrystallisation of this sample in course of the DSC experiment, but not by a true difference between the three samples, is supported. The small peak, which is detected at the diffraction angle of approximately 37° in the curve representing the spray - dried lactose treated by conventional mixing may be attributed to some error of the measuring device and may be classified as artefact.

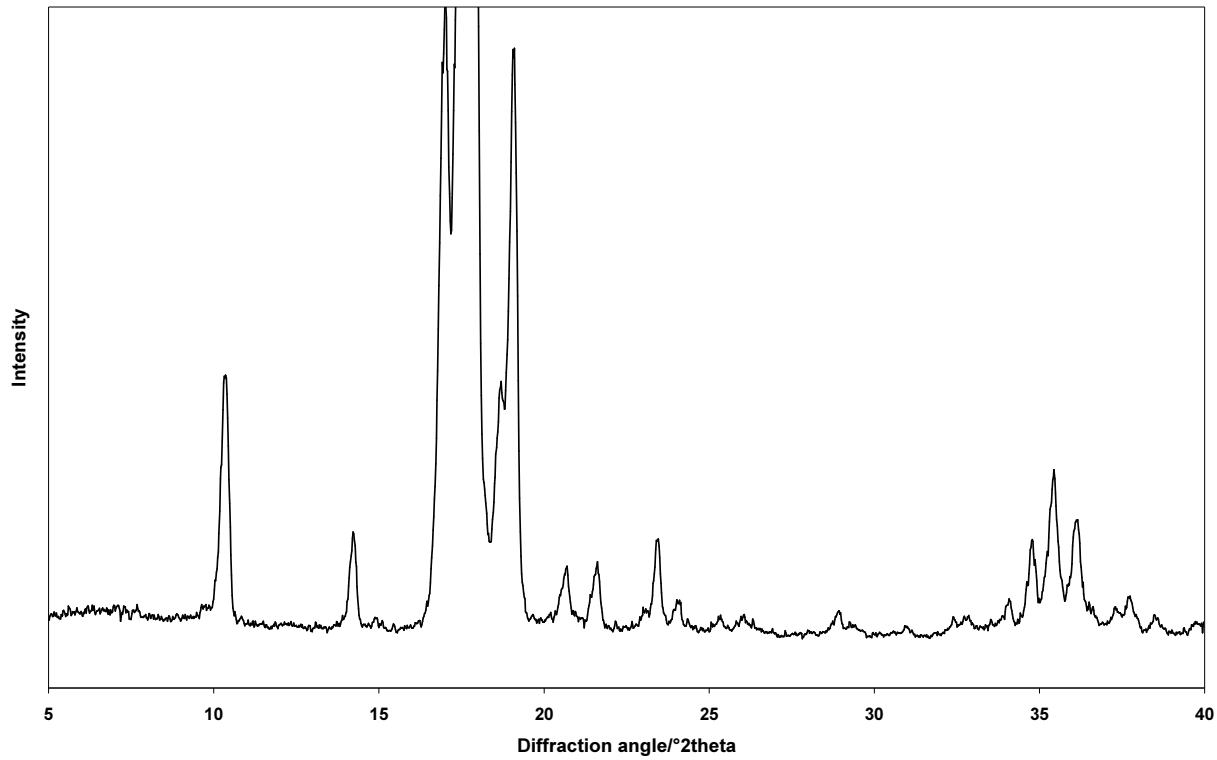

Figure 54: X - ray powder diffraction pattern of crystalline lactose, the curve of the first of two measurements is presented

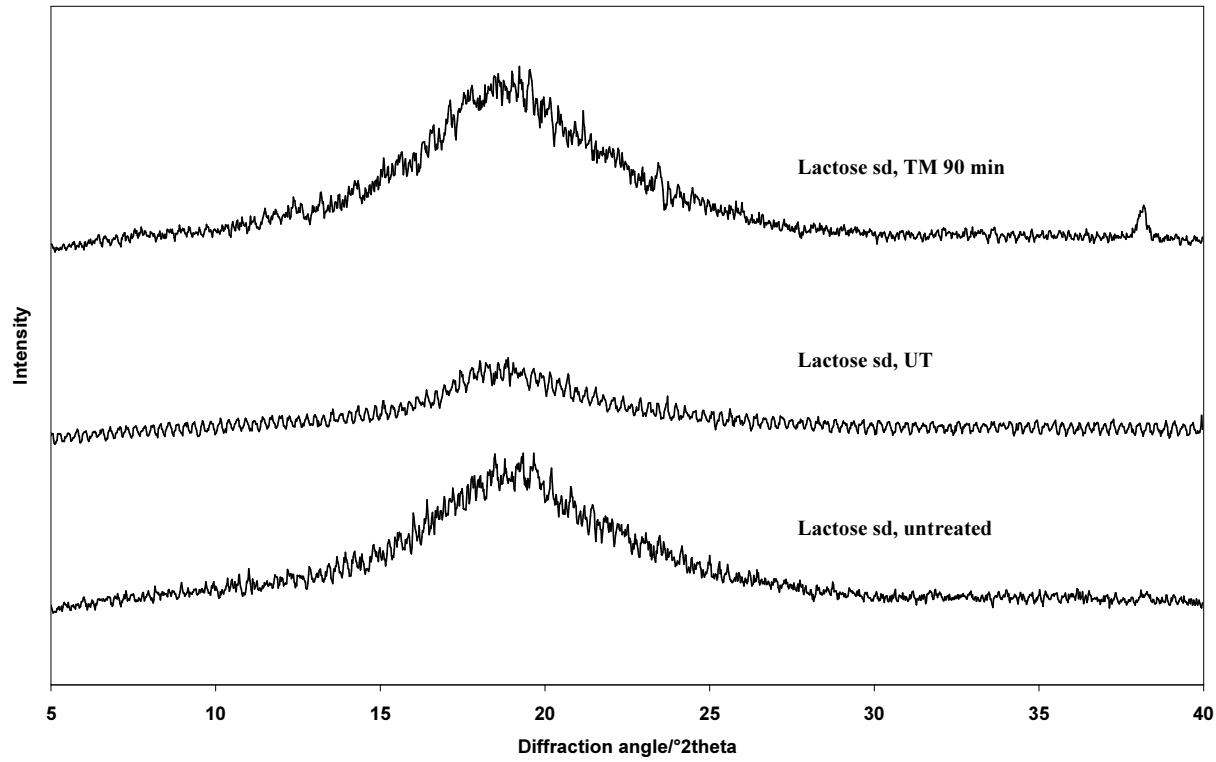

Figure 55: X - ray powder diffraction patterns of untreated spray - dried (sd) lactose and samples treated using electrostatically supported (UT) and conventional (TM 90 min) mixing, the curve of the first of two measurements is presented

3.3.3 Salbutamol base

The X - ray powder diffractogram of crystalline salbutamol base is shown in Figure 56. On the diffractogram the characteristic sharp diffraction peaks associated with a highly crystalline material are shown.

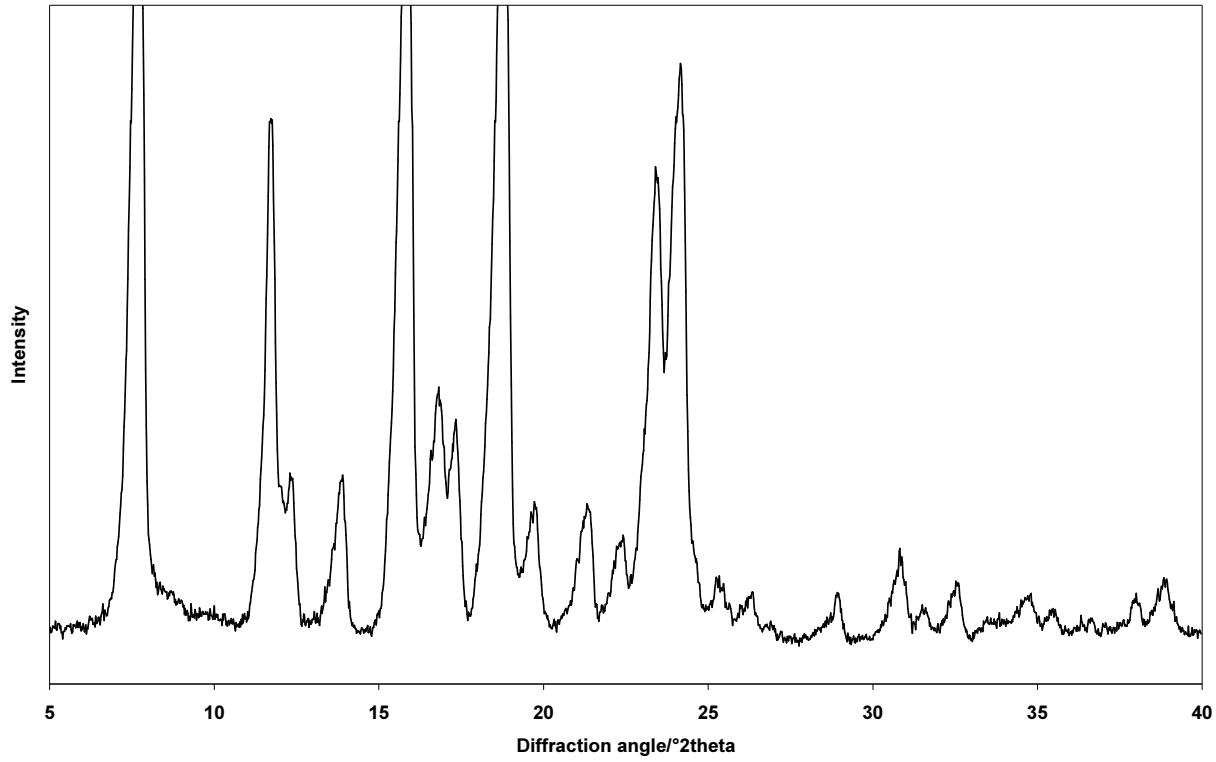

Figure 56: X - ray powder diffraction pattern of crystalline salbutamol base, the curve of the first of two measurements is presented

Figure 57 presents the X - ray traces of the spray - dried salbutamol base untreated and treated using conventional and electrostatically supported mixing. Sharp peaks, which indicate the crystallinity of all three samples, are found. No difference of the peak positions between the spray - dried and the crystalline samples is determined. However, the peak at the diffraction angle of approximately 15°, which is detected in the crystalline sample (Figure 56) is missing in the three spray - dried samples. This difference may be attributed to the fact that the shape of the crystalline particles (Figure 34 c) differs from the shape of the spray - dried particles (Figure 34 d), what may cause that the spray - dried particles take up another preferred orientation than the crystals of the crystalline salbutamol base samples, leading to a difference in the height of the diffraction peaks (Schoetlle, 2006).

No influence of the mixing mode on the amorphicity/crystallinity of the three spray - dried samples is found. These results are in good accordance with the results of moisture sorption and DSC investigations.

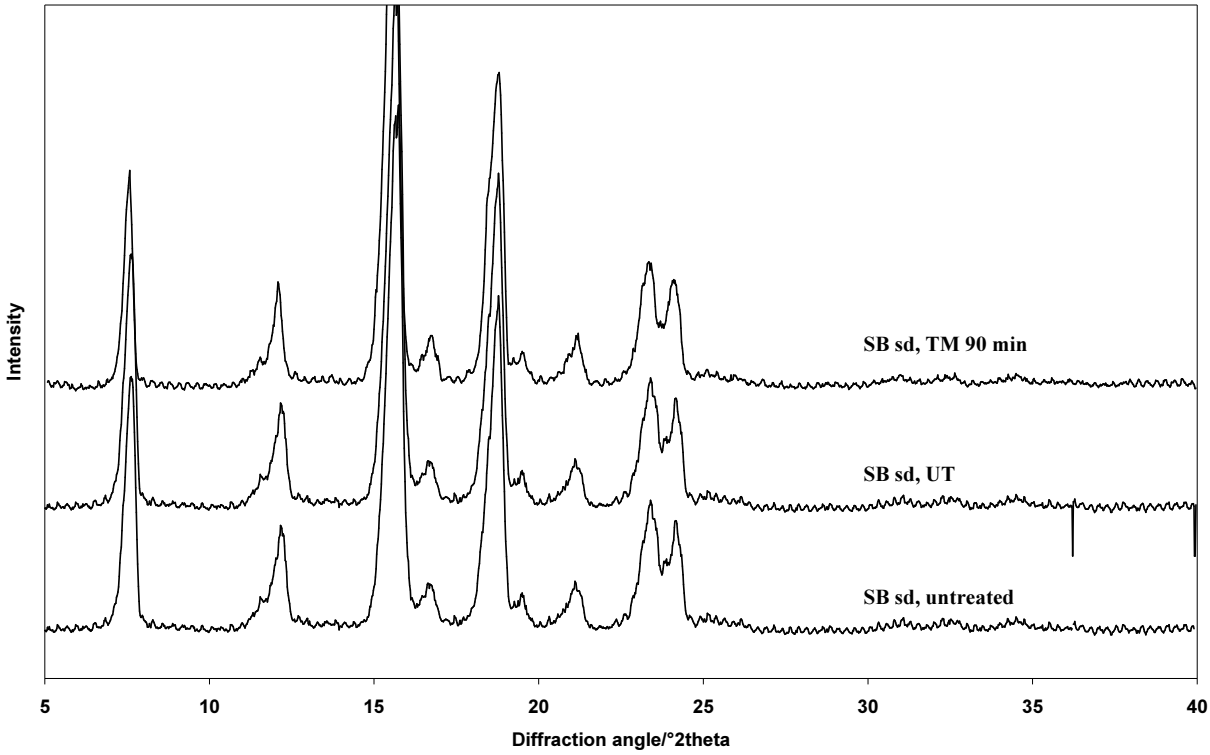

Figure 57: X - ray powder diffraction patterns of untreated spray - dried (sd) salbutamol base (SB) and samples treated using electrostatically supported (UT) and conventional (TM 90 min) mixing, the curve of the first of two measurements is presented

3.3.4 Salbutamol sulphate

Figure 58 presents the diffractogram of the crystalline salbutamol sulphate sample. Here the sharp peaks, as already was mentioned, affirm the crystalline nature of the sample (Young et al., 2007).

The spray - dried samples of untreated salbutamol sulphate and treated salbutamol sulphate using conventional and electrostatically supported mixing are found to be amorphous, due to the absence of the peaks, which are characteristic for the crystalline sample (Figure 59). Also no dependence of the mixing mode on the amorphicity/crystallinity of the samples is detected. This is in good accordance with the results of the DSC and moisture sorption analysis, with exception of salbutamol sulphate treated by electrostatically supported mixing. According the DSC (Figure 53) and X - ray measurements the spray - dried salbutamol sulphate sample treated by electrostatically supported mixing shows the behaviour characteristic for the amorphous powder. These results contrast with the results obtained by moisture sorption analysis. According to the moisture sorption diagram (Figure 48) the run of spray - dried salbutamol sulphate treated by electrostatically supported mixing suggests the crystalline nature. As was discussed in 3.2.4 it is probable, that the recrystallisation of spray - dried salbutamol sulphate took place at some time after the treatment by electrostatically supported mixing during storage or during the preparation of the sample for the moisture sorption measurements. If electrostatically supported mixing itself had caused recrystallisation, all three techniques would have identified the sample to be crystalline.

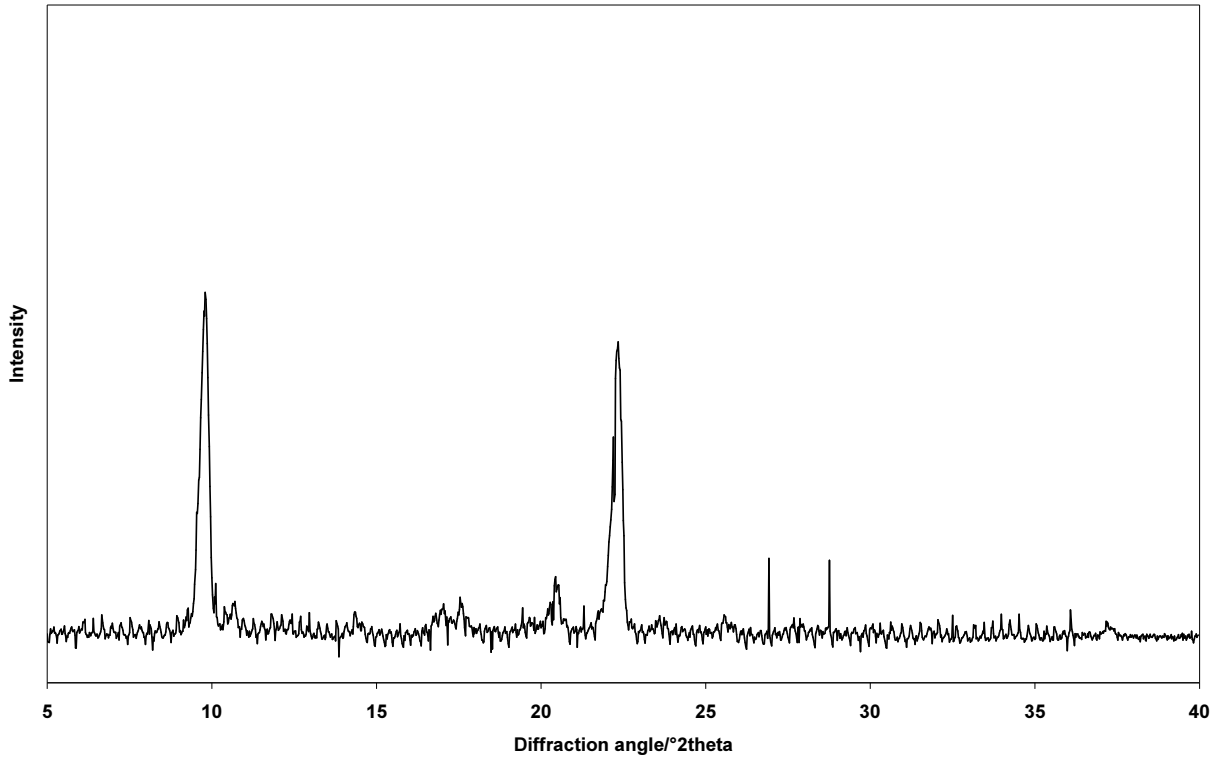

Figure 58: X - ray powder diffraction pattern of crystalline salbutamol sulphate, the curve of the first of two measurements is presented

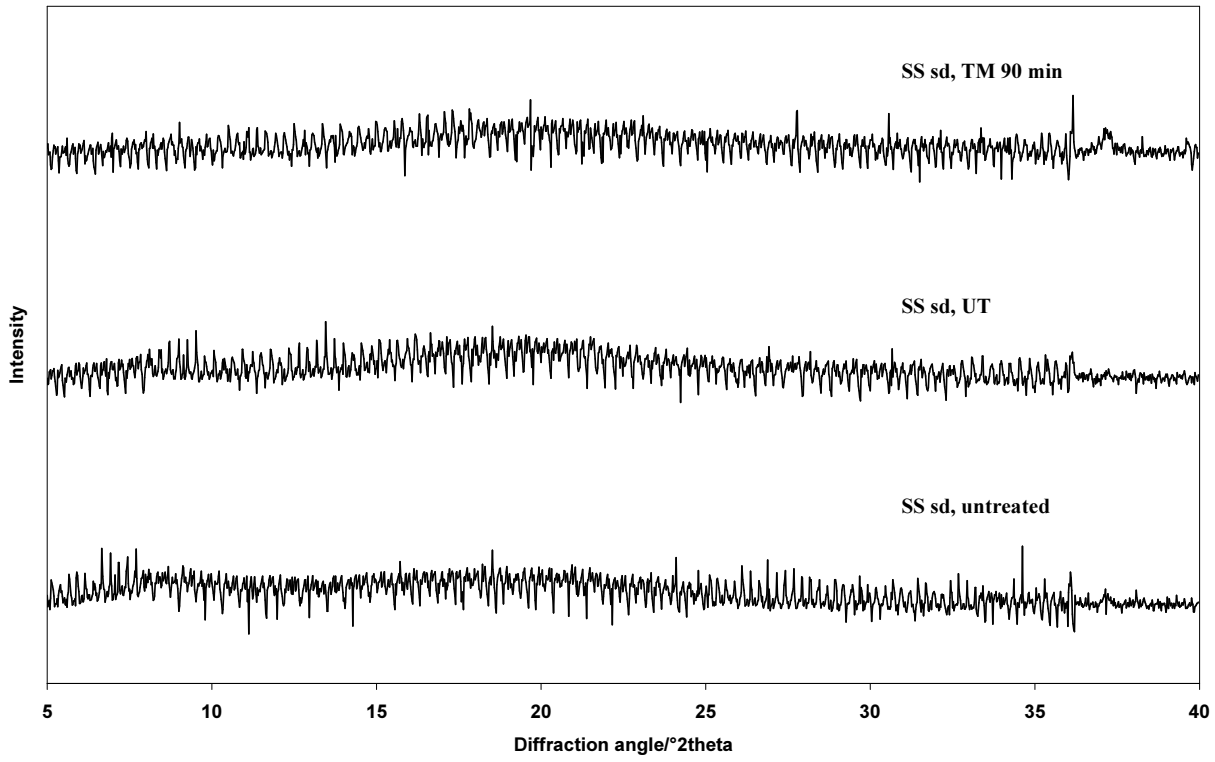

Figure 59: X - ray powder diffraction patterns of untreated spray - dried (sd) salbutamol sulphate (SS) and samples treated using electrostatically supported (UT) and conventional (TM 90 min) mixing, the curve of the first of two measurements is presented

3.3.5 Concluding remarks

With the help of the X - ray measurements it was possible to characterise the thermodynamic state of the investigated samples. In accordance with moisture sorption and DSC investigations, it was found out, that the spray - dried lactose and salbutamol sulphate show the behaviour, which is characteristic for the amorphous powder. In contrast to these results salbutamol base is shown to be crystalline.

In relation to the influence of the mixing mode on the crystallinity/amorphicity of spray - dried salbutamol sulphate, DSC and X - ray measurements reveal the spray - dried salbutamol sulphate sample treated by electrostatically supported mixing to be amorphous. These results contrast with the results obtained by moisture sorption analysis. According to the moisture sorption measurements spray - dried salbutamol sulphate treated by electrostatically supported mixing suggests the crystalline nature of the sample. As was discussed in 3.1.4 and 3.2.4, it is probable, that the recrystallisation of spray - dried salbutamol sulphate took place at some time after the treatment by electrostatically supported mixing during storage or during the preparation of the sample for the moisture sorption measurements. If electrostatically supported mixing itself had caused recrystallisation, all three techniques would have identified the sample to be crystalline. Anyway, the mentioned phenomenon recalls the problems associated with the instability of amorphous powders and reminds to take special care when handling amorphous materials. Furthermore, no changes of the crystallinity/amorphicity of spray – dried lactose treated by electrostatically supported mixing has been found using X - ray diffraction. This is in agreement with the results obtained by water vapour sorption, but does not correspond to the results obtained by DSC, where an enhanced enthalpy of recrystallisation of spray - dried lactose treated by electrostatically supported mixing has been found in comparison to the untreated spray - dried powder. This supports the hypothesis that the enhanced enthalpy of recrystallisation of the sample might be due to the spontaneous happening of recrystallisation during the DSC measurement itself, which by chance has not taken place in the other lactose samples under investigation.

3.4 Concluding remarks

Concluding the results of the chapter it has to be pointed out, that the investigation of crystallinity/amorphicity is quite complicated. Usually, it is not possible to characterise powders reliably by using just one technique. Therefore, it is very important to use different methods in order to investigate the stability of the samples in terms of crystallinity/amorphicity upon preparation and handling of the powder, such as micronisation, spray - drying and mixing. In this study, the combination of moisture sorption, DSC and X - ray techniques turned out to be reasonable. Moreover, the dependence of the sample behaviour on relative humidity (moisture sorption) and temperature (DSC) may be observed for the samples, which undergo such mechanical treatment as spray - drying, micronisation or mixing.

Combining moisture sorption, DSC and X-ray powder diffraction experiments, it has been found out, that spray - dried lactose and salbutamol sulphate are amorphous, whereas spray - dried salbutamol base is crystalline. Furthermore, micronisation of salbutamol base and salbutamol

sulphate does not change the crystallinity of the powders. In contrast, micronisation of lactose induces amorphous parts. In relation to the mixing mode, it has been shown, that there is no dependence of the crystallinity/amorphicity on the mixing mode.
According to these results salbutamol base may be recommended for the use in DPIs due to the thermodynamical stability of the material. Even spray – drying is resulting in a crystalline powder, which is not prone to change the thermodynamic state during further handling and processing.

4. Production of the interactive formulations

4.1 Conventional mixing

The preparation of the formulations, consisting of either spray - dried or micronised lactose, salbutamol base or salbutamol sulphate and different concentrations of nanoparticles (Aerosil® R972) were carried out using the TURBULA® mixer (see C.3.2 and E.4.1). According preliminary tests (the results of the tests are not presented in this work) the optimal mixing time is 90 min.

4.2 Electrostatically supported mixing

4.2.1 Preliminary remarks

An alternative way of mixing is electrostatically supported mixing (see C.3.3 and E.4.2). The aim of this method is to improve the homogeneity of the coating of the microparticulate active ingredient with nanoparticles and therefore to improve flowability, fluidisation and mass uniformity. The dispersion of each of the two mixing partners and the homogeneity of the coating depend on such parameters as time of mixing, speed of rotation of the rotor of the high - speed homogenator ULTRA - TURRAX® and nanoparticle - microparticle ratio. All these parameters influence the quality of the mixtures and will be analysed below.

Once the microparticles are coated with the nanoparticles, it is quite difficult to mechanically separate the nanoparticles from the microparticles again, because of the Van der Waals forces acting between nano - and microparticles. That is why the possibility of demixing is low and the nanoparticles are immobilised on the surface of the microparticles practically.

4.2.2 Dependence of charging on mixing parameters and particle concentrations

The following investigations of the parameters influencing the charging of the powder were carried out using the high - speed homogenator ULTRA - TURRAX®. As electrically non - conducting nonpolar fluid, liquid nitrogen was chosen. For the measurement of the induced charge a shielded measuring cup capacitor (Faraday cup), consisting of an isolated measuring cup (inner cup) and earthed protection cup (outer cup) in connection with a high - resistant electrometer was used (see C.3.3.5 and E.4.2).

At the beginning of the experiments, the influence of the different components of the experimental setup like measuring capacitor cup, electrically non - conducting fluid and ULTRA - TURRAX® disperser on the charge measured by the electrometer was investigated (Figure 60). At the beginning of the experiments, the timely fluctuations of the charge measured on the empty Faraday cup were measured during 600 s. Then 500 ml of the liquid nitrogen were poured into the cup and further measuring of the charge during another 600 s was done. At that point a minor shift of the charge is detected, though, the acquired charge stays stable during the following 600 s. Then the ULTRA - TURRAX® disperser was slowly inserted into the fluid and switched on at the rotation speed of 6200 rpm. At that point another shift of the charge is registered. The minor shift, that is measured, when the liquid nitrogen is poured into the Faraday

cup may be due to the charge of dust particles, which had been acquired from the surrounding air or stuck to the vessels where the liquid nitrogen has been filled in. By inserting the ULTRA - TURRAX® disperser and switching it on, these particles are charged causing another shift of the charge. Taking into consideration, that some changes regarding the charge in the Faraday cup may take place before the powder sample is added, it is important to wait, till the equilibration of the system due to the addition of liquid nitrogen and the switching on of the ULTRA - TURRAX® disperser is achieved and to make nullification before the powder under investigation is poured into the Faraday cup.

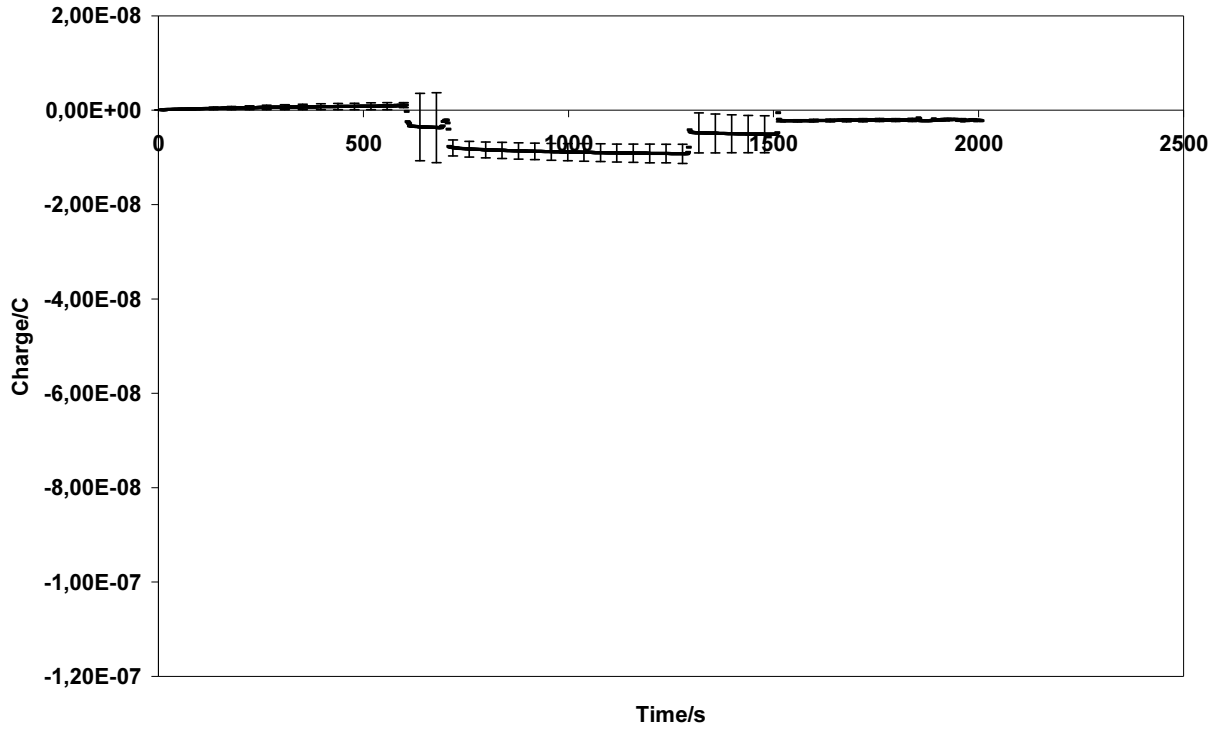

Figure 60: Mean ± s.d. of the of the charge measured on the Faraday cup: 0 s - 600 s: timely fluctuations of the charge measured on the empty Faraday cup; 600 s - 1200 s: charge measured on the Faraday cup containing liquid nitrogen; 1200 - 2000 s: charge measured on the Faraday cup after insertion and switching on of the ULTRA - TURRAX® disperser at the rotation speed of 6200 rpm (n = 3)

In course of the same experiment, the influence of the addition of a powder sample on the acquired charge was investigated using one of the three experiments carried out before for the investigation of the dependence of the acquired charge on the different components of the experimental setup (Figure 61). Therefore, 2 g of the test sample spray - dried lactose were poured into the Faraday cup. The suspension was stirred with 6200 rpm initially (time frame: 2000 s till 2600 s), and then the rotation speed was increased by 2000 rpm per 600 s. In relation to the amount of charge taken up by the powder sample, the contribution of the components of the system such as Faraday cup, liquid nitrogen and ULTRA - TURRAX® disperser to the acquired charge is only minor. It is observed, that the increase of the rotation speed leads to an increase of the measured negative charge. As the speed of the rotation of the rotor is shown to

influence the amount of the acquired charge, further investigations on this dependence were carried out.

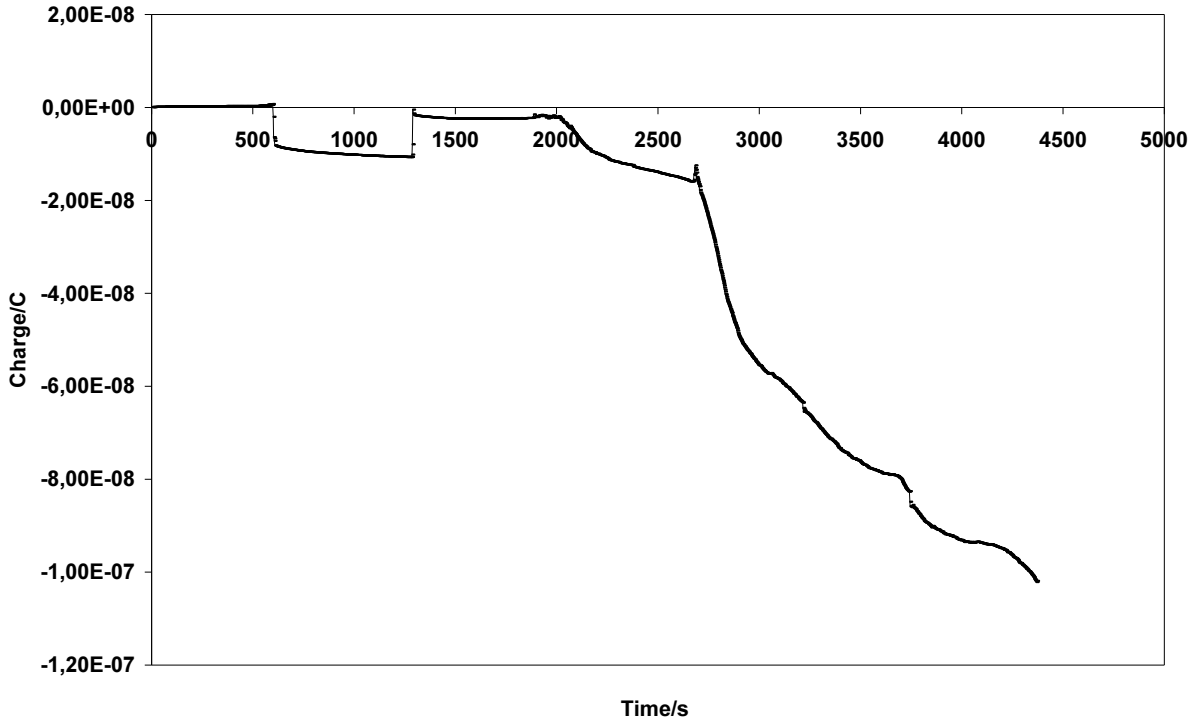

Figure 61: Charge measured on the Faraday cup: 0 s - 2000 s: see legend of Figure 60; 2000 s - 2600 s: addition of 2 g of spray - dried lactose and stirring at 6200 rpm; 2600 s - 4400 s: increasing of the rotation speed by 2000 rpm per 600 s (n = 1)

For the charging experiments 1 g and 2 g powder samples of spray - dried lactose were suspended in liquid nitrogen and stirred with the ULTRA - TURRAX® at different rotation speeds of the rotor, namely 6200 rpm (the lowest possible speed), 8200 rpm and finally 10200 rpm (Figure 62 and Figure 63). Further increasing of the rotation speed led to increasing of the wave of the rotor - stator system, inducing high turbulences inside the suspension and hindering the precise measurement of the acquired charge.

Comparing the acquired charge of the samples of 1 g powder at different rotation speeds, no difference between samples treated with 6200 rpm, 8200 rpm and 10200 rpm is detected (Figure 62). Probably, the acquired charge in relation to the scatter of the values is too low in order to obtain a significant difference between the samples treated at 6200 rpm, 8200 rpm and 10200 rpm. In case of samples treated at 10200 rpm, the standard deviations are especially high, indicating poor reproducibility. At this speed the generated wave might have been too high, leading to highly scattering results.

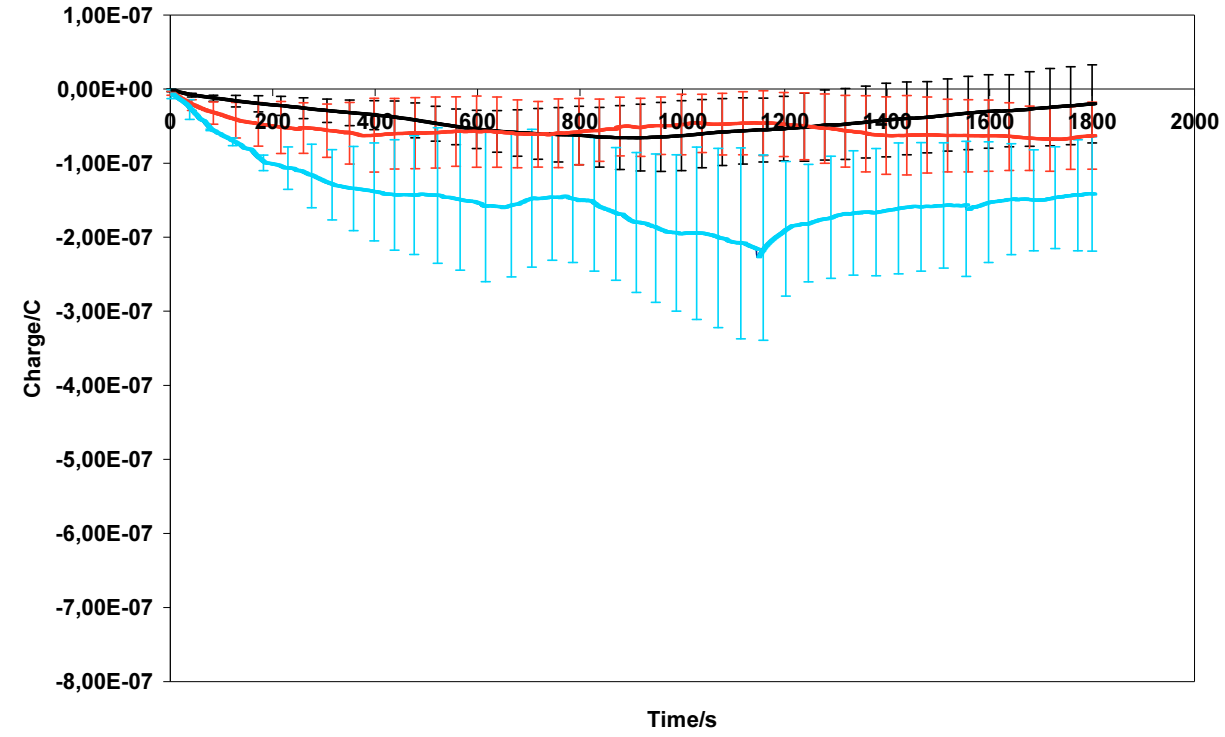

Figure 62: Mean ± s.d. of the acquired charge of 1 g of spray - dried lactose in dependence on the rotation speed of the ULTRA - TURRAX® rotor: 6200 rpm (black curve), 8200 rpm (red curve), 10200 rpm (blue curve) (n = 3)

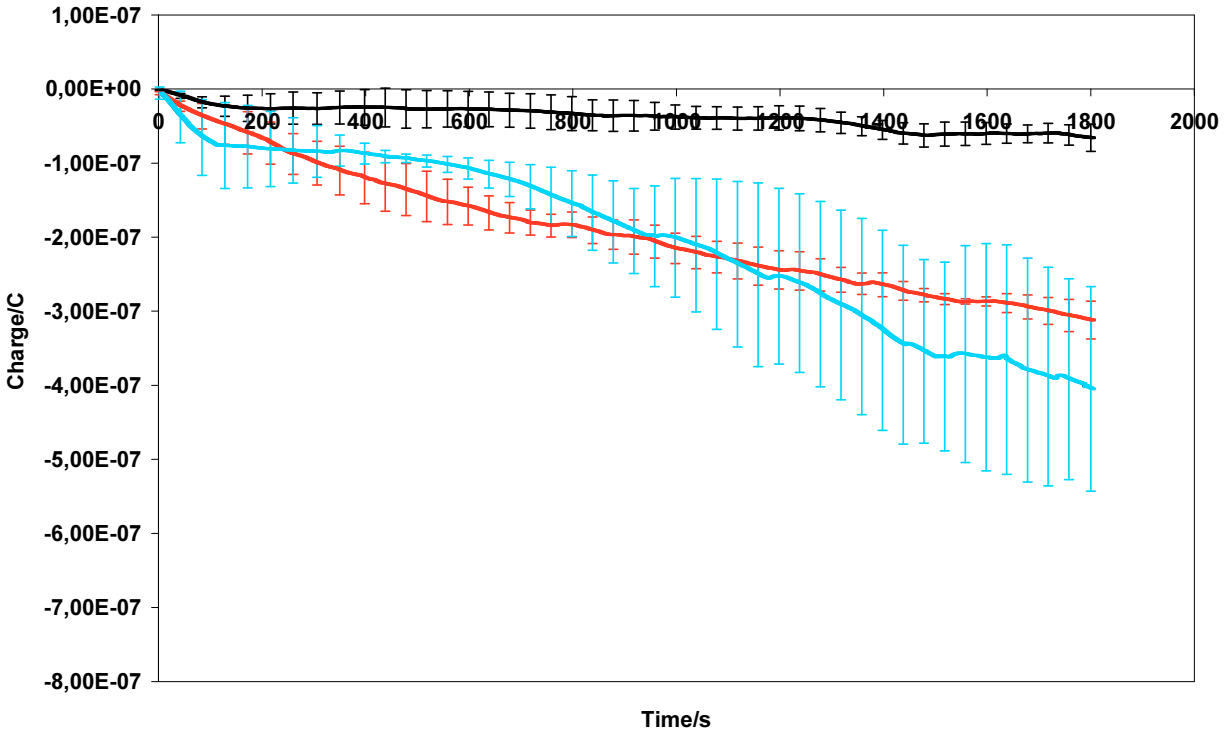

Figure 63: Mean ± s.d. of the acquired charge of 2 g of spray – dried lactose in dependence on the rotation speed of the ULTRA - TURRAX® rotor: 6200 rpm (black curve), 8200 rpm (red curve), 10200 rpm (blue curve) (n = 3)

Figure 63 shows the results of the charging experiments of the 2 g samples. Reproducible results in terms of the acquired charge were achieved by stirring at 6200 rpm and 8200 rpm. In contrast to these curves, the reproducibility of the charging, which was carried out at 10200 rpm is quite poor, also indicating that the speed of rotation at 10200 rpm is too high.
In comparison to the sample stirred at 6200 rpm, the induced charge of the particles stirred at 8200 rpm is increased, because the energy transferred upon tribocharging at 6200 rpm is lower in comparison to 8200 rpm resulting in a lower over all charge of the sample. In comparison to the 1 g sample, the charge acquired with the 2 g sample is higher due to the higher absolute surface of the 2 g sample.
According to the results of the preliminary charging experiments, the amount of the acquired charge is dependent on the rotation speed of the rotor, duration of the charging experiment and concentration of the particles in the suspension. The best charging conditions in terms of reproducibility are achieved using 2 g of the sample, dispersed at the rotation speed of 8200 rpm. These parameters were used during the following investigation of the dispersion and charging of the powder mixtures.

4.2.3 Dependence of charging on chemical identity

The charging behaviour of spray - dried and micronised lactose, salbutamol base and salbutamol sulphate was investigated. 2 g of each powder sample were suspended in approximately 500 ml of liquid nitrogen and were stirred during 800 s at the rotation speed of 8200 rpm.
Figure 64 - Figure 66 show the mean of the acquired charge of three charging experiments. It is noticeable, that the charge acquirement of salbutamol base and salbutamol sulphate differs from the one of lactose. The induced charge of the salbutamol base and sulphate particles is positive, in contrast to that of the lactose particles, which is negative. These differences may be explained by the differences in chemical structure and work functions of the three substances (Linsenbuehler et al., 2002; Linsenbuehler et al., 2004; Bailey, 1993).
The induced charge of the micronised products in case of salbutamol base and salbutamol sulphate is lower in comparison to the spray - dried products. In case of lactose the micronised product acquired a higher negative charge in comparison to the spray - dried particles. The differences in the values of the acquired charge between spray - dried and micronised powders may be explained by the differences in particle size, shape, surface, specific surface area and also crystallinity (see C.3.3).
The high scatter of the acquired charge represents the high sensitivity of the charging experiments and the charge measurements, which are not easy to reproduce. Reproducible experimental results on electrostatically supported mixing are difficult to obtain, because charging of surfaces is very sensitive to numerous parameters, such as roughness, contact pressure, the size of the object and the rubbing or gliding velocity between the surfaces but also temperature and relative humidity (Poppe, 1999).

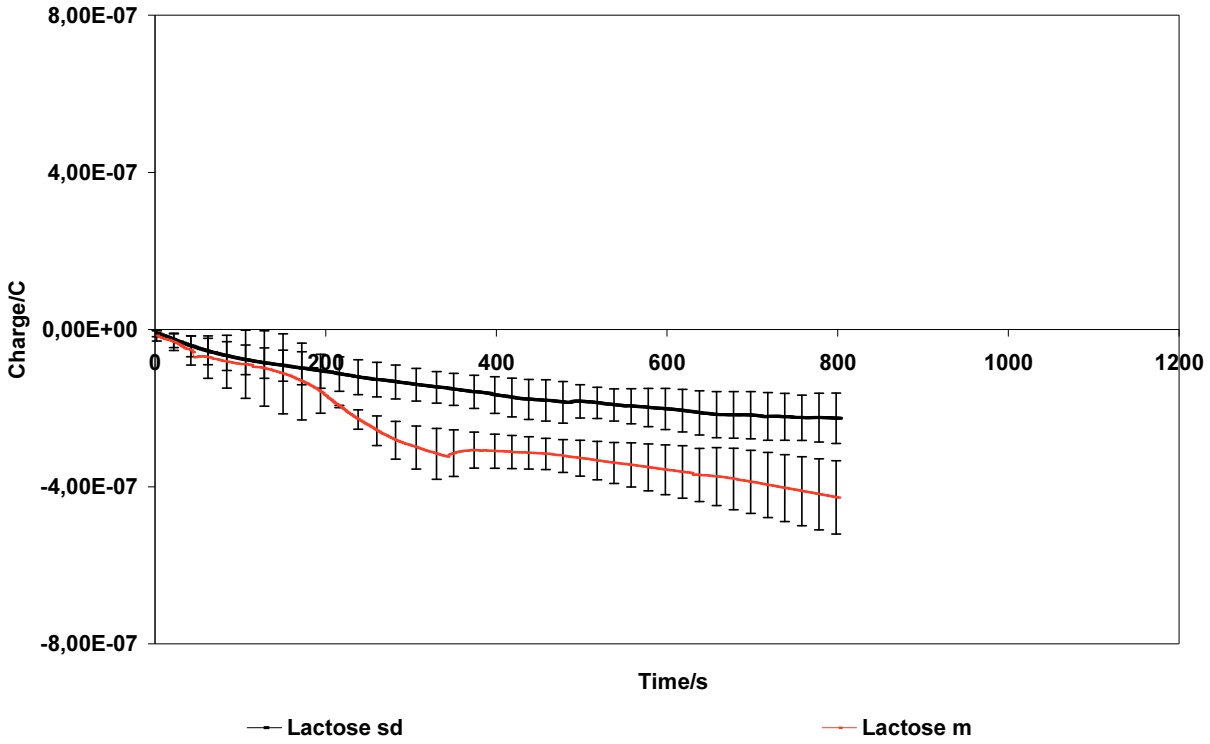

Figure 64: Mean ± s.d. of the acquired charge of 2 g of spray – dried (sd) lactose (black curve) and micronised (m) lactose (red curve) at 8200 rpm during 800 s (n = 3)

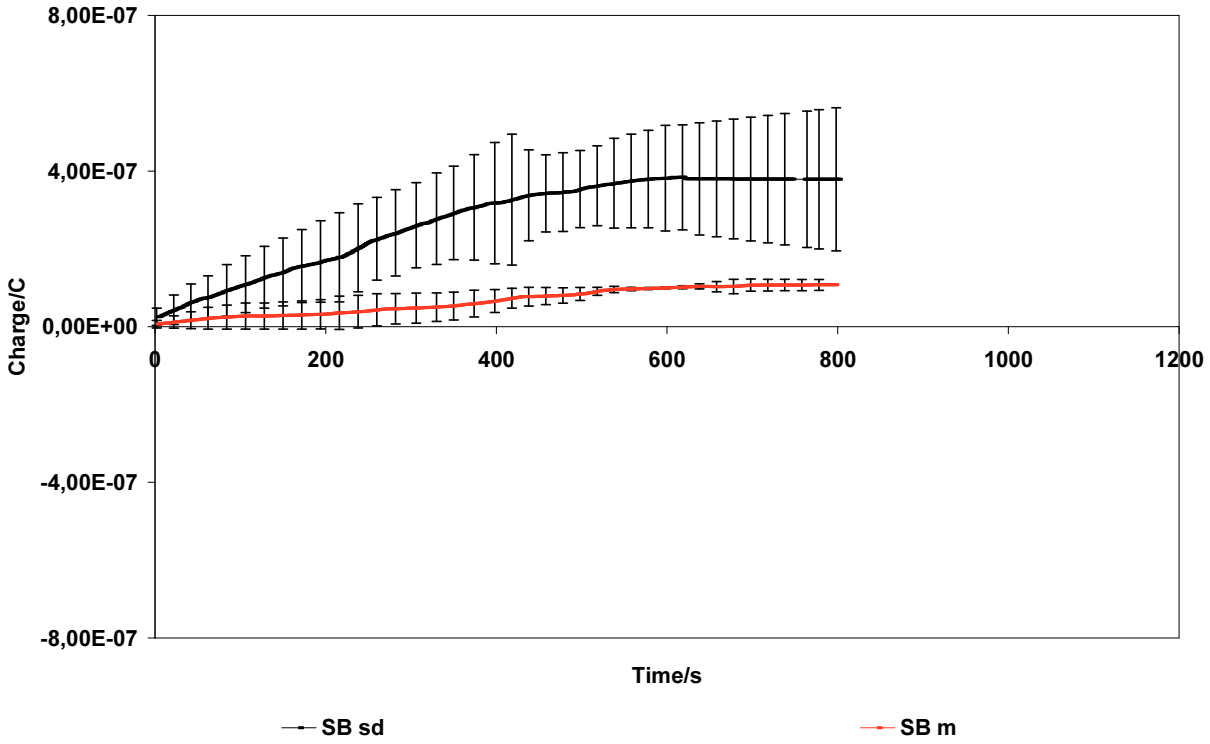

Figure 65: Mean ± s.d. of the acquired charge of 2 g of spray – dried (sd) salbutamol base (SB) (black curve) and micronised (m) salbutamol base (SB) (red curve) at 8200 rpm during 800 s (n = 3)

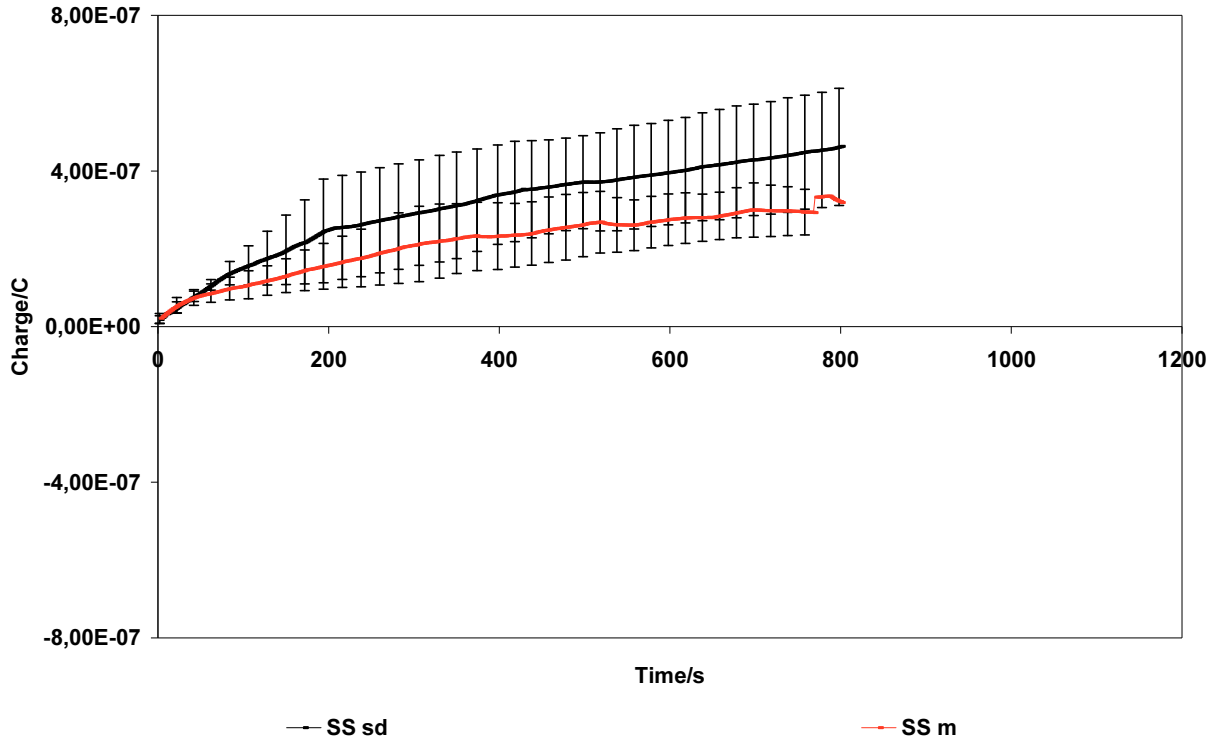

Figure 66: Mean ± s.d. of the acquired charge of 2 g of spray – dried (sd) salbutamol sulphate (SS) (black curve) and micronised (m) salbutamol sulphate (SS) (red curve) at 8200 rpm during 800 s (n = 3)

4.2.4 Charging behaviour of the nanoparticle fraction

The following investigations with Aerosil® R972 were carried out in order to investigate the charging behaviour of the nanoparticles. As the sample mass was chosen to be 2 g and as the nanoparticle concentration was chosen to be 0.5 %, 2.5 % and 12.5 % (see 1.4), nanoparticle samples of 0.01 g, 0.05 g and 0.25 g of Aerosil® R972 were prepared. The investigation of the charging behaviour was carried out on these samples at the rotation speed of 8200 rpm. Figure 67 presents the results of the charging experiments. The dependence of the acquired charge on the amount of nanoparticles in the suspension is detected. The lower the amount of the nanoparticles the lower the total acquired charge of the nanoparticle sample is. This can be explained by the fact that the absolute surface of the particles increases with the increase of the mass of the nanoparticles.

It is also observed, that in case of the sample with 0.5 % Aerosil® R972 at the beginning of the experiments the particles acquire a negative charge, later on they give off electrons again. The reversal of the polarity of hydrophobic Aerosil® R972 was also observed by Linsenbuehler, who investigated the charging behaviour of Aerosil® R972 (Linsenbuehler, 2005). Additionally, Harper reported, that the polarity of the obtained charge may reverse to the opposite without obvious reason (Harper, 1967). The scatter of the values of the acquired charge represents again the high sensitivity of the charging experiments and charge measurements to a variety of parameters.

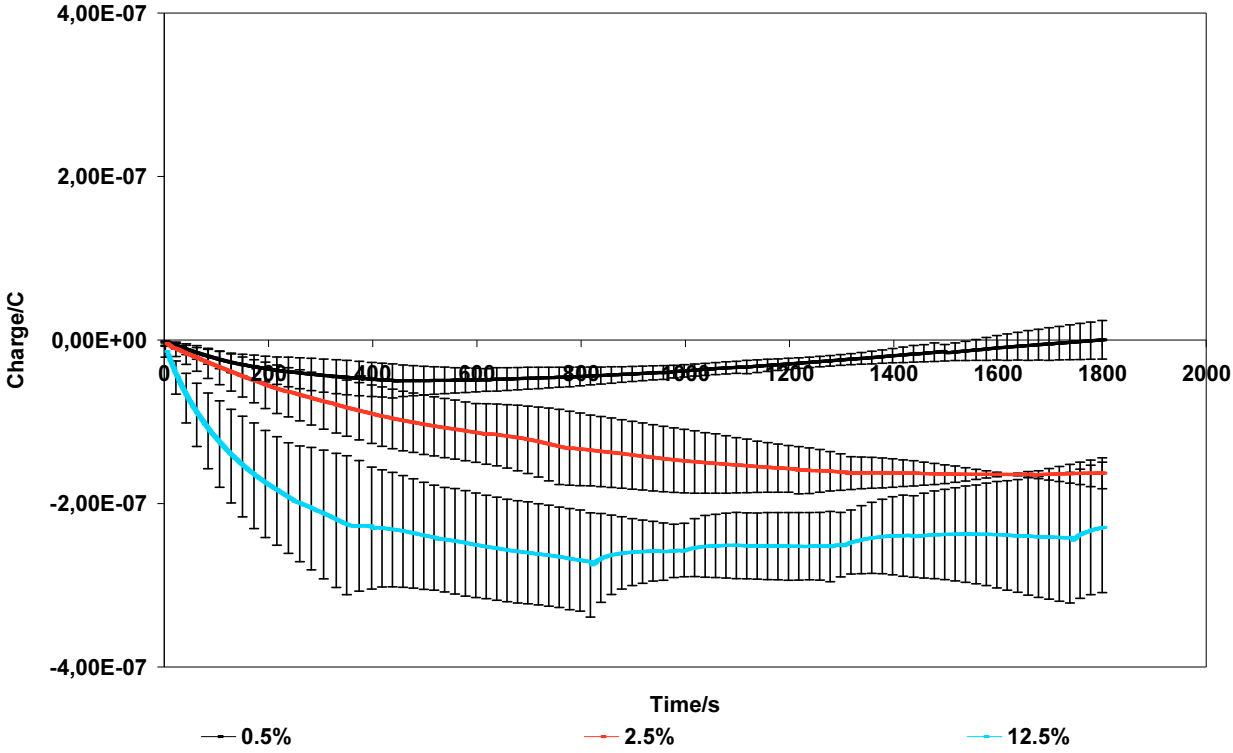

Figure 67: Mean ± s.d. of the acquired charge of 0.01 g (black curve), 0.05 g (red curve) and 0.25 g (blue curve) Aerosil® R972 at 8200 rpm during 1800 s (n = 3)

4.2.5 Charging process of different powder mixtures

As the dispersion of particles becomes more difficult as particle size decreases, nanoparticles were charged first in order to ensure proper dispersion. Afterwards, the microparticles were added to the nanoparticle suspension. The nanoparticles were suspended in liquid nitrogen. They were stirred and dispersed at 8200 rpm till the acquired charge was maximum or reached a plateau. Then, the microparticle fraction was given to the Aerosil® R972 suspension. At that point not only charging and dispersion of like particles, but also attraction and charge diffusion between micro - and nanoparticles and therefore the coating of microparticles with nanoparticles takes place. Finally, liquid nitrogen was allowed to evaporate leaving behind the dry powder mixture consisting of microparticles covered with nanoparticles.

On Figure 68 and Figure 69 examples of the charging curves of powder mixtures containing 2.5 % Aerosil® R972 and spray - dried or micronised lactose, salbutamol base and sulphate are displayed in order to give a rough idea about the charging behaviour. The same experiments were carried out with the mixtures containing 0.5 % and 12.5 % Aerosil® R972 and spray - dried or micronised lactose, salbutamol base or sulphate (results are not presented). As was already shown, the salbutamol base and salbutamol sulphate samples are positively charged, so after the adding of the microparticle fraction to the nanoparticle suspension, the curve drifts in the positive direction. The charging of the powder samples was carried out till the total measured charge of the system was zero, meaning that the total charge of the whole amount of the powder mixture is neutral. In case of lactose, the adding of the microparticle fraction leads to further increase of the negative charge. The charging experiment is completed after the equilibrium state

inside the system had been achieved, which is indicated by the run of the measuring curve parallel to the x - axis.

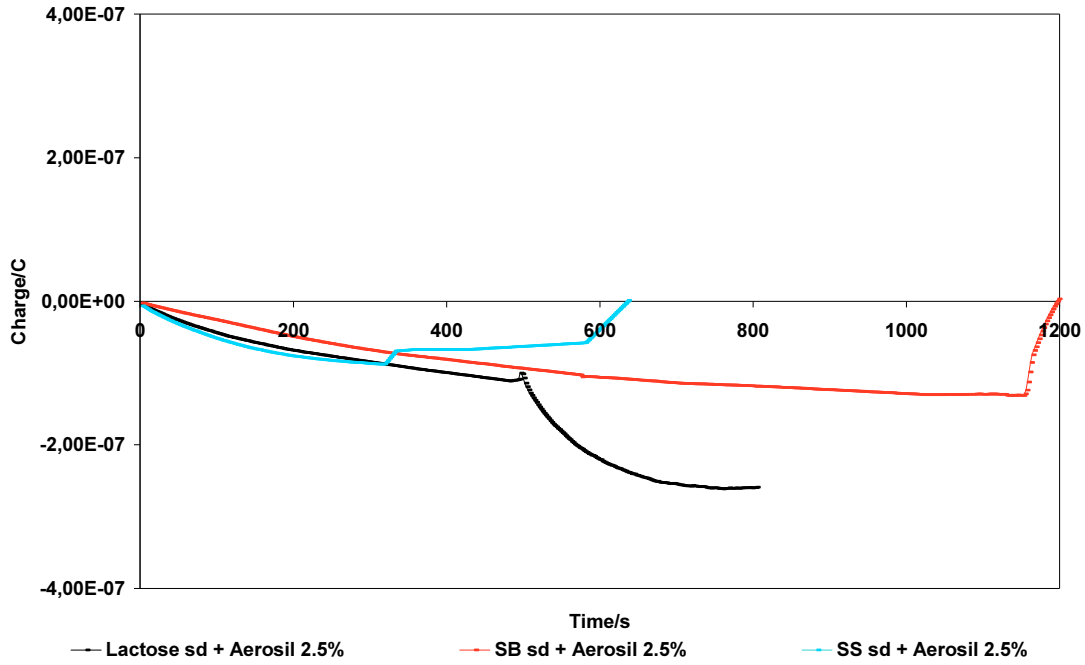

Figure 68: Acquired charge of spray - dried (sd) lactose (black curve), salbutamol base (SB) (red curve) and salbutamol sulphate (SS) (blue curve) with 2.5 % Aerosil® R972 in each sample in liquid nitrogen using ULTRA - TURRAX® disperser at 8200 rpm, the curve of the first of three measurements is presented

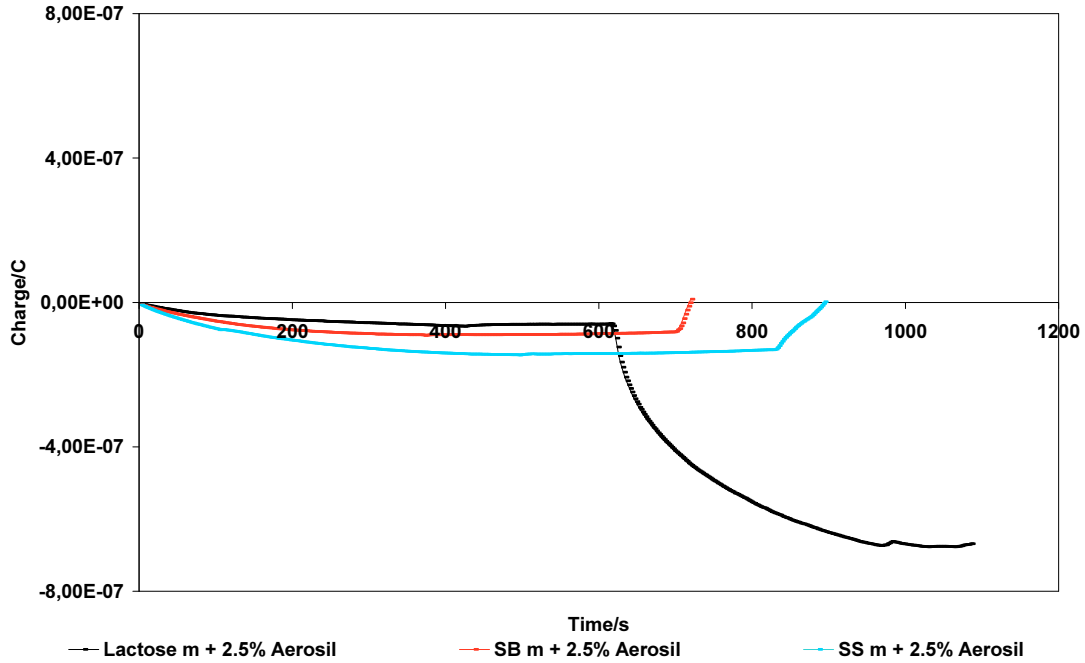

Figure 69: Acquired charge of micronised (m) lactose (black curve), salbutamol base (SB) (red curve) and salbutamol sulphate (SS) (blue curve) with 2.5 % Aerosil® R972 in each sample in liquid nitrogen using ULTRA - TURRAX® disperser at 8200 rpm, the curve of the first of three measurements is presented

4.2.6 Concluding remarks

Observing the results of the electrostatically supported mixing the impossibility to precisely control the acquired charge and difficulties in ensuring reproducible results in terms of the acquired charge are striking. This is due to the circumstances, that triboelectrical charging is a very complex phenomenon and is not fully investigated. There are a lot of factors, such as material properties, stirring conditions, relative humidity and temperature, which have an enormous influence on the results of the experiments and therefore further in - depth analysis has to be carried out, in order to understand the whole complexity of the charging. This, however, was not the focus of this study. Even without the perfect reproducibility of charging, it will be shown in the following chapters, that flowability, uniformity of mass and respirable fraction is quite reproducible. This means, that even charging may be poorly reproducible, the effect of electrostatically supported mixing on the quality of the powder inhalate is quite clear.

5. Flow behaviour of the interactive formulations

5.1 Flowability measurements

5.1.1 Preliminary remarks

For the measurement of the flowability different tests were carried out. These tests were done only with the untreated spray - dried lactose and powders treated by TURBULA® mixing, because they require at least 100 ml of powder. As this exceeds by far the batch size obtainable by electrostatically supported mixing, powders obtained by electrostatically supported mixing have not been examined. Investigations on the flowability of salbutamol base and sulphate were not performed either, because the material needed would have been too costly.

5.1.2 Ring shear tester

Markefka (Markefka et al., 2005) was able to show, that the ring shear tester, due to the sensitive detection of the differences in powder flowability, may be successfully used for the measuring of the flowability of powders which are intended for the use in dry powder inhalers. The average of the ff_c values (see C.4.1.1 and E.5.1) of untreated spray - dried lactose and spray - dried lactose treated by conventional mixing is shown in Figure 70.

Untreated spray - dried lactose and spray - dried lactose without Aerosil® R972 treated by conventional mixing show the lowest ff_c values indicating poor flowability. This means a cohesive behaviour. Mixtures of spray - dried lactose containing 0.5 %, 2.5 % or 12.5 % Aerosil® R972 show higher ff_c values than pure spray - dried lactose. This means an improvement of the flowability obtained by coating of the lactose particles with nanoparticles. Ring shear testing allows not only to differentiate between pure spray - dried lactose and mixtures containing different concentrations of Aerosil® R972, but also to rate the improvement of the flow behaviour among the mixtures with different nanoparticle concentrations in the ascending order 12.5 %, 2.5 % and finally 0.5 %.

As was mentioned earlier in relation to the improvement of the flow behaviour, the optimum coating level is supposed to be in between the upper and lower coating limit (see B.3.3). For the mixtures with 0.5 % and 2.5 % Aerosil® R972, the concentrations of Aerosil® R972 lay definitely below the upper coating limit, because in both cases, the host particles are not completely covered with a monolayer of guest particles (see 1.4). In case of the coating of the host particles with 12.5 % of Aerosil® R972, the amount of the Aerosil® R972 lays beyond the upper coating limit (see 1.4).

Starting from the concentration of 0 % Aerosil® R972 and moving to 0.5 % Aerosil® R972, flowability is enhanced at first, due to the decrease of interparticle interactions caused by the increasing number of nanoparticles acting as spacers. Increasing the nanoparticle concentration further to 2.5 % and finally to 12.5 %, leads to a decrease of flowability, probably caused by the emergence of mechanical interlocking exerted by the increasing number of nanoparticles on the microparticle surface.

In order to find out the precise concentration of the guest particles in the mixture, which ensures the highest improvement of the flowability, a fine tuning in the range between 0 % and 2.5 % would have to be done, because the optimum may lay between 0 % and 0.5 % of Aerosil® R972 as well as in between 0.5 % and 2.5 %. Anyway, considering the decrease of the flowability

when increasing the Aerosil® R972 concentration from 0.5 % to 2.5 %, the optimum won't definitely exceed 2.5 %.

The achieved results are in good accordance with the results obtained by Linsenbuehler (Linsenbuehler, 2005), who found, that the ff_c of a untreated spray - dried lactose mixture with 0 % Aerosil® R106 is the poorest. By increasing the Aerosil® R106 concentration flowability improved. He obtained the best results with a mixture containing 0.9 % (w/w) of Aerosil® R106, prepared using electrostatically supported mixing. The mean particle size of the spray - dried lactose was x_{50} = 3.68 µm. Further increasing of the concentration of the guest particles led to the deterioration of the ff_c values (Linsenbuehler, 2005). Taking into account, that the median of the particle size distribution of the spray – dried lactose used in this study is higher (x_{50} = 8.37 µm) and provided that the materials and procedures used by Linsenbuehler are quite similar, the optimum nanoparticle concentration for the formulations of this study is expected to be below 0.9 %, which is in the range indicated above.

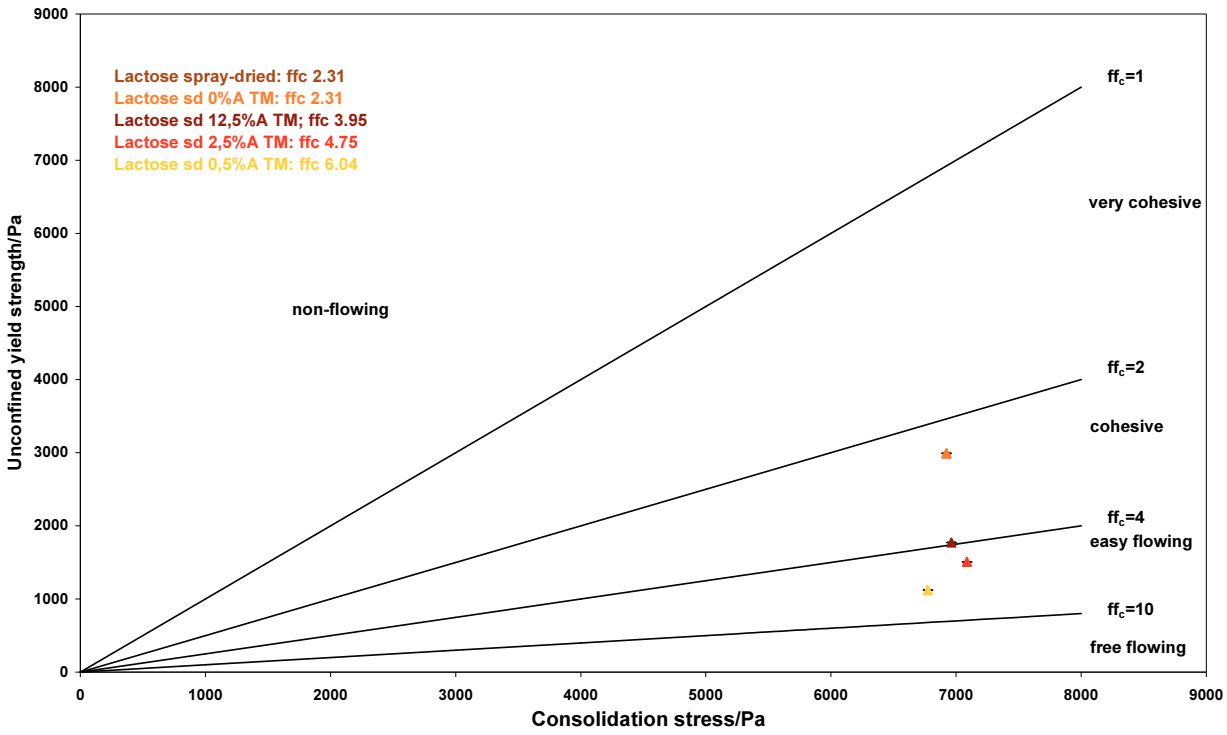

Figure 70: Mean ± s.d. of the ff_c - values of samples of untreated spray - dried (sd) lactose and mixtures containing spray - dried lactose and 0 %, 0.5 %, 2.5 % and 12.5 % Aerosil® R972 (A) prepared by conventional mixing (TM) (n = 3)

According to Meyer (Meyer, 2003) the concentration of 0.2 % (w/w) Aerosil® 200 is theoretically the ideal concentration for the coating of corn starch particles with the mean diameter of x_{50} = 22.0 µm. The best ff_c values (ff_c = 11) were obtained after mixing the powder fractions in the TURBULA® mixer for 360 minutes. Although the corn starch particles differ from lactose, at least, they are spherical like the spray – dried lactose particles used in the present study. As they are larger in comparison to the spray – dried lactose particles used in this study (x_{50} = 8.37 µm), the optimum nanoparticle concentration for the formulations of this study is

expected to be above 0.2 %, which also is in the range indicated above. However, it has to be kept in mind that the investigations by Meyer and the present study differ not only by the identity of the host and guest particles but also by the mixing time (360 min versus 90 min). Nevertheless, if these differences are discarded, the optimum nanoparticle concentration is expected to be in between 0.2 % (Meyer) and 0.9 % (Linsenbuehler), which is in good accordance to the results of this study.
According to the results of the measurements of the flowability using the ring shear tester, the coating of the host particles with nanoparticles by conventional mixing improves the flow behaviour of the powder samples. The key factor of flowability enhancement represents the amount of the guest particles in the sample. If the amount of the nanoparticles is too low, the guest particles are not able to act as spacers, the contact distance between the host particles is not increased and the powder is poorly flowable. If the amount of the nanoparticles is too high, mechanical interactions will take place deteriorating flowability also.

5.1.3 Hausner ratio

Another measure for the flowability of powders is the Hausner ratio. The lower the Hausner ratio and therefore the value of the volume of the loosely poured powder at the beginning of the experiment divided by the volume after tapping the powder a defined number of taps, the better the flowability of the powder (see C.4.1.2 and E.5.2).
Generally, uncoated spray - dried lactose exhibits a higher Hausner ratio than lactose coated with nanoparticles (Figure 71). Addition of Aerosil® R972 decreases the apparent volume and thereby the Hausner ratio of the spray - dried powder. Because of adhering of the nanoparticles on the surface of the microparticles, the interparticle forces between lactose particles are reduced and the particles are able to arrange themselves in the final densest packing, already when they are poured into the glass cylinder without additional energy input by tapping. Again, as with the ff_c values determined by ring shear testing, the best results were achieved by the powder mixture with 0.5 % Aerosil® R972. Differences between the mixtures with 0 % and 0.5 % and 0.5 % and 2.5 % Aerosil® R972 are significant. However, the difference between mixtures containing 2.5 % and 12.5 % Aerosil® R972 is not significant.
In a similar approach Kawashima (Kawashima et al., 1998) tried to improve the dispersibility of pranlukast hydrate by surface modification with light anhydrous silica acid. In that study the drug particles were coated with 2 %, 5 % and 10 % Aerosil® 200 using physical, Theta - composing mixing methods and also combined freeze and spray - drying methods. Though only a bulk density, which allows the calculation of the apparent volume, was determined, it was still possible to find out that the bulk density of the original uncoated pranlukast hydrate particles was higher than that of the coated particles. These results are in contrast to the present study and were attributed to the formation of agglomerates, caused by strong cohesive properties between the drug particles. The lowest value regarding bulk density of the powder mixtures was achieved by the mixture with 10 % Aerosil® 200 which was produced by physical mixing in a glass vessel with a vortex mixer, at the beginning, and in a mortar with a pestle at the end of the mixing process. The differences between the results obtained by Kawashima and in this study may be explained by the fact that not only two very different

mixing methods were used for the preparation of the powder samples, but also chemical identity and particle size, but most important particle shape especially of the used microparticulate powder fractions differ.

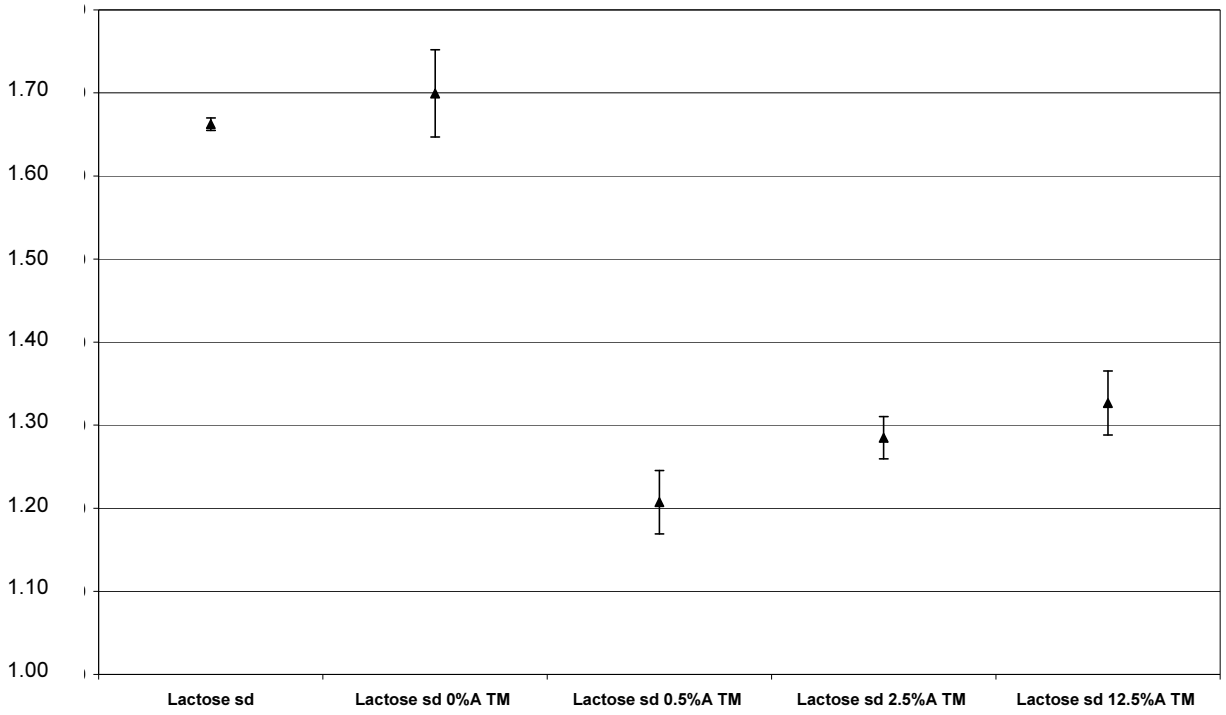

Figure 71: Mean ± s.d. of the Hausner ratio of mixtures containing spray - dried (sd) lactose and 0 %, 0.5 %, 2.5 % and 12.5 % Aerosil® R972 (A) prepared by conventional mixing (TM) (n = 3)

5.1.4 Flow rate and angle of repose

In flow rate tests, the time, which is needed to release 100 ml of the powder through the outlet of a funnel, is measured (see C.4.1.3 and E.5.3) (Figure 72). The better the flowability of the powder is, the greater is the amount of the powder passing the outlet of the funnel per time unit. The determination of the flow rate for spray - dried lactose containing no Aerosil® R972 was not possible due to its very poor flow properties. In this case the interparticle interactions were superior to the gravitational force and the powder stuck in the funnel.

In contrast, the determination of the angle of repose (see C.4.1.4 and E.5.4) of the mixtures containing spray - dried lactose and 0 %, 0.5 %, 2.5 % and 12.5 % Aerosil® R972 respectively, was possible. Measurements of the angle of repose were carried out using the powder funnel according Dr. Pfrengle. The powder under examination flows through the outlet of the glass funnel and forms a pile of a certain height on a round plate placed below the funnel. For the measurements of the angle of repose of the powders showing poor flow properties, such as powder samples with 0 % and 12.5 % Aerosil® R972, a stirring device was used. In order to calculate the angle of repose the height of the pile has to be divided by the radius of the plate, which is known. Figure 72 represents the results of the performed experiments.

Data obtained by the measurements of the flow rate and the angle of repose (Figure 72) support the statement that mixing of spray - dried lactose with 0.5 % Aerosil® R972 leads to the most pronounced enhancement of the flowability. In comparison to mixtures containing 0.5 % Aerosil® R972, mixtures containing 2.5 % exhibit a lower flowing rate and higher angle of repose, which deteriorate even more for the mixtures containing 12.5 %. However, mixtures containing 2.5 % and 12.5 % Aerosil® R972 do not differ significantly with respect to their angle of repose which is indicative for the lower sensitivity of angle of repose measurements to changes of flowability. This was also observed by Markefka (Markefka et al., 2005).
In order to improve the flowability of corn starch (x_{50} = 15 µm), Yang (Yang et al., 2005) coated corn starch particles with different silicas with size ranges from 20 nm to 2 µm using a magnetic assisted impaction coater, hybridizer coater and V - shaped blender. For the evaluation of the dry coating processes and influence of the silica, the angle of repose was measured. The best results were achieved by the mixture with 1.0 % CAB - O - SIL EH 5 silica (primary particle size x_{50} = 20 nm), which were produced with the help of the magnetic assisted impaction coater. Generally, due to the coating of the corn starch particles with the silica particles the flowability of the host particles may be increased, because the silica particles play the role of the spacers. However, the amount of guest particles, which is needed for the improvement of the flow behaviour in the study performed by Yang and this study, can not be compared simply, due to the differences of chemical identity, mean particle size of the used materials and very much differing mixing methods. Nevertheless, a maximum in flowability enhancement was obtained in both studies.

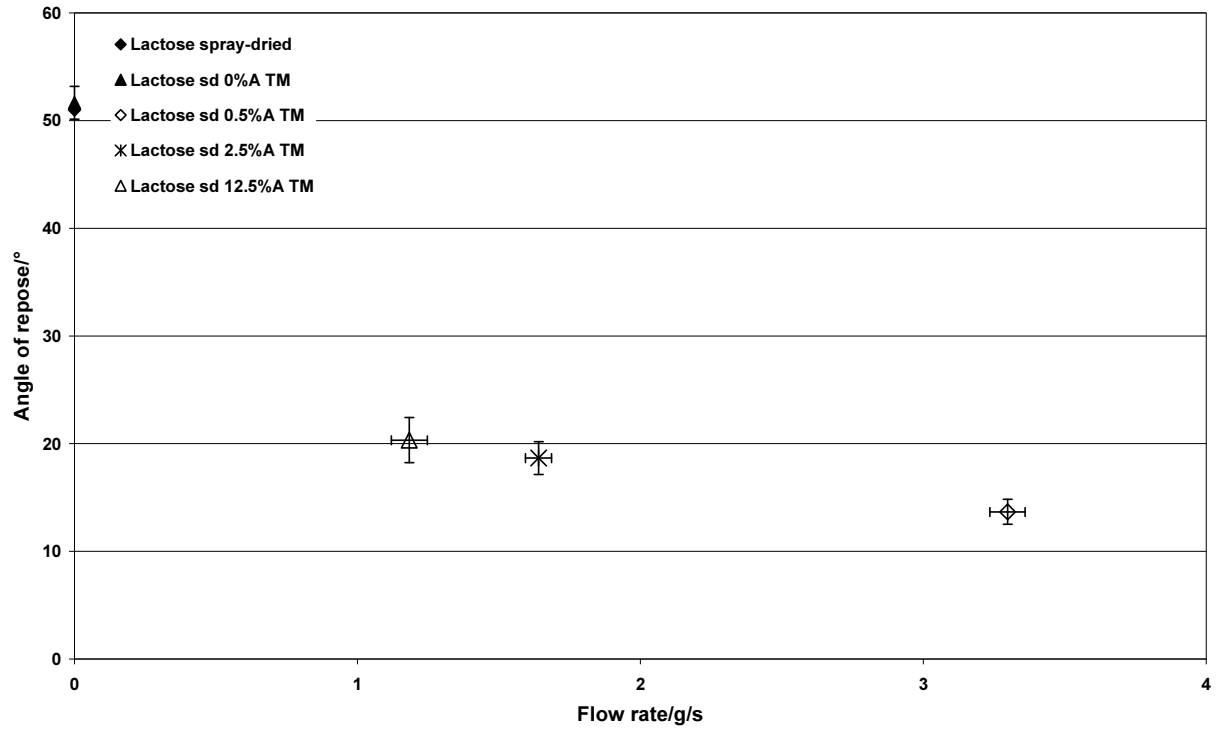

Figure 72: Mean ± s.d. of the angle of repose and flow rate values of mixtures containing spray - dried (sd) lactose and 0 %, 0.5 %, 2.5 % and 12.5 % Aerosil® R972 (A) prepared by conventional mixing (TM) (n = 3)

5.1.5 Concluding remarks

According to all measuring techniques spray - dried lactose containing no nanoparticles shows the worst flow characteristics. This is attributed to the fact that the lactose particle come in close contact with each other, therefore the contact area is high, enhancing also the interparticle interaction. It is shown, that coating the spray - dried lactose with 0.5 % Aerosil® R972 enhances the flow behaviour. Coating with higher amounts of Aerosil® R972 deteriorates the powder flow characteristics again, probably caused by the increase of mechanical interlocking phenomena, though a significant difference of the flow behaviour between powder mixtures containing 2.5 % and 12.5 % is not detected by measuring the Hausner ratio and the angle of repose. Comparing the different methods applied to determine flowability it has to be mentioned, that two, namely ring shear testing and powder flow rate measurements are appropriate to differentiate between all powders under investigation. According these measurements, flowability of the mixtures containing different concentrations of Aerosil® R972 decreases in the order 0.5 % > 2.5 % > 12.5 % Aerosil® R972. Nevertheless, all flowability measuring techniques identified the mixture containing 0.5 % Aerosil® R972 as the mixture, which exhibits the highest flowability.

5.2 Uniformity of mass of the dispensed dose

5.2.1 Preliminary remarks

Uniformity of mass was investigated by discharging the powder sample 40 or 10 times, depending on the drug, using the multi dose dry powder inhaler NOVOLIZER® (see C.4.2 and E.6). The relative standard deviation of the masses of the delivered doses was used as a measure for the uniformity of mass. A low value of the relative standard deviation means good uniformity of mass, in contrast to high values, which indicate high scattering of the delivered doses and poor uniformity of mass. The mass of the single dose was calculated by subtracting the weight after the powder discharge from the one before discharge. The mean of the obtained relative standard deviation values of three batches of each formulation was calculated. The powder mixtures were produced using electrostatically supported and conventional mixing. The measurements were carried out with both, spray - dried and micronised products. In both cases the mixtures of the active ingredient model with 0 %, 0.5 %, 2.5 % and 12.5 % Aerosil® R972 were investigated. The significance of the differences between the different mixtures was investigated using statistical methods of calculation (see E.9).

5.2.2 Spray - dried lactose

The results of the measurements of the samples of spray - dried lactose with 0 %, 0.5 %, 2.5 % and 12.5 % Aerosil® R972 prepared by conventional and electrostatically supported mixing are shown in Figure 73. The uniformity of mass was investigated by discharging the powder from one sample 40 times using a NOVOLIZER® DPI and the relative standard deviation of the mass of the 40 discharged doses was calculated.

Comparing the mixtures prepared with the help of the conventional mixing the following trends may be observed:

- Relative standard deviation of the mixtures with 0 % Aerosil® R972 is higher than of the mixtures containing 0.5 % Aerosil® R972.
- Increasing the nanoparticle concentration from 0.5 % to 2.5 % Aerosil® R972 does not lead to a significant change of the relative standard deviation.
- Increase of the nanoparticle concentration from 2.5 % to 12.5 % Aerosil® R972 significantly reduces the relative standard deviation.

These results are in fairly good accordance with the results obtained by flowability measurements using the ring shear tester and with measurements of the powder flow rate, with the exception that there was a significant decrease of flowability detected when increasing the nanoparticle concentration from 0.5 % to 2.5 % Aerosil® R972 (see 5.1).

Comparing the mixtures prepared with the help of electrostatically supported mixing the following is assessed:

- Addition of 0.5 % Aerosil® R972 results in the significant enhancement of the uniformity of mass in comparison to the mixture with 0 % Aerosil® R972, indicated by the low relative standard deviation.
- Further addition of nanoparticles results in the significant deterioration of the uniformity of mass of mixtures when increasing the nanoparticle concentration from 0.5 % to 2.5 %.

- Increase of the nanoparticle concentration to 12.5 % Aerosil® R972 does not alter the uniformity of mass significantly.

Comparing two mixing methods it has to be pointed out:

- The uniformity of mass of spray - dried lactose with 0 % Aerosil® R972 treated by conventional and electrostatically supported mixing is poor and not significantly differs from each other.
- The uniformity of mass of mixtures containing 0.5 % Aerosil® R972 prepared by electrostatically supported mixing is significantly superior compared to conventionally prepared mixtures containing the same amount of Aerosil® R972.
- The uniformity of mass of mixtures containing 2.5 % and 12.5 % Aerosil® R972 prepared by electrostatically supported mixing does not differ significantly from the conventionally prepared mixtures containing the same amount of Aerosil® R972.

Summarizing the results, the uniformity of mass of mixtures consisting of spray - dried lactose and 0.5 % of Aerosil® R972 are superior to pure spray - dried lactose and mixtures containing higher amounts of Aerosil® R972, namely 2.5 % and 12.5 % (electrostatically supported mixing) and 12.5 % (conventional mixing), respectively. The probable underlying mechanism of the enhancement of the uniformity of mass is the decrease of interparticle interactions by increasing the distance between the microparticulate host particles by the nanoparticulate Aerosil® R972.

Increasing the nanoparticle concentrations of mixtures prepared by conventional and electrostatically supported mixing from 0.5 % to 2.5 % and 12.5 % do not lead to a further improvement of the uniformity of mass. In contrary, in some cases described above, a significant deterioration of the results is observed. Exceeding the optimum amount of nanoparticles may cause mechanical interlocking on the one hand, by the excess of nanoparticles forming large agglomerates on the lactose surface and degrading thereby the dispersion of the lactose particles. On the other hand, depending on the size of the Aerosil® R972 agglomerates, they may disconnect themselves from the lactose particles, if the gravitational forces get stronger than the attracting forces between the microparticles and nanoparticle agglomerates. In this case, the possibility of the contact between lactose particles increases, especially on the sites of the lactose surfaces without nanoparticles, which also leads to deterioration of the dispersion of the lactose particles. The deterioration of the dispersion manifests itself in the decrease of uniformity of mass of mixtures containing 2.5 % and 12.5 % of Aerosil® R972 (electrostatically supported mixing), respectively 12.5 % (conventional mixing) in comparison to mixtures containing 0.5 % Aerosil® R972.

The uniformity of mass of mixtures containing 0.5 % Aerosil® R972 prepared by electrostatically supported mixing is significantly superior compared to conventionally prepared mixtures containing the same amount of Aerosil® R972. This might be explained by the fact that electrostatically supported mixing enhances dispersion of the nanoparticle and also microparticle fractions during the mixing process before the nanoparticles are attached to the microparticles. Thereby agglomerates are destroyed, leading to an electrostatically supported homogeneous distribution of the guest particles on the host microparticle surface, resulting in the efficient reduction of the interparticle forces. Probably, in case of conventional mixing the nanoparticle agglomerates cannot be dispersed as successful as in case of the electrostatically supported

mixing, where not only shear forces, but also electrostatic forces support the dispersion of the agglomerates, therefore the distribution of the spacers on the surface of the host particles.

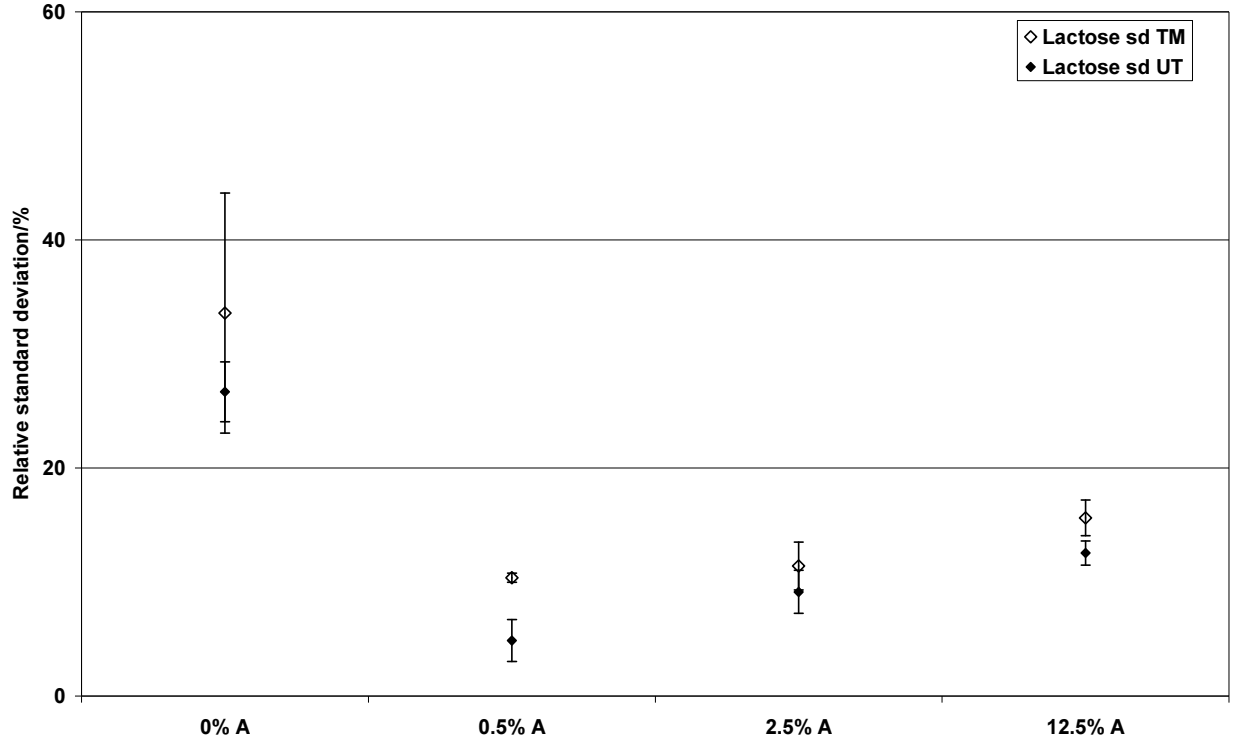

Figure 73: Mean ± s.d. of the relative standard deviation of the mass of 40 doses of mixtures containing spray - dried (sd) lactose and 0 %, 0.5 %, 2.5 % and 12.5 % Aerosil® R972 (A) prepared by conventional mixing (TM) or electrostatically supported mixing (UT) (n = 3)

5.2.3 Spray - dried salbutamol base

Spray - dried salbutamol base mixtures with 0 %, 0.5 %, 2.5 % and 12.5 % Aerosil® R972 were treated the same way as the spray - dried lactose mixtures with the exception that the uniformity of mass was investigated by discharging the powder 10 times using a NOVOLIZER® DPI. The relative standard deviation of the mass of 10 discharged doses was calculated. The results of the measurements are plotted in Figure 74.

Comparing the formulations prepared by conventional mixing the following observations can be made:

- Relative standard deviation of the mixtures with 0 % Aerosil® R972 is high, which indicates poor flowability, dispersibility and uniformity of mass.
- Coating of the micropartices with 0.5 %, 2.5 % and 12.5 % Aerosil® R972 does not lead to a significant enhancement of the uniformity of mass.

Comparing the relative standard deviation of spray - dried salbutamol base samples, which were prepared by electrostatically supported mixing the following points have to be discussed:

- Addition of 0.5 % and 2.5 % Aerosil® R972 leads to a significant decrease of the relative standard deviation in comparison to the mixture with 0 % Aerosil® R972.

- Increase of the nanoparticle concentration from 0.5 % to 2.5 % and 12.5 % in mixtures of spray - dried salbutamol base does not lead to a significant change of the uniformity of mass.

Comparing conventional and electrostatically supported mixing the following results are assessed:

- Mixtures with 0.5 % Aerosil® R972 prepared by electrostatically supported mixing show a significantly lower relative standard deviation and therefore an enhanced mass uniformity compared to the corresponding mixture produced by conventional mixing.
- The mixing mode does not make any significant difference in relation to the uniformity of mass for mixtures containing 2.5 % and 12.5 % Aerosil® R972.

In summary, it was possible to improve the uniformity of mass by coating spray - dried salbutamol base with 0.5 % and 2.5 % Aerosil® R972 using electrostatically supported mixing. However, the improvement is moderate in comparison to spray - dried lactose samples, which may be due to the irregular shape and higher surface roughness of the spray - dried salbutamol base particles in comparison to the spray - dried lactose particles (see 2.3). The roughness provides cavities for the nanoparticles to be placed in without leading to the reduction of interparticle interactions and to the improvement of the uniformity of mass on the one hand. On the other hand nanoparticles are trapped within the cavities without giving raise to mechanical interactions on the microparticle surface at higher nanoparticle concentrations thereby preventing the deterioration of the uniformity of mass when increasing the Aerosil® R972 concentration from 0.5 % to 2.5 %, which is in contrast to the corresponding lactose samples. Furthermore, due to the fact, that the x_{50} of the salbutamol base particles is lower than that of spray - dried lactose (see 2.2), the specific surface area of these particles is higher and therefore a higher amount of nanoparticles may be placed on the surface of the microparticles before mechanical interlocking may occur.

The uniformity of mass of mixtures containing 0.5 % Aerosil® R972 prepared by electrostatically supported mixing is significantly superior compared to conventionally prepared mixtures containing the same amount of Aerosil® R972. This might be explained by the fact that electrostatically supported mixing enhances dispersion of the nanoparticle and also microparticle fractions during the mixing process thereby destroying agglomerates and leading to an electrostatically supported homogeneous distribution of the guest particles on the host microparticle surface. This homogeneous distribution allows the reduction of interparticle interactions more efficiently than distributions obtained by conventional mixing especially at low nanoparticle concentrations, where each nanoparticle counts. This difference between conventional and electrostatically supported mixing diminishes at higher nanoparticle concentrations of 2.5 % and 12.5 %. However, no significant differences regarding the uniformity of mass were achieved at nanoparticle concentrations of 0.5 %, 2.5 % and 12.5 % obtained by conventional mixing in comparison to nanoparticle free samples. As the improvement of the uniformity of mass was only moderate in case of the samples prepared by electrostatically supported mixing anyway, the effect of nanoparticle addition by conventional mixing was not significant.

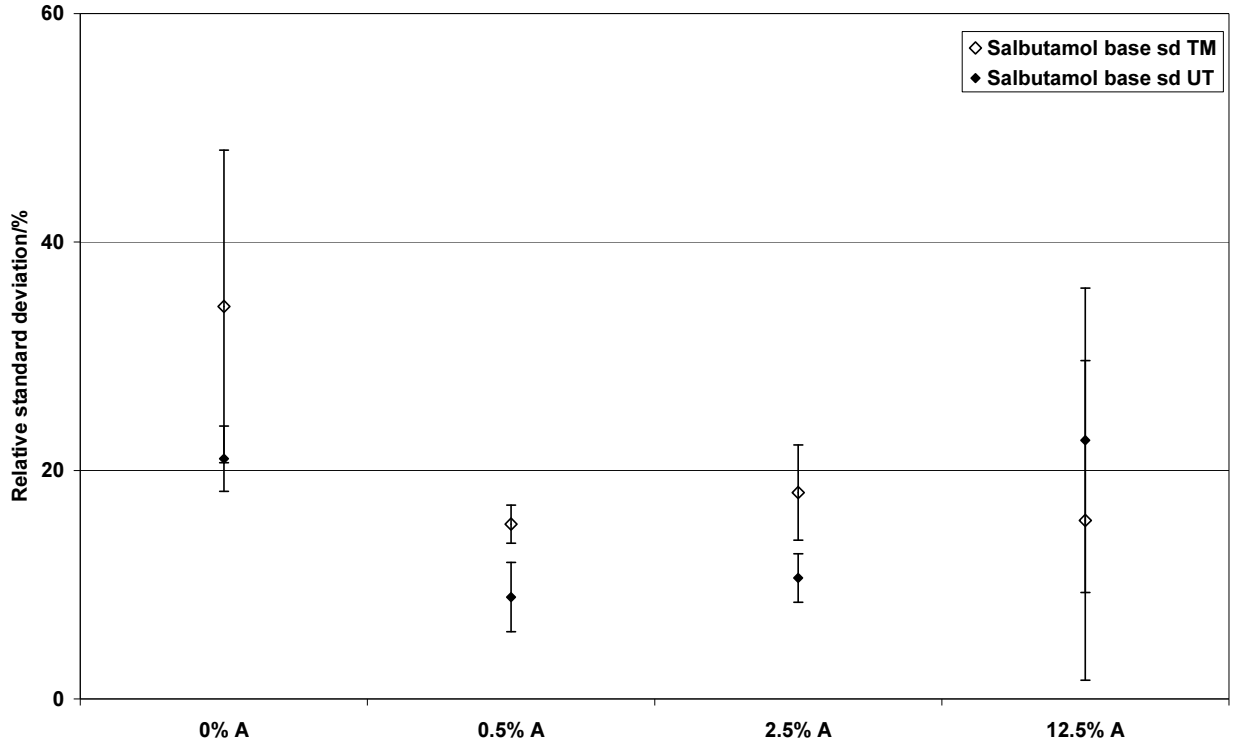

Figure 74: Mean ± s.d. of the relative standard deviation of the mass of 10 doses of mixtures containing spray - dried (sd) salbutamol base and 0 %, 0.5 %, 2.5 % and 12.5 % Aerosil® R972 (A) prepared by conventional mixing (TM) or electrostatically supported mixing (UT) (n = 3)

5.2.4 Spray - dried salbutamol sulphate

The determinations of the uniformity of mass of the spray - dried salbutamol sulphate mixtures coated with 0 %, 0.5 %, 2.5 % and 12.5 % of nanoparticles were carried out. The uniformity of mass was investigated by discharging the powder 10 times using a NOVOLIZER® DPI and the relative standard deviation of the mass of the 10 discharged doses was calculated. The results of the tests are presented in Figure 75.

In contrast to spray - dried lactose and salbutamol base samples the uniformity of mass was not improved by adding Aerosil® R972 neither using conventional nor electrostatically supported mixing. This is somewhat surprising at the first sight. However, according the investigations on the crystallinity of spray - dried salbutamol sulphate, salbutamol sulphate is amorphous initially after spray - drying, but is prone to recrystallise. This has been shown on samples prepared by electrostatically supported mixing that were examined by moisture sorption (see 3.1.4). Presumably, recrystallisation had taken place upon sample preparation for the moisture sorption studies. Keeping in mind, that recrystallisation of amorphous salbutamol sulphate is likely to occur, in contrast to for example amorphous lactose, which had not undergone recrystallisation neither during processing nor during handling, it might well happen, that recrystallisation of salbutamol sulphate takes place at some stage during handling or processing. The effect of recrystallisation accompanied by molecular rearrangement may give raise to the formation of solid bridges between particles, thereby increasing interparticle interactions and probably superimposing the interaction reducing effect of the nanoparticles. Consequently, discussing the obtained results in terms of the interaction reducing properties and the enhancing of the mass

uniformity due to the adding of the nanoparticle fraction to the microparticle fraction is not possible under these circumstances.

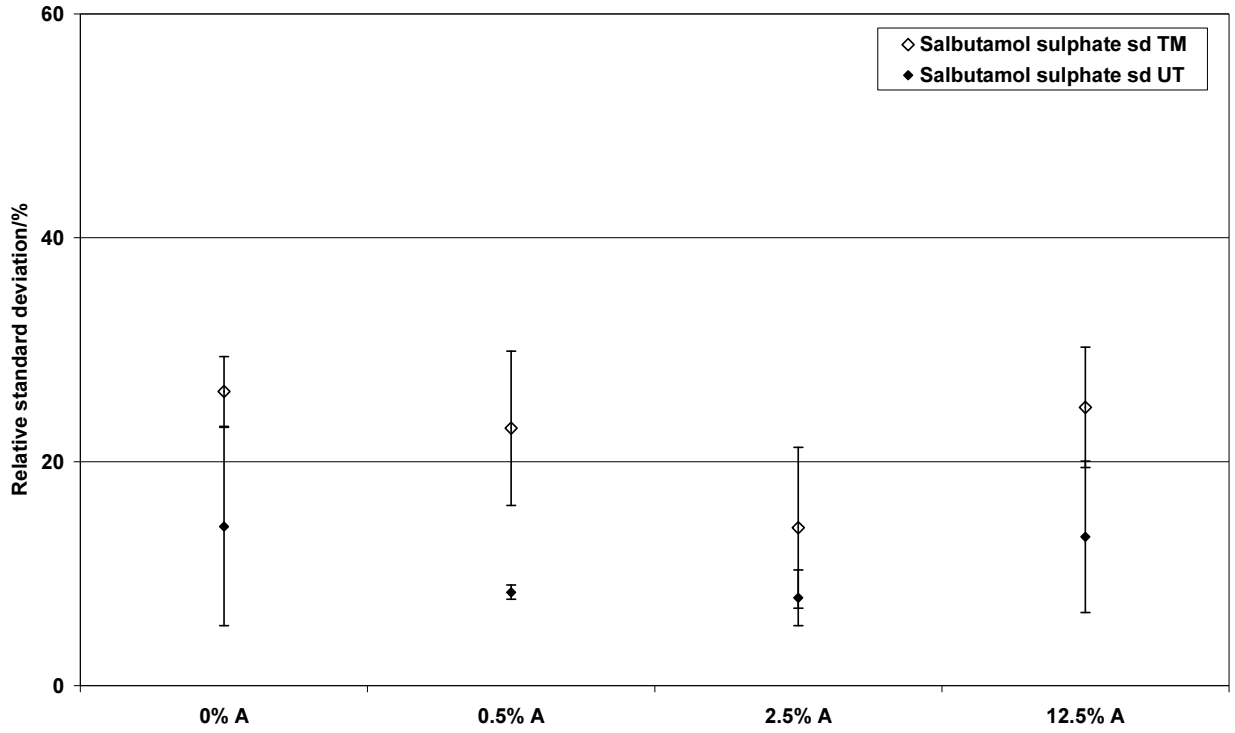

Figure 75: Mean ± s.d. of the relative standard deviation of the mass of 10 doses of mixtures containing spray - dried (sd) salbutamol sulphate and 0 %, 0.5 %, 2.5 % and 12.5 % Aerosil® R972 (A) prepared by conventional mixing (TM) or electrostatically supported mixing (UT) (n = 3)

5.2.5 Micronised lactose

Mixtures with micronised lactose and 0 %, 0.5 %, 2.5 % and 12.5 % Aerosil® R972 were prepared using conventional and electrostatically supported mixing. Uniformity of mass was investigated by discharging the powder 40 times using a NOVOLIZER® DPI. The relative standard deviation of the mass of the 40 discharged doses was calculated. The results of the measurements are plotted in Figure 76.

In case of the mixtures prepared using conventional mixing the following is observed:

- No significant change of the uniformity of mass between mixtures containing 0.5 %, 2.5 % and 12.5 % Aerosil® R972 and those without Aerosil® R972 is detected.

Looking on the mixtures prepared using electrostatically supported mixing following trends are observed:

- No significant change of the uniformity of mass between mixtures containing 0.5 %, 2.5 % and 12.5 % Aerosil® R972 and those without Aerosil® R972 is detected.

The most probable explanation for the lack of improvement of mass uniformity is, that the micronised lactose particles exhibit considerable amounts of fine particles on their surface already (see Figure 34 b), which themselves may act as spacers between the coarser lactose particles. The addition of further amounts of nanoparticles like Aerosil® R972 will not

significantly alter interparticle interactions anymore. Another reason for the lack of improvement of mass uniformity may be that the nanoparticles are entrapped in the asperities of the surface of the micronised particles, not being able to act as spacers and interparticle interaction reducing agents. This indicates that the described carrier free concept is unsuitable for micronised products, at least if they contain fines on their surface, which play the spacer role.

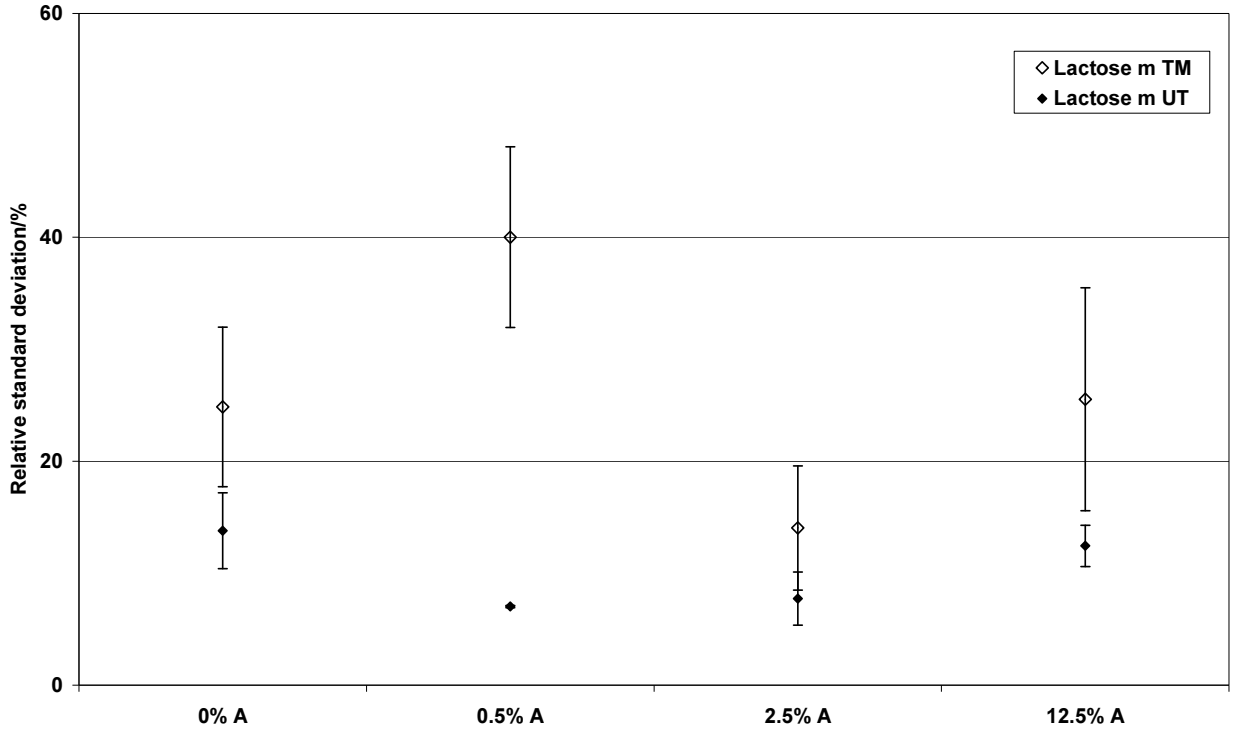

Figure 76: Mean ± s.d. of the relative standard deviation of the mass of 40 doses of mixtures containing micronised (m) lactose and 0 %, 0.5 %, 2.5 % and 12.5 % Aerosil® R972 (A) prepared by conventional mixing (TM) or electrostatically supported mixing (UT) (n = 3)

5.2.6 Micronised salbutamol base

Micronised salbutamol base mixtures with 0 %, 0.5 %, 2.5 % and 12.5 % Aerosil® R972 were treated the same way as the spray - dried salbutamol base mixtures. The uniformity of mass was investigated by discharging the powder 10 times using a NOVOLIZER® DPI and the relative standard deviation of the mass of the 10 discharged doses was calculated. The results of the measurements are plotted in Figure 77.

With mixtures prepared using the conventional mixing method, the following is observed:

- No significant change of the uniformity of mass between the mixtures containing 0 % and those containing 0.5 %, 2.5 % and 12.5 % Aerosil® R972 is detected.

Looking on the mixtures prepared using electrostatically supported mixing the following is observed:

-No significant change of the uniformity of mass between the mixtures containing 0 % and those containing 0.5 %, 2.5 % and 12.5 % Aerosil® R972 is detected.

As already mentioned in the previous chapter in the case of micronised lactose, the most probable explanation for the lack of improvement of the uniformity of mass is, that micronised salbutamol base particles exhibit considerable amounts of fine particles on their surface already (see Figure 34 d) acting themselves as spacers between the coarse salbutamol base particles. Another reason might be the entrapment of nanoparticles in the asperities of the surface of the coarse particles, not being able to act as interparticle interaction reducing agents. This supports the hypothesis, that the described carrier free concept is unsuitable for micronised products, at least if they contain fines on their surface, which play the spacer role.

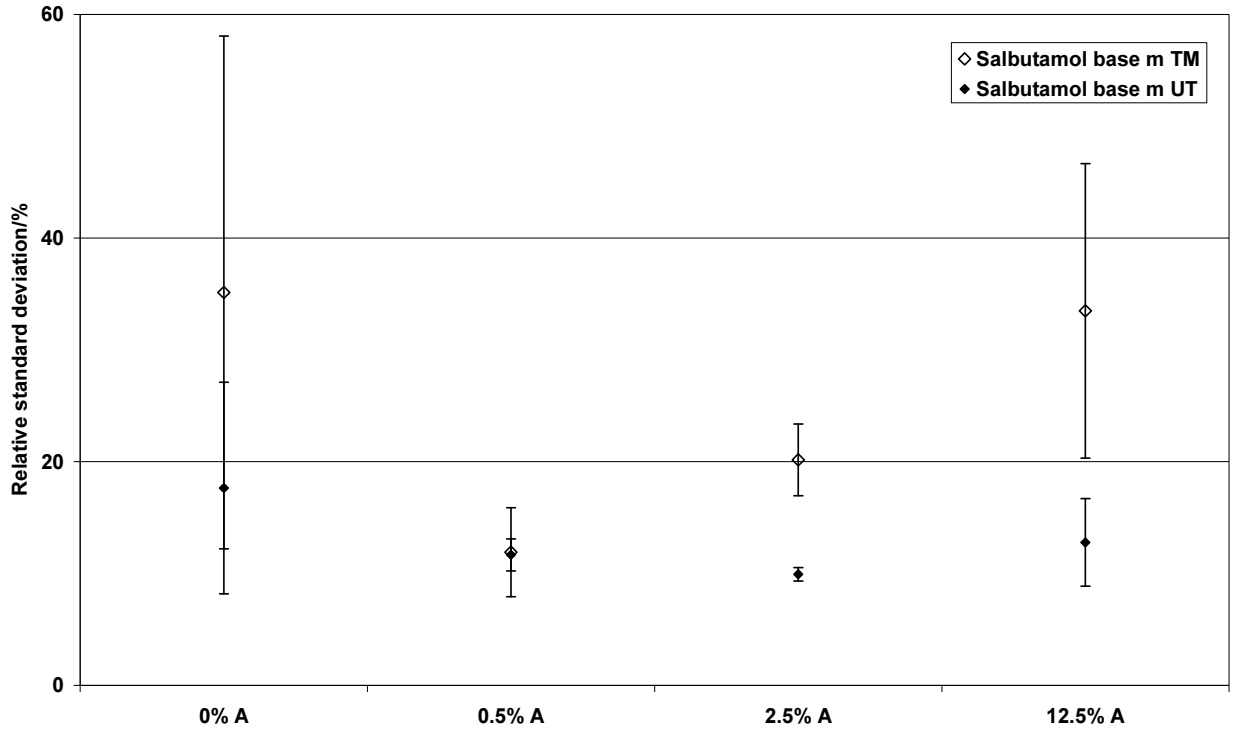

Figure 77: Mean ± s.d. of the relative standard deviation of the mass of 10 doses of mixtures containing micronised (m) salbutamol base and 0 %, 0.5 %, 2.5 % and 12.5 % Aerosil® R972 (A) prepared by conventional mixing (TM) or electrostatically supported mixing (UT) (n = 3)

5.2.7 Micronised salbutamol sulphate

Micronised salbutamol sulphate mixtures with 0 %, 0.5 %, 2.5 % and 12.5 % Aerosil® R972 were treated the same way as the spray - dried salbutamol sulphate mixtures. The uniformity of mass was investigated by discharging the powder 10 times using a NOVOLIZER® DPI and the relative standard deviation of the mass of the 10 discharged doses was calculated. The results of the measurements are plotted in Figure 78.

As in the case of micronised lactose and micronised salbutamol base no significant change of the uniformity of mass by adding nanoparticles is obtained, irrespective of whether the mixtures were prepared by conventional or electrostatically support mixing. As already discussed in the two previous chapters (see 5.2.5 and 5.2.6), the most probable explanation for this lack of improvement of mass uniformity are the considerable amounts of fine particles on the particle

surface (see Figure 34 f) acting themselves as spacers between the coarser particles and the entrapment of nanoparticles in the asperities of the coarse particles. Again, this supports the hypothesis, that this formulation concept is unsuitable for micronised salbutamol sulphate products.

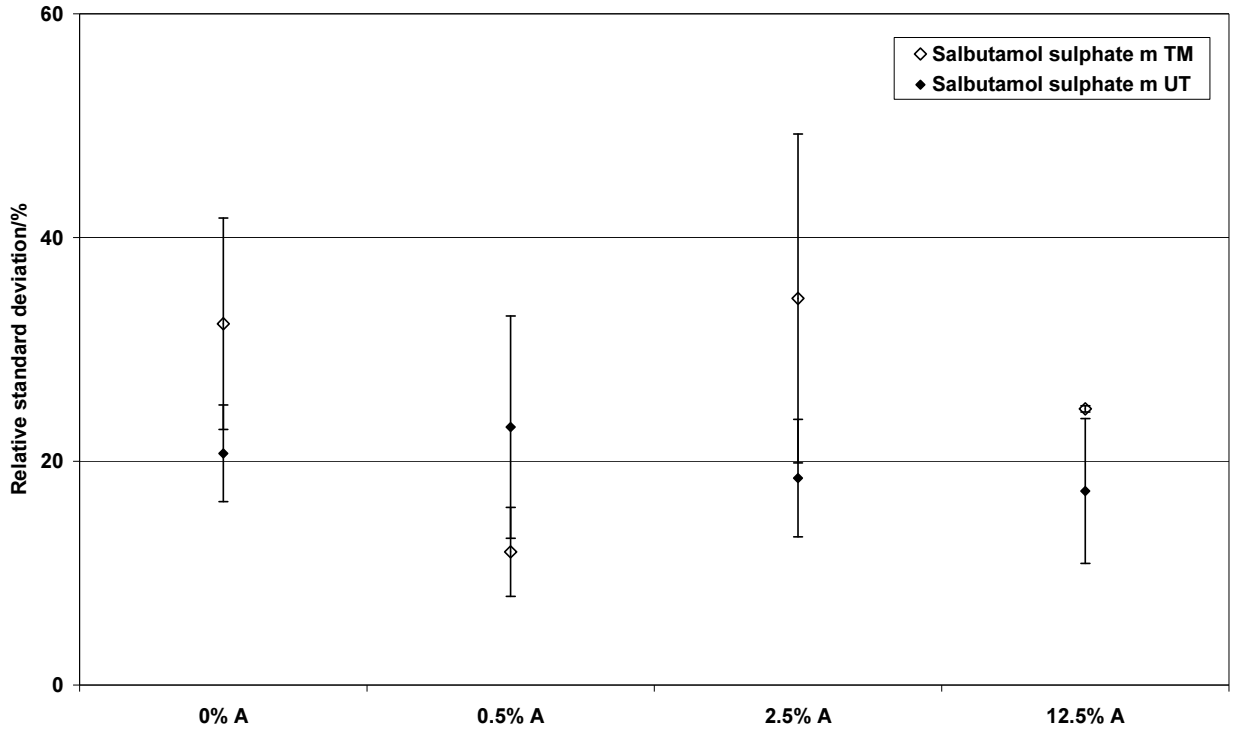

Figure 78: Mean ± s.d. of the relative standard deviation of the mass of 10 doses of mixtures containing micronised (m) salbutamol sulphate and 0 %, 0.5 %, 2.5 % and 12.5 % Aerosil® R972 (A) prepared by conventional mixing (TM) or electrostatically supported mixing (UT) (n = 3)

5.2.8 Concluding remarks

Generally, by coating of spray - dried lactose and salbutamol base microparticles with nanoparticles it is possible to increase the mass uniformity of the powder, which is released from the dry powder inhaler. This does not apply for spray - dried salbutamol sulphate, where the additional impact of recrystallisation on interparticle interaction may affect uniformity of mass considerably. It is possible to show, that the concentration of the nanoparticles plays an important role in the improvement of the uniformity of mass, low concentrations leading to a reduction of interparticle interaction and an enhancement of the uniformity of mass, whereas further increasing the nanoparticle concentration may cause mechanical interlocking leading to the deterioration of the uniformity of mass again. The nanoparticle concentration ensuring the improvement of the uniformity of mass has been shown to be dependent on particle size and particle surface topography. Comparing conventional and electrostatically supported mixing, electrostatically supported mixing is more efficient with respect to the increase of the uniformity of mass at low spacer concentrations. This has been shown for spray - dried lactose and spray - dried salbutamol base containing 0.5 % Aerosil® R972 and is explained by the

distribution of the guest particles on the host microparticle surface, which is supposed to be more homogeneous when using electrostatically supported mixing. At low concentrations, this homogeneous distribution ensures the non - contact and the reduction of interparticle interactions, whereas less homogeneous distributions obtained by conventional mixing still exhibit spacer free surface areas allowing contact between the drug particles.

Concluding the discussion of the results of the uniformity of mass of micronised samples, it can be said, that coating of the micronised powders with nanoparticles does not lead to enhancing of the mass uniformity. Probably, the fines present in the powder samples already play the role of spacers and further mixing with nanoparticles does not affect the uniformity of mass considerably. Furthermore, the nanoparticles may be entrapped inside the asperities of the surface of the micronised particles, not being able to act as spacers and interparticle interaction reducing agents. This has been shown for micronised lactose, salbutamol base and salbutamol sulphate.

5.3 Aerodynamic assessment of fine particles

5.3.1 Preliminary remarks

The aerodynamic assessment of fine particles (see E.7C.4.3 and E.7) was carried out using the Next Generation Impactor (NGI). The fine particle fraction (FPF) is the dose of the particles exhibiting an aerodynamic diameter of 5 µm and below divided by the delivered dose. This percentage of the powder is assumed to be able to reach the lower parts of the lung of the patient (Hickey et al., 1996). The mixtures containing spray - dried or micronised lactose, salbutamol base and salbutamol sulphate and 0 %, 0.5 %, 2.5 % and 12.5 % Aerosil ® R972 were released from the reservoir of the multi dose dry powder inhaler NOVOLIZER®.

5.3.2 Spray - dried lactose

The fine particle fractions (FPF) of spray - dried lactose with 0 %, 0.5 %, 2.5 % and 12.5 % Aerosil® R972 prepared by conventional and electrostatically supported mixing are shown in Figure 79.

Comparing the mixtures prepared by conventional mixing the following results are obtained:

- FPF of mixtures containing 0.5 % Aerosil® R972 is significantly higher than the one of the samples without nanoparticles.
- FPF of the mixtures with 0.5 % Aerosil® R972 is significantly higher than the one of the mixtures containing 2.5 % and 12.5 % Aerosil® R972.
- There is no significant difference of the FPF between mixtures containing 2.5 % and 12.5 % Aerosil® R972.

These results are in good accordance with the results obtained by flowability measurements using the ring shear tester and the flow rate measurements (see 5.1.2 and 5.1.4) with the exception, that there was a significant decrease of the flowability detected when increasing the Aerosil® R972 concentration from 2.5 % to 12.5 %. Also, they are in good agreement with the results obtained by the determination of mass uniformity (see 5.2.2), with the exception, that there was a significant decrease of the mass uniformity detected when increasing the Aerosil® R972 concentration from 2.5 % to 12.5 %, but no change when increasing the concentration from 0.5 % to 2.5 %.

Comparing the mixtures prepared with the help of electrostatically supported mixing the following trends are observed:

- FPF of the mixture with 0 % Aerosil® R972 is significantly lower than of the mixtures containing 0.5 % Aerosil® R972.
- Further addition of nanoparticles to obtain 2.5 % Aerosil® R972 results in the significant deterioration of the FPF.
- Increase of the nanoparticle concentration from 2.5 % to 12.5 % Aerosil® R972 does not alter the FPF significantly.

This agrees perfectly with the results obtained by the assessment of the uniformity of mass (see 5.2.2).

Comparing the FPFs which were obtained using the two mixing methods it has to be pointed out:

- FPF of the mixtures containing 0.5 % Aerosil® R972 prepared by electrostatically supported mixing is significantly superior compared to conventionally prepared mixtures containing the same amount of Aerosil® R972.
- FPFs of mixtures containing 0 %, 2.5 % and 12.5 % Aerosil® R972 prepared by electrostatically supported mixing do not differ significantly from the FPFs of conventionally prepared mixtures containing the same amount of Aerosil® R972. This corresponds perfectly with the results of the mass uniformity (see 5.2.2).

The FPF of mixtures containing 0.5 % Aerosil® R972 prepared by electrostatically supported mixing is superior compared to conventionally prepared mixtures containing the same amount of Aerosil® R972, due to the possibility that electrostatically supported mixing may enhance the dispersion and blending of the nanoparticle and microparticle fractions. As already mentioned previously (see 5.2.2), the enhanced dispersibility and improved blending during the mixing process may provide good conditions for the homogeneous attachment of the nanoparticles on the surface of the microparticles, resulting in the efficient reduction of the interparticle forces and enhanced FPF. Probably, in case of conventional mixing the shear forces are not high enough and nanoparticle agglomerates cannot be dispersed as successful as in case of the electrostatically supported mixing, therefore the distribution of the spacers on the surface of the host particles is not homogeneous enough to ensure the non - contact of the host particles at low nanoparticle concentration, when every nanoparticle counts.

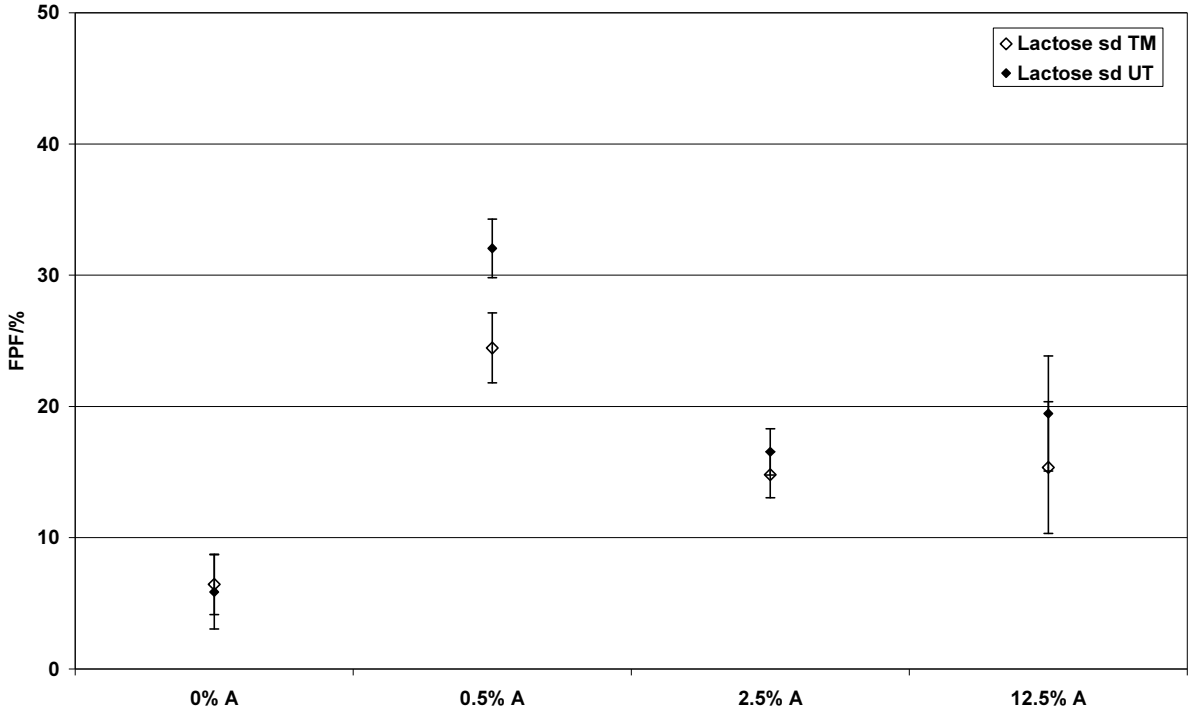

Figure 79: Mean ± s.d. of the fine particle fraction of mixtures containing spray - dried (sd) lactose and 0 %, 0.5 %, 2.5 % and 12.5 % Aerosil® R972 (A) prepared by conventional mixing (TM) or electrostatically supported mixing (UT) (n = 3)

Summarizing the results, the FPF of mixtures consisting of spray - dried lactose and 0.5 % of Aerosil® R972 are superior to pure spray - dried lactose and mixtures containing higher amounts of Aerosil® R972, namely 2.5 % and 12.5 %. As already mentioned in the previous chapter (see 5.2.2), nanoparticle concentrations, that are too low, result in insufficient spacing of the microparticles on the one hand. Nanoparticle concentrations exceeding the optimum amount may cause mechanical interlocking on the other hand, due to the excess of nanoparticles forming large agglomerates on the host particle surface. Furthermore, depending on the size of the Aerosil® R972 agglomerates, the guest particles may disconnect themselves from the surface of the host particles at high guest concentrations. This may happen, if the gravitational forces get stronger than the attracting forces between the microparticles and nanoparticle agglomerates. The possibility of the contact on the sites of the lactose surfaces without nanoparticles may increase, leading to possible deterioration of the dispersion of the lactose particles.
The minor differences of the results obtained by the flowability measurements or the measurements of the uniformity of mass and the aerodynamic assessment of the fine particle fraction are attributed to the different forces acting during the measurements.

5.3.3 Spray - dried salbutamol base

The FPFs of the samples of spray - dried salbutamol base with 0 %, 0.5 %, 2.5 % and 12.5 % Aerosil® R972 prepared by conventional and electrostatically supported mixing are shown in Figure 80.
Observing the FPF results of the mixtures prepared by conventional mixing the following trends are observed:
- No significant difference between the FPF values of the mixtures with 0 % and 0.5 % and 0 % and 12.5 % Aerosil® R972 is detected.
- FPF of the mixtures containing 2.5 % Aerosil® R972 is significantly higher than the FPF of the samples without nanoparticles. However, the increase is moderate. This is in contrast to the results of the mass uniformity, where no difference of the performance the samples is detected irrespective of the nanoparticle concentration, presumably, due to the different acting forces during the measurements of the uniformity of mass and the aerodynamic assessment of the fine particle fraction.
Comparing the results of the FPF of the mixtures prepared with the help of electrostatically supported mixing the following trends are observed:
- FPF of the mixture with 0 % Aerosil® R972 is significantly lower than of the mixtures containing 0.5 % Aerosil® R972.
- Increase of the nanoparticle concentration from 0.5 % to 2.5 % does not alter the FPF significantly.
- Further increase of the nanoparticle concentration from 2.5 % to 12.5 % Aerosil® R972 leads to a significant decrease of the FPF.
These results are in good accordance with the results of the mass uniformity measurements (see 5.2.3), with the exception that there was no significant change of mass uniformity detected when increasing the Aerosil® R972 concentration from 2.5 % to 12.5 %.

Comparing the values of the FPF which were obtained using the two mixing methods the following is observed:

- The FPF of the mixtures containing 0.5 % Aerosil® R972 prepared by electrostatically supported mixing is significantly higher than the FPF of the mixtures containing the same amount of Aerosil® R972 prepared with the help of conventional mixing.
- There is no significant difference between the FPF of mixtures prepared by both conventional and electrostatically supported mixing at concentrations of 0 %, 2.5 % and 12.5 % Aerosil® R972, which is in perfect accordance with the results of the mass uniformity (see 5.2.3).

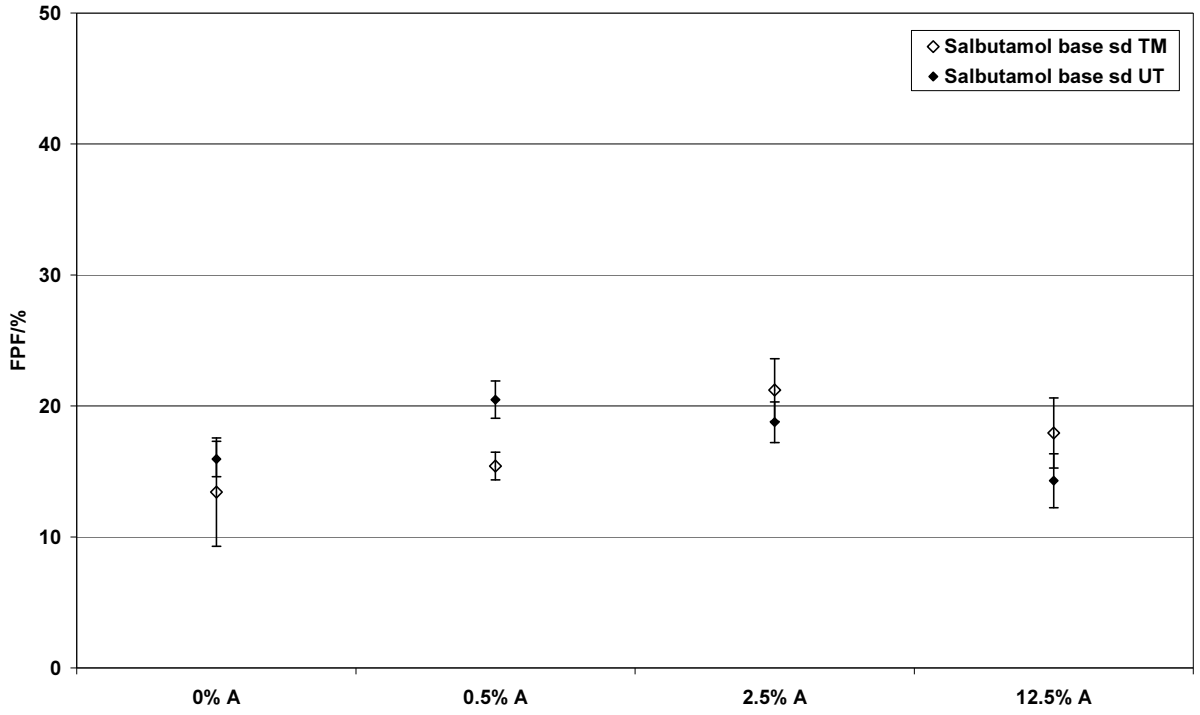

Figure 80: Mean ± s.d. of the fine particle fraction of mixtures containing spray - dried (sd) salbutamol base and 0 %, 0.5 %, 2.5 % and 12.5 % Aerosil® R972 (A) prepared by conventional mixing (TM) or electrostatically supported mixing (UT) (n = 3)

Summarizing, the FPF of mixtures containing 0.5 % Aerosil® R972 prepared by electrostatically supported mixing is significantly superior compared to conventionally prepared mixtures, which contain the same amount of Aerosil® R972. In case of conventional mixing the improvement of the FPF is obtained only by adding 2.5 % Aerosil® R972. Also it may be worth mentioning, that at the concentration of 2.5 % there is no significant difference between the FPFs of mixtures prepared by conventional and electrostatically supported mixing. These results may be due to the enhanced dispersion and blending of the nanoparticle and microparticle fractions by electrostatically supported mixing. Therefore, a lower amount of nanoparticles is needed to ensure non - contact of the spray - dried salbutamol base particles when electrostatically supported mixing is used. Further increasing of the nanoparticle concentration does not lead to the enhancement of the FPF, but to a decrease in some cases, for example when the nanoparticle concentration of samples prepared by electrostatically supported mixing is increased from 2.5 %

to 12.5 %. Probably this is due to the increased possibility of mechanical interlocking between the nanoparticles.
Nevertheless, it has to be mentioned, that the results obtained by aerodynamic assessment of the fine particle fraction do not perfectly correspond to the results obtained for the uniformity of mass, where no significant alteration of the uniformity of mass is found when adding Aerosil® R972 by conventional mixing. However, this may be attributed to the different forces acting during the measurements of the uniformity of mass and the aerodynamic assessment of the fine particle fraction.

5.3.4 Spray - dried salbutamol sulphate

The results of the determinations of the FPF of the spray - dried salbutamol sulphate mixtures coated with 0 %, 0.5 %, 2.5 % and 12.5 % of nanoparticles are displayed on Figure 81.
Observing the FPF results of the mixtures prepared by conventional mixing the following is observed:
- FPF of the mixtures containing 0.5 % Aerosil® R972 is significantly higher than of the samples with 0 % Aerosil® R972.
- Increasing the nanoparticle concentration from 0.5 % Aerosil® R972 to 2.5 % Aerosil® R972 results in a decrease of the FPF.
- Further increasing the nanoparticle concentration from 2.5 % to 12.5 % leads to a significant increase of the FPF again.
These results do not correspond to the results obtained by the investigations on mass uniformity, where the FPF of spray - dried salbutamol sulphate was not changed by adding Aerosil® R972.
In contrast to the FPF of spray - dried lactose and salbutamol base samples, the FPF of spray - dried salbutamol sulphate was not improved by adding Aerosil® R972 using electrostatically supported mixing. This is in a good accordance with the results of the mass uniformity of spray - dried salbutamol sulphate (see 5.2.4).
According to the investigations on the crystallinity of spray - dried salbutamol sulphate, salbutamol sulphate is amorphous initially after spray - drying, but is prone to recrystallise. This has been shown on samples prepared by electrostatically supported mixing that were examined by moisture sorption (see 3.1.4). The recrystallisation of amorphous salbutamol sulphate may occur at some stage during handling or processing, leading to the formation of solid bridges between particles, most probably superimposing the effect of the nanoparticles and causing arbitrary results like the increase of the FPF when increasing the nanoparticle concentration from 0 % to 0.5 %, the decrease of the FPF by further concentration increase to 2.5 % and finally the increase again by concentration increase to 12.5 %. Another phenomenon caused by the spontaneous transformation from the amorphous to the crystalline state may be the difference of the FPF of samples without nanoparticles prepared either by conventional or electrostatically supported mixing. Therefore, as already mentioned (see 5.2.4), the discussion of the obtained results in terms of the influence of nanoparticle addition on the FPF is not possible without further investigations.

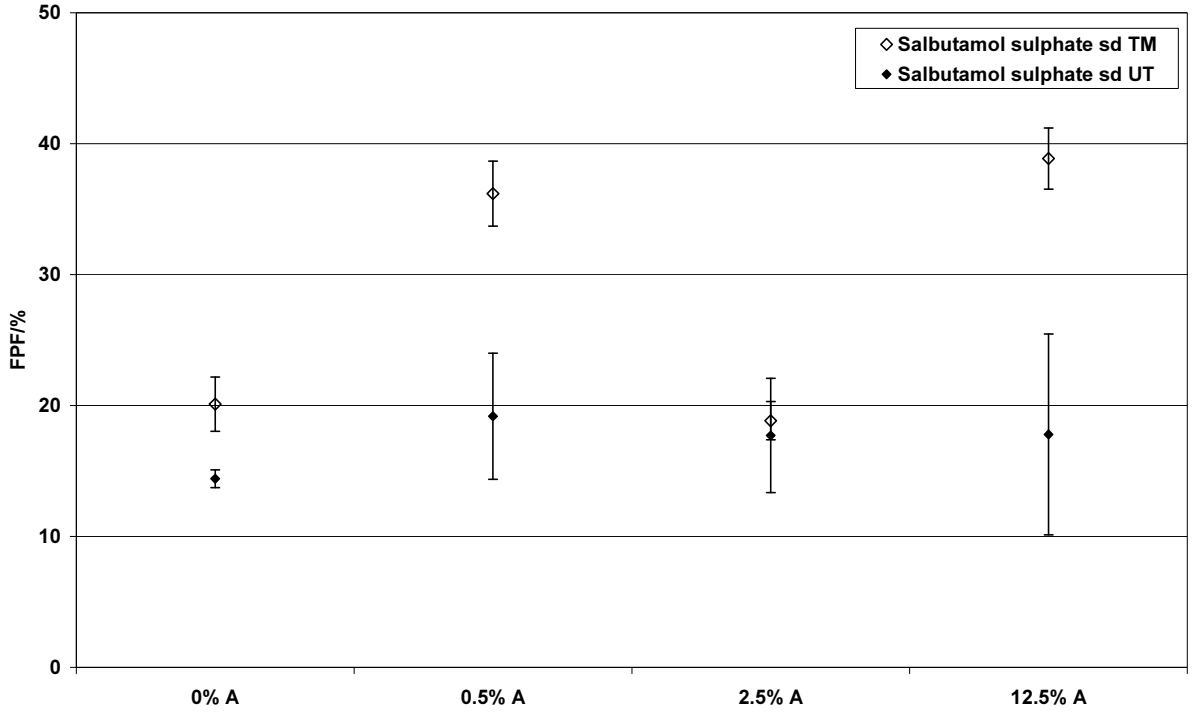

Figure 81: Mean ± s.d of the fine particle fraction of mixtures containing spray - dried salbutamol sulphate (SS) and 0 %, 0.5 %, 2.5 % and 12.5 % Aerosil® R972 (A) prepared by conventional mixing (TM) or electrostatically supported mixing (UT) (n = 3)

5.3.5 Micronised lactose

The results of the assessment of the fine particle fraction of mixtures of micronised lactose and 0 %, 0.5 %, 2.5 % and 12.5 % Aerosil® R972 prepared using conventional and electrostatically supported mixing are shown in Figure 82.

Comparing the FPF of the mixtures of micronised lactose prepared using conventional mixing no significant differences of the FPF of mixtures containing different nanoparticle concentrations are detected. This is in good accordance with the results of the measurements of the uniformity of mass and may be explained by the fact that micronised lactose particles exhibit considerable amounts of fine particles on their surface already (see Figure 34 b), which themselves may act as spacers between the coarser particles. The addition of further amounts of nanoparticles like Aerosil® R972 will not significantly alter interparticle interactions anymore. Another reason for the lack of improvement may be the entrapment of the nanoparticles in the asperities of the surface of the micronised particles.

Comparing the results of the FPF of the mixtures prepared using electrostatically supported mixing the following observations are made:

- FPF of mixtures containing 0.5 %, is significantly higher than that of the mixture with 0 % Aerosil® R972.
- FPF of the mixtures containing 0.5 % does not differ from the mixture containing 2.5 % Aerosil® R972 significantly.
- Further increase of the nanoparticle concentration from 2.5 % to 12.5 % Aerosil® R972 leads to a significant decrease of the FPF.

In comparison to the micronised lactose sample without nanoparticles treated by conventional mixing, it is striking, that the sample without nanoparticles treated by electrostatically supported mixing shows a significantly decreased FPF. This might be due to the alteration of the surface characteristics of the micronised product by the high speed homogenator. It might well be, that the dispersion of the powder in liquid nitrogen may have reduced the amount of fines on the particles´ surface resulting in an increase of interparticle interactions and a decrease of the FPF. This removal of fines is more likely to occur when treating the sample by electrostatically supported than by conventional mixing, firstly because of the higher energy input and secondly because of the higher dielectricity constant of the liquid nitrogen facilitating the detachment of the fines. Given the fact, that samples without nanoparticles differ from each other in relation to the FPF when prepared either by conventional or electrostatically supported mixing, it would not be good practice to compare samples containing nanoparticles either prepared by conventional or electrostatically supported mixing, because the treatment by the ULTRA - TURRAX® itself exerts an influence on the FPF even of nanoparticle free micronised samples.

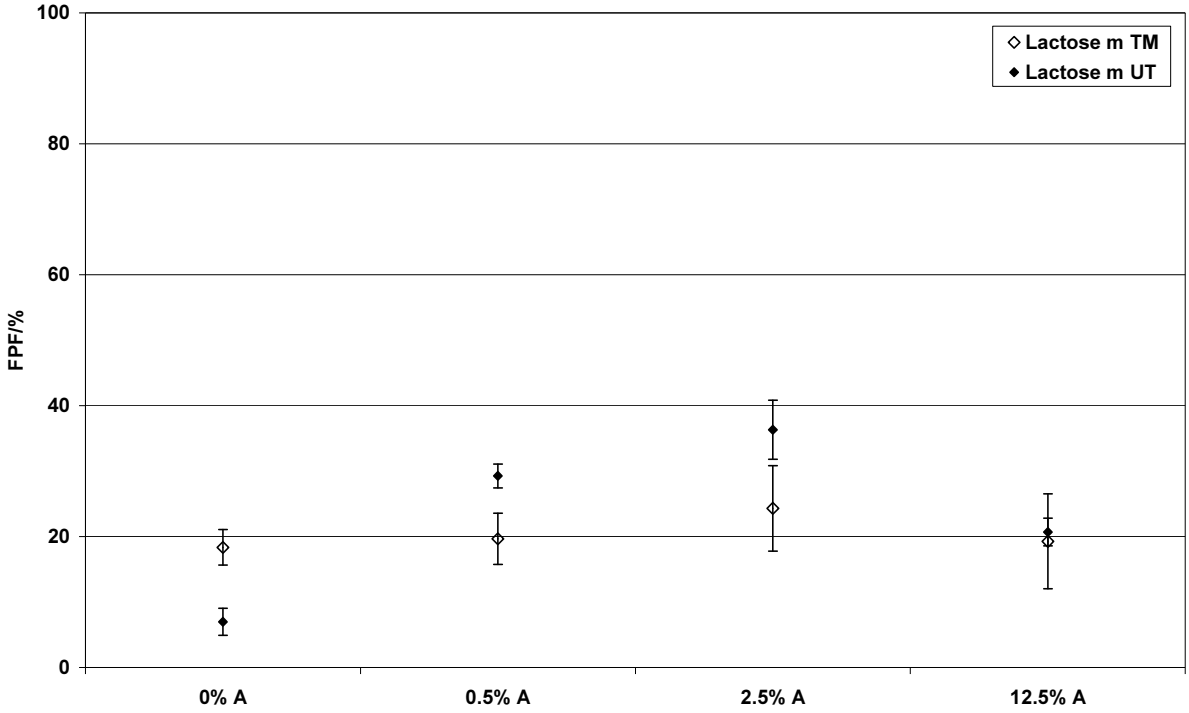

Figure 82: Mean ± s.d. of the fine particle fraction of mixtures containing micronised (m) lactose and 0 %, 0.5 %, 2.5 % and 12.5 % Aerosil® R972 (A) prepared by conventional mixing (TM) or electrostatically supported mixing (UT) (n = 3)

5.3.6 Micronised salbutamol base

Micronised salbutamol base mixtures with 0 %, 0.5 %, 2.5 % and 12.5 % Aerosil® R972 were treated the same way as the spray - dried salbutamol base mixtures. The results of the measurements are plotted in Figure 83.

Comparing the results of the mixtures prepared using conventional mixing the following is observed:

- FPF is significantly improved when increasing the nanoparticle concentration from 0 % to 0.5 % Aerosil® R972.
- There is no significant change of the FPF when increasing the nanoparticle concentrations from 0.5 % to 2.5 % and further to 12.5 % Aerosil® R972.

These results are in contrast to the results of the measurements of the uniformity of mass, where the addition of nanoparticles had no significant influence on the uniformity of mass. However, it is striking, that the standard deviation of the mass uniformity of the nanoparticle free sample is extraordinarily high, possibly hindering the detection of a significant effect of the addition of nanoparticles on the mass uniformity. Anyway, as described previously, differences of the results obtained by the aerodynamic assessment of fine particles and the measurements of the uniformity of mass may be attributed to the different acting forces during these measurements, also.

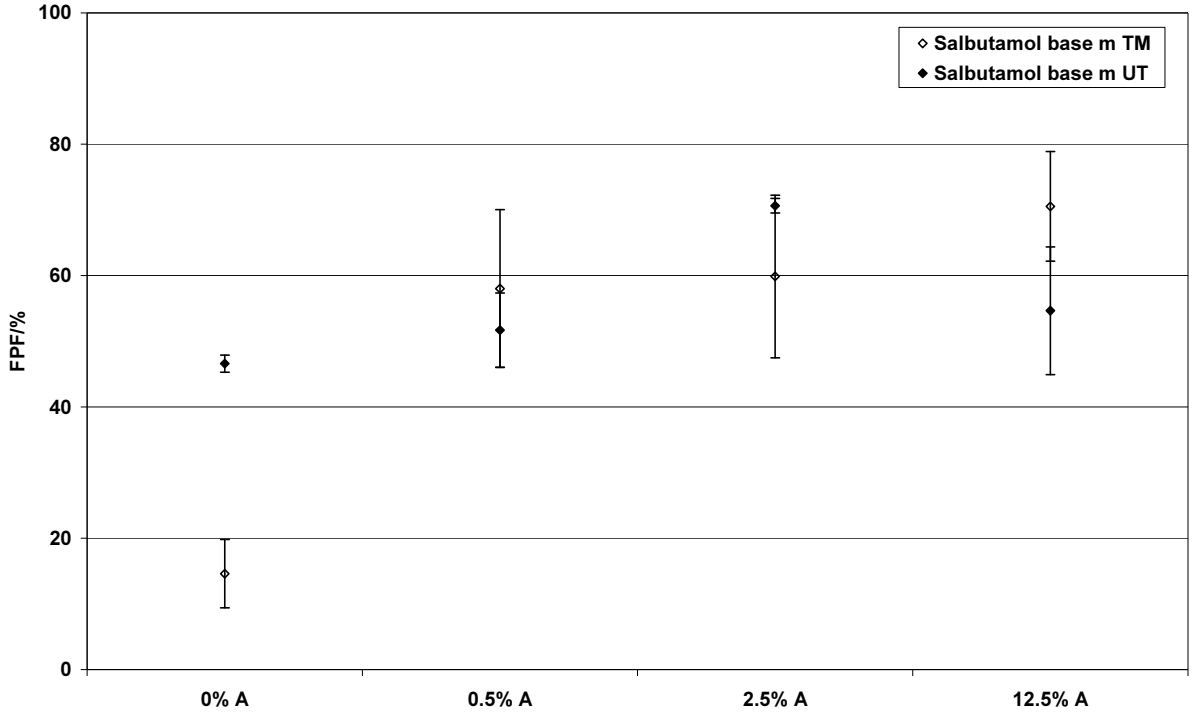

Figure 83.: Mean ± s.d. of the fine particle fraction of mixtures containing micronised (m) salbutamol base and 0 %, 0.5 %, 2.5 % and 12.5 % Aerosil® R972 (A) prepared by conventional mixing (TM) or electrostatically supported mixing (UT) (n = 3)

Comparing the results of the mixtures prepared by electrostatically supported mixing to the ones obtained by conventional mixing, a significant difference between the samples containing 0 % Aerosil® R972 is detected. The FPF of mixtures prepared by electrostatically supported mixing is significantly higher in comparison to conventional mixing. This may be caused by the enhanced dispersion of the micronised salbutamol base particles, which takes place during the treatment with the ULTRA - TURRAX® and results in an enhanced FPF. Another explanation, one may think of, is the comminution of the drug particles by the ULTRA - TURRAX®. However, it has

been shown in preliminary experiments, that treatment by the ULTRA - TURRAX® does not significantly alter the particle size of the drug powders used in this study, neither of the spray - dried nor of the micronised products (results are not shown). Due to the irregular shape of the micronised particles, the redispersion by the ULTRA - TURRAX® leads to a decrease of the bulk density of the possibly densified powder bed, thereby decreasing interparticle interactions and increasing the FPF. The effect of redispersion in case of the corresponding spherical spray - dried particles is assumed to be minor. However, in case of conventional mixing the energy input is not as high as in the case of electrostatically supported mixing, leading to a lower FPF.

Under the circumstances, that the samples without nanoparticles differ from each other in relation to the FPF when prepared either by conventional or electrostatically supported mixing, it is not good practice to compare the impact of the mixing mode on the FPF, as already mentioned in the previous chapter.

5.3.7 Micronised salbutamol sulphate

The determination of the FPF of the micronised salbutamol sulphate mixtures coated with 0 %, 0.5 %, 2.5 % and 12.5 % of nanoparticles were carried out. The results of the measurements are plotted in Figure 84.

Observing the FPF results of the mixtures prepared by conventional mixing the following is observed:

- FPF values of the mixtures with 0 % Aerosil® R972 are significantly lower than the ones of the mixtures with 0.5 % Aerosil® R972.
- FPF values of the mixtures with 0.5 % Aerosil® R972 are significantly higher than of the mixtures containing 2.5 % Aerosil® R972.
- Further addition of nanoparticles leads to a significant decrease of the FPF when increasing the nanoparticle concentration from 2.5 % to 12.5 % Aerosil® R972.

These results are in contrast to the results of the measurements of the uniformity of mass, where the addition of nanoparticles had no significant influence on the uniformity of mass. However, the changes of the FPF are moderate. So, it seems to be justified to attribute the differences in the results obtained by the determination of mass uniformity and the aerodynamic assessment of fine particles to the different forces acting during the measurements of the uniformity of mass and the aerodynamic assessment of fine particles.

Although the FPFs of samples without nanoparticles prepared by conventional and electrostatically supported mixing do not differ significantly, the possibility of the induction of changes to the nanoparticle free powder caused by the different mixing procedures is given, as already described in the two previous chapters for samples of micronised lactose (see 5.3.5) and salbutamol base (see 5.3.6). The absence of any significant difference of the FPF of the nanoparticle free micronised salbutamol sulphate samples may be caused by the simultaneous appearance of two counteracting mechanisms, namely the removal of fines decreasing the FPF and the enhanced dispersion by the ULTRA - TURRAX® increasing the FPF. However, the impact of these counteracting mechanisms may well vary in dependence on the presence or absence of nanoparticles, in other words, in dependence on the nanoparticle concentration,

leading to somewhat arbitrary results like the significant reduced FPF in case of samples containing 0.5 % Aerosil® R972 prepared by electrostatically supported mixing in comparison to the ones prepared by conventional mixing, although there is no significant difference between the nanoparticle free samples.
Last but not least, it is striking, that the FPF of the nanoparticle free micronised salbutamol sulphate treated by conventional mixing is considerably higher than the one of the corresponding spray - dried sample. This may be taken as another clue for the hypothesis, that solid bridge formation of initially amorphous spray - dried salbutamol sulphate upon recrystallisation takes place, which in turn, results in the low FPF of the spray - dried product (see 5.3.4).

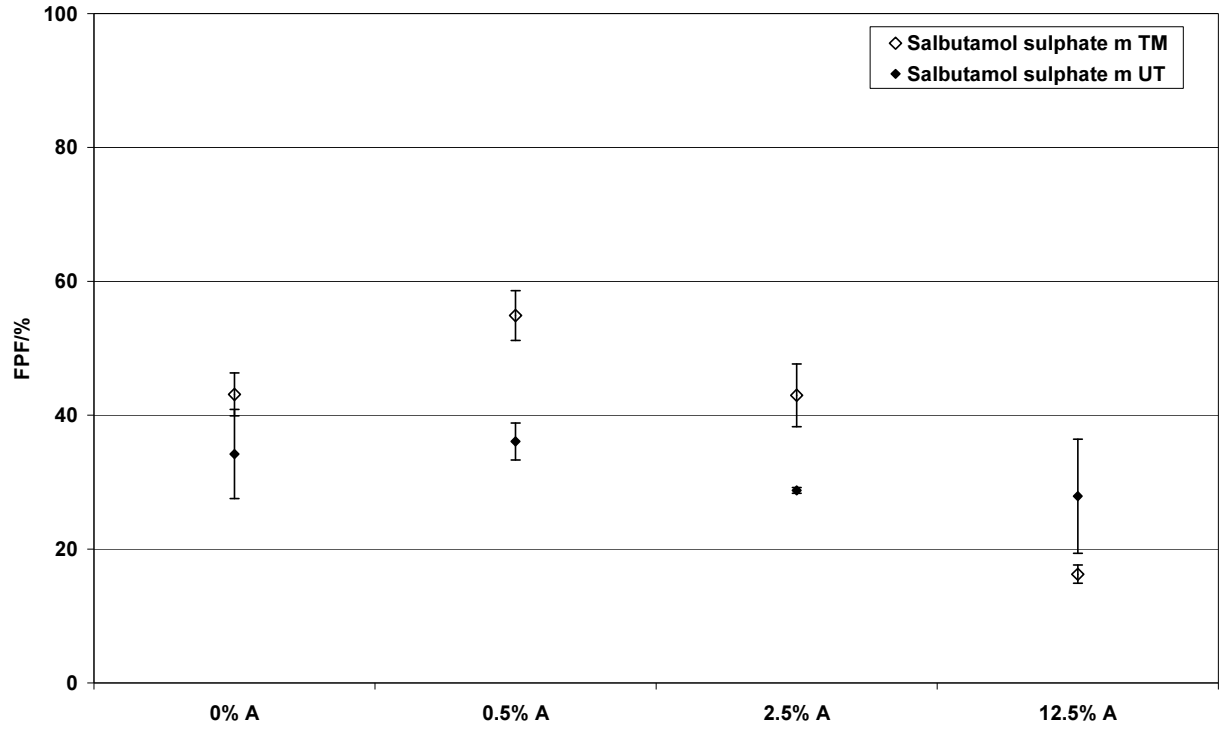

Figure 84: Mean ± s.d of the fine particle fraction of mixtures containing micronised (m) salbutamol sulphate (SS) and 0 %, 0.5 %, 2.5 % and 12.5 % Aerosil® R972 (A) prepared by conventional mixing (TM) or electrostatically supported mixing (UT) (n = 3)

5.3.8 Concluding remarks

Adding nanoparticles to spray - dried lactose or salbutamol sulphate particles causes an increase of the FPF, probably due to the ensuring of the non - contact of the microparticles and to the enhancing of the FPF at first. Further increasing of the nanoparticle amount does not lead to a further increase, but a decrease or no change of the FPF. Probably when the amount of nanoparticles exceeds optimum, mechanical interlocking may take place. Also, due to the excess of nanoparticles large agglomerates on the microparticles´ surface may be formed, which may disconnect themselves from the drug surface, if the gravitational forces get stronger than the attracting forces between microparticles and nanoparticle agglomerates. In this case, the interparticle forces between microparticles on the sites of the surface without nanoparticles increase, which also leads to the deterioration of the FPF.

It has been found out, that electrostatically supported mixing is advantageous regarding the FPF. The FPF of mixtures containing 0.5 % Aerosil® R972 prepared by electrostatically supported mixing is significantly superior compared to conventionally prepared mixtures containing the same amount of Aerosil® R972. These results are attributed to the enhanced dispersion of the nano - and microparticle fractions as well as the more homogeneous coating of the microparticle surface by nanoparticles when applying electrostatically supported mixing. The results obtained by the aerodynamic assessment of fine particles are in good agreement with the results obtained by the assessment of the mass uniformity (see 5.2), even if the nanoparticle concentrations, at which the FPF or mass uniformity was best, may not be exactly the same, but shifted towards higher or lower values. These shifts are attributed to the different forces acting during the measurements.

Although it is possible to increase the FPF of spray - dried lactose and salbutamol base by coating the microparticles with nanoparticles, it is not for spray - dried salbutamol sulphate samples, because the additional impact of recrystallisation on interparticle interaction may affect the FPF considerably. This has been shown for the uniformity of mass previously (see 5.2).

In relation to the micronised powders, it turned out, that the addition of Aerosil® R972 by conventional mixing does not change the FPF of lactose significantly. This is in agreement with the results of the determinations of the uniformity of mass. However, an increase of the FPF was found for micronised salbutamol base and sulphate when adding nanoparticles, which, upon further addition of Aerosil® R972 decreases again in the case of micronised salbutamol sulphate. Although these effect have not been observed by the investigations on mass uniformity, the results may well be explained by the effect of the nanoparticles acting as spacers at low concentrations and the effect of mechanical interlocking at high concentrations, as was already discussed previously (see 5.2.8). The differences between the results obtained by the determination of mass uniformity and the aerodynamic assessment of fine particles are attributed to the different forces acting during the measurements of the uniformity of mass and the aerodynamic assessment of fine particles.

Treating the micronised powders by conventional and electrostatically supported mixing turned out to induce changes to the nanoparticle free powders. This has been shown on nanoparticle free samples of micronised lactose and salbutamol base, which significantly differ from each other in relation to the FPF depending on the mixing mode. The differences found are attributed to two counteracting mechanisms, namely the removal of fine particles present on the surface of the micronised powders by the treatment with the ULTRA - TURRAX® enhancing interparticle interactions and reducing the FPF, and the efficient dispersion of the probably densified powder bed of the micronised samples by the treatment with the ULTRA - TURRAX® decreasing interparticle interactions and enhancing the FPF. The first mechanism seems to prevail in the case of micronised lactose, whereas the second one in the case of micronised salbutamol base. With respect to micronised salbutamol sulphate both mechanisms are assumed to affect the powder properties similarly. The removal of the fines as well as the dispersion of a possibly densified powder bed are more likely to occur when treating the samples by electrostatically supported than by conventional mixing, firstly because of the higher energy input and secondly because of the higher dielectricity constant of the liquid nitrogen facilitating the detachment of

the fines. Furthermore, micronised powders are more susceptible to the fines removal than spray - dried powders, because the first contain a considerable amount of fines, whereas the latter do not. And finally, the impact of redispersion is higher for micronised powders due to their irregular shape than for the corresponding, almost perfectly spherical spray – dried samples. Given the fact, that the treatment by electrostatically supported mixing itself alters the properties of the samples, it is not possible to discuss the changes of the FPF in dependence on the mixing mode. Finally, it has to be recalled, that the changes induced by the different mixing methods, that cause the FPF of the nanoparticle free samples prepared by conventional and electrostatically supported mixing to differ from each other, were not detected when examining the mass uniformity (see 5.2.5, 5.2.6, 5.2.7). This is attributed to the high standard deviations of the values of the relative standard deviation determined in course of the mass uniformity evaluation of the nanoparticle free samples (see Figure 76 - Figure 78).

E. Experimental part

1. Used materials

Acetic acid (100 %)	Rotipuran, Carl Roth GmbH & Co, Karlsruhe, Germany
Acetone	Sigma Aldrich Laborchem., Seelze, Germany
Acetonitril	Rotisolv, Carl Roth GmbH & Co, Karlsruhe, Germany
Demineralised water	produced by reverse osmosis
Dichlormethan	Fisher Scientific, Loughborough, UK
Glycerol (anhydrous)	Caesar & Loretz GmbH, Hilden, Germany
GranuLac 200	Molkerei MEGGLE Wasserburg GmbH & Co. KG, Wasserburg, Germany
Isopropanol	Chromasolv, Riedel - de - Haen, Seelze, Germany
Liquid nitrogen 5.0	Linde AG, Muenchen, Germany
Polyoxyethylen - 20 - cetylether (Brij 59)	Uniquema, Everberg, Belgium
Salbutamol base	FDC Limited, Deli, India
Salbutamol sulphate	FDC Limited, Deli, India
Silica dioxide Aerosil® R972	Degussa AG, Duesseldorf, Germany

2. Pre - treatment of the drug substances

2.1 Air jet milling

α - lactose - monohydrate and salbutamol sulphate were milled with the air jet mill (50 AS, Hosokawa Alpine AG, Augsburg, Germany). The feeding rate of the substances to the milling chamber was adjusted to approximately 1 g min^{-1}. The injector pressure was set to 3.5 bar and the milling pressure to 2.0 bar. After gathering of the micronised powder, the samples were stored over silica gel at least for 24 hours before further processing took place.

2.2 Spray - drying

Lactose was spray - dried by Molkerei MEGGLE Wasserburg GmbH & Co. KG, Wasserburg, Germany using Spray Dryer Mobile Niro Atomizer Typ M - 02 by following parameters:

- 10 % (w/w) solution of α - lactose - monohydrate in demineralised water
- Inlet temperature 134 °C ± 5 °C
- Outlet temperature 80 °C ± 5 °C
- Air flow rate 800 L h^{-1}
- Aspirator level 90 %
- Pump speed 5 ml min^{-1}.

Salbutamol base was spray - dried using mini spray dryer Buechi B - 191 (Buechi Labortechnik GmbH, Essen, Germany) by following parameters:

- 0.8 % (w/w) solution of salbutamol base in demineralised water
- Inlet temperature 80 °C ± 5 °C
- Outlet temperature 53 °C ± 5 °C
- Liquid nitrogen flow rate 414 L h^{-1}
- Aspirator level 100 %
- Pump speed 30 %.

Salbutamol sulphate was spray - dried using a mini spray dryer Buechi B - 191 (Buechi Labortechnik GmbH, Essen, Germany) using following parameters:

- 10 % (w/w) solution of salbutamol sulphate in demineralised water
- Inlet temperature 150 °C ± 5 °C
-Outlet temperature 80 °C ± 5 °C
- Air flow rate 800 L h^{-1}
- Aspirator level 90 %
- Pump speed 5 ml min^{-1}.

After spray - drying, the powders were stored in a desiccator containing silica gel at least for 24 hours until the further processing was performed.

2.3 Freeze - drying

Amorphous salbutamol base was prepared by freeze - drying of the 0.8 % (w/w) aqueous solution of salbutamol base using the LYOVAC GT2 FINN - AQUA (SANTASALO - SOHLBERG GmbH, Huerth; Germany). The aqueous salbutamol base solution (50 ml) was frozen in a 1 l flask with the help of frozen acetone. Afterwards the frozen solution

was subject to freeze - drying. A vacuum of $9.5*10^{-1}$ mbar was applied. The process of freeze - drying took 24 hours. After freeze - drying, the amorphous salbutamol base was stored in a desiccator containing silica gel until further analyses were performed.

3. Characterization of the materials

3.1 Laser diffraction

The particle size distributions of all powder samples were determined using a Sympatec HELOS H1402/KF - Magic laser diffractometer (Sympatec GmbH, Clausthal - Zellerfeld, Germany). The powder samples were placed evenly on the furrow of the Vibri - conveying unit (Sympatec GmbH) and then transported to the powder funnel of the dry dispersion unit RODOS. This unit allows the dry dispersion of the powder sample via a Venturi nozzle with the help of compressed air. During the measurements the dispersion pressure of 2.0 bar and a negative pressure between 60 mbar and 70 mbar were set up. For the determination of the particle size distribution the lens was used, which allows the measurement in the range between 0.25/0.45 µm and 87.5 µm. The results of the measurements were evaluated using the device software Windox 4.0. In this work the diffraction patterns of the drug microparticles were evaluated according the Fraunhofer theory. In order to characterise the average particle size of the powder samples the x_{50} - value (median) was used in this work. All measurements were performed in triplicate. Before the start of the investigations all powder samples were stored in the a desiccator containing silica gel at least for 24 hours until analyses were performed.

3.2 Scanning electron microscopy

Geometry and surface of the used materials were examined by scanning electron microscopy. The samples were fixed on a double - sided electro - conductive adhesive tape, which was fixed on a aluminium stub, and sputter - coated with gold during 180 s in an argon atmosphere using the Agar Sputter Coater B7340 (Agar Scientific Ltd., Essex, United Kingdom). The scanning electron micrographs were taken using a LEO VP 1430 (Carl Zeiss NTS GmbH, Germany) at 20 kV voltage under vacuum. Images were taken with 1000x, 2000x, 3000x and 4000x magnification. Before the start of the investigations all powder samples were stored in the a desiccator containing silica gel at least for 24 hours until analyses were performed.

3.3 Density

Pycnometric density measurements of the solid particles were carried out using a He - pycnometer AccuPyc^{TM} 1330 device (Micromeritics, Norcross, USA) at 25 °C ± 0.1 °C. The powder samples were introduced into the sample chamber of 10 cm^3 volume and were flushed tenfold with helium gas. The applied pressure for cleaning and filling of the 10 cm^3 sample chamber was 134 kPa. Obtained helium density values are the mean of five density measurements for each sample. Prior to investigations all powder samples were stored at least 24 hours in a desiccator containing silica gel.

3.4 Moisture sorption

The moisture sorption measurements of the powder samples were carried out in a humidity and temperature controlled chamber using the moisture sorption system SPS11 (Projekt Messtechnik, Ulm, Germany). The results of the measurements were evaluated with the device software Release 2.2.8 (Projekt Messtechnik). The temperature of the chamber was set to 25 °C and the equilibrium condition was angled to 0.01 % mass change per 60 minutes. The samples were weighed in time intervals of six minutes. The relative humidity was first set to 0 %. In steps of 10 % the relative humidity was raised to 90 % and finally to 95 %. Subsequently, the relative humidity was decreased to 0 % RH the same way. This cycle was repeated once more. After each raising of the RH the samples were allowed to equilibrate. Then the humidity was raised further to the next level. The weight of each sample was approximately 2 g. Before the beginning of each series of measurements the samples were stored, and therefore dried, in the humidity chamber at 0 % RH for 24 hours. All measurements were performed in duplicate. The results of the first measurement are shown in the diagrams.

3.5 Differential Scanning Calorimetry

Thermodynamic studies were performed using a DSC 821e (Mettler Toledo GmbH, Giessen, Germany). Temperature and enthalpy were calibrated using indium. Approximately 2 - 3 mg of the powder under investigation was introduced in a 40 µl standard aluminium pan with a pierced lid. As a reference an empty aluminium pan was used. The measuring cell was flushed with liquid nitrogen at a flow rate of 50 ml min^{-1}. The samples were heated from 0 °C to 350 °C with a heating rate of 10 °C min^{-1}. For the evaluation of the results of the measurements the device software STARe - Software Version 6.01 (Mettler Toledo GmbH) was used. Before the start of the investigations all powder samples were stored in the a desiccator containing silica gel at least for 24 hours until analyses were performed. All DCS curves presented are standardised by the weight of the samples. The measurements were done in duplicate.

3.6 X - Ray Powder Diffraction

Samples were examined by powder X - ray diffraction (Rigaku Miniflex, Rigaku Denki Co. Ltd, Tokio, Japan). Samples were placed in aluminium holders and scanned isothermally at 25 °C. In this device the anode is made from copper, Cu Kα - radiation was used, the acceleration voltage was 30 kV, the current flow 10 mA. For the measurements the 2 theta - angle - range between 5° and 40° was scanned, the measuring range of 2000 cps was used with the scanning velocity of 2 °/min and with the distance between two data points of 0.02°. All samples were stored over silica gel at least for 24 hours before the measurements were carried out. The measurements were done in duplicate.

4. Production of the powder formulations

4.1 Conventional mixing

Different mixtures of spray - dried and micronised active ingredients (lactose, salbutamol base and salbutamol sulphate) and 0 %, 0.5 %, 2.5 % and 12.5 % Aerosil® R972 (batches weight 200 g in case of spray - dried lactose, and 2 g in case of the other active ingredients) were

prepared by mixing the components 90 minutes in a 25 ml (in case of the other active ingredients) or 2500 ml (in case of spray - dried lactose) glass vial using a TURBULA® shaker mixer (T2C, Willy A. Bachofen AG Maschinenfabrik, Basel, Switzerland) at 65 rpm. For the preparation of the different mixtures, one half of the active ingredient was put inside the glass vial at first, further Aerosil® R972 was added and at last the second half of the microparticles was filled in. In order to keep the preparation conditions similar for all samples, the samples containing 0 % Aerosil® R972 were treated in the mixer under the same conditions as the mixtures containing 0.5 %, 2.5 % and 12.5 % Aerosil® R972. The relative standard deviation of the drug model content was below 1 %. After the preparation the mixtures were stored over silica gel in dessicator at least for 24 hours till the further proceeding took place. Powder mixtures of the above mentioned concentrations were prepared in triplicate.

4.2 Electrostatically supported mixing

At the beginning of the experiment approximately 500 ml of liquid nitrogen were poured in a 600 ml beaker, which was placed in the inner cup of a Faraday cup. Then the high - speed homogenator ULTRA - TURRAX® T25 basic (IKA® - Werke GmbH & Co. KG, Staufen, Germany) was switched on and slowly inserted into the liquid nitrogen. It has been waited till the equilibrium of the system in relation to the in charge measured was established (see D.4.2). After that, the nanoparticle fraction Aerosil® R972 was suspended in the liquid nitrogen. The nanoparticle dispersion was stirred at 8200 rpm with a high - speed homogenator ULTRA - TURRAX® T25 basic till the acquired charge of the powder reached a negative maximum or plateau. Then the microparticulate active ingredient fraction was added. In case of salbutamol base and sulphate charging was continued until the charge equalled unity. In case of lactose further decreasing of the charge took place, until the equilibrium was reached indicated by a plateau of the acquired charge. The measurements of the induced charge were carried out using a shielded cup capacitor (Faraday cup) which was connected to the electrometer Keithley 6514 (Keithley Instruments GmbH, Germering, Germany). The Faraday cup consisted of an inner and outer cup. The inner cup (measuring cup) is isolated from the ground and connected to the electrometer. The earthed outer cup (protection cup) works not only as a screening for the measuring cup, but prevents from the measurement of external charges. For the grounding the outer cup is connected to the shield of the coaxial cable.

Mixtures of active ingredient models and 0 %, 0.5 %, 2.5 % and 12.5 % Aerosil® R972 (batches of approximately 2 g) were prepared by electrostatically supported mixing. The relative standard deviation of the drug model content was below 1 %. After the preparation of the mixtures they were stored over silica gel in a dessicator at least for 24 hours till the further proceeding took place. Powder mixtures of the above mentioned concentrations were produced in triplicate.

5. Flowability measurements

5.1 Ring shear tester

Before carrying out the flowability measurements, after the preparation of the powder mixtures, all blends were stored over silica gel at least for 24 hours. In order to measure the flow properties of the fine - grained solids a ring shear tester type RST - 01.pc (Dietmar Schulze,

Schuettgutmesstechnik, Wolfenbuettel, Germany) was used. For the measurements the cell type MV10, v1.1 with internal volume of 267.04 cm^3 was used. At the beginning of the measurement during the pre - shear step the consolidation of the powder with the vertical normal load of 4000 Pa took place. For the construction of the yield limit during the second shear step the same powder blend was sheared under different normal loads of 800, 1600, 2400, 3200 Pa. During one run approximately 120 g of each powder blend was used. The testing was carried out on three batches.

5.2 Hausner ratio

At the beginning of the experiment the powder was loosely poured into the 250 ml glass cylinder and the volume V_{beg} is read. The present measurements were performed according the procedure described in the Monograph "Apparent and tapped volume" of the European Pharmacopoeia 6.0. At the end of the test the volume of the tapped powder V_{end} was also read. The Hausner ratio is a quotient of V_{beg} to V_{end}. A high Hausner ratio means poor flowability. The testing was carried out on three batches.

5.3 Flow rate

This conventional method is used for the characterisation of the flow behaviour of powders. The time, which 100 ml of the powder need to pass the outlet of a funnel, is determined. Measurements were carried out using the funnel described in the Monograph "Flow behaviour" of the European Pharmacopoeia 6.0, the diameter of the outlet orifice was 10 ± 0.01 mm. The testing was carried out on three batches.

5.4 Angle of repose

Measurements were carried out using the equipment as described in the German Industry Norm DIN 53916: "Surface active agents - Powders and granules - Measurement of the angle of repose; Proceeding according Pfrengle". For powders showing poor flow properties a stirring device was used. During the test the powder flows out of the funnel and settles as a cone on a plastic plate of 100 mm diameter. 100 ml of each powder were tested. The angle of repose is the angle between the sloping surface of the sample pile and the horizontal. All measurements were done in triplicate. The testing was carried out on three batches.

6. Uniformity of mass of the dispensed dose

In order to determine the uniformity of the dispensed mass, the multiple - unit reservoir NOVOLIZER® DPI (MEDA Pharma GmbH & Co. KG, Bad Homburg, Germany) containing the mixture was weighed before and after each dose discharge. 40 doses in case of the mixtures containing the spray - dried and micronised lactose, in all other cases 10 doses were discharged during each test. The mass of each dose was calculated by subtracting the weight of the multi dose reservoir after discharge from the weight before discharge. The relative standard deviation of the mass of the 40 or 10 doses, depending on the material, was calculated and taken as a measure for the uniformity of mass. The testing was carried out on three batches. Prior the

measurements of the mass uniformity, powder samples were stored over silica gel for at least 24 hours.

7. Aerodynamic assessment of the fine particles

During the NGI experiments the device is configured analogue to Figure 85, only the sample collection tube is replaced by the impactor. The collection cups of stage 1 and the micro orifice collector were coated with 2 ml of a mixture consisting of isopropanol 95 %, glycerol anhydrous 4.75 % and polyoxyethylene 20 cetyl ether (Brij® 58) 0.25 %. Due to the geometrical construction of the preseparator it was not coated at all. The collection cups of the stages 2 – 7 were coated with 1 ml of the mixture. Isopropanol was allowed to evaporate during at least 1 hour, the collection cups were put in the body of the NGI and the device was closed.

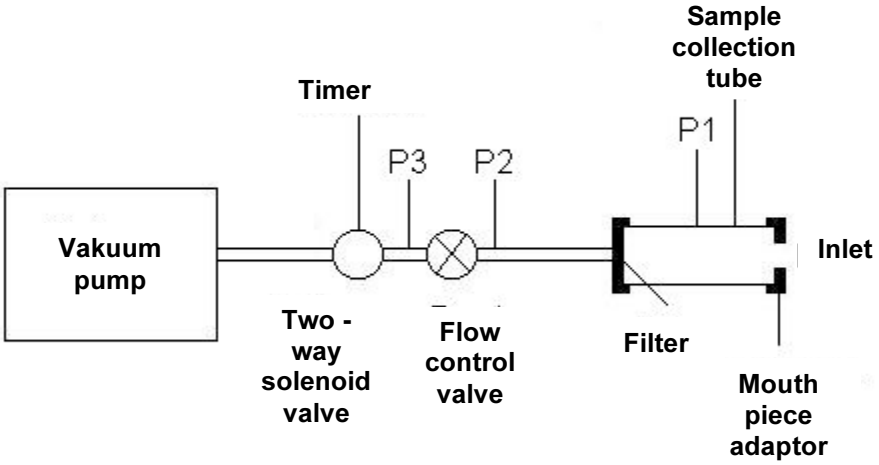

Figure 85: Sampling apparatus for DPIs (taken from Copley Scientific booklet 2007)

In case of spray - dried and micronised lactose approximately 0.6 g of the powder were released into the impactor, the NGI was then dismantled and the weight gain on each of the stages was determined gravimetrically. The FPF was calculated as percentage of the mass of particles smaller than 5 µm and the total mass of the released dose, which was considered to be 100 %.
In case of the mixtures of spray - dried or micronised salbutamol base or salbutamol sulphate approximately 0.04 g of the powder were released into the impactor. At the end of the experiment the NGI was opened and 20.0 ml of diluted acetic acid (pH 3) were added on each plate. The tray with the plates was shaken moderately for 10 minutes, afterwards 5.0 ml of the solution were taken from each plate and introduced into a glass volumetric flask and were filled up ad 50.0 ml with diluted acetic acid (pH 3). The preseparator was washed with the above mentioned solvent and filled into a glass volumetric flask. Solvent was added ad 50.0 ml. The concentrations of the solutions were determined by high - pressure liquid chromatography (HPLC). The testing was carried out on three batches.

8. HPLC Analysis

In - vitro deposition of the powder blends was determined by high - pressure liquid chromatography (HPLC). The HPLC system (LC 6A Shimadzu, Duisburg, Germany) consisted of the pump LC6A, the UV - VIS spectrometric detector SPD - 6AV ($\lambda = 276$ nm, flow rate: 0,52 ml/min, mobile solvent 55 % acetic acid/ 45 % acetonitrile), the autosampler SK - 6B, the integrator C - R4AX Chromatopac (Shimadzu, Duisburg, Germany), the column Nucleosil 100 - 5C18 HD, 250 - 4 (Macherey & Nagel, Dueren, Germany). During the measurements the column was tempered with the column oven (Thermasphere TS - 430, Phenomenex, Aschaffenburg, Germany) at the temperature of 35 °C. Before each series of measurements of each produced mixture three weighted concentrations of the analyte for the determination of linearity and after each ten samples one external standard were measured to check system suitability. The injected volume of each probe was 10 µl. All samples were injected twice.

9. Statistical methods of calculation

The statistical analysis of the experimental data was carried out using the two - sample two - tailed t - test. The two - sample (independent groups) t - test is used to determine whether the unknown means of two populations significantly differ from each other based on independent samples from each population. In cases, where the preliminary F - test for equality of variances indicated that the variances of the two groups were significantly different, a two - sample t - test was performed that does not assume equal variances. If the two - sample means are sufficiently different from each other, then the population means are declared to be significantly different. The statistical probability *p - value was 0.05.

F. Conclusion

The purpose of this study was to develop and evaluate a novel carrier free formulation for the use in dry powder inhalers. It is generally accepted that the mean size of the drug particles for dry powder inhalers has to be between 1 µm and 5 µm. As the weight of such fine particles is very low, particle interactions are much higher than the gravity forces. With the increase of cohesion forces the agglomeration of the drug particles takes place and flowability, dosing and redispersion becomes difficult.

In this study, cohesion forces are claimed to be reduced by covering the microparticulate drug with particles in the nanometer range. The nanoparticles are supposed to act as spacers, thereby declining cohesion forces between drug particles and promoting flowability, redispersion and dosing of the powder intended for the use in dry powder inhalers.

The nanoparticle - microparticle - mixtures were prepared using either a TURBULA® shaker mixer or an ULTRA - TURRAX® high speed homogenator providing mixing by suspending the nanoparticles as well as the microparticles in liquid nitrogen and charging them by triboelectrification. During this process not only charging and dispersion of like particles, but also attraction and charge diffusion between unlike charged micro - and nanoparticles occur, thereby presumably enhancing mixing homogeneity.

The coating ratio, which is defined as the percentage of nanoparticles in the nanoparticle - microparticle - mixture is assumed to play an important role in interparticle interaction reduction. Theoretically, it is supposed to be in between the so - called upper and lower coating limit in order to reduce interparticle interactions most effectively. The lower limit is achieved by mixing microparticles with such an amount of nanoparticles, that direct contact between two larger particles is not longer possible. The upper coating limit is achieved when the host particle is coated with a monolayer of the guest particles. The lower coating limit has been calculated using the model proposed by Bresges (Bresges et al., 2008) which is especially dedicated to the calculation of the minimum number of nanoparticles needed to ensure non - contact of the microparticulate host particles. However, mixing in real conditions may considerably differ from ideal conditions. Therefore, the calculations were used just as a basis for the estimation of the appropriate coating ratio. In order to verify the calculations and to check the coating of the microparticles with the nanoparticles in dependence on the nanoparticle concentration, SEM images were taken and the coating ratio was adjusted accordingly.

In this study, spray - dried lactose, salbutamol base and sulphate as well as micronised lactose, salbutamol base and salbutamol sulphate were used as model microparticles, Aerosil® R972 was taken as the model nanoparticle. Experiments with different Aerosil® R972 concentrations, namely 0 %, 0.5 %, 2.5 % and 12.5 % were carried out.

Scanning electron micrographs reveal the shape of the spray - dried products to be more or less spherical. In contrast to spray - dried spherical particles, micronised particles show an irregular shape. Also, the presence of fines in the samples of micronised lactose, salbutamol base and salbutamol sulphate is striking.

The flowability measuring tests on spray - dried lactose mixtures containing 0 %, 0.5 %, 2.5 % and 12.5 % Aerosil® R972 obtained by TURBULA® mixing reveal the worst flow characteristics for nanoparticle free samples. This is attributed to the close contact between the lactose particles enhancing interparticle interactions. Coating the spray - dried lactose with 0.5 % Aerosil® R972 enhances the flow behaviour, due to the nanoparticles acting as spacers between the lactose particles thereby reducing interparticle interaction. Coating with higher amounts of Aerosil® R972 deteriorates the powder flow characteristics again probably caused by the increase of mechanical interlocking phenomena. According to the results obtained by ring shear testing and flow rate measurements, flowability of the mixtures containing different concentrations of Aerosil® R972 decreases in the order 0.5 % > 2.5 % > 12.5 > 0 % Aerosil® R972.

In relation to the uniformity of mass, which is a functional factor for the performance of any multi dose dry powder inhaler, it has been found out, that by coating spray - dried microparticles with nanoparticles, it is possible to increase the mass uniformity. This has been shown for spray - dried lactose and salbutamol base. Due to recrystallisation phenomena in case of amorphous spray – dried salbutamol sulphate, dose uniformity enhancement is not observed. As already shown for the flow behaviour, the increase of the coating level improves the uniformity of mass at first due to the decrease of interparticle interactions, further increasing of the nanoparticle concentration leads to a deterioration of the uniformity of mass again, probably provoked by mechanical interlocking of excess nanoparticles. These results are in good accordance with the results of the flowability measurements, where also the dependence of the flowability on the nanoparticle concentration in the mixtures was observed.

Comparing conventional and electrostatically supported mixing, electrostatically supported mixing is more efficient with respect to the increase of the uniformity of mass at low nanoparticle concentrations. This has been shown for spray - dried lactose and spray - dried salbutamol base containing 0.5 % Aerosil® R972 and is explained by the distribution of the guest particles on the host microparticle surface, which is supposed to be more homogeneous when using electrostatically supported mixing. At low concentrations, this homogeneous distribution ensures the non – contact of the microparticles and the reduction of interparticle interactions, whereas less homogeneous distributions obtained by conventional mixing still exhibit spacer free surface areas allowing contact between the microparticles.

In contrast to these results, the effect of the addition of nanoparticles to micronised drug model powders by conventional mixing is not significant. This may be explained by the fact, that the fines present in micronised powders already play the role of spacers and further mixing with nanoparticles does not enhance the uniformity of mass anymore.

However, it is not possible to evaluate the effect of the mixing mode on the mass uniformity of micronised samples, because it has turned out, that the treatment of micronised powders using the ULTRA - TURRAX® high speed homogenator induces changes to the drug powder itself making a sound comparison between the mixing modes impossible.

Finally, it is possible to increase the FPF by coating spray – dried microparticles with nanoparticles. This has been shown for spray - dried lactose and salbutamol base samples. When increasing the amount of nanoparticles too much, mechanical interlocking may take place

resulting in the deterioration of the results in terms of the FPF. These results correspond very well to the ones obtained by the determination of mass uniformity.
However, in contrast to the results obtained by the investigations on mass uniformity of micronised drug particles, where no dependence of the mass uniformity on the nanoparticle concentration has been found, an increase of the FPF of micronised salbutamol base and salbutamol sulphate is obtained upon the addition of nanoparticles by conventional mixing. The main reason, which may be encountered for the deviation of the results obtained by the investigations on mass uniformity and on the FPF, is the different acting forces during the measurements of the uniformity of mass and the aerodynamic assessment of fine particles.
The effect of electrostatically supported mixing in comparison to conventional mixing using micronised drug models is difficult to judge, because, as already mentioned, the treatment of micronised powders using the ULTRA - TURRAX® high speed homogenator turned out to induce changes to the drug powder itself. In this sense, the application of electrostatically supported mixing to micronised powders is not beneficial.
In conclusion it can be said, that nanoparticle - microparticle - mixtures for the use in dry powder inhalers can be considered as an alternative approach to enhance flowability, uniformity of mass and respirable fraction in vitro. However, there will be various obstacles to be overcome before this approach will find its way into commercial products. First of all, Aerosil® R972 was used as nanoparticle model in this study. As Aerosil® R972 is not approved for the use in dry powder inhalers, toxicological studies will have to be carried out or even other nanoparticle models, which are approved for pulmonary application, have to be thought of. Secondly, the extent of the improvement of the uniformity of mass and the FPF strongly depends on the drug model. The FPF of spray – dried lactose, for example, increases approximately four fold when adding 0.5 % Aerosil® R972 by conventional mixing and approximately six fold when adding 0.5 % Aerosil® R972 by electrostatically supported mixing in comparison to the nanoparticle free sample, the FPF of which is below 10 %. In contrast, the improvement of the FPF by the addition of Aerosil® R972 to spray – dried salbutamol base is less than doubled with respect to the nanoparticle free sample, the FPF of which is around 15 %. Finally, the advantage of electrostatically supported mixing over conventional mixing in relation to the mass uniformity and FPF improvement is limited. The FPF of the mixture containing spray - dried lactose and 0.5 % Aerosil® R972, for example, is 24 % when prepared by conventional mixing and 32 % when prepared by electrostatically supported mixing. In case of spray - dried salbutamol base and 0.5 % Aerosil® R972 the obtained results are similar. Furthermore, electrostatically supported mixing was not at all shown to be superior to conventional mixing when applying to micronised powders. Given these figures and the problems associated with electrostatically supported mixing, like the cost intensive equipment and use of liquid nitrogen as well as the difficulties in scaling up the process, which is caused by the extensive use of liquid nitrogen, a thorough evaluation of the profitability would have to proceed, in order to be able to call electrostatically supported mixing a technique relevant in comparison to conventional mixing for the improvement of the performance of dry powder inhalates.

G. List of symbols and abbreviations

a	Distance
A_H	Hamaker - Van - der - Waals constant
A_h	Total surface area of host particles
A_{hex}	Required area for one particle in the hexagon model
$A_{p\ total}$	Total area of the particles
A_s	Surface area
c	Concentration
c_{VdW}	Van - der - Waals coefficient
D	Diffusion coefficient
d	Diameter of roughness/sphere
d_{ae}	Aerodynamic diameter of a particle
d_g	Geometric diameter of a particle
d_p	Diameter of a particle
e	Charge of an electron
E_F	Fermi level
E_f	Electric field strength
E_R	Electrostatic potential
E_V	Vacuum level, which represents the energy an electron from a given solid would have just outside the solid
F	Force
F_A	Attraction forces
F_{CB}	Capillary force
F_{el}	Electrostatic forces
ff_c	Flowability value
F_g	Gravity force
Fr	Froude - number
F_{VdW}	Van der Waals forces
g	Gravitational acceleration
h	Height
h_V	Planks quantum
i	Guest particle in Bresges model
K	Boltzmann constant
l	Edge length of the hexagon
m_d	Mass of the droplet
m_p	Mass of the particle
N	Number of hemispheres/roughnesses/guest particles on the surface of the large/host particles
$N_{p\ total}$	Total number of the particles in a sample
N_s	Density of the surface states of the insulator
N_t	Number of triangles needed to cover the surface of the host particle
q	Electrical charge

P	Pressure
R	Radius of the large/host particle
R_a	Airway radius
r_c	Radius of the mixing cylinder
r_p	Radius of the particle
r	Radius of hemisphere/roughness/guest particle
r_{min}	Radius of hemisphere at which minimum attraction between the partners occurs
$r + x_0$	Distance of the median line to the intersection of all median lines/side length
S	Contact area between the particles
S_p	Sectional plane
T	Absolute temperature
t	Time
x_{50}	Median
V	Electrostatic potential of the metal surface relative to the insulator at equilibrium in the work function model
V_a	Air velocity
V_{beg}	Apparent volume
V_e	Potential energy
V_{end}	Tapped powder
V_p	Volume of a spray - dried particle
V_{REF}	Volume of the reference chamber in a pycnometer
V_S	Volume of the sample under investigation using helium pycnometrie
V_{SC}	Volume of the chamber with a sample in a pycnometer
V_t	Velocity of the sedimentation
W	Work functions after the charge transfer
u	Dipole moment
U	Contact potential
ΔU	Potential difference
x	Contact distance between two guest particles in Meyer model
x_1	Half of the distance between the two guest particles in Meyer model
y	Contact distance between two host particles in Meyer model
y_1	Half distance between two host particles
α	Half of the interior angle of the equilateral triangle
α_p	Polarisability
ε	Permittivity
ε_e^F	Kinetic energy
ε_f	Electric field constant
ε_0	Dielectric permittivity in vacuum

ε_r	Relative dielectricity constant
Φ^M	Work function
$\hbar$	Planck's constant
$\hbar\varpi$	Lifschitz - Van - der - Waals constant
η_a	Air viscosity
ω	Angular speed
ϖ	Mean frequency from the absorption spectrum
ρ	Relative surface coverage
ρ_a	Density of the air
ρ_d	Density of the droplet
ρ_n	Number density of the molecules
ρ_p	Density of the particle
ϑ	Contact angle
σ	Surface charge density
σ_1	Consolidation stress
σ_c	Unconfined yield strength
ν	Characteristic frequency of the material
γ	Surface tension
Δ	Root mean square displacement
φ	Angle of repose

CFC	Chlorofluorocarbons
COPD	Chronic obstructive pulmonary diseases
CR	Coating ratio
CRc	Critical coating ratio
DIN	Deutsches Institut fuer Normung
DPI	Dry powder inhaler
DSC	Differential Scanning Calorimetry
FPD	Fine Particle Dose
FPF	Fine Particle Fraction
HPLC	High Pressure Liquid Chromatography
MDI	Meter dose inhaler
MOC	Micro - Orifice Collector
NGI	Next Generation Impactor
RH	Relative humidity
s.d.	Standard deviation
SEM	Scanning electron microscopy
STK	Stokes´ number
Tg	Glass transition temperature
XRD	X - ray powder diffraction

H. Bibliography

Bailey, A.G. Charging of Solids and Powders. Journal of Electrostatics 30 (1993) 167 - 180

Bresges, C., Urbanetz, N.A. Determination of the minimum number of spacer particles ensuring non - contact between host particles - A new approach by numerical modelling. Powder Technology doi: 10.1016/j.powtec.2008.03.002

Brodka - Pfeiffer, K., Langgut, P., Grass, P., Haeusler, H. Influence of mechanical activation on the physical stability of salbutamol sulphate. European Journal of Pharmaceutics and Biopharmaceutics 56 (2003) 393 - 400

Buckton, G. Interfacial phenomena in drug delivery and targeting. Chichester Harwood Academic Publishers (1995) (b)

Buckton, G. Surface characterization: Understanding sources of variability in the production and use of pharmaceuticals. Journal of Pharmacy and Pharmacology 47 (1995) 265 - 275 (a)

Buckton, G. The assessment and pharmaceutical importance of the solid/liquid and the solid/vapour interface: a review with respect to powders. International Journal of Pharmaceutics 44 (1988) 1 - 8

Buckton, G., Darcy, P. The use of gravimetric studies to assess the degree of crystallinity of predominantly crystalline powders. International Journal of Pharmaceutics 123 (1995) 265 - 271 (c)

Chidavaenzi, O.C., Buckton, G., Koosh, F., Pathak, R. The use of thermal techniques to assess the impact of feed concentration on the amorphous content and polymorphic forms present in a spray - dried lactose. International Journal of Pharmaceutics 159 (1997) 67 - 74

Columbano, A., Buckton, G., Wikeley, B. A study of the crystallisation of amorphous salbutamol sulphate using water vapour sorption and near infrared spectroscopy. International Journal of Pharmaceutics 237 (2002) 171 - 178

Copley Scientific: Quality Solutions for Solid Dosage Testing. Company brochure. January Edition (2003)

Coste, J., Pechery, P. Contribution to the study of charges by friction between metals and polymers. In: Proceedings IIème Congres International de l'Electrostatique, Grenoble; 20 - 22.04.1977 (1977)

Cross, J. Electrostatics: Principles, Problems and Applications. Adam Hilger, Bristol (1987)

Degussa AG: Hydrophobes Aerosil - Herstellung, Eigenschaften und Anwendungen. Schriftenreihe Pigmente; 6 (1993)

Degussa AG: Hydrophobe Aerosil® - Typen und ihr Einsatz in der Lack - Industrie; Schriftenreihe Pigmente. 18 (2000)

Degussa AG: Synthetische Kieselsaearen als Fliesshilfsmittel und Traegersubstanz; Schriftenreihe Pigmente. 11 (2002)

Derjaguin, B.V., Abrikosova, I.I., Lifschitz, E.M. Молекулярное притяжение конденсированных тел. Успехи физических наук T. LXIV 3 (1958) 494 - 528

Derjaguin, B.V., Muller V.M., Topotov Y.P. Effect of Contact Deformations on the Adhesion of Particles. Journal of colloid and Interface Science 53 (1975) 314 - 326

Duenisch, S. Untersuchung der Wirkungsweise von Nanomaterialien. PhD Thesis. Wuerzburg, Germany (2005)

Eber, M. Wirksamkeit und Leistungsfaehigkeit von nanoskaligen Fliessregulierungsmitteln. PhD Thesis. Wuerzburg, Germany (2004)

Elamin, A.A., Sebhatu, T., Ahlneck C. The use of amorphous model substances to study mechanically activated materials in the solid state. International Journal of Pharmaceutics 119 (1995) 25 - 36

European Pharmacopoeia 6.0; Council of Europe, Strasbourg; (2007)

Figura, L.O. The physical modification of lactose and its thermoanalytical identification. Thermochimica Acta; 222 (1993) 187 - 194

Gebhardt, J., Heyder, J., Stahlhofen, W. Deposition von Aerosolteilchen im menschlichen Atemtrakt bei therapeutischer Applikation von Aerosolen. Atemwegs - Lungenkrankheiten 4 (1978) 384 - 386

German Industry Norm DIN 53916: “Surface active agents - Powders and granules - Measurement of the angle of repose; Proceeding according Pfrengle”

Gerthsen, C., Vogel, H. Physik. Springer - Verlag, Berlin, Heidelberg, New York (1997)

Gombás, Á., Szabó-Révész, P., Kata, M., Regdon, Jr. G., Eroes I. Quantitative Determination of Crystallinity of α - lactose monohydrate by DSC. Journal of thermal analysis and calorimetry 68 (2002) 503 - 510

Gorny, M., Jakobs, M., Mykhaylova, V., Urbanetz, N.A. Quantifying the degree of disorder in micronised salbutamol sulphate using moisture sorption analysis. Drug Development and Industrial Pharmacy 33 (2007) 235 - 243

Greason, W.D. Electrostatic discharge: a charge driven phenomenon. Journal of Electrostatics 28 (1992) 199 - 210

Gruetzmann, R., Schmidt, P. C. Pulverinhalatoren und Dosieraerosole richtig anwenden. Pharmazeutische. Zeitung 24 (2004)

Guchardia, R., Freia, M., Johna E., Kaerger, J.S. Influence of fine lactose and magnesium stearate on low dose dry powder inhaler formulation. International Journal of Pharmaceutics 348 (2008) 10 - 17

Hamaker, H.C. The London - Van der Waals attraction between spherical particles. Physica IV I0(1937) 1058 - 1072

Hancock, B.C., Zografi G. Characteristics and Significance of the Amorphous State in Pharmaceutical Systems. Journal of Pharmaceutical Science 86 (1997) 1 - 11

Harper, W.R. Contact and frictional electrification. Oxford, Clarendon (1967)

Hickey, A.J., Martonen, T.B., Yang, Y. Theoretical relationship of lung deposition to the fine particle fraction of inhalation aerosols. Pharmaceutica Acta Helvetiae 71 (1996) 185 - 190

Huber, G. Elektrostatisch unterstuetztes Mischen und Beschichten hochdisperser Pulver in fluessigem Stickstoff. PhD Thesis. Erlangen – Nuernberg, Germany (2001)

Huber G., Wirth K.E. Electrostatically supported surface coating of solid particles in liquid nitrogen for use in dry powder inhalers. Powder Technology 134 (2003) 181 - 192

Hunnius C., Burger A. Hunnius pharmazeutisches Woerterbuch. Walter de Gruyter, Berlin, New York (1993)

Israelachvili, J.N. Forces, Intermolecular and Surface Forces. Academic Press, London (2000)

Itoh, T., Satoh, M., Adachi, S. Differential Thermal Analysis of α - lactose - monohydrate. Journal of Dairy Science 60 (1977) 1230 - 1235

Jenike, A. W. Storage and flow of solids; Bulletin of the University of Utah Nr 123.v Engineering Experiment Station, University of Utah, Salt Lake City (1964)

Jonat, S., Hasenzahl, S., Drexhsler M., Albers, P., Wagner K.G., Schmidt P.C. Investigation of compacted hydrophilic and hydrophobic silicon dioxides as glidants for pharmaceutical excipients. Powder Technology 141 (2004) 31 - 43

Kawashima, Y., Serigano, T., Hino, T., Yamamoto, H., Takeuchi, H. Design of inhalation dry powder of pranlukast hydrate to improve dispersibility by the surface modification with light anhydrous silicic acid (AEROSLI 200). International Journal of Pharmaceuticals 173 (1998) 243 - 251

Keithley Instruments GmbH; Elektrometer 6517 - A. Keithley Instruments GmbH, Germering (1988)

Kirk, J.H., Dann, S.E., Blatchford, C.G. Lactose: a guide to polymorph determination. International Journal of Pharmaceuticals 334 (2007) 103 - 144

Kurfess, D., Hinrichsen, H., Zimmermann, I. Statistical model of the powder flow regulation by nanomaterials. Powder Technology 159 (2005) 63 - 70

Krupp, H. Particle Adhesion - Theory and Experiment. Advanced Colloid Interface Science. I (1967) 111 - 239

Lane, R.A., Buckton, G. The novel Combination of dynamic vapour sorption gravimetric analysis and near infra - red spectroscopy as a hyphenated technique International Journal of Pharmaceuticals 207 (2000) 49 - 56

Lerk, C.F. Alterations of α - lactose During Differential Scanning Calorimetry. Journal of Pharmaceutical Science 73 (1984) 856 - 857

Lerk, C.F. Physikalisch - pharmazeutische Eigenschaften von Lactose. Pharmazie in unsere Zeit Nr.2 (1987)

Lifschitz, E.M. The Theory of Molecular Attractive Forces between Solids. Journal of Experimental and Theoretical Physics. 28 (1956) 73 - 83

Linsenbuehler, M. Herstellung und Charakterisierung funktionalisierter Composite - Partikel. PhD Thesis. Erlangen - Nuernberg, Germany (2005)

Linsenbuehler, M., Huber, G., Wirth, K.-E. Dispersing, Mixing and Coating of highly disperse Particles. In: Mueller, E.; Oestreich, C. Handling of highly dispersed powders. Shaker Verlag, Aachen 150 - 157 (2004) (a)

Linsenbuehler, M., Wirth, K.-E. A powder on the move.. In: European Coatings Journal 14 - 21 (2002) (b)

Linsenbuehler, M., Wirth, K.E. Ein Pulver lernt fliessen. In: Lacke&Farbe 85 - 90 (2002) (a)

Linsenbuehler, M., Wirth, K.-E. Properties of tailor - made functionalized micro - particles. In: Proceedings PARTEC 2004, Nuernberg; 16.03 - 18.03 (2004) (b)

Lohrmann, M. Adhaesionskraefte in interaktiven Mischungen fuer Pulverinhalatoren. PhD Thesis. Duesseldorf, Germany (2005)

Markefka, P. Assessment of low levels of amorphous content in lactose by DVS and isothermal microcalorimetry. Pharmaceutical and Medical Chemistry 335 (2002) 116

Markefka, P., Steckel, H. Powder flowability analysis as predictor for delivered mass uniformity from dry powder inhalers. Pharmind 7 (2005) 823 - 829

Marple, V.A. Next generation pharmaceutical impactor (a new impactor for pharmaceutical inhaler testing), Part I: Design. Journal of Aerosol Medicine and Pulmonary Drug Delivery 16 (2003) 283 - 299

Meyer, K. Nanomaterialien als fliessregulierungmittel. PhD Thesis. Wuerzburg, Germany (2003)

Moren, F. Aerosols in Medicine. Principles, Diagnosis and Therapy; Elsevier, Amsterdam - London - New York - Tokyo (1993)

Mueller, R.H., Schuhmann, R. Teilchengroessenmessung in Laborpraxis. Wissenschftliche Verlagsgesellschaft GmbH, Stuttgart (1996)

Mykhaylova, V., Urbanetz, N.A. New nanoparticle - microparticle formulations for use in dry powder inhalers. In: Proceeding of the Joint Meeting of the Czech, German and Hungarian Pharmaceutical Societies. Marburg, Germany (2006)

Najafabadi, A.R., Asgarian, R., Tajerzadeh, H., Gilani, K., Vatanara, A., Darabi, M. The effects of fine lactose as a third component on aerosolization of cerotaxime sodium from dry powder formulations. DARU 14 (2006) 155 - 163

Neumann, B.S. The flow properties of powders. In: Bean, H.S., Beckett, A.H., Carless, J.E.; Advances in Pharmaceutical Sciences. Academic Press, London 2 (1967) 181 - 221

Pahl, M.H., Wicke R. Haftkraefte in kompaktierten Schuettguetern. Aufbereitungs - Pfinztal 17.06 - 18.06 (2004)

Podczeck, F. Evaluation of the Adhesion Properties of Salbutamol Sulphate to Inhaler Materials. Pharmaceutical Research 15 (1998) 806 - 808 (a)

Podczeck, F. Optimization of the operation conditions of an Andersen - Cascade impactor and the relationship to centrifugal adhesion measurements to aid the development of dry powder inhalations. International Journal of Pharmaceutics 149 (1997) 51 - 61 (a)

Podczeck, F. Pulveraerosole zur Inhalation. Deutsche Apotheken. Zeitung 137 (1997) 73 - 79 (b)

Podczeck, F. The relationship between particulate properties of carrier materials and the adhesion force of drug particles in interactive powder mixtures. Journal of Adhesion Science and Technology 11 (1997) 1089 - 1104 (c)

Podczeck F. The relationsship between physical properties of lactose monohydrate and the aerodynamic behaviour of adhered drug particles. International Journal of Pharmaceutics 160 (1998) 119 - 130 (b)

Pohl, M., Schubert, H. Dispergieren und Desagglomerieren von Nanopartikeln mit Ultraschall. In: Teipel, U. (Hrsg.) Produktgestaltung in der Partikeltechnologie (2004)

Poppe, T., Blum, J., Henning, T. Experiments on collisional grain charging of micron - sized preplanetary dust. The Astrophysical Journal 533 (2000) 472 - 480

Price, R., Young, P., Edge, S., Staniforth, J.N. The influence of relative humidity on particulate interactions in carrier - based dry powder inhaler formulations. International Journal of Pharmaceutics 246 (2002) 47 - 59

Rumpf, H. Grundlagen und Methoden des Granulierens. Chemie Ingenieur Technik 3 (1958) 144 - 158

Rumpf, H. Particle Adhesion. In: Sastry, K.V.S. Agglomeration 77, Proceedings of the 2nd International Symposium on Agglomeration 1 (1977) 97 - 129

Saint - Lorant, G., Leterme, P., Gayot, A., Flament M.P. Influence of carrier on the performance of dry powder inhalers. International Journal of Pharmaceutics 334 (2007) 85 - 91

Saleki - Gerhardt, A., Ahlneck, C., Zografi, G. Assessment of disorder in crystalline solids. International Journal of Pharmaceutics 101 (1994) 237 - 247

Schoettle, I.A. Spruehgetrocknete Polylaktid, Poly(laktid - co - glykolid) Mikropartikel zur Steuerung der Freisetzung aus pulmonalen Arzneiformen. PhD Thesis. Mainz, Germany (2006)

Schubert, H. Food particle technology. Part I: Properties of particles and particulate food systems. Journal of food Engineering 6 (1987) 1 - 32

Schubert, H. Haftung zwischen Feststoffteilchen aufgrund von Fluessigkeitsbruecken. Chemie Ingenieur Technik 46 (1974) 333 - 224

Schubert, H. Mechanische Verfahrenstechnik. 3., erweit. u. durchges. Aufl..Deutscher Verlag fuer Grundstoffindustrie Leipzig (1977)

Schulze, D. Flowability and time consolidation measurements using a ring shear tester. Powder handling and processing 8 (1996) 221 - 226

Schulze, D., Wittmaier, A. Flow properties of highly dispersed powders at very small consolidation stresses. Chemical Engineering and Technology 26 (2003) 133 - 137

Schwedes, J., Schulze, D. Measurement of Flow Properties of Bulk Solids. Powder Technology. 61 (1990) 59 - 68

Steckel, H. Inhalationspulver - Neuere Entwicklungen bei Pulverinhalatoren. PZ Prisma 10 (2003) 145 - 157 (a)

Steckel, H. Therapie des Asthma bronchiale - Darreichungsformen fuer inhalative Glucocorticoide. Pharmazie in unserer Zeit. 4 (2003) 314 - 322 (b)

Steckel H., Bolzen N. Alternative sugars as potential carriers for dry powder inhalations. International Journal of Pharmaceutics 270 (2004) 297 - 306

Steckel, H., Markefka. P., Wierikte H., Kanmelar, R. Effect on milling and sieving on functiionality of dry powder inhalation products. International Journal of Pharmaceutics 309 (2006) 51 - 59

Steckel, H., Mueller, B.W. In vitro evaluation of dry powder inhalers: drug deposition of commonly used devices. International Journal of Pharmaceutics 154 (1997) 19 - 29

Tee, S.K., Marriott, C., Zeng, X.-M., Martin, G.P. The use of different sugars as fine and coarse carriers for aerosolised salbutamol sulphate. International Journal of Pharmaceutics 208 (2000) 111 - 123

Urbanetz, N.A. Physikalische Einfluesse steuern die pulmonale Deposition. Pharmazeutische Zeitung 40 (2006)

Vercoulen, P.H.W. Electrostatic processing of particles. PhD Thesis. Delft, Netherland (1995)

Visser, J. Van der Waals and other cohesive forces affecting powder fluidization. Powder Technology. 58 (1989) 1 - 10

Young, P.M., Chiou, T.T., Traini, D., Chan, H.-K., Thielmann, F., Burnett, D. The Use of Organic Vapor Sorption to Determine Low Levels of Amorphous Content in Processes Pharmaceutical Powders. Drug Development and Industrial Pharmacy 33 (2007) 91 - 97

Yang, J., Sliva, A., Banerjee, A., Dave R.N., Pfeffer R. Dry particle coating for improving the flowability of cohesive powders. Powder Technology. 158 (2005) 21 - 33

Zeng, M.Z., Martin, G.P., Marriott C. Particulate Interactions in Dry Powder Formulations for Inhalation. Taylor&Francis London (2001)

Zeng, X.-M., Martin G.P., Marroitt C.M., Pritchard J. Lactose as a Carrier in Dry Powder Formulations: The Influence of Surface Characteristics on Drug Delivery. Journal of Pharmaceutical Science 90 (2002) 1424 - 1434

Zeng, X.-M., Martin G.P., Tee, S.-K., Choush, A.A., Marriot C.M. Effects of particle size and adding sequence of fine lactose on the deposition of salbutamol sulphate from a dry powder formulation. International Journal of Pharmaceutics 182 (1999) 133 - 144

Zeng, X.-M., Martin G.P., Tee, S.-K., Marriot C.M. The role of fine particle lactose on the dispersion and deaggregation of salbutamol sulphate in an air stream in vitro. International Journal of Pharmaceutics 176 (1998) 99 - 110

Selbsttätigkeitserklärung

Die hier vorgelegt Dissertation habe ich eigenständig und ohne unerlaubte Hilfe angefertigt. Die Dissertation wurde in der vorgelegten Form bei keiner anderen Institution eingereicht. Ich habe bisher keine erfolglosen Promotionsversuche unternommen.

Düsseldorf, den 11.01.2009

Mykhaylova Viktoriya

Acknowledgements

This work would not take place without Prof. Dr. Nora Anne Urbanetz. I thank her wholeheartedly for the absolute support, patience, understanding and for giving me the opportunity to work in her research group. Her highly scientific, interesting ideas and suggestions were very helpful for the development of this work.

I deeply thank Prof. Dr. Peter Kleinebudde for the evaluation of this thesis and for excellent organising and heading of the Institute of the Pharmaceutics and Biopharmaceutics. I particularly thank him for allowing me to work in the Institute of Pharmaceutics and Biopharmaceutics at Heinrich - Heine University, Duesseldorf.

I´m especially grateful Prof. Dr. Bernhard Lippold for his kind support at the beginning of my work in the Institute of the Pharmaceutics and Biopharmaceutics.

I would like to express thanks to my colleague Carsten Bresges for developing of the computing program, which was very important for this thesis, for his support in solving of the difficult scientific problem.

A special appreciation is given to Annemarie Schmitz for the developing of the measuring method, which allowed me the evaluation of the results of the measurements with the help of High - Liquid - Chromatography and for her kind support and interesting discussions during my time at the institute.

I would like to thank the Company Molkerei MEGGLE Wasserburg GmbH & Co. KG, Wasserburg, Germany for the spray - dried lactose.

I gratefully thank the employees and colleagues of the Institute of Pharmaceutics and Biopharmaceutics, especially Karin Matthée for the performance of the numerous DSC measurements and also Martina Smikala, Karin Matthée, Dorothy Eikeler and for the performance of the SEM measurements.

I would like to thank my colleagues Caroline Kablitz, Seon - Hie Yoo, Claudia Reitz, Hind Jaeda and Andrea Michalk for the great time at the institute.

I am really very grateful to my colleague and friend Dejan Djuric for ensuring of the unforgettable time at the institute.

My best thanks to my friend Olga Yemchenko for her support and help.

I also very grateful to my mother for her understanding and supporting me and her believe in me.

The most deepest thank I would like to express to my husband Ruslan Monchuk, who enabled my PhD studies, always stand by my side and supported me absolutely.